Graduate School ETD Form 9
(Revised 12/07)

PURDUE UNIVERSITY
GRADUATE SCHOOL
Thesis/Dissertation Acceptance

This is to certify that the thesis/dissertation prepared

By Carmen Michelle Dumaual

Entitled
Expression and Function of the PRL Family of Protein Tyrosine Phosphatase

For the degree of Doctor of Philosophy

Is approved by the final examining committee:

Cynthia Stauffacher
Chair

Stephen Randall

Anna Malkova

George Sandusky

To the best of my knowledge and as understood by the student in the *Research Integrity and Copyright Disclaimer (Graduate School Form 20)*, this thesis/dissertation adheres to the provisions of Purdue University's "Policy on Integrity in Research" and the use of copyrighted material.

Approved by Major Professor(s): Stephen Randall

Approved by: Cynthia Stauffacher 11/06/2012
Head of the Graduate Program Date

Graduate School Form 20
(Revised 9/10)

PURDUE UNIVERSITY
GRADUATE SCHOOL

Research Integrity and Copyright Disclaimer

Title of Thesis/Dissertation:

Expression and Function of the PRL Family of Protein Tyrosine Phosphatase

For the degree of Doctor of Philosophy

I certify that in the preparation of this thesis, I have observed the provisions of *Purdue University Executive Memorandum No. C-22,* September 6, 1991, *Policy on Integrity in Research.**

Further, I certify that this work is free of plagiarism and all materials appearing in this thesis/dissertation have been properly quoted and attributed.

I certify that all copyrighted material incorporated into this thesis/dissertation is in compliance with the United States' copyright law and that I have received written permission from the copyright owners for my use of their work, which is beyond the scope of the law. I agree to indemnify and save harmless Purdue University from any and all claims that may be asserted or that may arise from any copyright violation.

Carmen Michelle Dumaual

Printed Name and Signature of Candidate

11/06/2012

Date (month/day/year)

*Located at http://www.purdue.edu/policies/pages/teach_res_outreach/c_22.html

EXPRESSION AND FUNCTION OF THE PRL FAMILY OF PROTEIN TYROSINE PHOSPHATASE

A Dissertation

Submitted to the Faculty

of

Purdue University

by

Carmen Michelle Dumaual

In Partial Fulfillment of the

Requirements for the Degree

of

Doctor of Philosophy

December 2012

Purdue University

Indianapolis, Indiana

For those who believed in me and have stood by me throughout the years

For John and Coz, who will never be forgotten

And for Mike

ACKNOWLEDGEMENTS

First and foremost, I would like to thank my friend, committee member, and mentor, Dr. George Sandusky, for encouraging me to apply to graduate school in the first place and whose enthusiasm for science has been an inspiration to me throughout my career. I am also greatly indebted to my graduate advisor, Dr. Stephen Randall for his guidance, support, and unending patience throughout the course of this project. His mentorship has helped to provide me with the necessary tools to become a successful, independent scientist. In addition, I would like to express my deepest appreciation to the remaining members of my committee, Dr. Cynthia Stauffacher, Dr. Martin Smith, and Dr. Anna Malkova for their valuable insight, advice, and many other contributions to both my dissertation project and my personal development and growth.

The completion of this project could not have been possible without the resources and expertise provided by many individuals along the way. Most notably, I would like to recognize Dr. Han Weng Soo, Dr. Mark Farmen, and Dr. Boyd Steere for their statistical and bioinformatic data analysis support; Dr. Tom Barber for the use of his laboratory and equipment; and Dr. Zhong-Yin Zhang and Chad Walls whose collaboration made a large portion of this work possible.

I am also grateful to my many friends, family and loved ones for their constant understanding, encouragement, and support. Completing a graduate degree while working full time has not been an easy road, but their reassurance and belief in me has helped me to overcome many setbacks and to keep my sanity through it all. Finally, I would like to thank Cosmo, the cat, for overseeing the writing of this dissertation and for having the ability to bring a smile to my face at the beginning and end of every day, even in the hardest of times.

TABLE OF CONTENTS

LIST OF TABLES

LIST OF FIGURES

LIST OF ABBREVIATIONS

Å	Angstrom
Asp	Aspartate
B2M	Beta-2 microglobulin
BamHI	*Bacillus amyloliquefaciens* HI
BLAST	Basic Local Alignment Search Tool
BSA	Bovine serum albumin
C	Celsius
C2	Protein kinase C, conserved region 2
CAAX	Cysteine, aliphatic, aliphatic, any amino acid
CDC	Cell division cycle
Cdk	Cyclin-dependent kinase
cDNA	Complementary deoxyribonucleic acid
CH2	Cdc25 homology region 2
CHO	Chinese hamster ovary
Csk	C-terminal Src kinase
Ct	Threshold Cycle
C-Terminal/C-termini	Carboxyl terminal/termini
Cys	Cysteine

Da	Dalton
DAB	Diaminobenzadine
DMEM	Dulbecco’s Modified Eagle Medium
DNA	Deoxyribonucleic acid
DSP	Dual specificity phosphatase
EDTA	Ethylenediaminetetraacetic acid
eIF2A	Eukaryotic translation initiation factor 2A
EMBL	European Molecular Biology Laboratory
EMT	Epithelial-to-mesenchymal transition
ER	Endoplasmic reticulum
ERK	Extracellular signal-regulated kinase
F-actin	Filamentous actin
FAK	Focal adhesion kinase
FC	Fold Change
FDR	False discovery rate
FERM	4.1/Ezrin/Radixin/Moesin
FFPE	Formalin-fixed paraffin-embedded
FITC	Fluorescein isothiocyanate
FTI	Farnesyltransferase inhibitor
GAP	GTPase activating protein
GAPDH	Glyceraldehyde-3-phosphate dehydrogenase
GCOS	GeneChip Operating System
GEF	Guanine nucleotide exchange factor

G Protein	GTP-binding protein
GDI	Guanine nucleotide dissociation inhibitor
GDP	Guanosine diphosphate
GGT	Geranylgeranyl transferase
GTP	Guanosine triphosphate
HEK	Human embryonic kidney
HPLC	High Performance Liquid Chromatography
Hr	Hour
ISH	In situ hybridization
IUPUI	Indiana University-Purdue University Indianapolis
JNK	c-Jun-N-terminal kinase
Ka	Dissociation constant
KAP	Kinase-associated phosphatase
KDa	Kilodalton
LSAB	Labeled streptavidin biotin
M	Molar
MAPK	Mitogen-activated protein kinase
Mas5	Microarray Analysis Suite 5.0
Min	Minute
miR/miRNA	MicroRNA
MKP	MAPK phosphatase
ml	Milliliter
mM	Millimolar

MMP	Matrix metalloproteinase
M_r	Relative molecular mass
mRNA	Messenger ribonucleic acid
MS	Mass spectrometry
μg	Microgram
μl	Microliter
μm	Micrometer
NaCl	Sodium chloride
NaOH	Sodium hydroxide
NCL	Nucleolin
ncRNA	Non-coding RNA
ng	Nanogram
NLS	Nuclear localization signal
NRPTP	Non-receptor protein tyrosine phosphatase
NSCLC	Non-small cell lung cancer
N-terminus/N-terminal	Amino terminus/terminal
OMFP	3-O-methylfluorescein phosphate
%P	Percent present
PAK	p21-activated kinase
PBS	Phosphate-buffered saline
PCR	Polymerase chain reaction
PI3K	Phosphoinositide 3-kinase
PIP	Phosphatidylinositol phosphate

PIP2	Phosphatidylinositol-4,5-bisphosphate; $PI(4,5)P_2$
PIP3	Phosphatidylinositol-3,4,5-trisphosphate; $PI(3,4,5)P_3$
PK	Protein kinase
pKa	Negative log of dissociation constant (Ka)
PKR	Protein kinase, RNA-dependent
PNPP	para-Nitrophenyl Phosphate
PP	Protein phosphatase
PPM	Protein phosphatase Mg^{2+}/Mn^{2+} dependent
PPP	Phosphoprotein phosphatase
PRL	Phosphatase of regenerating liver
pSer	Phosphoserine
PTEN	Phosphatase and tensin homolog deleted on chromosome 10
pThr	Phosphothreonine
PTP	Protein tyrosine phosphatase
PTP1B	Protein tyrosine phosphatase 1B
pTyr	Phosphotyrosine
QC	Quality control
qRT-PCR	Quantitative, Real-Time, Reverse Transcription PCR
RIPA	Radio-immunoprecipitation assay
RNA	Ribonucleic acid
RNase	Ribonuclease
RNAi	RNA interference

RPTP	Receptor protein tyrosine phosphatase
rRNA	Ribosomal RNA
RT	Room temperature
SAPK	Stress-activated protein kinase
SD	Standard deviation
SDS	Sodium dodecyl sulfate
SDSS	Sequence detection system software
Sec	Seconds
SH2/SH3	Src homology 2/Src homology 3
shRNA	Short hairpin RNA
siRNA	Small interfering RNA
SS	Staining score
SSC	Standard saline citrate
Stat	Signal transducer and activator of transcription
TAE	Tris-Acetate-EDTA
TBS	Tris-Buffered Saline
TBST	Tris-Buffered Saline with 0.05% Tween-20
TE	Tris-EDTA
UBC	Ubiquitin C
VEGF	Vascular endothelial growth factor
VHR	Vaccinia H1-related
vtRNA	Vault RNA
WT	Wild type

ABSTRACT

Dumaual, Carmen, Michelle Ph.D., Purdue University, December 2012.
Expression and Function of the PRL Family of Protein Tyrosine Phosphatase.
Major Professor: Stephen K. Randall.

The PRL family of enzymes constitutes a unique class of protein tyrosine phosphatase, consisting of three highly homologous members (PRL-1, PRL-2, and PRL-3). Family member PRL-3 is highly expressed in a number of tumor types and has recently gained much interest as a potential prognostic indicator of increased disease aggressiveness and poor clinical outcome for multiple human cancers. PRL-1 and PRL-2 are also known to promote a malignant phenotype *in vitro*, however, prior to the present study, little was known about their expression in human normal or tumor tissues. In addition, the biological function of all three PRL enzymes remains elusive and the underlying mechanisms by which they exert their effects are poorly understood. The current project was undertaken to expand our knowledge surrounding the normal cellular function of the PRL enzymes, the signaling pathways in which they operate, and the roles they play in the progression of human disease. We first characterized the tissue distribution and cell-type specific localization of PRL-1 and PRL-2 transcripts in a variety of normal and diseased human tissues using *in situ* hybridization. In normal, adult human tissues we found that PRL-1 and PRL-2 messages were

almost ubiquitously expressed. Only highly specialized cell types, such as fibrocartilage cells, the taste buds of the tongue, and select neural cells displayed little to no expression of either transcript. In almost every other tissue and cell type examined, PRL-2 was expressed strongly while PRL-1 expression levels were variable. Each transcript was widely expressed in both proliferating and quiescent cells indicating that different tissues or cell types may display a unique physiological response to these genes. In support of this idea, we found alterations of PRL-1 and PRL-2 transcript levels in tumor samples to be highly tissue-type specific. PRL-1 expression was significantly increased in 100% of hepatocellular and gastric carcinomas, but significantly decreased in 100% of ovarian, 80% of breast, and 75% of lung tumors as compared to matched normal tissues from the same subjects. Likewise, PRL-2 expression was significantly higher in 100% of hepatocellular carcinomas, yet significantly lower in 54% of kidney carcinomas compared to matched normal specimens. PRL-1 expression was found to be associated with tumor grade in the prostate, ovary, and uterus, with patient gender in the bladder, and with patient age in the brain and skeletal muscle. These results suggest an important, but pleiotropic role for PRL-1 and PRL-2 in both normal tissue function and in the neoplastic process. These molecules may have a tumor promoting effect in some tissue types, but inhibit tumor formation or growth in others. To further elucidate the signaling pathways in which the PRLs operate, we focused on PRL-1 and used microarray and microRNA gene expression profiling to examine the global molecular changes that occur in response to stable PRL-1 overexpression in HEK293 cells. This

analysis led to identification of several molecules not previously associated with PRL signaling, but whose expression was significantly altered by exogenous PRL-1 expression. In particular, Filamin A, RhoGDIα, and SPARC are attractive targets for novel mediators of PRL-1 function. We also found that PRL-1 has the capacity to indirectly influence the expression of target genes through regulation of microRNA levels and we provide evidence supporting previous observations suggesting that PRL-1 promotes cell proliferation, survival, migration, invasion, and metastasis by influencing multi-functional molecules, such as the Rho GTPases, that have essential roles in regulation of the cell cycle, cytoskeletal reorganization, and transcription factor function. The combined results of these studies have expanded our current understanding of the expression and function of the PRL family of enzymes as well as of the role these important signaling molecules play in the progression of human disease.

PUBLICATIONS

The Journal of Histochemistry & Cytochemistry

Volume 54(12): 1401–1412, 2006
Journal of Histochemistry & Cytochemistry
http://www.jhc.org

ARTICLE

Cellular Localization of PRL-1 and PRL-2 Gene Expression in Normal Adult Human Tissues

Carmen M. Dumaual, George E. Sandusky, Pamela L. Crowell, and Stephen K. Randall

Department of Biology, Indiana University–Purdue University Indianapolis, Indianapolis, Indiana (CMD,PLC,SKR), and Department of Pathology, Indiana University School of Medicine, Indianapolis, Indiana (GES)

SUMMARY Recent evidence suggests that the PRL-1 and -2 phosphatases may be multifunctional enzymes with diverse roles in a variety of tissue and cell types. Northern blotting has previously shown widespread expression of both transcripts; however, little is known about the cell type-specific expression of either gene, especially in human tissues. Therefore, we investigated expression patterns for PRL-1 and -2 genes in multiple normal, adult human tissues using in situ hybridization. Although both transcripts were ubiquitously expressed, they exhibited strikingly different patterns of expression. PRL-2 was expressed heavily in almost every tissue and cell type examined, whereas PRL-1 expression levels varied considerably both between tissue types and between individuals. Widespread expression of PRL-1 and -2 in multiple organ systems suggests an important functional role for these enzymes in normal tissue homeostasis. In addition, the variable patterns of expression for these genes may provide distinct activities in each tissue or cell type. **(J Histochem Cytochem 54:1401–1412, 2006)**

KEY WORDS
PRL-1
PRL-2
normal human tissues
in situ hybridization
mRNA
differential expression
cellular localization

THE PRL FAMILY of phosphatases constitutes a distinct class of protein tyrosine phosphatase (PTP), consisting of three members (PRL-1, -2, and -3). These three closely related enzymes are distinctive in that they are among the smallest of the PTPs consisting primarily of a catalytic domain, and their amino acid sequences contain a carboxy terminal CAAX motif that is posttranslationally isoprenylated. This posttranslational modification, unique among PTPs, is critical to the subcellular localization and biological activity of the PRL enzymes (Cates et al. 1996; Zeng et al. 2000; Si et al. 2001). Specific substrates and cellular roles of the PRLs remain to be defined; however, their high degree of conservation (Cates et al. 1996; Zeng et al. 1998), as well as their similarity to several dual-specificity phosphatases (DSPs) involved in cell cycle and cell growth control (Zeng et al. 1998; Kozlov et al. 2004; Sun et al. 2005), suggests a critical role for these PTPs in cellular regulation. Recent evidence suggests that these may be pleiotropic-signaling molecules that play diverse roles in various tissue and cell types (Diamond et al. 1996; Rundle and Kappen 1999).

Correspondence to: Carmen M. Dumaual, IUPUI, Dept. of Biology, 723 West Michigan St., Room SL306, Indianapolis, IN 46202. E-mail: cdumaual@lilly.com

Received for publication May 12, 2006; accepted August 1, 2006 [DOI: 10.1369/jhc.6A7019.2006].

PRL-1, the first identified PRL family member, was initially characterized and named for its expression in a number of proliferating cell types including rat liver during hepatic regeneration (Mohn et al. 1991; Diamond et al. 1994), mouse liver cells and NIH3T3 mouse fibroblasts stimulated by a primary mitogen (Diamond et al. 1996; Columbano et al. 1997), rat cerebral cortex following transient forebrain ischemia (Takano et al. 1996), and multiple human tumor cell lines (Diamond et al. 1994; Wang et al. 2002a). Further indicating a role for PRL-1 in cellular growth and proliferation, it has been found that PRL-1 phosphatase activity is required for progression of cells through mitosis (Wang et al. 2002a), and that overexpression of either PRL-1 or -2 in cells leads to accelerated entry into S phase (Werner et al. 2003). Additionally, all three PRL enzymes have been linked to cellular transformation and tumorigenesis (Cates et al. 1996; Wang et al. 2002b; Bardelli et al. 2003; Zeng et al. 2003; Wu et al. 2004).

Although these results are all consistent with a role for the PRL enzymes in cell growth, analysis of the normal tissue expression of PRL transcripts revealed all three genes to be predominantly expressed in terminally differentiated tissues such as skeletal muscle (Diamond et al. 1994; Zeng et al. 1998; Matter et al. 2001), brain (PRL-1) (Diamond et al. 1994), and cardiac muscle (PRL-3) (Matter et al. 2001). Consistent

0022-1554/06/$3.30

The Journal of Histochemistry & Cytochemistry

with this pattern of PRL expression, Diamond et al. (1996) noted high levels of PRL-1 protein in the differentiated villus but not in the proliferating crypt enterocytes of rat intestine and high levels of PRL-1 mRNA in confluent differentiated CaCo2 cells, but little to no expression in proliferating CaCo2 cells. Guo et al. (2003) found the PRL-1 gene to be significantly overexpressed in more differentiated parous breast tissues as compared with proliferative nulliparous breast tissues. Scarlato et al. (2000) found that PRL-1 mRNA is upregulated in oligodendroglial progenitor cells that are capable of terminal differentiation in comparison to immature oligodendroglial progenitors, which do not terminally differentiate.

Together these results suggest a dual role for the PRL gene family in regulation of both cellular proliferation and differentiation. Consistent with this notion, PRL-1 mRNA was predominantly expressed in proliferating chondrocytes in early development of mouse embryos but was localized primarily to differentiated, hypertrophic chondrocytes in later stages of development (Rundle and Kappen 1999). PRLs have also been implicated in more complex biological processes including embryonic development (Rundle and Kappen 1999; Kong et al. 2000), angiogenesis (Guo et al. 2004), cardiomyopathy (Matter et al. 2001), cell movement (Zeng et al. 2003), and sexual differentiation in the brain (Carter 1998).

Whereas multi-tissue analysis has revealed PRL-3 expression to be largely confined to heart and skeletal muscle in normal tissues (Zeng et al. 1998; Matter et al. 2001), PRL-1 and -2 are reported to be more widely expressed (Montagna et al. 1995; Zeng et al. 1998; Rundle and Kappen 1999; Kong et al. 2000). Given that the biological effects of the PRL enzymes may be tissue specific, characterization of the tissues and cell types that express PRL-1 and -2 is important to elucidating the physiological function of the normal genes and to understanding their roles in the pathogenesis of disease. However, studies of normal PRL-1 or -2 expression, to date, have been limited largely to animal systems and to human cell line or tissue Northern blots. To our knowledge, no study has yet described the cell type-specific expression patterns of any of the PRL genes in a diverse panel of human tissues. Therefore, we sought to characterize the cellular localization and tissue distribution of PRL-1 and -2 mRNA in a broad range of normal adult human tissues using in situ hybridization (ISH). With non-radioactive ISH, we detected some level of PRL-1 and -2 message in nearly all human tissues studied, confirming reports of their ubiquitous expression. Our results also show that the two genes display distinct expression levels and patterns from one another, as well as distinct patterns of expression among different tissues, supporting a potential multi-functional role for these genes in normal cellular regulation.

Materials and Methods

Tissue Procurement

Samples of normal human tissues consisting of postmortem tissue specimens, surgical biopsy samples, and surgically resected organs were obtained from the Cooperative Human Tissue Network, National Disease Research Interchange, and Indiana University School of Medicine, Department of Pathology. Samples were collected in accordance with the guidelines of Indiana University with approval from the Indiana University–Purdue University Indianapolis Institutional Review Board. Specimens were fixed in 10% neutral-buffered formalin, processed, and embedded in paraffin. Five-μm-thick serial sections were cut and mounted on Fisherbrand Superfrost/Plus slides (Fisher Scientific; Pittsburgh, PA). Tissues included adrenal gland (n=3), appendix (n=3), bladder (n=5), brain (n=7), breast (n=18), cervix (n=5), colon (n=6), eye (n=3), gallbladder (n=1), heart (n=5), kidney (n=18), liver (n=6), lung (n=10), lymph node (n=6), ovary (n=12), pancreas (n=20), parathyroid (n=1), placenta (n=2), prostate (n=20), skeletal muscle (n=9), skin (n=3), duodenum (n=4), jejunum (n=4), spleen (n=10), stomach (n=7), testis (n=5), thyroid (n=4), tongue (n=2), and uterus (n=8).

Oligonucleotide Probes

Specific 45-mer oligonucleotide probes for PRL-1 and -2 mRNA were designed using Oligo Primer Analysis Software (Molecular Biology Insights; Cascade, CO). Oligonucleotide sequences were verified using a BLAST search of EMBL and GenBank databases to ensure that there was no significant homology with other mRNA species. Probes were custom synthesized by Midland Certified Reagent Company Inc. (Midland, TX) and were labeled with fluorescein isothiocyanate (FITC) at both the 5′ and 3′ ends. PRL-1 (5′-GGC CAA CAG AAA AGA AGT GCA CTG AGG TTT ACC CCA TCC AGG TCA-3′) and PRL-2 (5′-TGG CAA ATA AAA AGT GTG AGC GTG CGT GTG AGT GTG ATG GGG AAA-3′) antisense probes are complementary to nucleotides 150–194 and 19–63 of the human PRL-1 (GenBank U48296) and PRL-2 (GenBank U48297) mRNA sequences, respectively. Corresponding control, sense oligonucleotides for PRL-1 and -2, were also generated. PRL probes were chosen from a region covering all known transcript variants.

Slot-blot Hybridization

Slot-blot hybridization was performed to verify specificity of the oligonucleotide probes. PRL-1 cDNA and PRL-2 cDNA, both cloned in pUC19 vectors (Cates et al. 1996), and PRL-3 cDNA, cloned in a pET-15b vector (a gift from Millenium Pharmaceuticals; Cambridge, MA), were linearized with BamHI. Linearized DNA samples of 100, 50, 10, and 5 ng each were denatured by the addition of 0.4 M NaOH and 10 mM EDTA and by heating for 10 min at 100C. Samples were then neutralized with an equal volume of cold 2 M ammonium acetate, pH 7.0. Two hundred μl of each denatured DNA solution was spotted on a nitrocellulose membrane (Protran; Schleicher and Schuell Bioscience, Keene, NH) using a Bio-Dot SF Microfiltration Apparatus (Bio-Rad; Hercules, CA) according to the manufacturer's instructions. Samples were immobilized on the membrane using a Stratalinker UV

The Journal of Histochemistry & Cytochemistry

Crosslinker 1800 (Stratagene; La Jolla, CA). Slot-blots were prehybridized for 30 min at 37C in prewarmed PerfectHyb Plus hybridization buffer (Sigma; St Louis, MO), followed by hybridization with FITC-labeled oligonucleotide antisense probes for PRL-1 and -2, diluted to 100 ng/ml in prewarmed PerfectHyb Plus buffer. Hybridization was allowed to proceed overnight at 37C. Posthybridization, membranes were washed two times for 5 min each in 2X SSC + 0.1% SDS at room temperature, followed by one 20-min wash in 0.5X SSC + 0.1% SDS at 37C, and a 5-min wash at room temperature in TBST (50 mM Tris–HCl, 150 mM NaCl, pH 7.6, plus 0.05% Tween-20). Prior to detection, membranes were blocked for 2 hr with 3% BSA in TBST and additionally for 30 min with Serum Free Protein Block (Dako; Carpinteria, CA). FITC-labeled probes were detected for 30 min using a mouse anti-FITC primary antibody (Dako) diluted 1:1000 in Dako Antibody Diluent, followed by Dako LSAB2 Peroxidase Link and Peroxidase Conjugated Streptavidin Label (10 min each). Reactions were visualized using the Dako DAB substrate chromogen system. Development was allowed to occur for 5 min, and the reactions were stopped by rinsing membranes in TBST followed by distilled water. Membranes were washed three times, 5 min each, in TBST, between each step of the procedure.

Non-radioactive ISH

Paraffin sections were dewaxed in xylene and rehydrated through a graded series of ethanol (100%, 95%, and 75%) to water. Sections were permeabilized with 200 μl of 10 μg/ml, nuclease-free Proteinase K (Sigma). Optimal length of time for Proteinase K digestion was determined empirically for each tissue type (data not shown). Deproteination reaction was stopped by washing slides two times, 3 min each, in Nanopure (Chesterland, OH) ultrapure water. Slides were subsequently dehydrated by sequential washes in 95% ethanol and 100% ethanol and allowed to air dry for 1 hr at room temperature. Tissue sections were hybridized with 750 ng/ml PRL-1, -2, or control probe in PerfectHyb Plus (Sigma) hybridization buffer, sealed with parafilm, and hybridized 12–14 hr at 37C in a humidity chamber. Coverslips were dislodged and nonspecifically bound probe was removed by soaking slides for 5 min each in two changes of 2X SSC plus 0.1% SDS at room temperature. Slides were then washed stringently in prewarmed 0.5X SSC + 0.1% SDS at 37C for 20 min, followed by a 10-min rinse in TBS (50 mM Tris–HCl, 150 mM NaCl, pH 7.6) + 0.1% SDS at room temperature.

Histochemical Detection

Detection of hybridized probe was performed by standard immunohistochemical techniques using a catalyzed signal-amplification procedure. All staining steps were performed on a Dako Autostainer at room temperature, and slides were rinsed for 5 min in TBST + 0.05% Tween-20 between each step of the procedure. Nonspecific background staining was blocked by incubation with Dako Serum-Free Protein Block for 30 min, followed by a 30-min incubation with mouse anti-FITC primary antibody (Dako), and diluted to 22 μg/ml in Dako Antibody Diluent. Bound primary antibody was detected using the labeled streptavidin–biotin method (LSAB2; Dako) combined with the Renaissance Tyramide Signal Amplification (TSA Biotin; PerkinElmer Life Sciences, Boston, MA) kit. Briefly, slides were incubated sequentially with Dako LSAB2 Peroxidase Link for 30 min, Dako LSAB2 Label for 10 min, biotinyl tyramide (TSA Biotin System) diluted 1:50 in 1× amplification diluent for 10 min, and Dako LSAB2 Label again for 10 min. Antibody complexes were visualized using 3,3′-DAB substrate (Chromogen System; Dako) as the chromogenic substrate. Development was allowed to proceed for 2 to 5 min and was stopped by rinsing the slides in distilled water. Following immunohistochemical detection, sections were counterstained briefly with 1X Lerner's hematoxylin, dehydrated through graded alcohols, cleared in xylene, and coverslipped with permanent mounting media (Fisher).

Controls

Several positive and negative controls were used to confirm the specificity of the ISH signal. All controls were performed on serial sections of the same tissues as hybridized with the labeled PRL-1 and -2 probe, following the ISH procedures described above. Positive controls included (a) verification of the hybridization and detection procedure by hybridization of the PRL-1 and -2 antisense probes to a normal pancreas tissue (case #032,098) known to be positive for PRL-1 and -2 mRNA and (b) hybridization of tissues with a fluorescein-conjugated Poly d(T) probe (Novocastra Laboratories; New Castle upon Tyne, UK) to assess the preservation and integrity of the mRNA in each sample. Negative controls consisted of (a) omission of the oligonucleotide probes from the hybridization mixture, (b) substitution of the specific antisense probe with an equivalent concentration of labeled sense probe, (c) hybridization using a cocktail of randomly generated, FITC-conjugated, oligonucleotide sequences (NCL-CONTROL; Novocastra) to assess binding of nonspecific sequences, and (d) RNase pretreatment of tissue sections to demonstrate specificity of the signal for single-stranded RNA. For RNase pretreatment, RNase solution was prepared by diluting RNase A (RNase A; Sigma) in TE buffer (20 mM Tris, pH 7.5, 1 mM EDTA) to a final concentration of 250 μg/ml. Control sections were incubated with 200 μl RNase solution or TE buffer only for 2 hr at 37C and were subsequently washed three times for 5 min each in ultrapure water, immediately prior to tissue dehydration and probe hybridization.

Analysis of ISH Results

Evaluation of all slides was performed under brightfield microscopy. All sections of a particular tissue type were stained and analyzed in a single run and are therefore directly comparable. Tissue distribution, localization pattern, intensity of staining, and percentage of positive cells were evaluated by two investigators (GES and CMD) in a blinded fashion. Localization pattern was evaluated as cytoplasmic, nuclear, or perinuclear. Staining intensity was classified according to the following scale: (−) absent, (+/−) barely detectable, (+) weak, (++) moderate, and (+++) strong. In cases of heterogeneous staining, the average intensity across the section was taken as the score. Also, in a few cases where a patient sample was stained twice, the case was given a mean score based on evaluation of the two sections. Percentage of positive cells was estimated as the number of stained cells per total

The Journal of Histochemistry & Cytochemistry

number of cells counted. To confirm reproducibility of the analysis, 25% of the slides were randomly chosen and scored twice. Duplicate slides gave similar results.

Results

Specificity of Oligonucleotide Probes

To verify that the PRL-1 and -2 oligonucleotide probes were specific for their complementary sequences, a BLAST search was performed against the EMBL and GenBank databases. Neither sequence displayed significant similarity to any other known mRNA species. For confirmation that the labeled PRL-1 and -2 probes were not cross-hybridizing with sequences from closely related family members, slot-blot hybridization was carried out on PRL-1, -2, and -3 cDNA targets. Both antisense probes displayed a high degree of specificity for their target mRNA sequences (Figure 1) with minimal cross-reactivity. In addition, variable ISH expression patterns of PRL-1 and -2 and reduced levels of both transcripts in tissues known to heavily express PRL-3 (heart) suggested specificity of the probes for their respective targets. Therefore, we concluded that the probes were of sufficient specificity to accurately detect their appropriate PRL-1 or -2 transcripts.

ISH Controls

Several controls were used to confirm specificity of the staining signal and viability of the tissue mRNA. No specific hybridization was detected when tissue sections were hybridized with a control sense probe specific to PRL-1 or -2, a randomly generated "nonsense" oligonucleotide sequence, or in the absence of probe. In addition, pretreatment of slides with RNase A abolished the hybridization signals, indicating that staining was specific to RNA. A positive signal using a poly d(T) probe was detected in all cases, demonstrating the presence of mRNA in each sample (control data not shown).

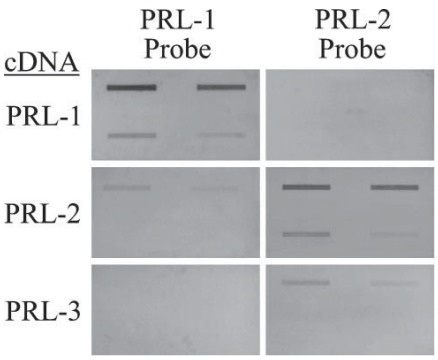

Figure 1 Specificity of the PRL-1 and -2 oligonucleotide probes. Denatured PRL-1, -2, and -3 cDNA were spotted onto a nitrocellulose membrane in various amounts and hybridized with PRL-1 or -2 FITC-labeled oligonucleotide probes. Clockwise from the upper left of each panel are 100, 50, 5, and 10 ng of spotted cDNA. Hybridized probe was detected using standard immunohistochemical techniques. Both probes displayed a high degree of specificity for their respective targets.

Expression Patterns of PRL-1 and -2 in Normal Human Tissues

Cellular localization and tissue distribution of PRL-1 and -2 mRNA were examined in zinc formalin-fixed, paraffin-embedded human tissues using non-isotopic ISH. ISH revealed widespread nuclear expression of both transcripts in histologically normal tissues. PRL-2 was generally expressed at higher levels than PRL-1. In addition, whereas PRL-2 was expressed at moderate to high levels in all tissues and most cell types examined, expression of PRL-1 was much more variable. Distribution and expression levels of PRL-1 and -2 in various tissues are described below and are further summarized in Table 1.

Skin

Intense and widespread expression of PRL-2 mRNA was observed throughout the epidermis (Figure 2B) and in the skin appendages. All epithelial cells in the coiled secretory portion of the eccrine sweat glands and within the hair follicles demonstrated heavy staining for this transcript (not pictured). Abundant expression was also observed in the fibroblasts of the dermis (Figure 2B) and in the endothelial cell layer of the tissue microvasculature. Expression of PRL-1, however, was more variable. One patient case expressed PRL-1 transcripts at similar levels to those observed for PRL-2, whereas in two of three cases, PRL-1 was expressed at a lower intensity. In these cases, PRL-1 transcripts were localized to all epithelial cells of the dermal appendages (not shown) but to a smaller percentage of cells within the epidermis and dermis (Figure 2A).

Gastrointestinal Tract

Moderate expression of PRL-1 and strong expression of PRL-2 were noted in the stratified squamous epithelium of the tongue, whereas neither transcript was detected in the taste buds of the circumvallate papillae. PRL-1 message was also absent from the sublingual salivary glands, but scattered staining at a moderate intensity was observed for PRL-2. In the stomach, PRL-1 expression varied from mild to heavy, depending on the region analyzed. Staining for PRL-1 was generally weak to absent in the mucous producing cells of the cardiac and body (Figure 2C) mucosa, but moderate to heavy in the pyloric mucosa (Figure 2D). PRL-1 expression in the parietal and chief cells varied from

The Journal of Histochemistry & Cytochemistry

Table 1 Average PRL-1 and -2 mRNA expression in normal human tissues[a]

Tissue	PRL-1	PRL-2	Tissue	PRL-1	PRL-2
Skin	++	+++	Heart	–	++
Tongue			Coronary arteries	–	++
Epithelia	++	+++	Cerebral cortex		
Taste buds	–	–	Neurons	–	+
Salivary glands	–	++	Neuroglia	–	+
Stomach	++	+++	Cerebellum		
Small intestine	+++	+++	Molecular layer	+/–	++
Large intestine	++	+++	Granular layer	++	+++
Appendix	++	+++	Purkinje cells	+/–	+
Pancreas			Thyroid		
Endocrine	++	+++	C cells	+	+
Exocrine	++	+++	Follicular cells	++	+++
Liver			Parathyroid		
Hepatocytes	+/–	++	Chief cells	++	+++
Ductal cells	+/–	+++	Oxyphil cells	+	++
Gallbladder	+++	+++	Adrenal gland		
Oviduct	+++	+++	Cortex	+	+
Ovary			Medulla	++	++
Epithelia	+++	+++	B-lymphocytes	++	++
Granulosa	++	+++	T-lymphocytes	+++	+++
Cervix	+++	+++	Spleen	+	++
Uterus			Connective tissue		
Endometrium	+++	+++	Adipocytes	+++	+++
Myometrium	+	++	Fibrocartilage	–	–
Placenta	++	+++	Hyaline cartilage	–	+++
Breast	++	+++	Stromal fibroblasts	++	+++
Prostate	++	+++	Eye		
Testis	+++	+++	Cornea	++	+++
Bladder	++	+++	Sclera	++	+++
Kidney			Choroid	++	+++
Glomeruli	+	+++	Retina[b]		
Proximal tubules	++	+++	GCL	+	+++
Distal tubules	+/–	+++	IPL	–	–
Collecting tubules	++	+++	INL	++	+++
Interstitium	+	+++	OPL	–	–
Lung	+++	+++	ONL	+	+++
Skeletal muscle	+/–	+++	Rods/cones	–	–

[a]Results represent the average staining intensity across multiple samples. Degree of staining: –, undetectable; +/–, faint or barely detectable; +, weak expression; ++, moderate expression; +++, strong expression.
[b]GCL, ganglion cell layer; IPL, inner plexiform layer; INL, inner nuclear layer; OPL, outer plexiform layer; ONL, outer nuclear layer.

patient to patient with expression limited to a small number of cells in some cases (5–10%) and more widespread expression in others (90–95%). Expression in these cell types tended to be both nuclear and cytoplasmic, with the most frequent expression occurring closer to the base of the gastric glands. PRL-2 was heavily expressed in all regions of the stomach. As with PRL-1, the strongest expression of PRL-2 occurred toward the base of the gastric glands (Figure 2E), and both cytoplasmic and nuclear staining were noted in the parietal and chief cells (Figure 2F).

Both PRL-1 and -2 transcripts were expressed at a high intensity in the small intestine (Figure 2G). Equivalent levels of expression were noted in the villous epithelium, crypt epithelium, and muscularis mucosae of the duodenum and jejunum and in the Brunner's glands of the duodenum. PRL-2 was also heavily expressed in the muscularis and the vasculature. PRL-1, however, was found at slightly lower levels in these structures. PRL-2 expression in the colon mirrored that of the small intestine with heavy expression noted throughout the organ. PRL-1 expression was moderate and, as in the stomach, the percentage of stained cells was case dependent, ranging from 30% in one case to 95–100% in others. Similar patterns of expression were seen in the appendix where PRL-1 was moderately expressed and PRL-2 was heavily expressed in the mucosal epithelium and submucosa.

Exocrine and endocrine portions of the pancreas both stained strongly for PRL-1 and -2 mRNA expression. PRL-1 staining was mixed, with ~20–25% of acinar and islet cells displaying heavy expression and 75–80% cells expressing more moderate levels in each case. Ductal epithelial cells, on the other hand, always displayed high levels of PRL-1 transcript. The pancreatic vasculature also stained strongly for PRL-2 and at a slightly lower intensity for PRL-1. Expression in the pancreas was noted to be both nuclear and cytoplasmic for both markers. In normal liver, a large degree of interindividual variation was again noted for PRL-1. Hepatocytes in four of six cases examined were negative for PRL-1 message (Figure 2H). In the remaining cases, 25–50% of the hepatocyte nuclei were strongly positive. In most cases, PRL-1 expression was low to undetectable in the bile duct epithelia and varied from weak to moderate in the vasculature. PRL-2 message was expressed strongly in ~50% of hepatocyte nuclei, whereas the hepatocyte cytoplasm revealed only weak or mild expression. Bile duct epithelia displayed moderate to strong hybridization for PRL-2, and blood vessels stained intensely (Figure 2I). Gallbladder mucosa and microvasculature were highly positive for both PRL-1 and -2 mRNA. Lymphocytes throughout gut-associated lymphoid tissue also hybridized strongly for both transcripts. A large degree of interindividual variability was seen in the staining intensity and number of positive lymphocytes for PRL-1.

Central Nervous System

Expression of PRL-1 and -2 in the brain was heaviest in the granular layer of the cerebellum followed by cell bodies within the molecular layer. Purkinje cells displayed faint cytoplasmic expression for PRL-1 and mild cytoplasmic expression of PRL-2 (Figures 2J and 2K). PRL-1 was absent from the neurons outside the cerebellum in most cases (Figure 2L), whereas PRL-2 expression in the neurons of the cerebral cortex varied from absent or weak to strong expression, depending on the sample and region analyzed (Figures 2M and 2N). Expression in glial cells and capillary endothelial

The Journal of Histochemistry & Cytochemistry

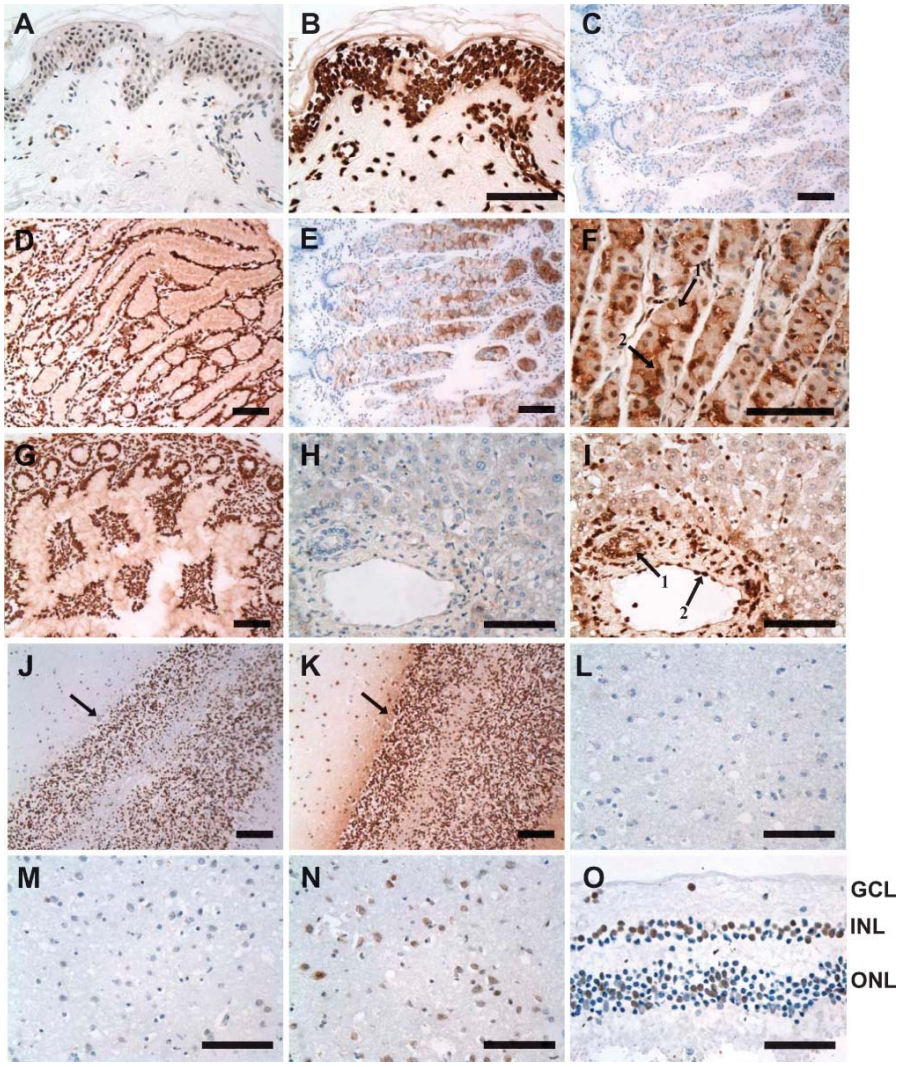

The Journal of Histochemistry & Cytochemistry

cells was also generally absent for PRL-1 and varied for PRL-2.

Sense Organs

In the eye, PRL-1 and -2 messages were localized to the outer nuclear, inner nuclear, and ganglion cell layers of the retina. Whereas PRL-2 was expressed heavily throughout the nuclei and cell bodies in each of these layers, PRL-1 expression was mild to moderate and found in only a limited number of cell bodies and nuclei, with predominantly nuclear expression (Figure 2O). Both transcripts were also present in the vascular endothelial cells, fibroblasts, and lymphocytes of the choroids, in the corneal epithelium and endothelium, and in the fibroblasts of the cornea and sclera. In the corneal epithelium, PRL-1 predominantly stained the more apical layers of cells. PRL-2 was expressed heavily in each of the named structures, whereas PRL-1 expression was generally mild to moderate and more diffuse. Only the endothelial cell layer of the cornea strongly expressed the PRL-1 transcript.

Female and Male Reproductive Tracts

In the ovary, PRL-1 expression was highest in the surface epithelium and oviduct. Hybridization was mild to heavy in the stroma, follicular cells, corpus luteum, and vasculature, each varying considerably on a case-by-case basis. PRL-2 expression was consistently heavy in all structures of the ovary but slightly less intense in the stromal cell nuclei and vascular endothelium than in the epithelial cells. PRL-1 and -2 showed parallel patterns of expression in the cervix. Both were expressed highly in the epithelial and stromal components of the ectocervix and endocervix as well as in the tissue vasculature. Placental chorionic villi also demonstrated abundant expression of both messages, with moderate staining observed for PRL-1 and heavy staining for PRL-2. Glandular epithelium of the uterus exhibited pronounced expression of PRL-1 and -2. Myometrial smooth muscle and endometrial stroma also displayed consistently moderate to high expression of PRL-2 mRNA, whereas variable levels of PRL-1 mRNA were observed. In 50% of the cases, no PRL-1 expression was observed in the myometrium, whereas in the other half of cases, PRL-1 myometrial expression was moderate to intense. Endothelial cells within the uterine vasculature strongly expressed both PRL-1 and -2.

Both transcripts were also abundant in the glandular epithelium and the vasculature of the breast. Whereas PRL-1 expression in the mammary duct varied slightly among individuals, mRNA was generally expressed at moderate to high levels. Within the stroma of the breast, tissues hybridized with PRL-1 displayed a more scattered and variable staining. Here expression varied from absent to heavy, depending on the individual. PRL-2 was always expressed heavily in both the mammary ducts and stromal fibroblasts. A similar trend was observed in the prostate, where PRL-1 expression in both the prostatic glands and stroma displayed a large degree of interindividual variation. Positive staining for PRL-1 was apparent in all cases studied, but the staining intensity varied from barely detectable to strongly positive. On average, staining of the glandular epithelium was moderate, whereas staining of stromal fibroblasts was mild and more diffuse (Figure 3A). PRL-2 expression was heavy in both the epithelium and fibroblasts of all cases examined (Figure 3B). In the testis, expression of each transcript was heavy in the seminiferous tubules with staining of the Sertoli cells, primary spermatogonia, and mature spermatocytes. Leydig cells in the interstitium also expressed both transcripts strongly. Stromal fibroblasts and the vasculature of the testes stained moderately for PRL-1 and heavily for PRL-2 mRNA expression.

Urinary System

In the urinary system, PRL-2 was again found to be consistently and heavily expressed, whereas PRL-1 expression varied in amount and intensity. In the urinary bladder, PRL-1 mRNA was expressed at weak to moderate levels in the urothelium, with the strongest expression occurring in the intermediate and basal cell layers (Figure 3C). Weak to moderate expression of PRL-1 was also noted in the stromal fibroblasts, smooth muscle nuclei, and vasculature of the bladder. Hybridization of PRL-1 in the kidney was extremely

Figure 2 Moderate and diffuse expression of PRL-1 mRNA (**A**) and strong expression of PRL-2 mRNA (**B**) in the stratified epithelia and elastocollagenous stroma of the skin. In the stomach, PRL-1 expression was mild in the body mucosa (**C**) but heavy in the pyloric mucosa (**D**). PRL-2 expression in the body of the stomach tended to be localized toward the base of the gastric glands (**E**) where both cytoplasmic and nuclear staining of the acid (arrow 1 in **F**) and enzyme (arrow 2 in **F**) producing cells was noted. PRL-1 expression in the jejunum was strong and mirrored the expression level of PRL-2 (**G**). PRL-1 transcripts were absent in the majority of liver tissues analyzed (**H**), whereas PRL-2 message was expressed strongly but not in all hepatocyte nuclei (**I**). High expression of PRL-2 was also noted in the bile duct epithelium (arrow 1 in **I**) and vascular endothelium (arrow 2 in **I**) of the liver. PRL-1 (**J**) and PRL-2 (**K**) were both highly expressed in the granular layer of the cerebellum. Purkinje cells displayed faint expression for PRL-1 and mild expression for PRL-2 (arrows). PRL-1 was generally not expressed in neurons or glial cells of the cerebral cortex (**L**). Two different sections taken from the same patient demonstrate that PRL-2 expression in the cerebral cortex was dependent on the location sectioned (**M,N**). Scattered PRL-1 expression was observed in the ganglion cell layer (GCL), inner nuclear layer (INL), and outer nuclear layer (ONL) of the retina (**O**). Bar = 100 μm.

The Journal of Histochemistry & Cytochemistry

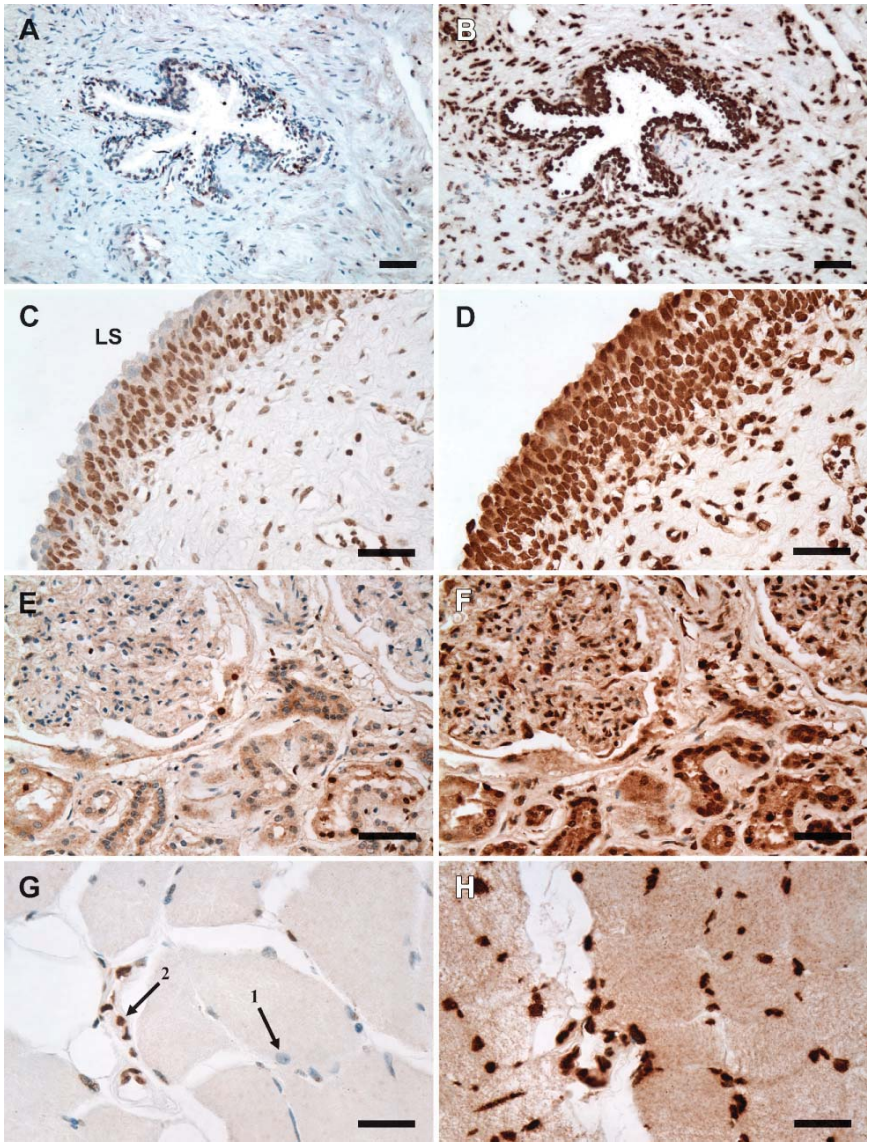

The Journal of Histochemistry & Cytochemistry

variable, with expression ranging from weak to strong in different patient samples. Some level of PRL-1 expression was detected in the proximal convoluted tubules, collecting tubules, glomeruli, interstitial cells, and vascular elements in all patient cases (Figure 3E). The percentage of PRL-1 positive cells, in each case, varied from as low as 30% to as high as 95%. In all but two cases, PRL-1 was also expressed in the distal convoluted tubules. Generally, expression was highest in the proximal tubules and collecting tubules followed by the interstitium, glomeruli, and distal tubules. In contrast to PRL-1, PRL-2 was expressed at high levels in all components of the urinary bladder (Figure 3D) and kidney (Figure 3F).

Respiratory System

Heavy nuclear staining of PRL-1 and -2 was observed in the alveolar and bronchiolar epithelia with PRL-1 expression in pneumocytes being slightly less intense than its expression in the bronchiolar epithelium. Endothelial cells within the lung vasculature also displayed heavy expression of both transcripts.

Skeletal Muscle and Heart

Skeletal muscle nuclei stained weakly, if at all, for PRL-1 message, whereas cells of the endomysium, perimysium, and vasculature stained heavily for the transcript (Figure 3G). PRL-2 expression, on the other hand, was high in the skeletal muscle nuclei and muscle fibers, in addition to the surrounding support tissue and vasculature (Figure 3H). The epicardium, myocardium, and endocardium of normal heart were all generally negative for PRL-1 gene expression. Likewise, in the coronary arteries, faint PRL-1 expression was found in only one of five cases. PRL-2 expression in the heart was stronger than PRL-1 but much less intense than the PRL-2 expression levels observed in other organs. Cardiac cell nuclei stained moderately for PRL-2, whereas epicardial and endocardial components stained only lightly. All layers of the coronary arteries moderately expressed PRL-2.

Endocrine Tissues

Follicular epithelial cells in the thyroid expressed moderate levels of PRL-1 and high levels of PRL-2 transcripts. C-cells expressed both transcripts mildly. The oxyphilic and chief cells of the parathyroid were both positive for PRL-1 and -2 expression, with slightly higher expression occurring in the chief cells and with stronger expression of PRL-2 than of PRL-1. It was noted that staining for both transcripts in the oxyphilic cells was nuclear, whereas expression in chief cells was mostly cytoplasmic. Adipocytes within the gland stained intensely for both transcripts. Mild to moderate expression of both PRL-1 and -2 were noted in the adrenal cortex and medulla.

Lymphoid Tissues

Both B- and T-cell areas of the lymph node strongly expressed PRL-1 and -2 transcripts, with moderate staining of B cells and heavy expression in T cells. In the spleen, PRL-1 expression was less intense and more variable. Three of ten samples tested were negative for PRL-1, whereas the remaining seven samples expressed mRNA mildly and diffusely in the splenic cords, venous sinuses, and lymphoid follicles. The fibrocollagenous capsule and microvasculature of the organ expressed PRL-1 message at more moderate levels. PRL-2 was expressed in all samples and generally displayed a moderate staining intensity in the red and white pulp areas of the spleen and strong intensity within the capsule.

Connective Tissues

In general, adipocytes stained heavily for both PRL-1 and -2 transcripts. Tendon fibrocartilage, on the other hand, was negative for each. Hyaline cartilage was commonly negative for PRL-1, whereas chondroblast and chondrocyte nuclei and the territorial matrix of the lacuna were strongly positive for PRL-2. Fibroblasts in all tissues stained heavily for PRL-2, whereas PRL-1 expression in fibroblasts varied widely among tissue types and between individual samples within a tissue type.

Discussion

A detailed knowledge of the cellular distribution of PRL-1 and -2 gene expression in different human tissues and cell types is essential to understanding both the role of these proteins in normal tissues and their potential involvement in the pathogenesis of disease. The present study is the first report describing the cell-specific pattern of expression for either PRL-1 or -2 in a variety of human tissues. Previous studies have shown preferential expression of PRL-3 in the heart and skeletal muscle of normal tissues (Zeng et al. 1998; Matter et al. 2001); thus, PRL-3 transcripts were not examined here.

Results obtained show widespread distribution of PRL-1 and -2 in tissues from the major organ systems.

Figure 3 Moderate expression of PRL-1 mRNA and strong expression of PRL-2 mRNA in the glandular epithelia of the prostate (**A,B**), urothelia of the bladder (**C,D**), and glomeruli and tubules of the kidney (**E,F**). In the urinary bladder (**C**), a lack of staining for PRL-1 was noted in most luminal surface (**LS**) cells. Skeletal muscle cell fibers and nuclei were generally negative for PRL-1 (arrow 1 in **G**), although the surrounding support tissue was strongly positive for the transcript (arrow 2 in **G**). Skeletal muscle cell fibers and nuclei, as well as the surrounding support tissue, displayed strong expression of PRL-2 (**H**). Bar = 50 μm.

The Journal of Histochemistry & Cytochemistry

PRL-1 expression was more variable and generally less intense than the level of PRL-2 expression in the same tissue or cell types. Only in the pyloric region of the stomach, small intestine, gallbladder, oviduct, testis, lung, and adipose tissue were levels of PRL-1 expression equivalent to PRL-2 in both intensity and total number of positive cells. PRL-1 expression was most abundant in the duodenum, jejunum, gallbladder, testis, lung, adipose, skin appendages, lymph node, oviduct, cervix, surface epithelium of the ovary, and endometrial glands of the uterus. Moderate expression of PRL-1 was seen in several other tissues and cell types including the skin and tongue epithelium, colon, appendix, pancreas, breast, placenta, prostate, bladder, and the eye. Lowest levels of PRL-1 expression were found in the liver and skeletal muscle, and no PRL-1 message could be detected in the taste buds, salivary glands, heart, coronary arteries, cerebral cortex, or cartilage.

In the urinary bladder, PRL-1 appeared to be localized to the more immature, intermediate, and basal cell layers of the uroepithelium and not to the more differentiated and highly specialized superficial cell layer. It would be interesting to examine the colocalization of PRL-1 with the cytokeratins (CKs) and/or uroplakins, which can serve as markers of urothelial cell proliferation and differentiation. For example, CK20 is restricted mainly to the superficial layer of the urothelium, whereas CK13 is present only in the basal and intermediate layers (Mallofre et al. 2003; Varley et al. 2004). Such studies could help to elucidate a specific role for PRL-1 in this tissue type.

A large degree of interindividual variation was noted for PRL-1 in some tissues, most notably skin, stomach, liver, pancreas, breast, prostate, bladder, and kidney. Such differences could be attributed to allelic variants, environmental factors, lifestyle factors, and/or homeostatic control mechanisms. Differential expression in the breast, for example, could be a factor of the donor's reproductive history because Guo et al. (2004) found that PRL-1 is significantly overexpressed in parous breast tissue, which has been stimulated to differentiate during pregnancy.

In contrast to PRL-1, PRL-2 mRNA was found in almost every cell type examined, and the majority of tissues exhibited intense expression of the transcript. More moderate levels of PRL-2 were observed in the salivary glands, heart, coronary arteries, adrenal gland, spleen, and uterine smooth muscle. Purkinje cells of the cerebellum and C-cells of the thyroid demonstrated weak expression of the PRL-2 transcript. Only the taste buds of the tongue, fibrocartilage of the tendon, and photoreceptors and cell processes of cells within the retina were negative for PRL-2 expression. In the liver, PRL-2 was heavily expressed in the hepatocytes, but only 40–50% of hepatocyte nuclei were positive for expression. In comparison, 95–100% of cells were generally positive for expression in other tissues. In the cerebral cortex, PRL-2 expression in neurons and glial cells varied from specimen to specimen and between different sections within the same specimen. When expressed, PRL-2 levels in the cortex varied from weak to moderate. A more extensive analysis of PRL-2 expression in various areas of the brain and cerebral cortex may reveal region-specific localization patterns.

These results are generally consistent with previous reports on PRL-1 or -2 mRNA expression in human tissues. In a panel of cDNA libraries from adult hematopoietic tissues, Gjorloff-Wingren et al. (2000) noted ubiquitous expression of both transcripts with PRL-1 always expressed at equivalent or lower levels than PRL-2. Using multiple tissue Northern blots, Montagna et al. (1995) and Zhao et al. (1996) also reported widespread PRL-2 expression with moderate to high levels of PRL-2 transcripts in all tissue types examined. Additionally, Zhao et al. reported comparatively low levels of three PRL-2 variants in the liver. Our data both confirm and expand on this finding by suggesting that the lower levels of PRL-2 observed in the liver are not due to reduced PRL-2 expression across all cells, but rather to a smaller percentage of cells actually expressing the gene.

Comparison of our results with patterns of PRL-1 and -2 expression in other species reveals further similarities. The current study showed PRL-1 transcripts to be barely detectable in normal adult human liver or skeletal muscle and completely undetectable in the heart. In agreement with these findings, several researchers have reported a virtual absence of PRL-1 gene transcription in the liver of normal adult rats (Diamond et al. 1994,1996; Peng et al. 1999). In addition, Northern analysis, ISH, and immunohistochemistry have all consistently shown an absence of both PRL-1 mRNA and protein in murine heart tissue (Diamond et al. 1994; Rundle and Kappen 1999; Kong et al. 2000). Studies using ISH have also indicated an absence of PRL-1 in mouse skeletal muscle (Rundle and Kappen 1999). Northern analysis, on the other hand, has shown heavy expression of PRL-1 in rat skeletal muscle tissue (Diamond et al. 1994). Our analysis in human skeletal muscle tissues agrees with both findings, revealing a strong reactivity of the connective tissue and vasculature directly surrounding the muscle cells, whereas the muscle fibers and nuclei themselves were generally negative. PRL-2 was heavily expressed in human skeletal muscle, but weakly expressed in the brain cerebral cortex. In accordance with these results, Zeng et al. (1998) found heavy expression of PRL-2 in mouse skeletal muscle and comparatively low expression in the mouse brain.

In several cases, patterns of PRL-1 mRNA expression also appear to correlate well with reports of PRL-1 protein expression. For example, we found that PRL-1 mRNA expression in the regions of the stomach closest

The Journal of Histochemistry & Cytochemistry

to the esophagus was weak, whereas expression in regions more distal to the esophagus was high. Further, our analysis showed decreased levels of PRL-1 mRNA in the colon as compared with the duodenum and jejunum. Kong et al. (2000) noted a lack of PRL-1 protein expression in the esophagus of the adult rat and found a gradient of PRL-1 protein expression within the small intestine, with highest levels of expression observed in the proximal intestine (duodenum and jejunum) and lower levels evident in the more distal ileum. Together these results suggest that PRL-1 may be differentially expressed along the longitudinal axis of the digestive tract, increasing from esophagus and cardiac stomach to pyloric stomach and proximal small intestine, then decreasing again in the distal intestine and the colon. Such spatial differences in PRL-1 expression suggest a specialized role for the enzyme within the digestive tract.

Variable expression of PRL-1 protein has also been observed along the crypt–villus axis of the intestine. Diamond et al. (1996) and Kong et al. (2000) each reported significantly greater expression of PRL-1 protein in villus enterocytes than in crypt enterocytes. In the current study, however, we observed heavy expression of PRL-1 mRNA throughout both villus and crypt enterocytes. Although some of these observations could be explained by species-specific patterns of expression, such differences between mRNA and protein levels also raise the possibility that PRL-1 expression may be regulated posttranscriptionally.

In conclusion, the present results help to define the basal gene expression of the PRL-1 and -2 phosphatases in adult human tissues and provide a foundation for the recognition and interpretation of the changes in these patterns that may be associated with cancer or other disease states. Widespread tissue distribution of PRL-1 and -2 mRNA suggests a fundamental biological function for these enzymes. Whereas PRL-2 was highly expressed in the majority of tissues examined, PRL-1 expression was highly variable. PRL-1, therefore, appears to be regulated spatially in a cell type- and tissue-specific manner in the adult. Both transcripts showed widespread expression in both proliferating and quiescent normal cells, indicating that each tissue or cell type may display a unique physiological response to these genes. Further studies aimed at elucidating the specific substrates and other interacting molecules for the PRL enzymes will help clarify the specific cellular functions of PRL-1 and -2 and provide insight into their varied expression patterns in human tissues.

Acknowledgments

This work was supported in part by Public Health Service, NIH Grant CA-72450 (to PLC and SKR) and by an Indiana University Cancer Center–Cathy Peachey Foundation grant (to PLC).

Literature Cited

Bardelli A, Saha S, Sager JA, Romans KE, Xin B, Markowitz SD, Lengauer C, et al. (2003) PRL-3 expression in metastatic cancers. Clin Cancer Res 9:5607–5615

Carter DA (1998) Expression of a novel rat protein tyrosine phosphatase gene. Biochim Biophys Acta 1442:405–408

Cates CA, Michael RL, Stayrook KR, Harvey KA, Burke YD, Randall SK, Crowell PL, et al. (1996) Prenylation of oncogenic human PTP (CAAX) protein tyrosine phosphatases. Cancer Lett 110: 49–55

Columbano A, Ledda-Columbano GM, Pibiri M, Piga R, Shinozuka H, De Luca V, Cerignoli F, et al. (1997) Increased expression of c-fos, c-jun and LRF-1 is not required for in vivo priming of hepatocytes by the mitogen TCPOBOP. Oncogene 14:857–863

Diamond RH, Cressman DE, Laz TM, Abrams CS, Taub R (1994) PRL-1, a unique nuclear protein tyrosine phosphatase, affects cell growth. Mol Cell Biol 14:3752–3762

Diamond RH, Peters C, Jung SP, Greenbaum LE, Haber BA, Silberg DG, Traber PG, et al. (1996) Expression of PRL-1 nuclear PTPase is associated with proliferation in liver but with differentiation in intestine. Am J Physiol 271:G121–129

Gjorloff-Wingren A, Saxena M, Han S, Wang X, Alonso A, Renedo M, Oh P, et al. (2000) Subcellular localization of intracellular protein tyrosine phosphatases in T cells. Eur J Immunol 30:2412–2421

Guo K, Li J, Tang JP, Koh V, Gan BQ, Zeng Q (2004) Catalytic domain of PRL-3 plays an essential role in tumor metastasis: formation of PRL-3 tumors inside the blood vessels. Cancer Biol Ther 3:945–951

Guo S, Russo IH, Russo J (2003) Difference in gene expression profile in breast epithelial cells from women with different reproductive history. Int J Oncol 23:933–941

Kong W, Swain GP, Li S, Diamond RH (2000) PRL-1 PTPase expression is developmentally regulated with tissue-specific patterns in epithelial tissues. Am J Physiol Gastrointest Liver Physiol 279:G613–621

Kozlov G, Cheng J, Ziomek E, Banville D, Gehring K, Ekiel I (2004) Structural insights into molecular function of the metastasis-associated phosphatase PRL-3. J Biol Chem 279:11882–11889

Mallofre C, Castillo M, Morente V, Sole M (2003) Immunohistochemical expression of CK20, p53, and Ki-67 as objective markers of urothelial dysplasia. Mod Pathol 16:187–191

Matter WF, Estridge T, Zhang C, Belagaje R, Stancato L, Dixon J, Johnson B, et al. (2001) Role of PRL-3, a human muscle-specific tyrosine phosphatase, in angiotensin-II signaling. Biochem Biophys Res Commun 283:1061–1068

Mohn KL, Laz TM, Hsu JC, Melby AE, Bravo R, Taub R (1991) The immediate-early growth response in regenerating liver and insulin-stimulated H-35 cells: comparison with serum-stimulated 3T3 cells and identification of 41 novel immediate-early genes. Mol Cell Biol 11:381–390

Montagna M, Serova O, Sylla BS, Feunteun J, Lenoir GM (1995) A 100-kb physical and transcriptional map around the EDH17B2 gene: identification of three novel genes and a pseudogene of a human homologue of the rat PRL-1 tyrosine phosphatase. Hum Genet 96:532–538

Peng Y, Du K, Ramirez S, Diamond RH, Taub R (1999) Mitogenic up-regulation of the PRL-1 protein-tyrosine phosphatase gene by Egr-1. Egr-1 activation is an early event in liver regeneration. J Biol Chem 274:4513–4520

Rundle CH, Kappen C (1999) Developmental expression of the murine Prl-1 protein tyrosine phosphatase gene. J Exp Zool 283:612–617

Scarlato M, Beesley J, Pleasure D (2000) Analysis of oligodendroglial differentiation using cDNA arrays. J Neurosci Res 59:430–435

Si X, Zeng Q, Ng CH, Hong W, Pallen CJ (2001) Interaction of farnesylated PRL-2, a protein-tyrosine phosphatase, with the beta-subunit of geranylgeranyltransferase II. J Biol Chem 276: 32875–32882

Sun JP, Wang WQ, Yang H, Liu S, Liang F, Fedorov AA, Almo SC, et al. (2005) Structure and biochemical properties of PRL-1, a

phosphatase implicated in cell growth, differentiation, and tumor invasion. Biochemistry 44:12009–12021

Takano S, Fukuyama H, Fukumoto M, Kimura J, Xue JH, Ohashi H, Fujita J (1996) PRL-1, a protein tyrosine phosphatase, is expressed in neurons and oligodendrocytes in the brain and induced in the cerebral cortex following transient forebrain ischemia. Brain Res Mol Brain Res 40:105–115

Varley CL, Stahlschmidt J, Smith B, Stower M, Southgate J (2004) Activation of peroxisome proliferator-activated receptor-gamma reverses squamous metaplasia and induces transitional differentiation in normal human urothelial cells. Am J Pathol 164: 1789–1798

Wang J, Kirby CE, Herbst R (2002a) The tyrosine phosphatase PRL-1 localizes to the endoplasmic reticulum and the mitotic spindle and is required for normal mitosis. J Biol Chem 277:46659–46668

Wang Q, Holmes DI, Powell SM, Lu QL, Waxman J (2002b) Analysis of stromal-epithelial interactions in prostate cancer identifies PTPCAAX2 as a potential oncogene. Cancer Lett 175:63–69

Werner SR, Lee PA, DeCamp MW, Crowell DN, Randall SK, Crowell PL (2003) Enhanced cell cycle progression and down regulation of p21(Cip1/Waf1) by PRL tyrosine phosphatases. Cancer Lett 202: 201–211

Wu X, Zeng H, Zhang X, Zhao Y, Sha H, Ge X, Zhang M, et al. (2004) Phosphatase of regenerating liver-3 promotes motility and metastasis of mouse melanoma cells. Am J Pathol 164: 2039–2054

Zeng Q, Dong JM, Guo K, Li J, Tan HX, Koh V, Pallen CJ, et al. (2003) PRL-3 and PRL-1 promote cell migration, invasion, and metastasis. Cancer Res 63:2716–2722

Zeng Q, Hong W, Tan YH (1998) Mouse PRL-2 and PRL-3, two potentially prenylated protein tyrosine phosphatases homologous to PRL-1. Biochem Biophys Res Commun 244:421–427

Zeng Q, Si X, Horstmann H, Xu Y, Hong W, Pallen CJ (2000) Prenylation-dependent association of protein-tyrosine phosphatases PRL-1, -2, and -3 with the plasma membrane and the early endosome. J Biol Chem 275:21444–21452

Zhao Z, Lee CC, Monckton DG, Yazdani A, Coolbaugh MI, Li X, Bailey J, et al. (1996) Characterization and genomic mapping of genes and pseudogenes of a new human protein tyrosine phosphatase. Genomics 35:172–181

The Journal of Histochemistry & Cytochemistry

Am J Transl Res 2012;4(1):83-101
www.ajtr.org /ISSN:1943-8141/AJTR1112002

Original Article

Tissue-specific alterations of PRL-1 and PRL-2 expression in cancer

Carmen M Dumaual[1], George E Sandusky[2], Han Weng Soo[3], Sean R Werner[4], Pamela L Crowell[5], Stephen K Randall[1]

[1]Department of Biology, Indiana University-Purdue University Indianapolis, 723 West Michigan St., Room SL306, Indianapolis, Indiana, 46202, USA; [2]Department of Pathology and Laboratory Medicine, Indiana University School of Medicine, Van Nuys Medical Science Building, 635 Barnhill Drive, Room A128, Indianapolis, IN, 46202, USA; [3]Ministry of Defence, Singapore, MINDEF building, 303 Gombak Drive #B1-36, Singapore 669645, Singapore; [4]Cook Medical Inc., 750 North Daniels Way, Bloomington, IN, 47404, USA; [5]Department of Pharmaceutical Sciences, College of Pharmacy and Health Sciences, Butler University, 4600 Sunset Ave., Indianapolis, IN, 46208, USA

Received December 6, 2011; accepted December 30, 2011; Epub January 5, 2012; Published January 15, 2011

Abstract: The PRL-1 and PRL-2 phosphatases have been implicated as oncogenic, however the involvement of these molecules in human neoplasms is not well understood. To increase understanding of the role PRL-1 and PRL-2 play in the neoplastic process, *in situ* hybridization was used to examine PRL-1 and PRL-2 mRNA expression in 285 normal, benign, and malignant human tissues of diverse origin. Immunohistochemical analysis was performed on a subset of these. PRL-1 and PRL-2 mRNA expression was also assessed in a small set of samples from a variety of diseases other than cancer. Where possible, associations with clinicopathological characteristics were evaluated. Alterations in PRL-1 or -2 expression were a frequent event, but the nature of those alterations was highly tumor type specific. PRL-1 was significantly overexpressed in 100% of hepatocellular and gastric carcinomas, but significantly underexpressed in 100% of ovarian, 80% of breast, and 75% of lung tumors. PRL-2 expression was significantly increased in 100% of hepatocellular carcinomas, yet significantly downregulated in 54% of kidney carcinomas. PRL-1 expression was correlated to patient gender in the bladder and to patient age in the brain and skeletal muscle. PRL-1 expression was also associated with tumor grade in the prostate, ovary, and uterus. These results suggest a pleiotropic role for PRL-1 and PRL-2 in the neoplastic process. These molecules may associate with tumor progression and serve as clinical markers of tumor aggressiveness in some tissues, but be involved in inhibition of tumor formation or growth in others.

Keywords: Phosphatase of regenerating liver, PRL-1, PRL-2, in situ hybridization, cancer

Introduction

The PRL family of phosphatases has gained much attention in recent years as potential targets for therapeutic intervention in a variety of tumor types. The family consists of three closely related members (PRL-1, PRL-2, and PRL-3), which constitute a novel class of protein tyrosine phosphatase (PTP). The PRLs are among the smallest of the PTPs, having molecular masses of 20-22kDa and consisting primarily of a catalytic domain. In addition, the PRL enzymes are the only PTPs known to be post-translationally isoprenylated. This post-translational modification is critical to their subcellular localization and biological activity [1-3].

Accumulating evidence points to a role for the PRL family in tumor formation, invasion, and metastasis. Functional studies have shown that overexpression of PRL-1, -2, or -3 in non-tumorigenic rodent cells leads to rapid cellular growth and a transformed phenotype in culture and to tumor formation in athymic, nude mice [1, 4-7]. Moreover, PRL-3 overexpression enhances the growth of human embryonic kidney fibroblasts in culture [5] and can transform a low metastatic potential melanoma cell line into a highly metastatic line both *in vitro* and *in vivo* [6]. Stable expression of PRL-1 or PRL-3 leads to enhanced cell motility and invasive ability, whereas downregulation of either of these molecules causes a significant reduction in migratory

ability *in vitro* and suppression of metastatic tumor formation *in vivo* [7-14]. The most well studied PRL family member, in relation to human cancer, is PRL-3. Widespread interest in this gene was generated after Saha et al. [15] identified 144 gene transcripts with increased expression in liver metastases compared to their primary colorectal tumors and demonstrated that PRL-3 was the only gene consistently overexpressed in all 18 of the metastatic cases examined. A gradient in PRL-3 expression was also noted, with low levels of PRL-3 message in normal colorectal epithelium, intermediate levels in the primary tumors, and high expression in each of the liver metastases. Bardelli et al. [16] later showed that PRL-3 mRNA overexpression was not limited to liver metastases, but that PRL-3 was expressed more highly in all colorectal carcinoma metastases examined, regardless of the site of metastasis. PRL-3 overexpression has since been linked to such clinical parameters as disease progression, tumor aggressiveness, lymphatic invasion, venous invasion, presence and extent of metastasis, or poor patient prognosis in colon/colorectal [17-20], cervical [21], ovarian [22, 23], breast [24-26], gastric [27-35], non-small cell lung [36], esophageal [37], nasopharyngeal [12], brain [38], hepatocellular [39] and bile duct [40] cancers. These data suggest PRL-3 as a potential prognostic indicator of disease aggressiveness and clinical outcome for multiple tumor types.

In contrast to PRL-3, little data is currently available on the expression of PRL-1 or PRL-2 in human malignancies, yet it is clear from cell line and murine studies that these genes also play important roles in tumor formation, invasion, and metastasis [1, 7, 41-43]. In the current study, we provide further insight into the role that both PRL-1 and PRL-2 play in the development and progression of human disease by performing a retrospective analysis on 342 human tissue specimens from 243 individual subjects. The expression of PRL-1 and PRL-2 mRNA was assessed in a variety of normal and tumor tissues of diverse tissue origin using *in situ* hybridization. Where possible, correlations between PRL-1 or -2 mRNA expression and several clinicopathological features, including patient age and gender, tumor type and grade, and presence or absence of local or distant metastases were investigated. A comparison between mRNA and protein expression levels was also made in a subset of these tissues. In addition, because PRL-3 overexpression in mouse models has previously been linked to cardiovascular disease [5] and PTPs in general have been implicated in the progression of several cardiovascular, neurological, metabolic, and autoimmune diseases [44-47], we also examined the relationship between PRL-1 and PRL-2 expression and a variety of disease states other than cancer.

Materials and methods

Tissue procurement

Formalin-fixed, paraffin-embedded tissue samples were obtained from archival paraffin blocks. Tissues were acquired from the Cooperative Human Tissue Network (CHTN), National Disease Research Interchange (NDRI), or Indiana University School of Medicine, Department of Pathology, collected in accordance with the guidelines of Indiana University and with approval from the IUPUI Institutional Review Board. Tissue sections of each specimen were stained with Hematoxylin and Eosin (H&E) and were examined by a pathologist, with no prior knowledge of the available patient data, to confirm histopathologic diagnosis and tumor grading. For all cases, representative tissue sections were chosen for *in situ* hybridization (ISH) and/or immunohistochemical (IHC) analysis.

In situ hybridization

Non-isotopic ISH was performed using FITC-labeled oligonucleotide probes specific for PRL-1 or PRL-2 mRNA, as previously described [48]. Briefly, 5μm thick tissue sections were deparaffinized, rehydrated through graded alcohols to distilled water and permeabilized with 200μl of 10μg/mL proteinase K for 5-20 minutes depending on tissue type. The deproteination reaction was stopped by washing slides two times, three minutes each in Nanopure ultrapure water, followed by sequential washes in 95% and 100% ethanol for three minutes each. Slides were allowed to air dry for one hour at room temperature (RT), prior to hybridization. Tissue sections were then incubated in a humidified chamber overnight (12-14 hours) at 37°C with 50μL of PRL-1, PRL-2, or control probe diluted to a final concentration of 750 ng/mL in PerfectHyb™ Plus hybridization buffer (Sigma-Aldrich, St. Louis, MO, USA). Following hybridization, non

-specifically bound probe was removed by washing slides two times in 2X SSC (300mM NaCl, 30mM Sodium Citrate, pH 7.0) plus 0.1% SDS for five minutes RT, one time in pre-warmed 0.5X SSC (75mM NaCl, 7.5mM Sodium Citrate, pH 7.0) + 0.1% SDS at 37ºC for 20 minutes, and one time in tris-buffered saline (TBS; 50mM Tris-HCL, 150mM NaCl, pH 7.6) + 0.1% SDS at RT for 10 minutes. Detection of hybridized probe was performed by standard immunohistochemical techniques using a catalyzed signal amplification procedure. Non-specific background staining was blocked by incubation with DAKO Serum-Free Protein Block (DAKO Corporation, Carpenteria, CA, USA) for 30 minutes, followed by 30 minutes incubation with a mouse anti-FITC primary antibody (DAKO), diluted to 22µg/mL in DAKO Antibody Diluent. Bound primary antibody was detected using the labeled streptavidin-biotin method (LSAB2, DAKO) combined with the Renaissance® Tyramide Signal Amplification kit (TSA™ Biotin, PerkinElmer Life Sciences, Inc., Boston, MA, USA). Peroxidase bound, antibody complexes were visualized using DAB (DAB Substrate/Chromogen System, DAKO) as the chromogenic substrate. Development was allowed to proceed for 2-5 minutes and was stopped by rinsing the slides in distilled water for five minutes. Sections were counterstained briefly with 1X Lerner's hematoxylin, dehydrated through graded alcohols, cleared in xylene, and coverslipped with permanent mounting media (ThermoFisher Scientific, Inc., Waltham, MA, USA). All staining steps were performed on a DAKO Autostainer at room temperature and slides were rinsed for five minutes in TBS + 0.05% Tween-20 between each step of the procedure. Normal adjacent and tumor tissue sections from one organ type were always processed simultaneously.

Immunohistochemistry

Rabbit antibodies against peptides corresponding to amino acids 50-65 of human PRL-1 and 47-62 of human PRL-2 were generated by Genemed Synthesis, Inc (San Antonio, TX, USA). The antibodies were affinity purified against E. coli expressed PRL proteins. Slides containing 5µm tissue sections were deparaffinized for 9 minutes in xylene then rehydrated through a series of 100%, 80%, and 70% ethanol for 5 minutes each, followed by a 5 minute rinse in PBS. Antigen retrieval was performed by heating in a microwave for 5 minutes in 5mM Sodium Citrate. Following retrieval, slides were allowed to cool at room temperature for 15 minutes. Endogenous peroxidase activity was quenched by incubation in 3% H_2O_2 for 5 minutes. Sections were blocked for 15 minutes in 3% non-fat dry milk, 1% BSA, then incubated 90 minutes at 37°C with primary antibody diluted 1:200 in blocking solution. This was followed by a 30 minute incubation with biotinylated secondary, anti-rabbit antibody (Biogenex Laboratories, Inc., Fremont, CA, USA) diluted 1:20 in blocking buffer and a 30 minute incubation with streptavidin peroxidase (Biogenex). A 5 minute phosphate buffered saline (PBS) rinse was incorporated after each step in the immunostaining procedure. Colorimetric detection was carried out using AEC and allowed to proceed until color was detected in the tissues by microscopic examination at which point the reaction was quenched by rinsing the slides in distilled water. Sections were counterstained in Hematoxylin for 30 seconds and again rinsed with water.

Controls

Several positive and negative controls were used, concurrently, to confirm the specificity of the ISH or IHC signal. All controls were performed on serial sections of the same tissues as examined with the PRL-1 and PRL-2 probes or antibodies, utilizing the ISH and IHC procedures described above. For the ISH experiments, positive controls included: (a) verification of the hybridization and detection procedure by hybridization of the PRL-1 and PRL-2 antisense probes to a normal pancreas tissue (case # 032098), known to be positive for PRL-1 and PRL-2 mRNA and (b) hybridization of tissues with a fluorescein-conjugated Poly d(T) probe (Novocastra Laboratories, New Castle upon Tyne, UK) to assess the preservation and integrity of the mRNA in each sample. Negative controls consisted of: (a) omission of the oligonucleotide probes from the hybridization mixture and incubation of the tissue specimens with only PerfectHyb™ hybridization buffer, (b) substitution of the specific antisense probe with an equivalent concentration of labeled sense probe to examine the stringency of the assay, (c) hybridization using a cocktail of randomly generated, FITC-conjugated, oligonucleotide sequences (NCL-CONTROL, Novocastra), to assess binding of nonspecific sequences, and (d) Pretreatment of tissue sections with 250µg/mL RNase A (Sigma-Aldrich) for 2 hours at 37ºC to

demonstrate the specificity of the signal for single stranded RNA. Probe specificity was also verified by slot-blotting and shown previously [48]. As negative controls for IHC, tissue sections were incubated either in the presence of no primary antibody, no secondary antibody, or primary antibody blocked with the peptide used to generate the anti-PRL-1 or anti-PRL-2.

Staining interpretation

Evaluation of all slides was performed under bright-field microscopy. The intensity of staining and the percentage of positive normal and tumor cells for the ISH studies were evaluated with the aid of a single, experienced pathologist, in a blinded fashion. For the IHC experiments, scoring of images was performed independently by three separate individuals and the mean reading was taken for each tissue section. The appearance of a brownish-red stain over the cells was used to indicate probe hybridization or antibody binding and thus reflect the cellular levels of PRL-1 and PRL-2 mRNA or protein. Immunostaining was scored using established methods [49, 50]. Briefly, staining intensity was classified according to the following scale: (-) absent, (+/-) barely detectable, (+) weak, (++) moderate, and (+++) strong. In cases of heterogeneous staining, the average intensity across the tissue was taken as the score. Also, in a few cases where a patient sample was stained twice, the case was given a mean score, based on evaluation of the two sections. The percentage of positive cells was estimated as the number of stained cells, per total number of cells counted. The localization of staining within the cells of each tissue was also examined and noted as nuclear, cytoplasmic, membranous, or a combination of these. For semiquantitative analysis of the results, the staining intensity was assigned an arbitrary value, on a scale of 0-3, as follows: (-) = 0, (+/-) = 0.5, (+) =1, (++) = 2, (+++) = 3. An overall staining score (SS) was calculated for each sample, by multiplying the staining intensity times the percentage of positive cells. After multiplication of both values, results were graded from 0 (negative) to 300 (all cells display strong staining intensity). To confirm the reproducibility of the analysis, 25% of the slides were randomly chosen and scored twice. Duplicate readings gave similar results. Images were acquired using a SPOT digital camera and imaging software (Diagnostic Instruments, Inc., Sterling Heights, MI, USA).

Statistical analysis

Statistical calculations were executed using Statistical Analysis System software (SAS version 8.2, SAS Institute, Inc., Cary, NC). Analyses of differences in PRL expression between cancerous and noncancerous tissues were performed using a Student's paired t-test. Results are expressed as mean ± standard error of the mean (SEM) and $P < 0.05$ was considered statistically significant. For most samples, the medical histories of the patients and pathological reports for each specimen were also available. These were reviewed and correlations between PRL expression and patient clinicopathological features such as patient age and gender; tumor type, subtype, and grade; and presence of local or distant metastasis were calculated using a mixed model analysis of variance. Again, $P < 0.05$ was deemed statistically significant.

Results

PRL-1 and PRL-2 transcripts are expressed in a broad variety of normal and tumor tissues

A total of 285 normal, benign, and malignant human tissue samples of diverse origin were obtained from archival paraffin blocks and subjected to ISH, in order to examine expression of PRL-1 and PRL-2 mRNA transcripts (**Table 1**). PRL-2 message was found to be expressed at moderate to high levels in almost all (279/285) of the normal and tumor tissues examined. Low levels of PRL-2 were noted only in a single case of renal cell carcinoma, one normal lymph node, one ovarian carcinoma, and three normal specimens from the spleen. PRL-1 mRNA was also expressed in the vast majority of tissues examined, however the degree and intensity of PRL-1 staining varied considerably between tissue types and between individual cases within a single tissue type. This transcript was expressed at detectable levels in 97% (133/137) of histologically normal tissues examined, as well as in 93% (14/15) of breast carcinomas, 83% (5/6) of endometrial adenocarcinomas, 78% (14/18) of ovarian tumors, 77% (10/13) of renal cell carcinomas, and in 100% of primary tumors derived from the bladder (n=9), cervix (n = 1), colon (n = 5), liver (n = 4), lung (n = 8), pancreas (n = 14), prostate (n = 28), skin (n = 1), stomach (n = 5), and testis (n = 4). PRL-1 was also expressed in all cases examined of B-

PRL-1 and PRL-2 expression in cancer

Table 1. Expression of PRL-1 and PRL-2 in various tumors and diseased tissues

		PRL-1			PRL-2		
Tissue Type/Histopathology	# Samples	Weak (%)	Moderate (%)	Strong (%)	Weak (%)	Moderate (%)	Strong (%)
Bladder							
Transitional Cell Carcinoma	7	0	71	29	0	0	100
Sarcomatoid Carcinoma	1	100	0	0	0	0	100
Undifferentiated Carcinoma	1	100	0	0	0	0	100
Hyperplastic Lesion	1	100	0	0	0	0	100
Brain							
Alzheimer's	4	25	75	0	25	0	75
Multiple Sclerosis	2	0	0	0	100	0	0
Breast							
Invasive Ductal Carcinoma	15	13	40	40	0	7	93
Benign Lesions	2	0	100	0	0	0	100
Cervix							
Squamous Cell (LCK)	1	0	100	0	0	0	100
Colon							
Adenocarcinoma	5	20	40	40	0	0	100
Metastatic Lesions in Liver	3	0	33	67	0	0	100
Crohn's Disease	2	0	0	100	0	0	100
Coronary Arteries							
30-60% Occlusion	3	33	0	0	0	33	33
60-90% Occlusion	2	0	0	0	0	50	0
Heart							
Heart Disease	7	43	0	0	14	86	0
Kidney							
Renal Cell Carcinoma	13	38	31	8	8	8	84
Liver							
Hepatocellular Carcinoma	4	0	100	0	0	0	100
Hepatitis	2	100	0	0	0	50	50
Steatosis	2	50	50	0	0	50	50
Lung							
Non Small Cell Lung Cancer	8	0	37	63	0	12	88
Lymph Node							
B-Cell Lymphoma	4	0	0	100	0	0	100
Hodgkin Lymphoma	1	0	0	100	0	0	100
Metastatic Lymphoma in Testes	1	0	0	100	0	0	100
Ovary							
Epithelial Tumor	17	41	35	0	6	12	82
Dysgerminoma	1	0	100	0	0	0	100
Pancreas							
Exocrine Tumor	12	0	8	92	0	0	100
Endocrine Tumor	2	0	0	100	0	0	100
Diabetic	8	0	0	100	0	0	100
Prostate							
Adenocarcinoma	28	25	25	50	0	0	100
Skeletal Muscle							
Diabetic	4	0	50	0	0	25	75
Skin							
Basal Cell Carcinoma	1	100	0	0	0	0	100
Spleen							
Chronic Lymphocytic Leukemia	1	100	0	0	0	100	0
Chronic Myelogenous Leukemia	1	0	0	100	0	0	100
Diabetic	3	0	67	0	0	33	67
Stomach							
Adenocarcinoma	4	0	0	100	0	0	100
Leiomyosarcoma	1	0	0	100	0	0	100
Testis							
Germ Cell Tumor	4	0	50	50	0	0	100
Uterus							
Adenocarcinoma	6	33	50	0	0	17	83
Sarcoma (MMMT)	1	0	0	100	0	0	100
Vasculature (Multi Tumor Tissues)	38	21	32	45	0	5	95
Stroma (Multi Tumor Tissues)	90	41	29	17	0	12	88

Abbreviations: LCK = Large Cell Keratinizing; MMMT = Malignant Mixed Mullerian Tumor

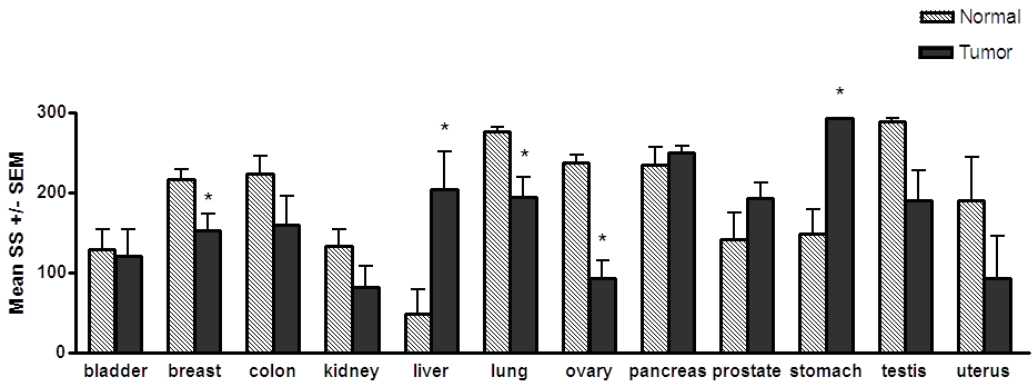

Figure 1. Levels of PRL-1 transcript in matched tumor and adjacent normal tissue pairs. The mean staining scores (SS) ± the SEM are shown. An asterisk indicates a statistically significant difference between the matched normal versus tumor tissue, as determined by paired t-tests ($P < 0.05$). A statistically significant increase in PRL-1 mRNA expression was found in hepatocellular carcinomas ($P = 0.0052$, $n = 4$), and carcinomas of the stomach ($P = 0.01$, $n = 5$), compared to matched normal tissues. A significant decrease in PRL-1 mRNA expression was found in breast tumor tissue ($P = 0.0058$, $n = 15$), lung tumors ($P = 0.015$, $n = 8$), and ovarian carcinomas ($P = 0.0007$, $n = 6$) compared to matched normal tissues.

cell lymphoma (n = 5, including one metastatic lesion in the testes), Hodgkin lymphoma (n = 1), chronic lymphocytic leukemia (CLL; n = 1), chronic myelogenous leukemia (CML; n = 1), colon metastases to the liver (n = 3), uterine sarcoma (n = 1), and benign lesions of the breast (n = 2). In the vast majority of cases (both normal and tumor), localization of PRL-1 and PRL-2 staining appeared to be nuclear, however in tissues of the breast, liver, pancreas, stomach, and uterus, both nuclear and cytoplasmic staining were observed.

Dysregulation of PRL-1 and PRL-2 mRNA expression in tumors is highly tissue specific

To provide further insight into the role of the PRL genes in cancer development, PRL-1 and PRL-2 mRNA expression were directly compared between the tumor and normal tissues examined by ISH. In both the normal and tumor tissues, a large degree of inter-individual variability was observed, particularly in PRL-1 expression, suggesting that comparisons between normal and diseased tissue from different patients could be misleading. To account for this, only case matched tumor and normal adjacent tissue (NAT) specimens from the same patient were utilized in this analysis. Of the tissues examined, there were 94 cases where both tumor and normal samples were available (188 total tissue specimens). These included case matched specimens from the bladder (n = 5), breast (n = 15), colon (n = 5), kidney (n = 13), liver (n = 4), lung (n = 8), ovary (n = 6), pancreas (n = 10), prostate (n = 13), spleen (n = 1), stomach (n = 5), testis (n = 4), and uterus (n = 5).

Direct comparison between normal and tumor samples revealed several significant, yet highly tissue specific differences in PRL-1 and PRL-2 mRNA expression (**Figures 1** and **2**). PRL-1 expression was significantly higher in 100% of the gastric carcinomas examined as compared to adjacent normal gastric tissue, with an almost 2-fold higher mean staining score in the cancerous tissue than in the noncancerous tissue ($P = 0.01$, Stomach, **Figures 1** and **3**). PRL-1 was also significantly overexpressed in 100% of hepatocellular carcinomas (HCC) compared to the matched normal tissues examined ($P = 0.0052$) with 4-fold higher expression occurring in the tumor tissues in this instance. PRL-2 message was also found to be upregulated in 100% of the hepatocellular carcinomas examined ($P = 0.0152$, Liver, **Figure 1**) with levels of PRL-2 expression in the HCC tissues, on average, approximately 2-fold higher than in normal hepatocytes ($P = 0.0152$).

Given the evidence for a role of the PRL en-

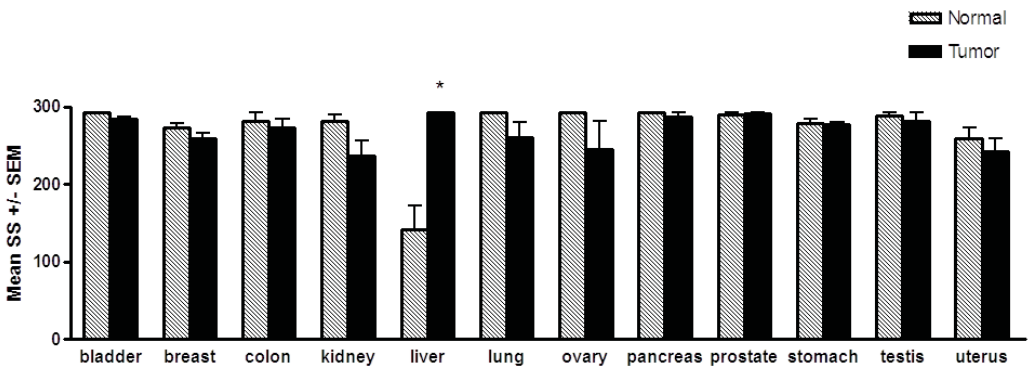

Figure 2. Levels of PRL-2 transcript in matched tumor and adjacent normal tissue pairs. The mean staining scores (SS) ± the SEM are shown. An asterisk indicates a statistically significant difference between the matched normal versus tumor tissue, as determined by paired t-tests ($P < 0.05$). Only hepatocellular carcinomas exhibited a statistically significant difference, with an approximately 2-fold increase in PRL-2 mRNA expression ($P = 0.015$, $n = 4$) in the tumors compared to normal liver tissue from the same subjects.

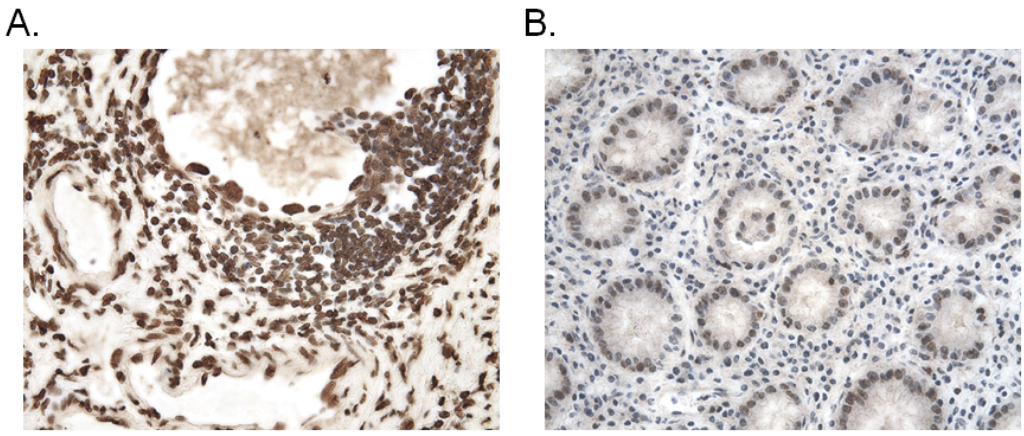

Figure 3. Increased levels of PRL-1 mRNA in carcinomas of the stomach. A representative example shows that PRL-1 message is expressed at significantly higher levels in a gastric adenocarcinoma (A) than in the normal gastric tissue from the same individual (B). Counterstained with hematoxylin. Magnification x 400.

zymes in tumor development and metastasis, it was not surprising to find PRL-1 and PRL-2 expression increased in a variety of tumor tissues. Unexpectedly however, expression of both genes was also found to be lower, relative to the normal adjacent tissues, in a number of tumor types. PRL-1 transcript levels were significantly decreased in 100% of ovarian carcinomas ($P = 0.0007$, Ovary, **Figure 1**), twelve (80%) of 15 benign and malignant breast tumors ($P = 0.0058$, **Figures 1** and **4**), and 6 (75%) of 8 lung carcinomas ($P = 0.0148$) with respect to the paired normal tissues for each. A similar downward trend appeared to occur for 80% of the colon carcinomas, 69% of the renal cell carcinomas, 80% of the testicular carcinomas, and 80% of the uterine carcinomas examined, however the differences in these tissues did not reach statistical significance. For PRL-2, seven (54%) out of 13 renal cell carcinomas showed a

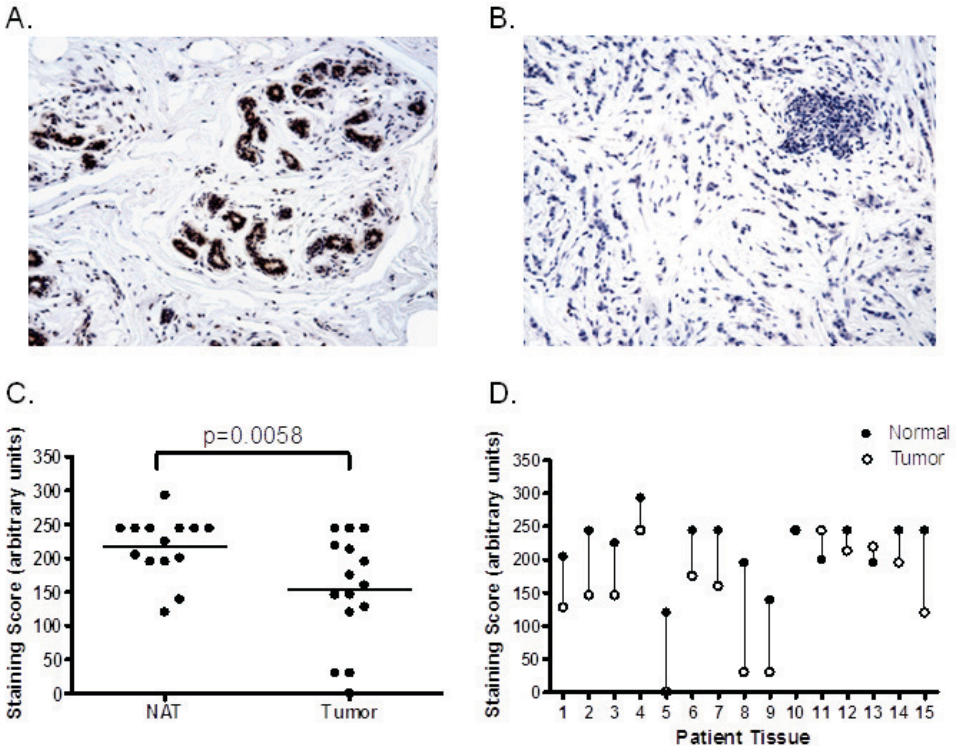

Figure 4. Decreased levels of PRL-1 mRNA in benign and malignant tumors of the breast. PRL-1 mRNA expression in (A) normal breast tissue and (B) a case matched, invasive ductal carcinoma of the breast. Counterstained with hematoxylin. Magnification x200. (C) Semi-quantitative analysis of PRL-1 mRNA expression in breast tumors (n = 15) and their matched normal adjacent tissues (n = 15). Horizontal lines represent the mean values for each group. Differences between the groups were found to be statistically significant by paired t-test (P = 0.0058). (D) PRL-1 mRNA expression in individual cases of matched tumor and adjacent normal tissue of the breast, showing a decrease in PRL-1 mRNA transcripts in 12/15 (80%) tumor tissues compared to their matched normal counterparts. Vertical lines connect matched tissue pairs from the same patient.

slight decrease in PRL-2 expression compared to the matched normal tissues (P = 0.049). Likewise, 38% of lung carcinomas, 40% of ovarian and 60% of uterine carcinomas showed a small decrease in PRL-2 mRNA levels compared to corresponding normal tissues, but these changes were not found to be statistically significant. Both PRL-1 and PRL-2 were also downregulated almost 2-fold in a single case of chronic lymphocytic leukemia compared to normal splenic B cells from the same patient, but, with only one tumor and matched normal sample in this case, statistical comparisons for this tumor type could not be made. No significant changes or trends in either PRL-1 or PRL-2 were observed in the overall mRNA expression between bladder, pancreatic, or prostate tumors and their respective matched normal adjacent tissues.

PRL-1 and PRL-2 mRNA expression in tumor stroma and vasculature

In addition to analyzing PRL-1 and PRL-2 expression patterns in multiple tumors and their normal cellular counterparts, expression of these transcripts was also compared between the stroma and vasculature of each subject's tumor (**Table 1**) and normal tissue. PRL-1 message was expressed in the vasculature of 100% of the normal tissues and 98% of the tumor tissues examined, with highly variable degree

and intensity of staining. Only one specimen, a uterine adenocarcinoma, did not display PRL-1 staining in the tumor vasculature, although very low levels of PRL-1 message were detectable in the glandular tissue of this tumor. In the stroma, PRL-1 was expressed in 95% of both the normal and tumor tissue sections examined, again with highly variable levels of expression from tissue to tissue. In most of the cases where an absence of PRL-1 staining was observed in the stroma, staining of all other structures within the tissue was also weak to absent. However, in 2/4 normal breast tissues where PRL-1 mRNA expression was not detected in the stroma, PRL-1 was expressed at moderate to high levels in the ductal epithelium. Likewise, in one squamous cell carcinoma of the lung which lacked PRL-1 expression in the stroma, PRL-1 was expressed at moderate levels in the tumor epithelium. PRL-2 was expressed at moderate to high levels in the vasculature and stroma of all 190 cases examined.

Similar to its upregulation in adenocarcinomas of the stomach, PRL-1 was also overexpressed in the stroma of each stomach tumor tissue examined (**Figure 3**), compared to the stroma of the corresponding normal adjacent tissues ($P = 0.0382$). In the bladder, although no clear differences in PRL expression existed between the normal and malignant urothelial cells, a significant decrease in PRL-1 expression was observed in both the bladder tumor vasculature ($P = 0.0199$) and the stroma surrounding the tumor ($P = 0.0182$), as compared to these structures in the normal adjacent tissue samples. PRL-2 expression was also significantly decreased in the stroma of bladder carcinomas ($P < 0.0001$). Unlike PRL-1, PRL-2 expression was not significantly altered in the bladder tumor vasculature and displayed high levels of expression in all normal and tumor tissues. Levels of PRL-1 and PRL-2 message in the stroma and vasculature were not significantly different between the normal and tumor tissue pairs of any other tissue type.

Expression of PRL-1 and PRL-2 transcripts in other human diseases

In addition to carcinogenesis, protein tyrosine phosphatases have also been implicated in susceptibility to, or progression of, various other diseases, such as inflammatory and autoimmune diseases, neurodegenerative diseases, and cardiovascular disease. The PRL family member PRL-3 itself has been linked to a role in heart disease [5]. Therefore, in an attempt to analyze the relationship between PRL expression and various other disease states, PRL-1 and PRL-2 mRNA expression were examined in the affected organs from patients with Alzheimer's disease (n = 4), multiple sclerosis (n = 2), crohn's disease (n = 2), heart disease (n = 7), coronary artery disease (n = 5), hepatitis (n = 2), liver steatosis (n = 2), insulin-dependent diabetes mellitus (n = 6), and noninsulin-dependent diabetes (n = 2). A student's t-test was used to compare the mean staining scores between each set of diseased tissues and a set of histologically normal samples of the same tissue type, from different subjects.

PRL-1 expression was again highly variable in all tissue types examined. PRL-2 message was expressed at moderate to high levels in all tissues examined, with the exception of the brain and heart where, like PRL-1, its expression was quite variable (**Table 1**). In the small sample set analyzed here, no significant correlations were found between either PRL-1 or PRL-2 gene expression and any of the disease states examined. There did appear to be a trend toward increased expression of PRL-1 in the brains of Alzheimer's disease patients, where 75% of subjects had a SS > 150 in sections from the cerebral cortex and hippocampus, while 60% of normal subjects displayed SS < 50 in the same regions. However, considering the correlations with patient age discussed below, this trend is unlikely to be significant.

Correlation between PRL-1 and PRL-2 mRNA expression and patient clinicopathological parameters

To evaluate the clinical relevance of PRL-1 and PRL-2 expression in each tissue type examined, where possible (sufficient sample size and available patient data), a mixed model analysis of variance was used to analyze the relationship between the PRL staining scores and several clinicopathological features, including patient age, patient gender, tumor type, tumor subtype, tumor grade, and evidence of tumor metastasis (**Tables 1** and **2**). The intensity of PRL staining was also compared to the localization of the staining (whether nuclear, cytoplasmic, membranous, or a combination of these) to examine any correlations between the two and the stain-

Table 2. Patient and sample characteristics

	Total Number			Gender			Age (years)		Tumor Grade				Metastasis		
Tissue Type	Samples	Subjects	Tumors	M	F	Unk	Mean	Range	High	Intermediate	Low	Unk	Y	N	Unk
Bladder	16	10	9	4	6	0	71	60-81	6	3	0	0	1	8	0
Brain	16	11	0	7	4	0	68	50-87	0	0	0	0	0	0	0
Breast	35	20	17	0	20	0	58	38-85	12	4	1	0	7	6	4
Cervix	6	6	1	0	6	0	40	30-44	0	1	0	0	0	1	0
Colon	16	11	8	7	3	1	69	29-94	2	4	2	0	7	1	0
Coronary Artery	5	5	0	4	1	0	57	37-78	0	0	0	0	0	0	0
Heart	11	11	0	7	4	0	45	9-73	0	0	0	0	0	0	0
Kidney	26	13	13	8	5	0	64	8-81	3	9	1	0	4	9	0
Liver	16	12	4	5	7	0	54	1-75	0	0	4	0	0	0	4
Lung	16	8	8	6	2	0	66	57-76	6	2	0	0	5	3	0
Lymph Node	11	11	5	7	4	0	44	7-82	3	0	2	0	1	0	4
Ovary	29	24	18	0	24	0	47	17-74	9	6	3	0	4	2	12
Pancreas	38	28	14	10	9	9	47	3-79	8	5	0	1	6	0	8
Prostate	41	28	28	28	0	0	63	51-75	14	10	4	0	2	3	23
Skeletal Muscle	9	9	0	5	3	1	55	16-90	0	0	0	0	0	0	0
Skin	4	4	1	1	1	2	52	51-52	0	0	1	0	0	1	0
Spleen	12	11	2	8	3	0	41	13-71	0	0	1	1	0	0	2
Stomach	10	5	5	4	1	0	72	46-85	4	1	0	0	4	0	1
Testis	10	5	4	5	0	0	45	28-82	2	1	1	0	0	1	3
Uterus	16	11	7	0	11	0	47	20-68	2	5	0	0	1	1	5

Abbreviations: M = male; F = Female; Unk = Unknown; Y = Yes; N = No

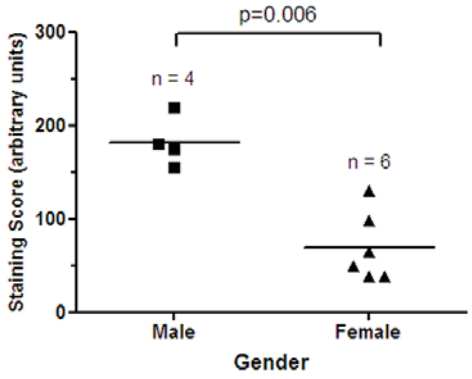

Figure 5. Gender specific expression of PRL-1 in the bladder. Semi-quantitative analysis of PRL-1 mRNA expression in male (n = 4) and female (n = 6) bladder tissues. Horizontal lines represent the mean values for each group. Differences between the two groups were found to be statistically significant by paired t-test (P = 0.006).

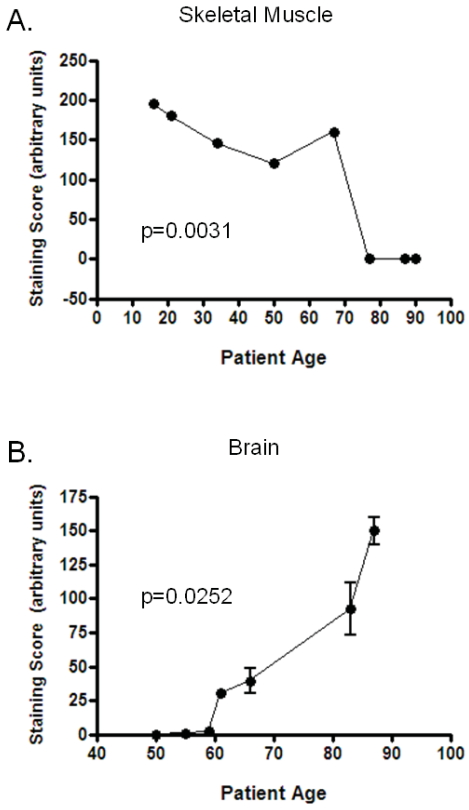

Figure 6. PRL-1 levels correlate with age in the skeletal muscle and brain. Semi-quantitative analysis showed that PRL-1 mRNA expression is negatively correlated with patient age in the skeletal muscle (A) and positively correlated with patient age in the brain (B). In both cases, mixed model analysis found the results to be statistically significant (P < 0.05). Brain specimens included tissue sections from the cerebrum, hippocampus, substantia nigra, and cerebellum. Different regions of the brain within the same individual displayed similar staining scores. The averages of these are represented.

ing localization was also individually compared to each of the various clinicopathological parameters.

Levels of PRL-1 expression were found to be correlated with patient gender in neoplasms of the bladder (P = 0.006), where the male subjects all exhibited significantly higher PRL levels than the female subjects (**Figure 5**). Expression levels of PRL-1 were also correlated with age in some tissue types. PRL-1 staining scores significantly decreased with patient age in the skeletal muscle (P = 0.0031, **Figure 6A**) with very low expression levels attained after ages greater than 75 years. In contrast, PRL-1 strongly increased with patient age in the brain (P = 0.0252, **Figure 6B**) with sharp increases observed in patients over the age of 60 years. In several tumor tissues, expression of PRL-1 and -2 was significantly correlated with increasing tumor grade (increasing severity). In the ovary (**Figure 7A**), well-differentiated tumors expressed little to no PRL-1, while the less organized moderately-differentiated and poorly differentiated tumors tended to express higher levels of the transcript (P = <0.0001). There were no well-differentiated carcinomas of the uterus in this study, however the poorly differentiated carcinomas expressed PRL-1 to a significantly higher degree than the moderately differentiated uterine tumors (P = 0.0441). In the prostate (**Figure 7B**), mean PRL-1 staining scores once more increased from the low grade, more differentiated tumors (Gleason grades 1-4) to the moderate grade tumors (Grades 5-7). However, the mean staining score again decreased in the more poorly differentiated, high grade (Grades 8-10) prostate tumors (P = 0.0126). In the testes, little to no PRL-2 expression was

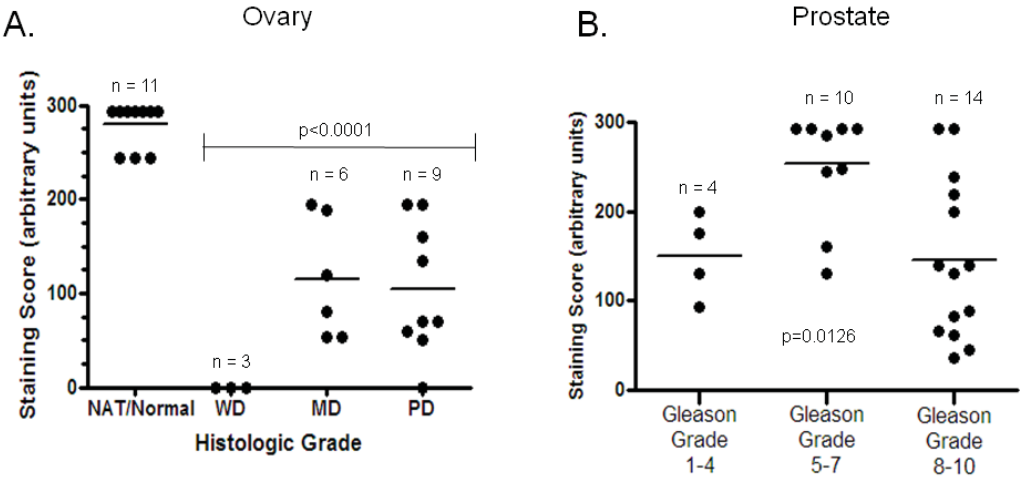

Figure 7. Correlation of PRL-1 expression with tumor grade in the ovary and prostate. (A) Expression levels, in arbitrary units, of PRL-1 mRNA in human ovarian carcinomas (n = 18) of varying histologic grade. WD = well-differentiated; MD = moderately differentiated; PD = poorly differentiated. (B) Expression levels, in arbitrary units, of PRL-1 mRNA in human prostate carcinomas (n = 28) of varying histologic grade. Horizontal lines represent the mean values for each group. In both tissue types, mixed model analysis found the results to be statistically significant ($P < 0.05$).

observed in a well-differentiated germ cell tumor, but high levels of PRL-2 were noted in both the moderately and poorly differentiated tumors. In this tissue type, however, the number of samples in each category was too small to make any statistical comparisons. No clear associations were found between the intensity of PRL-1 or PRL-2 staining and the localization of the staining, nor between the localization of staining and any of the clinicopathological parameters examined. There were also no correlations found, in this data set, between PRL-1 or -2 expression and histologic subtype (e.g. clear cell vs. chromophobe cell type renal cell carcinomas of the kidney; adenocarcinoma vs. squamous cell non-small cell cancer of the lung, etc.) or with the presence or absence of local or distant metastases in any tumor type.

Correlation of PRL mRNA and protein expression

To examine the relationship between PRL-1 and PRL-2 expression at the mRNA and protein levels, select cases from various tissue types and representing a wide range of expression levels via ISH (RNA) were also examined by IHC (protein). The degree of expression for each was scored, in a blinded fashion, by different individuals than those who scored the ISH results and the general levels of expression (high, medium, or low) for the mRNA and protein were then compared. Using this approach it is not possible to compare absolute levels of RNA and protein, however, the relative changes seen in comparing various tissues and in comparing tumor and normal adjacent tissue can be useful. In the majority of the 30 individual cases examined, PRL-1 mRNA and protein were expressed at similar relative levels (**Figure 8A**). In cases where the relative levels differed, staining was always more intense for PRL-1 mRNA than for the protein. In half of the same 30 tissue sections, PRL-2 mRNA staining intensity was also higher than that for PRL-2 protein (**Figure 8B**). In the remaining half of cases, PRL-2 mRNA and protein appeared to be expressed at similar levels (37%) or the staining intensity for the protein was higher than that for the mRNA (13%).

Within the 30 tissues probed by both ISH and IHC, there were 10 cases of paired tumor and normal adjacent tissue. Examination of these tissue pairs revealed that 6 of 10 cases for PRL-1 (concordance = 60%) and 8 of 10 cases for PRL-2 (concordance = 80%) displayed the same

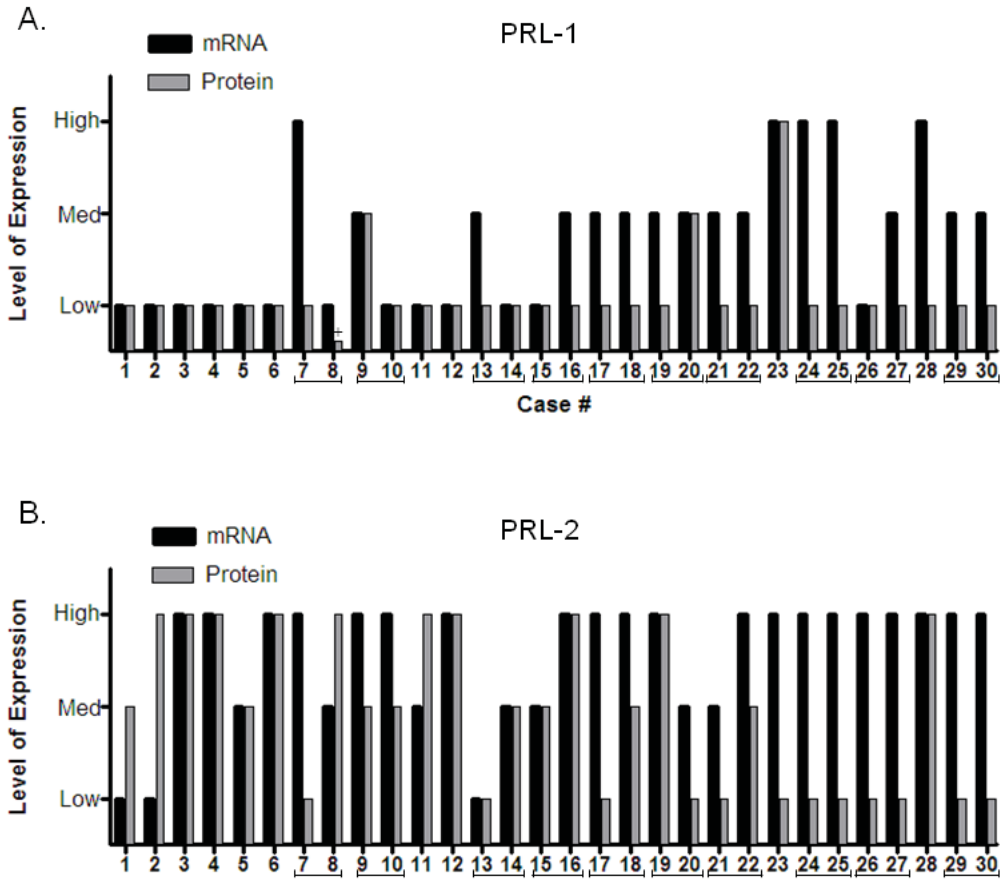

Figure 8. Comparison between mRNA and protein expression levels. PRL-1 (A) and PRL-2 (B) mRNA and protein expression levels were compared in a selection of 30 normal and tumor tissues from a variety of tissue types. Brackets indicate matched normal adjacent and tumor tissue pairs from the same individual. The plus sign in (A) denotes a sample for which no expression of PRL-1 protein was detected; however a small arbitrary value was assigned so that this sample would appear on the graph.

trends of expression between the RNA and protein (e.g. both increased from the normal adjacent to the tumor tissue; both decreased from the normal adjacent to the tumor tissue; or neither changed). This suggested that there was good overall concordance between the RNA and protein results and that, in general, changes occurring at the mRNA level here are reflective of those occurring at the protein level.

Discussion

Accumulating evidence has implicated the PRL family of phosphatases as having an oncogenic role in human cancers [1, 4-7]. For example, it is now well known that PRL-3 expression is generally absent from normal adult human tissues, but frequently elevated in a variety of benign and malignant human neoplasms, where it may serve as a marker for tumor aggressiveness, increased tumor angiogenesis, and/or poor prognosis [9, 10, 12, 18, 21-27, 31, 35-37, 51]. Here, we used in situ hybridization to examine the expression of PRL-1 and PRL-2 in human malignancies with the aim of providing further insight into the role these two PRL family mem-

bers play in disease pathogenesis.

PRL-1 and PRL-2 transcript levels were evaluated across 285 normal, benign, and malignant tumor tissues, where both transcripts were found to be ubiquitously expressed. While PRL-2 transcripts were consistently abundant across almost all specimens, PRL-1 expression was highly variable, not only between tissue types, but also from individual to individual within a given tissue type. Since such a high degree of patient-to-patient variability in PRL-1 expression could confound results when making comparisons between groups of unmatched normal and tumor tissues from different subjects, only matched tumor and normal adjacent tissue (NAT) samples taken from the same individuals were used to evaluate changes in PRL gene expression that might occur as a result of neoplastic transformation. Given current knowledge of the role that the PRL enzymes play in promoting tumor development and progression, we hypothesized that PRL-1 and PRL-2 gene expression would each be upregulated in a number of tumor types relative to their matched normal tissue specimens. In accordance with this theory, PRL-1 and PRL-2 transcripts were each found to be significantly overexpressed in 100% of hepatocellular carcinomas ($n = 4$; $p = 0.0052$ and 0.0152 respectively) and PRL-1 message was also significantly overexpressed in both the tumor ($p = 0.01$) and stroma ($p = 0.0382$) of 100% of carcinomas from the stomach ($n = 5$). Increased levels of PRL-3 expression have previously been associated with the progression and metastasis of gastric and liver carcinomas [27, 29-31, 34, 35, 39]. The current report is the first to suggest that PRL-1 and PRL-2 may also play an important role in the development and/or progression of these tumor types.

Surprisingly however, in other tissue types, a very different result was seen. In 100% of ovarian ($n=6$; $p = 0.0007$), 80% of breast ($n = 15$; $p = 0.0058$), and 75% of lung ($n = 8$; $p = 0.0148$) tumors, PRL-1 levels were found to be significantly lower in the neoplastic cells than in their matched, unaffected counterparts. Likewise, PRL-2 levels were significantly decreased in 54% of carcinomas from the kidney ($n = 13$; $p = 0.049$) relative to the matched normal controls. These results suggest that dysregulation of PRL-1 and PRL-2 is a highly tissue specific event. This is consistent with observations of normal tissues, which have suggested that the PRL enzymes may be pleiotropic signaling molecules with a diversity of roles in different tissues and cell types [52, 53].

In addition to a role in cancer, PTPs have been implicated in a growing number of human pathologies, including cardiovascular, immunological, infectious, neurological, and metabolic diseases [44-47]. Therefore, we also sought to examine PRL-1 and PRL-2 mRNA expression in a small cohort of available samples from patients with various pathological conditions. In the panel of tissues examined here, PRL-1 and -2 were widely expressed, however no significant correlations were found between PRL-1 or PRL-2 expression levels and Alzheimer's disease, multiple sclerosis, Crohn's disease, coronary artery disease, heart disease, liver steatosis, hepatitis, or diabetes.

To evaluate the extent to which deregulation of PRL expression might be related to known patient characteristics and clinicopathological variables, where possible, PRL-1 and -2 mRNA expression levels in each tissue type were correlated to such features as patient age, patient gender, tumor histologic subtype, tumor grade, and presence/absence of tumor metastasis. In neoplasms of the bladder, expression levels of PRL-1 were found to be correlated to patient gender ($p = 0.006$), with male subjects displaying significantly higher PRL-1 transcript levels than female subjects. A similar trend toward increased expression in male subjects was also noted for PRL-2 in the lung (data not shown). Carter et al. [54] previously observed gender based differences of PRL-2 expression in rat brains, where PRL-2 mRNA was expressed at 3-fold higher levels in the anterior pituitaries of male rats than in female rats. The current data thus support these prior observations that the PRL enzymes may play a sexually dimorphic role in select tissue types. Increased PRL-1 expression also correlated positively with patient age in the brain ($p = 0.0252$), yet negatively with patient age in the skeletal muscle ($p = 0.0031$). Advancing age of both the brain and skeletal muscle is associated with a decline in function as well as with several common accompanying changes in gene expression [55-57]. Interestingly, in one transcriptional profiling study, aimed at identifying gene signatures for human aging in the frontal cortex [55], PRL-2 appeared on the list of genes which are significantly upregulated in the aging human brain. These

data suggest that both PRL-1 and PRL-2 may be putative players in, or be heavily influenced by, the aging process. Taken together, these results suggest that age and gender should be taken into account when evaluating sample to sample variations in PRL abundance and further underscore the importance of using appropriately matched case controls in comparisons of PRL expression.

PRL-1 or -2 mRNA levels were found to be associated with tumor grade in some tissue types. Levels of PRL-1 in ovarian tumors increased significantly ($p < 0.0001$) in the moderate and poor grade tumors, relative to the low grade specimens, although this increase was to levels that remained appreciably lower than that seen in the NAT/normal specimens. A similar pattern of expression was observed for PRL-1 in the uterus and for PRL-2 in the testes. In the prostate, a wide range of PRL-1 expression levels were observed across the histologically normal tissue specimens, as well as across cases of prostatic intraepithelial neoplasia (PIN) and benign prostatic hyperplasia (BPH). However, in the prostate tumor specimens there was a significant increase in PRL-1 expression going from the lower grade to the more moderate grade tumors ($p = 0.0126$), followed by a subsequent decrease in the higher grade tumors. These data suggest that alterations in PRL expression are an early event of carcinogenesis in many organ systems and that PRL-1 and/or PRL-2 may serve as useful biomarkers for detection of tumorigenic lesions or for assessment of tumor aggressiveness in select tissue types. No correlations were found between PRL-1 or -2 expression and any of the clinicopathological features examined in the breast, heart, kidney, liver, pancreas, spleen, or stomach. Nor was any association seen between PRL expression and histologic subtype or tumor metastasis in any of the tumor types examined. There were also no significant correlations between PRL-1 or PRL-2 mRNA expression and clinical features related to colon cancer progression or metastasis, consistent with a previous report examining PRL-1 and PRL-2 protein in this tissue type [19].

To determine whether changes seen at the RNA level are reflective of what is occurring in these tissues at the protein level, immunostaining results from anti-peptide, affinity-purified polyclonal antibodies specific to PRL-1 and PRL-2 were directly compared to the ISH results in a subset of tissues from different tissue origin and demonstrating varied levels of PRL mRNA expression. Despite the presence of some variation between the absolute levels of PRL-1 or -2 mRNA and protein in the analysis of individual cases, there was a clear correlation between the two with respect to the changes occurring during tumorigenesis. In comparisons of matched normal and tumor samples from the same patient, the mRNA and protein both exhibited the same change (or conversely, lack of change) in expression 60% of the time for PRL-1 and 80% of the time for PRL-2. When differences in the general expression levels (high, medium, low) between mRNA and protein occurred, the mRNA was most often detected at higher levels than the protein. It is possible that, in each of these cases, changes occurring at the RNA level had not yet been reflected at the protein level. Alternatively, this could indicate post-transcriptional control of these molecules, perhaps through translational repression by PolyC-RNA-binding protein 1 (PCBP1) or a similar molecule, as was recently described for PRL-3 [58].

Only a handful of studies have yet examined PRL-1 or PRL-2 expression in human malignancies and even fewer have evaluated PRL-1 or PRL-2 in case matched normal and tumor samples. However, in general, the current results are in good agreement with previously published reports. In the present study, PRL-1 and PRL-2 levels were consistently lower in primary tumors from the ovary, compared to paired normal tissues, suggesting that higher levels of PRL -1 and -2 may be advantageous in this sample type. This is consistent with the observations of Reich et al. who showed that higher expression of PRL-1 or PRL-2 in ovarian cancer effusions correlated with better overall patient survival [59]. In contrast, the present data also show a relationship between increasing PRL-1 expression in ovarian carcinomas and advanced tumor grade. It is currently unclear how PRL-1 expression can be consistently downregulated in tumor specimens and positively correlated with improved patient outcome, yet also show positive correlation to increased tumor aggressiveness. However, with respect to outcome, Reich et al. did not observe the same beneficial effect of PRL-1 and -2 on patient survival when the molecules were expressed in solid tumors. It is possible then that, in solid ovarian tumors, an initial knockdown of PRL-1 expression is re-

quired for neoplastic transformation, following which enhanced levels of PRL-1 have no effect. Or PRL-1 could have an inhibitory effect on tumor formation in the early stages of ovarian carcinogenesis, but play a tumor-promoting role in the latter stages. A similar dual, opposing role has previously been reported for other molecules including Notch1 [60], MIC-1 [61], and for TGFβ [62], which has been shown to be an upstream regulator of PRL-3 [63]. In breast tissue, Hardy et al. [43] used real-time PCR to examine PRL-2 expression and found elevated levels of PRL-2 mRNA in primary breast tumors relative to matched normal tissue. The present data indicate a lack of change in PRL-2 expression between normal and neoplastic breast tissues, but PRL-2 levels in most breast tissues were extremely high and quite possibly at the limits of detection for the ISH system. In the pancreas, Stephens et al. [64] showed upregulation of PRL-1 and PRL-2 protein in 33% and 26% respectively of pancreatic tumors in relation to matched NAT specimens. In the current study, similar results were noted for PRL-1 mRNA with increased expression of PRL-1 seen in 46% of pancreatic tumor specimens with respect to matched normal controls. However, in 36% of samples, the opposite effect was seen, with an increase of PRL-1 expression in the NAT tissue relative to tumor. And, in 18% of samples, no differences were seen between the two. In the current data for PRL-2, staining was always heavy and no detectable differences between PRL-2 expression in the tumor and NAT samples were observed.

The results presented here show that, as with family member PRL-3, alterations in expression of PRL-1 and PRL-2 are a common event in human cancers; however, the nature of these alterations is highly tissue specific. In some tissue types, such as the stomach and liver, PRL-1 or -2 expression associates with tumor promotion, whereas in other tissue types, like the ovary and lung, expression of these molecules may normally serve a protective function. The frequent deregulation of these molecules in human neoplasms suggests that they may be useful markers for cancer diagnosis. They may also serve as valuable therapeutic targets and/or indicators of increasing tumor severity in select tissue types. The mechanisms of PRL action and regulation are currently poorly understood and the exact biological function of these molecules is unknown. Identifying the means by which their expression is regulated or the signaling pathways in which they act will be an important next step to provide insight into the pleiotropic role these molecules play in the carcinogenic process. Characterization of the PRL signaling pathways may also enhance our understanding of the observed gender and age related variations in PRL-1 expression. The present results help to expand our current understanding of the differences that exist between PRL-1 and PRL-2 levels in normal tissues and human malignancies and should facilitate larger scale retrospective or prospective studies examining the relevance of PRL-1 or PRL-2 in clinical cancer as well as in other human pathologies.

Acknowledgements

The authors would like to thank Dr. Mark Farmen for his oversight and review of the statistical analysis and Dr. Dean Wiseman and Jennifer Funke for their readings of the IHC slides. A portion of this work was supported in part by PHS, NIH grant CA72450, awarded to P.L.C.

Address correspondence to: Dr. Carmen M Dumaual, IUPUI, Dept. of Biology, 723 West Michigan St., Room SL306, Indianapolis, IN 46202, USA Tel: 317-277-9883; Fax: 317-277-7893; E-mail: cdumaual@gmail.com; Dr. Stephen K. Randall, IUPUI, Dept. of Biology, 723 West Michigan St., Room SL306, Indianapolis, IN 46202, USA Tel: 317-274-0592; Fax: 317-274-2846; E-mail: srandal@iupui.edu

References

[1] Cates CA, Michael RL, Stayrook KR, Harvey KA, Burke YD, Randall SK, Crowell PL and Crowell DN. Prenylation of oncogenic human PTP(CAAX) protein tyrosine phosphatases. Cancer Lett 1996; 110: 49-55.

[2] Si X, Zeng Q, Ng CH, Hong W and Pallen CJ. Interaction of farnesylated PRL-2, a protein-tyrosine phosphatase, with the beta-subunit of geranylgeranyltransferase II. J Biol Chem 2001; 276: 32875-32882.

[3] Zeng Q, Si X, Horstmann H, Xu Y, Hong W and Pallen CJ. Prenylation-dependent association of protein-tyrosine phosphatases PRL-1, -2, and -3 with the plasma membrane and the early endosome. J Biol Chem 2000; 275: 21444-21452.

[4] Diamond RH, Cressman DE, Laz TM, Abrams CS and Taub R. PRL-1, a unique nuclear protein tyrosine phosphatase, affects cell growth. Mol Cell Biol 1994; 14: 3752-3762.

[5] Matter WF, Estridge T, Zhang C, Belagaje R, Stancato L, Dixon J, Johnson B, Bloem L, Pickard T, Donaghue M, Acton S, Jeyaseelan R,

Kadambi V and Vlahos CJ. Role of PRL-3, a human muscle-specific tyrosine phosphatase, in angiotensin-II signaling. Biochem Biophys Res Commun 2001; 283: 1061-1068.

[6] Wu X, Zeng H, Zhang X, Zhao Y, Sha H, Ge X, Zhang M, Gao X and Xu Q. Phosphatase of regenerating liver-3 promotes motility and metastasis of mouse melanoma cells. Am J Pathol 2004; 164: 2039-2054.

[7] Zeng Q, Dong JM, Guo K, Li J, Tan HX, Koh V, Pallen CJ, Manser E and Hong W. PRL-3 and PRL-1 promote cell migration, invasion, and metastasis. Cancer Res 2003; 63: 2716-2722.

[8] Guo K, Li J, Tang JP, Koh V, Gan BQ and Zeng Q. Catalytic domain of PRL-3 plays an essential role in tumor metastasis: formation of PRL-3 tumors inside the blood vessels. Cancer Biol Ther 2004; 3: 945-951.

[9] Kato H, Semba S, Miskad UA, Seo Y, Kasuga M and Yokozaki H. High expression of PRL-3 promotes cancer cell motility and liver metastasis in human colorectal cancer: a predictive molecular marker of metachronous liver and lung metastases. Clin Cancer Res 2004; 10: 7318-7328.

[10] Li Z, Zhan W, Wang Z, Zhu B, He Y, Peng J, Cai S and Ma J. Inhibition of PRL-3 gene expression in gastric cancer cell line SGC7901 via microRNA suppressed reduces peritoneal metastasis. Biochem Biophys Res Commun 2006; 348: 229-237.

[11] Matsukawa Y, Semba S, Kato H, Koma Y, Yanagihara K and Yokozaki H. Constitutive suppression of PRL-3 inhibits invasion and proliferation of gastric cancer cell in vitro and in vivo. Pathobiology 2010; 77: 155-162.

[12] Zhou J, Wang S, Lu J, Li J and Ding Y. Overexpression of phosphatase of regenerating liver -3 correlates with tumor progression and poor prognosis in nasopharyngeal carcinoma. Int J Cancer 2009; 124: 1879-1886.

[13] Qian F, Li YP, Sheng X, Zhang ZC, Song R, Dong W, Cao SX, Hua ZC and Xu Q. PRL-3 siRNA inhibits the metastasis of B16-BL6 mouse melanoma cells in vitro and in vivo. Mol Med 2007; 13: 151-159.

[14] Nakashima M, Lazo JS. Phosphatase of regenerating liver-1 promotes cell migration and invasion and regulates filamentous actin dynamics. J Pharmacol Exp Ther 2010; 334: 627-633.

[15] Saha S, Bardelli A, Buckhaults P, Velculescu VE, Rago C, St Croix B, Romans KE, Choti MA, Lengauer C, Kinzler KW and Vogelstein B. A phosphatase associated with metastasis of colorectal cancer. Science 2001; 294: 1343-1346.

[16] Bardelli A, Saha S, Sager JA, Romans KE, Xin B, Markowitz SD, Lengauer C, Velculescu VE, Kinzler KW and Vogelstein B. PRL-3 expression in metastatic cancers. Clin Cancer Res 2003; 9: 5607-5615.

[17] Peng L, Ning J, Meng L and Shou C. The association of the expression level of protein tyrosine phosphatase PRL-3 protein with liver metastasis and prognosis of patients with colorectal cancer. J Cancer Res Clin Oncol 2004; 130: 521-526.

[18] Mollevi DG, Aytes A, Padulles L, Martinez-Iniesta M, Baixeras N, Salazar R, Ramos E, Figueras J, Capella G and Villanueva A. PRL-3 is essentially overexpressed in primary colorectal tumours and associates with tumour aggressiveness. Br J Cancer 2008; 99: 1718-1725.

[19] Wang Y, Li ZF, He J, Li YL, Zhu GB, Zhang LH and Li YL. Expression of the human phosphatases of regenerating liver (PRLs) in colonic adenocarcinoma and its correlation with lymph node metastasis. Int J Colorectal Dis 2007; 22: 1179-1184.

[20] Xing X, Peng L, Qu L, Ren T, Dong B, Su X and Shou C. Prognostic value of PRL-3 overexpression in early stages of colonic cancer. Histopathology 2009; 54: 309-318.

[21] Ma Y, Li B. Expression of phosphatase of regenerating liver-3 in squamous cell carcinoma of the cervix. Med Oncol 2011; 28: 775-780.

[22] Polato F, Codegoni A, Fruscio R, Perego P, Mangioni C, Saha S, Bardelli A and Broggini M. PRL-3 phosphatase is implicated in ovarian cancer growth. Clin Cancer Res 2005; 11: 6835-6839.

[23] Ren T, Jiang B, Xing X, Dong B, Peng L, Meng L, Xu H and Shou C. Prognostic significance of phosphatase of regenerating liver-3 expression in ovarian cancer. Pathol Oncol Res 2009; 15: 555-560.

[24] Radke I, Gotte M, Kersting C, Mattsson B, Kiesel L and Wulfing P. Expression and prognostic impact of the protein tyrosine phosphatases PRL-1, PRL-2, and PRL-3 in breast cancer. Br J Cancer 2006; 95: 347-354.

[25] Wang L, Peng L, Dong B, Kong L, Meng L, Yan L, Xie Y and Shou C. Overexpression of phosphatase of regenerating liver-3 in breast cancer: association with a poor clinical outcome. Ann Oncol 2006; 17: 1517-1522.

[26] Hao RT, Zhang XH, Pan YF, Liu HG, Xiang YQ, Wan L and Wu XL. Prognostic and metastatic value of phosphatase of regenerating liver-3 in invasive breast cancer. J Cancer Res Clin Oncol 2010; 136: 1349-1357.

[27] Miskad UA, Semba S, Kato H, Matsukawa Y, Kodama Y, Mizuuchi E, Maeda N, Yanagihara K and Yokozaki H. High PRL-3 expression in human gastric cancer is a marker of metastasis and grades of malignancies: an in situ hybridization study. Virchows Arch 2007; 450: 303-310.

[28] Miskad UA, Semba S, Kato H and Yokozaki H. Expression of PRL-3 phosphatase in human gastric carcinomas: close correlation with invasion and metastasis. Pathobiology 2004; 71: 176-184.

[29] Ooki A, Yamashita K, Kikuchi S, Sakuramoto S, Katada N and Watanabe M. Phosphatase of regenerating liver-3 as a prognostic biomarker

in histologically node-negative gastric cancer. Oncol Rep 2009; 21: 1467-1475.
[30] Pryczynicz A, Guzinska-Ustymowicz K, Chang XJ, Kisluk J and Kemona A. PTP4A3 (PRL-3) expression correlate with lymphatic metastases in gastric cancer. Folia Histochem Cytobiol 2010; 48: 632-636.
[31] Li ZR, Wang Z, Zhu BH, He YL, Peng JS, Cai SR, Ma JP and Zhan WH. Association of tyrosine PRL-3 phosphatase protein expression with peritoneal metastasis of gastric carcinoma and prognosis. Surg Today 2007; 37: 646-651.
[32] Wang Z, Cai SR, He YL, Zhan WH, Chen CQ, Cui J, Wu WH, Wu H, Song W, Zhang CH, Peng JJ and Huang XH. High expression of PRL-3 can promote growth of gastric cancer and exhibits a poor prognostic impact on patients. Ann Surg Oncol 2009; 16: 208-219.
[33] Wang Z, Cai SR, He YL, Zhan WH, Zhang CH, Wu H, Peng JJ, Xu JB, Zhang XH, Wang L and Song W. Elevated PRL-3 expression was more frequently detected in the large primary gastric cancer and exhibits a poor prognostic impact on the patients. J Cancer Res Clin Oncol 2009; 135: 1041-1046.
[34] Wang Z, He YL, Cai SR, Zhan WH, Li ZR, Zhu BH, Chen CQ, Ma JP, Chen ZX, Li W and Zhang LJ. Expression and prognostic impact of PRL-3 in lymph node metastasis of gastric cancer: its molecular mechanism was investigated using artificial microRNA interference. Int J Cancer 2008; 123: 1439-1447.
[35] Dai N, Lu AP, Shou CC and Li JY. Expression of phosphatase regenerating liver 3 is an independent prognostic indicator for gastric cancer. World J Gastroenterol 2009; 15: 1499-1505.
[36] Ming J, Liu N, Gu Y, Qiu X and Wang EH. PRL-3 facilitates angiogenesis and metastasis by increasing ERK phosphorylation and up-regulating the levels and activities of Rho-A/C in lung cancer. Pathology 2009; 41: 118-126.
[37] Ooki A, Yamashita K, Kikuchi S, Sakuramoto S, Katada N and Watanabe M. Phosphatase of regenerating liver-3 as a convergent therapeutic target for lymph node metastasis in esophageal squamous cell carcinoma. Int J Cancer 2010; 127: 543-554.
[38] Navis AC, van den Eijnden M, Schepens JT, Hooft van Huijsduijnen R, Wesseling P and Hendriks WJ. Protein tyrosine phosphatases in glioma biology. Acta Neuropathol 2010; 119: 157-175.
[39] Zhao WB, Li Y, Liu X, Zhang LY and Wang X. Evaluation of PRL-3 expression, and its correlation with angiogenesis and invasion in hepatocellular carcinoma. Int J Mol Med 2008; 22: 187-192.
[40] Xu Y, Zhu M, Zhang S, Liu H, Li T and Qin C. Expression and prognostic value of PRL-3 in human intrahepatic cholangiocarcinoma. Pathol Oncol Res 2010; 16: 169-175.
[41] Wang J, Kirby CE and Herbst R. The tyrosine phosphatase PRL-1 localizes to the endoplasmic reticulum and the mitotic spindle and is required for normal mitosis. J Biol Chem 2002; 277: 46659-46668.
[42] Wang Q, Holmes DI, Powell SM, Lu QL and Waxman J. Analysis of stromal-epithelial interactions in prostate cancer identifies PTPCAAX2 as a potential oncogene. Cancer Lett 2002; 175: 63-69.
[43] Hardy S, Wong NN, Muller WJ, Park M and Tremblay ML. Overexpression of the protein tyrosine phosphatase PRL-2 correlates with breast tumor formation and progression. Cancer Res 2010; 70: 8959-8967.
[44] Tautz L, Pellecchia M and Mustelin T. Targeting the PTPome in human disease. Expert Opin Ther Targets 2006; 10: 157-177.
[45] Wellcome Trust Case Control Consortium. Genome-wide association study of 14,000 cases of seven common diseases and 3,000 shared controls. Nature 2007; 447: 661-678.
[46] Muise AM, Walters T, Wine E, Griffiths AM, Turner D, Duerr RH, Regueiro MD, Ngan BY, Xu W, Sherman PM, Silverberg MS and Rotin D. Protein-tyrosine phosphatase sigma is associated with ulcerative colitis. Curr Biol 2007; 17: 1212-1218.
[47] Todd JA, Walker NM, Cooper JD, Smyth DJ, Downes K, Plagnol V, Bailey R, Nejentsev S, Field SF, Payne F, Lowe CE, Szeszko JS, Hafler JP, Zeitels L, Yang JH, Vella A, Nutland S, Stevens HE, Schuilenburg H, Coleman G, Maisuria M, Meadows W, Smink LJ, Healy B, Burren OS, Lam AA, Ovington NR, Allen J, Adlem E, Leung HT, Wallace C, Howson JM, Guja C, Ionescu-Tirgoviste C, Simmonds MJ, Heward JM, Gough SC, Dunger DB, Wicker LS and Clayton DG. Robust associations of four new chromosome regions from genome-wide analyses of type 1 diabetes. Nat Genet 2007; 39: 857-864.
[48] Dumaual CM, Sandusky GE, Crowell PL and Randall SK. Cellular localization of PRL-1 and PRL-2 gene expression in normal adult human tissues. J Histochem Cytochem 2006; 54: 1401-1412.
[49] Nitadori J, Ishii G, Tsuta K, Yokose T, Murata Y, Kodama T, Nagai K, Kato H and Ochiai A. Immunohistochemical differential diagnosis between large cell neuroendocrine carcinoma and small cell carcinoma by tissue microarray analysis with a large antibody panel. Am J Clin Pathol 2006; 125: 682-692.
[50] Jackel MC, Mitteldorf C, Schweyer S and Fuzesi L. Clinical relevance of Fas (APO-1/CD95) expression in laryngeal squamous cell carcinoma. Head Neck 2001; 23: 646-652.
[51] Kong L, Li Q, Wang L, Liu Z and Sun T. The value and correlation between PRL-3 expression and matrix metalloproteinase activity and expression in human gliomas. Neuropathology 2007; 27: 516-521.
[52] Diamond RH, Peters C, Jung SP, Greenbaum

LE, Haber BA, Silberg DG, Traber PG and Taub R. Expression of PRL-1 nuclear PTPase is associated with proliferation in liver but with differentiation in intestine. Am J Physiol 1996; 271: G121-129.
[53] Rundle CH, Kappen C. Developmental expression of the murine Prl-1 protein tyrosine phosphatase gene. J Exp Zool 1999; 283: 612-617.
[54] Carter DA. Expression of a novel rat protein tyrosine phosphatase gene. Biochim Biophys Acta 1998; 1442: 405-408.
[55] Lu T, Pan Y, Kao SY, Li C, Kohane I, Chan J and Yankner BA. Gene regulation and DNA damage in the ageing human brain. Nature 2004; 429: 883-891.
[56] Zahn JM, Sonu R, Vogel H, Crane E, Mazan-Mamczarz K, Rabkin R, Davis RW, Becker KG, Owen AB and Kim SK. Transcriptional profiling of aging in human muscle reveals a common aging signature. PLoS Genet 2006; 2: e115.
[57] Bischoff-Ferrari HA, Borchers M, Gudat F, Durmuller U, Stahelin HB and Dick W. Vitamin D receptor expression in human muscle tissue decreases with age. J Bone Miner Res 2004; 19: 265-269.
[58] Wang H, Vardy LA, Tan CP, Loo JM, Guo K, Li J, Lim SG, Zhou J, Chng WJ, Ng SB, Li HX and Zeng Q. PCBP1 suppresses the translation of metastasis-associated PRL-3 phosphatase. Cancer Cell 2011; 18: 52-62.
[59] Reich R, Hadar S and Davidson B. Expression and clinical role of protein of regenerating liver (PRL) phosphatases in ovarian carcinoma. Int J Mol Sci 2011; 12: 1133-1145.
[60] Talora C, Sgroi DC, Crum CP and Dotto GP. Specific down-modulation of Notch1 signaling in cervical cancer cells is required for sustained HPV-E6/E7 expression and late steps of malignant transformation. Genes Dev 2002; 16: 2252-2263.
[61] Mimeault M, Batra SK. Divergent molecular mechanisms underlying the pleiotropic functions of macrophage inhibitory cytokine-1 in cancer. J Cell Physiol 2010; 224: 626-635.
[62] Kretzschmar M. Transforming growth factor-beta and breast cancer: Transforming growth factor-beta/SMAD signaling defects and cancer. Breast Cancer Res 2000; 2: 107-115.
[63] Jiang Y, Liu XQ, Rajput A, Geng L, Ongchin M, Zeng Q, Taylor GS and Wang J. Phosphatase PRL-3 is a direct regulatory target of TGFbeta in colon cancer metastasis. Cancer Res 2010; 71: 234-244.
[64] Stephens B, Han H, Hostetter G, Demeure MJ and Von Hoff DD. Small interfering RNA-mediated knockdown of PRL phosphatases results in altered Akt phosphorylation and reduced clonogenicity of pancreatic cancer cells. Mol Cancer Ther 2008; 7: 202-210.

CHAPTER 1. INTRODUCTION

1.1 Phosphorylation in Signal Transduction

Modification of proteins through reversible phosphorylation is the most common form of post-translational modification, with a majority of the proteins in a mammalian cell being subject to phosphorylation at one or more sites (Khoury, Baliban, & Floudas, 2011; Olsen et al., 2006). Addition and removal of phosphate groups regulates protein function through modulation of enzymatic activity, protein stability, cellular localization, and/or protein-protein interactions (Johnson, 2009; Varedi, Ventura, Merajver, & Lin, 2010). It plays critical roles in controlling cellular responses to diverse signals and directs such fundamental biological processes as cell growth, differentiation, metabolism, adhesion, migration, cell cycle regulation, cell-to-cell communication, gene transcription and translation, apoptosis, ion channel activity, neural function, and immune response (Reviewed in: Cans, Mangano, Barila, Neubauer, & Superti-Furga, 2000; den Hertog, 2003; Hunter, 1998; Julien, Dube, Hardy, & Tremblay, 2011).

The phosphorylation state of cellular proteins is governed by the interplay between protein kinase (PK) and protein phosphatase enzymes that, respectively, attach or remove phosphate groups from their target proteins. Initially, it was

believed that protein kinases were the key regulators of phosphorylation-dependent signaling and that protein phosphatases constituted a small group of non-specific scavenger enzymes, which simply functioned as “off” switches to counteract PK effects. It is now appreciated, however, that protein phosphatases are a highly regulated and functionally diverse, multi-member family of enzymes, which carry out specific and active roles in cell signaling. Moreover, members of the protein phosphatase family can, not only, negatively regulate the actions of the PKs, but also potentiate PK signaling, depending on the cellular context. Also, while aberrant phosphorylation due to PK malfunction plays a well established role in the pathogenesis of many human diseases, most notably human cancers, it has become apparent that deregulation of phosphatase function can also lead to disease development and progression. Abnormal protein phosphatase activity has now been linked to a variety of human afflictions, including cancer, diabetes, metabolic syndromes, immune dysfunction, cardiovascular disease, Alzheimer’s and Parkinson’s diseases (Reviewed by: Braithwaite, Voronkov, Stock, & Mouradian, 2012; Cheng, Uetani, Lampron, & Tremblay, 2005; Ducruet, Vogt, Wipf, & Lazo, 2005; Julien et al., 2011; Tautz, Pellecchia, & Mustelin, 2006).

1.2 The Phosphatase Superfamilies

Proteins can be phosphorylated on nine amino acid residues (serine, threonine, tyrosine, cysteine, arginine, lysine, aspartate, glutamate, and histidine) (Hunter, 2004), but in eukaryotic cells, serine, threonine, and tyrosine

phosphorylation predominate (Olsen et al., 2006). The enzymes that dephosphorylate these (serine, threonine, and tyrosine) residues can be broadly classified into three major families (Table 1.1), based on structure, substrate preference, catalytic mechanism, and active site sequence (Moorhead, Trinkle-Mulcahy, & Ulke-Lemee, 2007; Mustelin, 2007). The first family consists of the protein serine/threonine phosphatases; a group of metalloenzymes that require metal ion cofactors for catalytic function and specifically dephosphorylate phosphoserine (pSer) and phosphothreonine (pThr) residues. The second major group is the protein tyrosine phosphatase (PTP) superfamily, which is defined by the active site sequence signature motif $C(X)_5R$ (using one letter amino acid code with X representing any amino acid). This family includes enzymes with substrate preferences for phosphotyrosine (pTyr) alone ("classical PTPs"), as well as a unique class of enzymes, termed dual specificity phosphatases (DSPs), with the ability to dephosphorylate pTyr, pSer, pThr and/or non-proteinaceous substrates. The third family is made up of the Asp-based phosphatases, which are characterized by a catalytic motif containing two aspartate residues (DXDXT/V). This is the most newly identified and recently classified family of phosphatase. Some of the molecules in this group, such as FCP1 [TFIIF-associating C-terminal domain (CTD) phosphatase] and SCP1 (Small CTD Phosphatase) exclusively dephosphorylate phosphoserine and are often classified with the serine/threonine phosphatase family, while others, like the Eyes absent transcription factors (Eya1-4) exhibit tyrosine-specific phosphatase activity and are frequently categorized within the PTP family.

1.2.1 The Serine/Threonine Phosphatase Superfamily

As the family name implies, the protein serine/threonine phosphatases specifically catalyze cleavage of phosphate from serine and threonine residues. All members of this superfamily appear to be metalloenzymes whose catalytic mechanism requires the presence of a dinuclear metal ion cofactor at the active site (Cohen, 2004; W. P. Taylor & Widlanski, 1995). The family can be divided into two further groups known as the PPP (phosphoprotein phosphatase) and PPM (protein phosphatase, Mg^{2+}/Mn^{2+}-dependent) families.

The PPP family consists of the prototypic member Protein Phosphatase 1 (PP1), as well as six other members named PP2A, PP2B (Calcineurin), and PP4-7. All family members share high sequence homology within a ~280 residue stretch of amino acids that contains a conserved catalytic domain and three characteristic sequence motifs (-GDXHG-, -GDXVDRG-, and -GNHE-) (Barford, 1996; Moorhead, De Wever, Templeton, & Kerk, 2009). Each PPP represents a unique catalytic subunit capable of forming diverse multimeric holoenzyme complexes with a wide variety of regulatory, scaffolding, targeting, and inhibitory proteins. It is these interacting partners, rather than the catalytic phosphatase subunits themselves, that drive the subcellular localization and substrate specificity of the PPP enzymes (Hubbard & Cohen, 1993; Pawson & Scott, 1997; Virshup & Shenolikar, 2009).

The PPM family includes PP2C, pyruvate dehydrogenase phosphatase (PDP), and other “PP2C-like” proteins (Cohen, 2004). Although no sequence homology exists between the PPM and PPP family members, structural

comparisons indicate an analogous catalytic mechanism, but with the PPM members specifically requiring Mg^{2+} or Mn^{2+} as their metal ion cofactors (Barford, 1996). The PPM phosphatases are thought to act as monomers and do not have known regulatory subunits. Instead, their protein sequences display a variety of domains that may confer added specificity and function.

1.2.2 The Protein Tyrosine Phosphatase Superfamily

The defining characteristic for members of the protein tyrosine phosphatase (PTP) superfamily, is the presence of a conserved active site signature sequence, $C(X)_5R$, in the catalytic domain, referred to as the PTP Signature Motif. An invariant cysteine residue within the signature motif resides at the bottom of a catalytic pocket and is absolutely required for PTP phosphatase activity (Yuvaniyama, Denu, Dixon, & Saper, 1996). Due to the unique environment of the PTP active site, this cysteine has an unusually low pKa (between 4.5 and 5.5, compared to a pKa of ~8.5 for a typical cysteine residue) (Z. Y. Zhang & Dixon, 1993). This low dissociation constant favors the function of the cysteine as a nucleophile, initiating attack on its phosphosubstrate targets. Other essential residues in the PTP sequence include an aspartic acid residue, outside the signature motif, that acts as a general acid/base (proton donor/proton acceptor) during the enzymatic reaction and an invariant arginine, in the active site motif, that functions in substrate binding and stabilization of the

transition state during phosphoryl displacement (Denu & Dixon, 1998). Unlike the serine/threonine phosphatases, the PTPs do not require metal ions for catalysis.

The general structures of the PTP catalytic domains are highly conserved; therefore specificity of PTP function is often gained through the presence of additional regulatory sequences or domains in the regions flanking the catalytic core. PTP regulatory domains can either directly modify catalytic activity or indirectly influence activity, by targeting the enzymes to particular subcellular locations, substrates, or interacting partners. Some examples of regulatory sequences/domains associated with particular PTP subgroups are listed in Table 1.1. Such domains include, but are not limited to: SH2 domains, which target molecules to phosphotyrosine containing proteins; SH3 domains which bind proline-rich sequences in other proteins; 14-3-3 domains for binding phosphoserine residues in other molecules; nuclear localization signals (NLS) and nuclear export signals (NES) to direct import into and export from the nucleus; and N-terminal myristoylation sequences, CAAX isoprenylation motifs, FERM, C2, and pleckstrin homology (PH) domains for targeting molecules to intracellular membranes or the plasma membrane (Alonso et al., 2004; Hunter, 1998). PTPs can also be modified and regulated post-translationally via a variety of other mechanisms, including phosphorylation, proteolysis, sumoylation, dimerization, and oxidation (den Hertog, Ostman, & Bohmer, 2008; Ostman, Frijhoff, Sandin, & Bohmer, 2011; Soulsby & Bennett, 2009).

Based on sequence and structure, the PTP enzymes are divided into three distinct classes (Table 1.1). The Class I PTPs comprise the so called "classical PTPs", which exclusively dephosphorylate phosphotyrosine residues. This same class also includes the dual specificity phosphatase (DSP) enzymes, whose family members vary considerably in substrate specificity. The Class II PTP family is represented by the small low molecular weight protein tyrosine phosphatases (LMPTP). And Class III is made up of three important cell cycle regulators (CDC25A, CDC25B, CDC25C). Between these three classes, more than 100 human PTPs have now been identified and several of them have demonstrated crucial roles in normal cellular homeostasis, as well as in pathogenesis of a variety of diseases (Cheng et al., 2005; Ducruet et al., 2005; Goldstein, 2002; Julien et al., 2011; Ostman, Hellberg, & Bohmer, 2006; Pulido & Hooft van Huijsduijnen, 2008; Tautz et al., 2006). Despite this, many of the PTP enzymes are largely uncharacterized and their function and biological substrates remain unknown. Further efforts toward defining PTP function will be crucial to understanding the biology of these enzymes and could ultimately lead to the development of novel therapies for disease treatment.

Table 1.1 The Phosphatase Superfamilies and Subfamilies

Phosphatase Family/Subgroup	Number of Members	Example Members	Substrate Specificity	Example Regulatory Domains[1]
I. **Ser/Thr Phosphatase Superfamily**	31			
A. PPP Family	13	PP1, PP2A, PP2B	pSer, pThr	Multi Regulatory Subunits
B. PPM Family	18	PP2C	pSer, pThr	ColBD
II. **PTP Superfamily**	104			
A. Class I Cys-based PTPs	99			
1. Classical PTPs	38			
a. RPTPs	21	CD45, PTPα, LAR	pTyr	FN, CA, Ig, MAM
b. NRPTPs	17	PTP1B, TCPTP, SHP1	pTyr	SH2, FERM, PDZ
2. DSPs	61			
a. MKPs	11	MKP1-5, MKP7, PAC-1	pTyr, pThr	CH2, KIM
b. Slingshots	3	SSH1, SSH2, SSH3	pSer	14-3-3, F-actin, SH3
c. PRLs	3	PRL-1, PRL-2, PRL-3	pTyr, Phosphoinositides	CAAX Box
d. Atypical DSPs	19	VHR, PIR1, STYX	pTyr, pThr, mRNA	SH4, CBD
e. CDC14s	4	CDC14A, CDC14B, KAP	pSer, PThr	NES
f. PTENs	5	PTEN, TPIP, Tensin	D3-Phosphoinositides	C2, PDZ
g. Myotubularins	16	MTM1, MTMR1-15	D3-Phosphoinositides	C2, PH, FYVE, PDZ
B. Class II Cys-based PTPs	2	LMPTP, SSU72	pTyr, pSer	
C. Class III Cys-based PTPs	3	CDC25A, CDC25B, CDC25C	pTyr, pThr	
III. **Asp-based Phosphatases**	13			
A. FCP/SCP Family	8			
1. FCP1	1	FCP1	pSer	BRCT
2. SCP	3	SCP1-3	pSer	
3. FCP/SCP-like	4	TIMM50, Dullard	pSer, pThr	
B. HAD Family	5*	EYA1-4, Chronophin	pTyr, pSer	

[1]Abbreviations: BRCT, Breast Cancer gene 1 (BRCA1) C-Terminus; C2, Protein kinase C, conserved region 2; CA, Carbonic Anhydrase-like; CAAX, Cysteine-Aliphatic-Aliphatic-Any amino acid (Isoprenylation motif); CBD, Carbohydrate Binding Domain; CH2, Cdc25 Homology region 2; ColBD, Collagen Binding Domain; F-actin, Filamentous actin binding domain; FERM, Band 4.1/Ezrin/Radixin/Moesin Homology; FN, Fibronectin-like; FYVE, Fab1/Yotb/Vac1p/Early endosomal antigen-1 homology; Ig, Immunoglobulin-like; KIM, Kinase Interaction Motif; MAM, meprin, A2, RPTPμ homology; NLS, Nuclear Export Signal; PDZ, Postsynaptic density-95/Discs large/ZO1 homology; PH, Pleckstrin Homology; SH2, Src Homology 2; SH3, Src Homology 3; SH4, Src Homology 4 (myristoylation signal). *Although this is a large superfamily of enzymes, so far only chronophin and Eya1-4 have been demonstrated to have protein phosphatase activity. Information included in this table was gathered from the references cited in the text for each phosphatase family..

1.2.2.1 The Class I Cysteine-Based PTPs: Classical PTPs

The Class I cysteine (Cys)-based PTP family, at 99 members, is by far the largest class of PTP. Class I members are divided into two groups: The classical PTPs and the DSPs. These are then further divided into several subgroups on the basis of sequence homology, overall structure, and substrate specificity (Alonso et al., 2004; Moorhead et al., 2007).

The 38 classical PTPs share extensive sequence similarity over an approximately 240-280 amino acid catalytic domain. They are strictly specific for hydrolysis of pTyr residues in protein substrates, due to the presence of a deep (9Å) substrate binding pocket that selectively accommodates the longer phosphotyrosine sidechains. Unlike pTyr, the pSer and pThr side chains are too short to reach the catalytic residues at the base of the pocket (Tonks & Neel, 2001). CD45 and PTP1B are the prototypic examples of the two types of classical PTPs, which include transmembrane, receptor-like PTPs (RPTPs) and non-membrane spanning, cytoplasmic enzymes, referred to as intracellular PTPs or non-receptor PTPs (NRPTPs).

The 21 RPTP enzymes are all type I, membrane spanning proteins, consisting of a variable extracellular domain, a single membrane spanning region, and an intracellular segment containing one or two catalytic domains. In most cases, where two catalytic domains exist, the membrane proximal domain is responsible for the majority of catalytic activity, while the membrane distal domain is either inactive or only weakly active. The function of the low activity domain is unknown, but it has been postulated to play a role in recruitment of

interacting molecules or in regulation of the more active domain (Blanchetot, Tertoolen, Overvoorde, & den Hertog, 2002; Krueger et al., 2003). The extracellular regions of RPTPs vary greatly in length and composition and can be used to further separate the RPTPs into eight smaller groups. Though the specific features of the extracellular segments differ between subgroups, almost all resemble the extracellular domains of cell adhesion molecules and include adhesion-type domains, such as meprin/A5/PTPmu (MAM) domains, fibronectin type-III-like repeats, and immunoglobulin-like domains (Paul & Lombroso, 2003; Tonks, 2006). The functional significance of these domains in the context of the PTPs remains an area of active study, but it appears that they may serve to promote homophilic interactions with identical molecules on adjacent cells (Aricescu et al., 2006; Cismasiu, Denes, Reilander, Michel, & Szedlacsek, 2004). Such interactions would allow the RPTPs to serve as bifunctional molecules, directly linking cell adhesion to intracellular signaling pathways.

The 17 NRPTPs all contain a single catalytic domain and are localized intracellularly. As with the RPTPs, the regions flanking the catalytic domain of NRPTPs are highly variable and contain sequences that, in this case, serve to regulate enzymatic activity, enhance interactions with other proteins, or direct the molecules to specific subcellular locations. For example, PTP1B and T-Cell PTP (TC-PTP) are NRPTPs that each contains a 20 amino acid hydrophobic sequence at their C-termini, which directs them to the cytoplasmic surface of the endoplasmic reticulum (Bourdeau, Dube, & Tremblay, 2005; Simoncic, McGlade, & Tremblay, 2006). This specific localization of the intracellular PTP enzymes

serves a regulatory function, either bringing the phosphatases in contact with or restricting them from their cellular substrates.

1.2.2.2 The Class I Cysteine-based PTPs: DSPs

In addition to the classical PTPs, the Class I family of Cys-based PTPs also contains a heterogeneous group of enzymes referred to as dual specificity phosphatases (DSPs), because the founding members of this class had the capability of dephosphorylating both pTyr and pSer/pThr residues. DSPs have now been identified that can also target non-proteinaceous substrates, including phosphatidylinositol phosphates (Maehama & Dixon, 1998; G. S. Taylor, Maehama, & Dixon, 2000) and mRNA (Deshpande, Takagi, Hao, Buratowski, & Charbonneau, 1999), making this the most diverse class of phosphatase enzymes in terms of substrate specificity. The ability of the DSPs to accommodate phospho-substrates other than pTyr lies in the presence of a shallower and often wider active site cleft for the DSPs than for the Tyr-specific PTPs. These structural differences permit, for example, the shorter side chains of Ser/Thr residues or the bulkier structure of the inositol ring, to access the DSP catalytic core (J. O. Lee et al., 1999; Yuvaniyama et al., 1996).

DSP enzymes are intracellular phosphatases containing a single catalytic domain that is smaller than the conserved domain of the classical tyrosine phosphatases, but includes the PTP signature motif. Outside the catalytic domain, DSP subfamilies bear little resemblance to one another or to any other

PTPs. Even so, all DSPs maintain similar secondary and tertiary structures and utilize the same basic catalytic mechanism as the tyrosine-specific PTPs (Denu & Dixon, 1998). There are a total of 61 DSP family members and these can be further divided into 7 subfamilies on the basis of sequence similarity as well as the presence of specific non-catalytic domain motifs (Alonso et al., 2004; Moorhead et al., 2007). The DSP family members include: 11 MPKs (Bermudez, Pages, & Gimond, 2010), 3 Slingshots (Y. Wang, Shibasaki, & Mizuno, 2005), 3 PRLs (Bessette, Qiu, & Pallen, 2008), 4 CDC14s (Mocciaro & Schiebel, 2010; Poon & Hunter, 1995), 19 Atypical DSPs (Bayon & Alonso, 2010), 5 PTENs (J. O. Lee et al., 1999; Leslie & Downes, 2004), and 16 Myotubularins (Kerk & Moorhead, 2010). The DSP phosphatase family is nicely reviewed by Alonso et al. (Alonso et al., 2004) and Patterson et al. (Patterson, Brummer, O'Brien, & Daly, 2009).

1.2.2.3 The Class II Cysteine-based PTPs

The Class II enzymes are low molecular weight molecules (~18kDa) that contain a minimal PTP signature sequence, which is uniquely found in the extreme N-terminus of the molecule. Aside from the PTP signature motif, these enzymes have little recognizable homology to other PTPs and share some resemblance with bacterial arsenate reductase enzymes (Alonso et al., 2004; Mustelin et al., 1999). Until recently, the Class II PTP family contained only one human member, known as low molecular weight PTP (LMPTP). However, a

second low molecular weight PTP (Ssu72) has recently been identified and, based on overall structure and location of the catalytic domain, was proposed to belong to the LMPTP class (Y. Zhang & Zhang, 2011). While LMPTP displays specificity for pTyr residues, this new, structurally related, family member preferentially dephosphorylates phosphoserine residues. These also exhibit highly distinct roles from one another. LMPTP is involved in control of cytoskeletal rearrangements and cell adhesion (Chiarugi et al., 2000), whereas Ssu72 is a transcriptional regulator that physically interacts with transcription initiation and termination complexes and dephosphorylates the C-terminal domain of RNA polymerase II (Ganem et al., 2003; Y. Zhang & Zhang, 2011).

1.2.2.4 The Class III Cysteine-based PTPs

The Class III family of PTP consists of three cell cycle regulators, CDC25A, CDC25B, and CDC25C. These have dual specificity for pTyr and pThr residues and are responsible for removing inhibitory phosphates from Threonine-Tyrosine motifs at the N-termini of cyclin dependent kinase (Cdk) enzymes. The CDC25s thus act as positive regulators of cell division by dephosphorylating and activating the Cdks, favoring cell cycle progression. The CDC25 enzymes share sequence similarity to bacterial rhodanese enzymes and are thought to have evolved from rhodanese-like proteins (Alonso et al., 2004; Hofmann, Bucher, & Kajava, 1998).

1.2.3 The Asp-based Phosphatase Superfamily

The Asp-based phosphatases carry out dephosphorylation through an unusual mechanism that involves the use of conserved aspartic acid residues in the active site motif (DXDXT/V) to catalyze nucleophilic attack of the phosphate group in a metal-dependent fashion (Moorhead et al., 2007; Rayapureddi et al., 2003). The family is often further divided into the FCP/SCP and HAD (haloacid dehalogenase) families, but both groups share the same conserved active site sequence and catalytic mechanism. The HAD superfamily is actually a much larger family of enzymes, which includes dehalogenases, ATPases, phosphomutases, and phosphonatases (Burroughs, Allen, Dunaway-Mariano, & Aravind, 2006) but, thus far, only five members have been demonstrated to have phosphatase activity. These include four Eyes absent (Eya) proteins which also serve as transcription factors with major roles in development (Rayapureddi et al., 2003) and chronophin which dephosphorylates and activates cofilin, an actin depolymerizing factor essential for cytoskeletal reorganization (Gohla, Birkenfeld, & Bokoch, 2005).

1.3 The PRL Family of Dual Specificity Phosphatase

There are three PRL phosphatases, PRL-1 (also known as PTP4A1 and PTP_{CAAX1}), PRL-2 (also known as PTP4A, PTP4A2, PTP_{CAAX2}, HH13, and OV-1), and PRL-3 (also known as PTP4A3) that constitute a unique DSP subfamily of unknown biological function. They were initially characterized and named, Phosphatase of Regenerating Liver, for the identification of PRL-1 as an

immediate early gene induced in proliferating rat liver during hepatic regeneration (Diamond, Cressman, Laz, Abrams, & Taub, 1994; Mohn et al., 1991). Each PRL enzyme is encoded by a different gene, with the PRL-1 gene found on chromosome 6q12, the PRL-2 gene on chromosome 1p35, and the PRL-3 gene mapping to chromosome 8q24.3 (Montagna, Serova, Sylla, Mattei, & Lenoir, 1996; Y. Peng, Genin, Spinner, Diamond, & Taub, 1998; B. J. Stephens, Han, Gokhale, & Von Hoff, 2005). This family of enzymes is distinctive in that they are among the smallest of the PTPs, having apparent molecular masses of 20-22kDa and consisting primarily of a centrally located catalytic domain that contains the canonical $C(X)_5R$ PTP active site signature sequence (Diamond et al., 1994; Matter et al., 2001; Sun et al., 2005). The PRL family members are further characterized by the presence of a C-terminal CAAX consensus motif, which targets them for post-translational modification by farnesylation (Cates et al., 1996). This post-translational modification is unprecedented among PTPs and is critical to the subcellular localization and biological activity of the PRL enzymes (Si, Zeng, Ng, Hong, & Pallen, 2001; J. Wang, Kirby, & Herbst, 2002; Zeng et al., 2000). The CAAX box is immediately preceded by a polybasic stretch of amino acids, which resembles a bipartite nuclear localization signal, but may instead serve in facilitating membrane interactions (Pascaru et al., 2009; Sun et al., 2007).

Also unique among PTPs is the ability of PRL-1 and PRL-3 to homotrimerize within the cell (Sun et al., 2007; Sun et al., 2005). PRL trimers are structured such that the active sites are facing outward and the C-terminal

farnesylation sites are clustered together on one face, ideally positioned to allow cooperative membrane binding (Jeong et al., 2005). This structure is likely to augment membrane attachment and may also represent a novel mechanism of PTP regulation, given that disruption of trimer formation was found to inhibit the effects of PRL-1 signaling (Sun et al., 2007).

Aside from these hallmarks and a few predicted protein phosphorylation sites (Diamond et al., 1994; Zeng, Hong, & Tan, 1998), the PRL enzymes lack any other apparent regulatory sequences or domains. A schematic representation of the PRL primary structure is displayed in Figure 1.1.

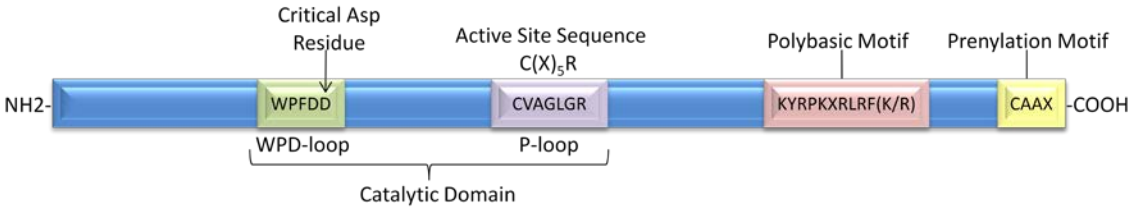

Figure 1.1. Schematic Diagram of Mammalian PRL Protein Primary Structure
The catalytic domain is responsible for the enzymatic activity of the PTPs and contains invariant cysteine (C), arginine (R), and aspartate (D) residues. The polybasic and prenylation motifs are important determinants of the intracellular localization of the proteins. The CAAX box sequence is CCIQ for PRL-1, CCVQ for PRL-2, and CCVM for PRL-3. This figure was created using information from the various references cited in this section of the text.

The full length PRL-1 and PRL-3 proteins are each 173 amino acids in length, while the PRL-2 sequence is slightly shorter at 167 amino acids (Kozlov et al., 2004). All three molecules share a high degree of amino acid sequence similarity with 87% identity between PRL-1 and PRL-2, 76% identity between

PRL-1 and PRL-3, and 75% identity between PRL-2 and PRL-3 (Zeng et al., 1998). In addition, the enzymes are well conserved between species with virtually 100% homology across all characterized mammalian proteins for each PRL (Yarovinsky et al., 2000; Yuan, Chen, Lin, Zhang, & Zhang, 2007). The mammalian enzymes also share at least 50% identity with PRLs found in the fruit fly, *Drosophila melanogaster*; the nematode *Caenorhabditis elegans*; and the protozoan parasite *Trypanosoma cruzi*. In all organisms, the active site sequence is 100% identical and the C-terminal prenylation motif is highly conserved (Cuevas, Rohloff, Sanchez, & Docampo, 2005; Kozlov et al., 2004; Y. Peng et al., 1998). Such remarkable conservation across species suggests an important evolutionary function for this family of enzymes.

Although the three PRL family members are highly similar to one another, they bear very little resemblance to other known PTPs. Sequence alignment suggest their closest relatives to be two DSPs; the cell cycle regulator CDC14 and the lipid phosphatase/tumor suppressor PTEN, each with which the PRLs share less than 30% sequence identity (Kim et al., 2004; Zeng et al., 1998). In contrast, structural alignments show the closest PRL relatives to be VHR (an atypical DSP), MKP, KAP (a member of the CDC14 family), and PTEN (Jeong et al., 2005; Kozlov et al., 2004). Little is currently known about the specific functions of the PRL enzymes and the signal transduction pathways in which they operate, however, their high degree of conservation, as well as their similarity to several DSPs involved in cell cycle and cell growth control, suggests a key role for these PTPs in cellular regulation.

1.3.1 Biological Function of the PRL Enzymes

Little is currently known about the specific functions of the PRL enzymes or the signal transduction pathways in which they participate. Recent evidence, however, suggests that these may be multifaceted molecules involved in a number of diverse biological processes.

The first identified PRL family member, PRL-1, was initially described as an immediate early gene induced as part of the proliferative response in regenerating rat liver after partial hepatectomy (Diamond et al., 1994; Mohn et al., 1991). PRL-1 expression has since been associated with a number of other proliferating cell types, including mitogen stimulated NIH 3T3 mouse fibroblasts (Diamond et al., 1994), mitogen or hepatocarcinogen treated mouse liver (Columbano et al., 1997), cytokine-stimulated human myeloma cells (Fagerli et al., 2008), hormone treated rat reproductive tissues (McLean, Friel, Pouchnik, & Griswold, 2002; Schmidt, de Avila, & McLean, 2006), rat cerebral cortex following transient forebrain ischemia (Takano et al., 1996), developing tissues of diverse origin (Diamond et al., 1996; Haber, Naji, Cressman, & Taub, 1995; W. Kong, Swain, Li, & Diamond, 2000; Rundle & Kappen, 1999), and multiple human tumor cell lines (Diamond et al., 1994; Fagerli et al., 2008; Hardy, Wong, Muller, Park, & Tremblay, 2010; Rouleau et al., 2006; Schwering et al., 2003; J. Wang et al., 2002). The up-regulation of PRL-1 in these instances suggested that it may have a positive role in the growth response. Reinforcing this notion, Wang et al. (2002) found that PRL-1 phosphatase activity is required for normal progression of cells through mitosis and Werner et al. (2003) showed that overexpression of either

PRL-1 or PRL-2 in D27 pancreatic ductal epithelial cells leads to accelerated entry into S phase. Similar results have since been shown for PRL-3 in mouse embryonic fibroblasts (MEFs; Basak et al., 2008) and SW480 colon carcinoma cells (Semba, Mizuuchi, & Yokozaki, 2010).

Further supporting a role for the PRL enzymes in promotion of cell growth and survival, researchers have shown that overexpression of any of the three PRL enzymes in non-tumorigenic cells can lead to enhanced cell growth, altered morphology concomitant with cellular transformation, and tumor formation upon injection of transformed cells into athymic nude mice (Cates et al., 1996; Diamond et al., 1994; Liang et al., 2007; Matter et al., 2001; Semba et al., 2010; X. Wu et al., 2004). Overexpression of either PRL-1 in HeLa cells (Min et al., 2009) or of PRL-3 in an esophageal squamous cell carcinoma (ESCC) cell line (Ooki et al., 2010) also causes inhibition of 5-Fluorouracil treatment-induced apoptosis. In addition, cells overexpressing PRL-2 exhibit reduced requirements for the growth factors erythropoietin and interleukin-3 (Akiyama, Dhavan, & Yi, 2010).

Although all of these results support a positive role for the PRL phosphatases in cell growth regulation, surprisingly, initial analysis of the normal tissue expression of PRL transcripts revealed that all three genes were predominantly expressed in skeletal muscle, a terminally differentiated tissue characterized by permanent withdrawal from the cell cycle (Diamond et al., 1994; Zeng et al., 1998). In addition, further analysis revealed an abundance of PRL transcripts in the brain (PRL-1) (Diamond et al., 1994; Takano et al., 1996) and

cardiac muscle (PRL-3) (Matter et al., 2001) and high levels of PRL-1 protein in the zymogen cells of the stomach and surface enterocytes of the gastrointestinal tract (W. Kong et al., 2000), all tissues/cell types that are considered to have little to no capacity for proliferation. In intestinal epithelium, which contains both proliferating and terminally differentiated cells, PRL-1 and PRL-3 were found only in the differentiated enterocyte villi and not in the proliferating crypt cells (Diamond et al., 1996; Zeng et al., 2000). Consistent with this pattern of expression, PRL-1 mRNA was also exclusively expressed in Caco-2 cells when they were in a differentiated state, but not when they were in a proliferative state (Diamond et al., 1996). Furthermore, Guo et al. (2003) found the PRL-1 gene to be significantly overexpressed in more differentiated parous breast tissues as compared to proliferative nulliparous breast tissues. Finally, Scarloto et al. (2000) demonstrated up-regulation of PRL-1 mRNA in oligodendroglial progenitor cells that are capable of terminal differentiation in comparison to immature oligodendroglial progenitors, which do not terminally differentiate. Taken together, these results suggest a dual role for the PRL enzymes, where they could have growth-associated functions under some circumstances and differentiation-associated functions in others. In keeping with this notion, PRL-1 mRNA was found to be expressed predominantly in proliferating chondrocytes during early development of mouse embryos, but was localized primarily to differentiated, hypertrophic chondrocytes in later stages of mouse development (Rundle & Kappen, 1999).

It is possible that cellular responses to PRL signaling may differ depending on the cell or tissue type. Another possibility is that the amplitude and duration of the PRL signal may govern its action. Along these lines, Diamond et al. reported that small levels of PRL-1 overexpression in NIH 3T3 cells resulted in a transformed phenotype, while higher levels of PRL-1 caused growth cessation (Diamond et al., 1994; Diamond et al., 1996). Similarly, Basak et al. (2008) found that basal expression of PRL-3 in mouse embryonic fibroblasts enhanced cell survival signaling through the PI3K/Akt pathway, whereas high levels of PRL-3 overexpression in the same cell line decreased PI3K/Akt activity and resulted in cell cycle arrest. These results were the first to demonstrate the critical dose-sensitive effects of PRL expression on cell cycle progression and to highlight the importance of properly maintaining basal PRL levels in order to ensure normal cell cycle control.

Overall, the specific actions of the PRLs in various cell types require further clarification. An enhanced understanding of the specific tissue expression patterns of the PRL genes and analysis of the signaling pathways in which they operate may help to further elucidate their natural biological functions.

1.3.2 Subcellular Localization of the PRL Proteins

The subcellular localization of a protein can sometimes provide clues regarding its biological function; however, reports on the intracellular localization of the PRL enzymes have been quite varied. PRL-1 was originally described as a nuclear protein by Diamond et al. (1994) who showed that NIH 3T3 cells

transiently or stably transfected with the enzyme displayed PRL-1 immunoreactivity in both the nucleus and cytoplasm, with the most predominant staining in the nucleus. The same authors found almost exclusively nuclear PRL-1 staining in proliferating rat liver and rat small intestine (Diamond et al., 1996). Subsequent studies, on the other hand, have largely described the PRLs as membrane associated proteins. In transiently transfected CHO cells and stably transfected NIH 3T3 cells, Zeng et al. (2000) found all three PRLs to localize to the plasma membrane and the early endosome. They later extended their study to show that, in stably transfected CHO cells, plasma membrane associated PRL-3 is concentrated at membrane structures such as ruffles, protrusions, and vacuolar-like membrane extensions (Zeng et al., 2003). All of these structures have been affiliated with cell movement and invasion, thus supporting a role for the PRL phosphatases in those processes.

PRL localization to membrane structures, whether it be the plasma membrane, early endosome membrane, nuclear membrane, or the surface of the endoplasmic reticulum, has also been observed in transiently transfected HEK293 cells, HeLa cells, SW480 colon adenocarcinoma cells, HCT-116 colorectal cancer cells, COS-7 cells, and mouse embryonic fibroblasts (Bardelli et al., 2003; Basak et al., 2008; Fiordalisi, Keller, & Cox, 2006; Jeong et al., 2005; Sun et al., 2007; Sun et al., 2005; J. Wang et al., 2002; X. Wu et al., 2004). Each of these studies, though, used overexpression systems, which have the possibility to result in non-physiological localization of a protein. For this reason, J. Wang et al. (2002) decided to examine the subcellular localization of

endogenously expressed PRL-1. In this analysis, they found the cellular distribution of PRL-1 to be cell-cycle dependent, with localization to the ER in non-mitotic HeLa cells and localization to the centrosomes and spindle apparatus in mitotic HeLa cells. Fagerli et al. (2008) also showed a cell-cycle dependent shuttling of endogenous PRL-3 between cellular compartments. In the OH-2 multiple myeloma cell line, PRL-3 was localized in the nucleus during G_0/G_1 phase, but then partially redistributed to the cytoplasm throughout the S and G_2M phases. In addition, Wu et al. (2004) noted that, in PRL-3 overexpressing COS-7 cells, PRL-3 was concentrated in the perinuclear region during interphase and became enriched at the metaphase plate during mitosis. Such data support a role for the PRL enzymes in cell cycle regulation.

Reports of endogenous PRL expression in other cell lines and in tissue sections have been highly incongruous, with some cell or tissue types displaying exclusively or primarily cytoplasmic expression (Dai, Lu, Shou, & Li, 2009; Fagerli et al., 2008; L. Kong, Li, Wang, Liu, & Sun, 2007; B. Stephens, Han, Hostetter, Demeure, & Von Hoff, 2008; Yarovinsky et al., 2000), some showing only membrane localization (Ooki et al., 2010), and others exhibiting a combination of these (J. Li et al., 2005; Ruan et al., 2010; Y. Wang et al., 2007). These data seem to suggest that PRL subcellular localization may be cell or tissue type specific; however, reports within a single tissue type also vary. In a single study, PRL-3 expression was predominantly cytoplasmic in 64% of cervical cancer cases and mostly nuclear in another 36% of cervical cancer specimens. Interestingly, the number of cases exhibiting cytoplasmic staining

was increased in lymph node metastases from these same tumors (Ma & Li, 2011). Also, in a study of developing and adult rat tissues, a number of tissues that showed evidence of cytoplasmic PRL-1 staining early in tissue development (e.g. lung) displayed more highly nuclear patterns of PRL-1 localization in the mature tissues (W. Kong et al., 2000).

Taken together, these data indicate that PRL distribution inside the cell may be influenced by a number of different factors, including cell cycle phase, tissue or cell type, tumor grade, and/or developmental stage. Post-translational modification also appears to be a factor, because treatment of cells with FTIs or expression of farnesylation site mutants in non-mitotic cells causes PRLs to dissociate from membrane structures and redistribute to the cytoplasm and/or nucleus (Fiordalisi et al., 2006; Jeong et al., 2005; Pascaru et al., 2009; Si et al., 2001; Sun et al., 2005; J. Wang et al., 2002; Zeng et al., 2000). Additional investigation will be required to further understand the dynamics of PRL subcellular localization and to elucidate the mechanisms by which the PRLs are translocated within the cell.

1.3.3 PRL Expression in Normal Tissues

As with the subcellular localization of a protein, the tissue and cell type specificity of a molecule can sometimes provide clues that contribute to understanding gene function. Multi-tissue analysis has revealed PRL-3 expression in normal tissues to be somewhat restricted, whereas PRL-1 and PRL-2 appear to be more widely distributed. The various normal tissues where

either positive or negative PRL expression has been observed are listed in Appendix A, Tables A.1 and A.2 respectively.

In normal human and rodent tissues, PRL-3 is preferentially enriched in the heart and skeletal muscle, although it is also expressed at moderate levels in the pancreas and at low levels in various other organs (K. Guo et al., 2006; Matter et al., 2001; X. Wu et al., 2004; Zeng et al., 1998; Zeng et al., 2000). PRL-1 expression has been found at differing levels in the bulk of tissues examined to date with heaviest expression noted in the rat brain, rat skeletal muscle (Diamond et al., 1994; Takano et al., 1996) and human reproductive tissue, small intestine, lung, (Dumaual, Sandusky, Crowell, & Randall, 2006) and developing liver (Gjorloff-Wingren et al., 2000; K. Guo et al., 2006). Tissues with the lowest PRL-1 expression levels include human thyroid and kidney, as well as adult liver tissues from both human and rat (Diamond et al., 1994; Dumaual et al., 2006; K. Guo et al., 2006). Like PRL-1, the tissue distribution of PRL-2 is nearly ubiquitous. The heaviest expression of PRL-2 has been noted in rodent skeletal muscle and heart (Carter, 1998; Zeng et al., 1998) and in human skeletal muscle and thymus (Dumaual et al., 2006; K. Guo et al., 2006; Montagna, Serova, Sylla, Feunteun, & Lenoir, 1995; Z. Zhao et al., 1996). Most tissues express PRL-2 at moderate to high levels, but lower levels of PRL-2 have been observed in human adrenal tissues (Dumaual et al., 2006; K. Guo et al., 2006) and in human and mouse spleen and cerebral cortex (Dumaual et al., 2006; K. Guo et al., 2006; Zeng et al., 1998). Expression of each of the PRLs in normal tissues seems to correlate most often with a differentiated state.

Although widely expressed, PRL-1 and PRL-2 do display very specific patterns of expression. For example, despite the fact that PRL-1 is expressed heavily in regenerating liver tissue, its expression is low to undetectable in most normal, quiescent liver samples (Diamond et al., 1994; Diamond et al., 1996; Dumaual et al., 2006; K. Guo et al., 2006; Haber et al., 1995; W. Kong et al., 2000). Additionally, PRL-1 expression in the primate retina exhibits selectivity in cone-type expression, with PRL-1 protein levels restricted to the red and green light-sensitive photoreceptors and no PRL-1 expression in the blue light-sensitive photoreceptors (Yarovinsky et al., 2000). In the human and rat gastrointestinal tract, PRL-1 exhibits a horizontal gradient of expression with highest levels noted in the proximal small intestine and lower levels in the more distal small intestine and colon (Dumaual et al., 2006; W. Kong et al., 2000). There is also a gradient of PRL expression along the crypt-villus axis of the small intestine, where significantly greater expression of PRL-1 and PRL-3 protein is present in the apical villus enterocytes than in the basal crypt enterocytes. Moreover, PRL-2 is expressed at significantly higher levels in the anterior pituitary glands of male Sprague-Dawley rats than in female rats, possibly suggesting a sexually dimorphic role for PRL-2 in anterior pituitary function (Carter, 1998). In a related manner, increased expression of PRL-1 mRNA was detected in rat Sertoli cells responding to follicule stimulating hormone (FSH) and in rat ovary upon stimulation with FSH and luteinizing hormone (McLean et al., 2002; Schmidt et al., 2006), raising the possibility that PRL expression may be influenced by the levels of specific hormones in particular organs or tissues.

Overall, while the mechanisms behind differential expression of the PRLs remain unclear, the near ubiquitous expression of PRL-1 and PRL-2 in both developing and adult tissues confirms an important cellular role for these molecules and indicates that they may function in regulation of basic physiological processes that are common to many tissues and cell types. The differential expression patterns seen between the three PRL molecules implies that, although the PRL family members are highly homologous, they are likely to be differentially regulated and may even serve divergent functions from one another.

1.3.4 PRL Expression and Cancer

Recent interest in the PRL family members relates to their relationship with cellular proliferation, as accumulating evidence points to a role for these proteins in the promotion of tumorigenesis and metastasis. Functional studies have shown that overexpression of PRL-1, -2, or -3 in varied cell types can lead to rapid cellular growth and a transformed phenotype, as evidenced by altered cell morphology, loss of contact inhibition, and gain of anchorage-independent growth, in culture (Cates et al., 1996; Diamond et al., 1994; Hwang et al., 2012; Matter et al., 2001; Werner et al., 2003). In addition, ectopic expression of any of the PRL phosphatases leads to enhanced cell motility and invasiveness and the ability to induce metastatic tumor formation in athymic nude mice (Akiyama et al., 2010; Fiordalisi et al., 2006; K. Guo et al., 2004; Hardy et al., 2010; Luo, Liang, & Zhang, 2009; Mizuuchi, Semba, Kodama, & Yokozaki, 2009; Nakashima & Lazo,

2010; Sun et al., 2007; Y. Wang & Lazo, 2012; X. Wu et al., 2004; Zeng et al., 2003). Conversely, down-regulation of endogenous PRL by RNA interference (shRNA, siRNA, miRNA) or blockage of PRL activity with small molecule inhibitors or PRL-specific antibodies has the opposite effect, reducing cell growth, abolishing cell invasion, and migration *in vitro*, and suppressing metastatic tumor formation *in vivo* (Achiwa & Lazo, 2007; Ahn et al., 2006; Daouti et al., 2008; Fiordalisi et al., 2006; K. Guo, Tang, Tan, Wang, & Zeng, 2008; Hardy et al., 2010; Kato et al., 2004; Z. Li et al., 2006; Matsukawa et al., 2010; Ming, Liu, Gu, Qiu, & Wang, 2009; Mizuuchi et al., 2009; Nakashima & Lazo, 2010; Ooki et al., 2010; Polato et al., 2005; Qian et al., 2007; B. Stephens et al., 2008; Sun et al., 2007; L. Wang et al., 2009; Y. Wang & Lazo, 2012; Z. Wang et al., 2008; X. Wu et al., 2004; Zhou, Wang, Lu, Li, & Ding, 2009). Expression of a catalytically inactive PRL mutant, a CAAX domain mutant, or a polybasic domain mutant also inhibits the ability of PRL expressing cells to undergo cellular transformation and acquisition of metastatic properties (Fiordalisi et al., 2006; K. Guo et al., 2004; Matter et al., 2001; McParland et al., 2011; Nakashima & Lazo, 2010; Sun et al., 2007; Y. Wang & Lazo, 2012; X. Wu et al., 2004; Zeng et al., 2003). Collectively, these data suggest that PRL expression plays a causal role in tumor cell growth and metastatic progression, rather than simply being a consequence of these events. Moreover, the phosphatase activity and membrane-binding properties of the PRLs are each required for this functionality.

The most well studied PRL family member, in relation to human cancer, is PRL-3. Widespread interest in this gene was generated after Saha et al. (2001)

identified 144 gene transcripts which were up-regulated in liver metastases compared to their matched primary colorectal tumors and discovered that, of 38 transcripts chosen for further analysis, PRL-3 was the only one consistently overexpressed in all 18 metastatic lesions examined. Bardelli et al. (2003) later found that PRL-3 mRNA overexpression was not limited to colorectal cancer (CRC) metastases to the liver, but that PRL-3 is expressed highly in all metastatic lesions derived from CRCs, regardless of the metastatic site (liver, lung, brain, or ovary). A gradient in PRL-3 expression was noted, with low levels of PRL-3 message in normal colorectal epithelium, intermediate levels in the primary CRC tumors, and high expression in each of the liver metastases. A similar trend of increasing PRL-3 expression with increased tumor aggressiveness has since been observed for a number of different tumor types (Fagerli et al., 2008; Guzinska-Ustymowicz, Pryczynicz, & Kemona, 2009; Hao et al., 2010; L. Kong et al., 2007; Z. Li et al., 2006; Lou, Liu, Guo, Lei, & Li, 2012; Ma & Li, 2011; Miskad et al., 2007; Miskad, Semba, Kato, & Yokozaki, 2004; Ooki et al., 2009; Radke et al., 2006; Schwering et al., 2003; Y. Wang et al., 2007; Y. Xu et al., 2010; Zhou et al., 2009). In addition, PRL-3 up-regulation has now been linked to such clinical parameters as tumor size, tumor grade/stage, lymphatic invasion, venous invasion, presence and extent of metastasis, and/or poor patient prognosis, not only in colon/colorectal carcinomas (Hatate et al., 2008; Kato et al., 2004; Mollevi et al., 2008; L. Peng, Ning, Meng, & Shou, 2004; Semba et al., 2010; Y. Wang et al., 2007; Xing et al., 2009), but also in cervical (Ma & Li, 2011), ovarian (Polato et al., 2005; T. Ren et al., 2009), breast (Hao et

al., 2010; Radke et al., 2006; L. Wang et al., 2006), gastric (Dai et al., 2009; Z. R. Li et al., 2007; Miskad et al., 2007; Ooki et al., 2011; Ooki et al., 2009; Pryczynicz, Guzinska-Ustymowicz, Chang, Kisluk, & Kemona, 2010; Z. Wang et al., 2009), non-small cell lung (Ming et al., 2009) esophageal (Y. Q. Liu, Li, Lou, & Lei, 2008; Ooki et al., 2010), nasopharyngeal (Zhou et al., 2009), hepatocellular (W. B. Zhao, Li, Liu, Zhang, & Wang, 2008) and bile duct (Y. Xu et al., 2010) cancers. These data suggest up-regulated PRL-3 expression as a potential prognostic indicator of disease aggressiveness and clinical outcome for multiple tumor types.

Several lines of evidence also point to a role for PRL-3 in angiogenesis, a key process that is required for invasive tumor growth and metastasis. For instance, PRL-3 expression is found in the endothelial cells of multiple tumor types and, in many cases, its expression is up-regulated in tumor endothelium with respect to the endothelium of histologically normal tissues (Bardelli et al., 2003; L. Kong et al., 2007; Miskad et al., 2007; Radke et al., 2006; St Croix et al., 2000). High PRL-3 expression is significantly correlated with increased venous and/or lymphatic invasion in human colorectal (Hatate et al., 2008; Kato et al., 2004; Mollevi et al., 2008; Semba et al., 2010), gastric (Z. R. Li et al., 2007; Miskad et al., 2007; Ooki et al., 2009), cervical (Ma & Li, 2011), bile duct (Y. Xu et al., 2010), and hepatocellular (W. B. Zhao et al., 2008) carcinomas. PRL-3 is capable of enhancing endothelial cell migration *in vitro* (Parker et al., 2004) and of recruiting endothelial cells and promoting vascular formation both *in vitro* and *in vivo* (K. Guo et al., 2006; Parker et al., 2004; Rouleau et al., 2006). In contrast, disruption of PRL-3 activity or expression suppresses vascular formation (J. Xu

et al., 2011). PRL-3 expressing cells injected into the tail veins of nude mice can form highly vascularized micro and macrometastatic solid tumors which can invade already established, host organ blood vessels (K. Guo et al., 2004). Furthermore, PRL-3 expression is positively associated with the expression of several pro-angiogenic factors, such as VEGF, VEGF-C, and ET_AR (Ming et al., 2009; Radke et al., 2006) and negatively associated with anti-angiogenic factors like IL-4 (K. Guo et al., 2006). Finally, in human umbilical vein endothelial cells (HUVECs), VEGF signaling can directly induce PRL-3 transcription (J. Xu et al., 2011). These results have led to speculation that PRL-3 could facilitate the spread of cancer cells by promoting establishment of tumor microvasculature, a requirement for tumor cell expansion. In this capacity, PRL-3 overexpression may be a prerequisite for the development of both local and distant metastatic lesions.

In contrast to PRL-3, PRL-1 and PRL-2 are much less well studied in human malignancies, however there is also evidence linking these two family members to malignant transformation and disease progression. High PRL-1 mRNA levels are found in a variety of tumor cell lines and expression levels in these tumor lines are often higher than those in the respective, non-tumorigenic lines. PRL-1 mRNA is associated with advancing disease in esophageal squamous cell carcinoma (ESCC) patient samples, where it is found at higher levels in ESCC tumor samples than in normal esophageal mucosa and is expressed more frequently in ESCC cases with lymph node metastasis than in those without (Y. Q. Liu et al., 2008). PRL-1 is also more highly expressed in

carcinomas of the stomach and liver than in the matching normal tissues (Dumaual et al., 2011). As with PRL-3, PRL-1 and PRL-2 are both expressed heavily in lymph node metastases from colonic adenocarcinomas, but expressed at lower levels in the primary adenocarcinomas, and often undetectable in colonic adenomas or normal colon sections (Y. Wang et al., 2007). Both PRL-1 and PRL-2, but not PRL-3 are up-regulated in pancreatic cancer cell lines and pancreatic tumor tissues as compared to normal pancreatic tissue (B. Stephens et al., 2008). Moreover, PRL-2 has been associated with tumor progression in breast (Hardy et al., 2010), lung (Hwang et al., 2012), liver (Dumaual et al., 2011) and prostate (Q. Wang, Holmes, Powell, Lu, & Waxman, 2002) carcinomas.

The potential pathogenic role of all three PRLs in the progression of human malignancies makes these enzymes attractive targets for development of novel anti-cancer therapeutics. However, little is currently known about the specific functions of these enzymes or the signal transduction pathways in which they participate. Identification of the signaling pathways in which the PRLs act is an important next step to understanding the biology of these proteins and the role they play in the carcinogenic process.

1.3.5 PRL Substrates and Signaling Pathways

Researchers are just beginning to learn about some of the cellular players with which the PRL phosphatases interact. Nevertheless, there is a lot of work remaining to be done in this arena before the cellular functions of the PRL enzymes are fully understood. The following sections summarize our current

knowledge of the signaling pathways, substrates, and interacting partners of each of the PRL family members. In combination, an overwhelming amount of evidence suggests that the PRL molecules leverage multiple signaling pathways, which exert effects mainly on the cell cycle, cytoskeleton, and cellular adhesions to promote cell proliferation and cell survival and favor the acquisition of invasive and metastatic properties.

1.3.5.1 PRL-1 Substrates and Signaling Pathways

No true *in vivo* substrates for PRL-1 have yet been identified; however PRL-1 does exhibit tyrosine phosphatase activity *in vitro* (Diamond et al., 1994; Yu et al., 2007). To date, it shows strongest activity as an autophosphatase, but it can also slightly dephosphorylate the proto-oncogenic kinase c-Src (Diamond et al., 1994) and the transcription factor ATF-7 (Peters et al., 2001). Although immunoprecipitation experiments have failed to find a direct interaction between PRL-1 and c-Src (Luo et al., 2009), a physical association between PRL-1 and ATF-7 has been confirmed (Peters et al., 2001). ATF-7 (activating transcription factor-7; also called ATF-5 or ATF-X) is a basic leucine zipper transcription factor which can bind cAMP-response (CRE) elements in DNA and functions as a pro-survival factor. Though PRL-1 may, in part, exert its effects through this molecule, the nature of the PRL-1/ATF-7 relationship has not been further characterized.

A number of other PRL-1 binding partners have also been identified. PRL-1 and PRL-3, but not PRL-2 can directly interact with α-tubulin, one of the major components of cytoskeletal microtubules (J. Wang et al., 2002). This association may be required for localization of PRL-1 to the spindle apparatus during mitosis, as suggested by J. Wang et al. (2002). Alternatively, it could be involved in the trafficking of PRL-1 from the ER to the plasma membrane, as has been proposed for K-Ras4B, which, like PRL-1, contains both a post-translational farnesylation motif and a C-terminal polybasic domain (Fu & Casey, 1999; Silvius, 2002). An association between the C-terminal polybasic domain of PRL-1 and several phosphoinositides has also been discovered and may contribute to PRL-1 membrane targeting (Sun et al., 2007). This relationship is completely non-enzymatic as, unlike PRL-3, PRL-1 does not demonstrate any lipid phosphatase activity (Sun et al., 2007; Yu et al., 2007). Other binding partners identified for PRL-1 include PRL-2 (Ewing et al., 2007); TNFα-induced protein 8 (TNFAIP8), a suppressor of TNF-mediated apoptosis (Ewing et al., 2007); the Rho GTPase activating protein (GAP) p115 RhoGAP (Bai et al., 2011); and FKBP38 (peptidyl prolyl cis/trans isomerase FK506-binding protein 38), a molecule which may promote proteosomal degradation of the PRL enzymes (M. S. Choi et al., 2011).

Among these PRL-1 interacting partners, p115 RhoGap (gene symbol ARHGAP4) was the most recently identified (Bai et al., 2011). This molecule is a member of the Slit-Robo (Sr) GAP family of molecules and normally functions to inhibit cell motility through the down-regulation of RhoA and MEKK1, two important mediators of actin cytoskeleton reorganization and cell migration. Bai

et al. (2011) have proposed that a direct physical interaction between PRL-1 and p115 RhoGAP may augment cell motility by both preventing p115 RhoGAP from promoting RhoA deactivation and blocking its inhibitory binding of MEKK1. Not only does PRL-1 co-immunoprecipitate with p115 RhoGAP, but it also co-immunoprecipitates with all other SrGAP family members, with which it interacts through their SH3 domains (Bai et al., 2011).

PRL-1 has also been implicated in a number of other signaling pathways which may contribute to its role in malignant transformation. Several studies indicate that PRL-1 may enhance proliferation by coordinately decreasing expression of negative cell cycle regulators and increasing expression of positive cell cycle regulators. For instance, overexpression of PRL-1 leads to down-regulation of the Cdk inhibitor $p21^{cip1/waf1}$ and up-regulation of the S phase cyclin, Cyclin A, resulting in increased activation of Cdk2 and stimulating early entry into S phase (Hwang et al., 2012; Werner et al., 2003). PRL-1 also participates as part of a negative feedback loop, whereby the tumor suppressor p53 can directly activate transcription of PRL-1, which in turn negatively regulates p53 protein stability through two independent pathways. Upon up-regulation by p53, PRL-1 signaling induces transcription of the early growth response (Egr-1 and Egr-2) transcription factors, which subsequently induce expression of the p53 induced protein with a RING-H2 domain (PIRH2) ubiquitin ligase. PRL-1 also leverages the PI3K/Akt signaling pathway to mediate activation of the mouse double minute 2 (Mdm2) ubiquitin ligase. These events culminate in the ubiquitination and proteosomal degradation of p53 and the inhibition of p53-mediated apoptosis

(Min et al., 2010; Min et al., 2009). Additionally, this causes suppression of the ability of p53 to transactivate both its own promoter and the p21 promoter, providing a potential mechanism for the independently observed PRL-1-mediated reductions in $p21^{cip1/waf1}$ levels (Hwang et al., 2012; Min et al., 2009; Werner et al., 2003).

Recent studies have identified a relationship between the PRLs and various components of the integrin-mediated cell signaling pathways. In response to extracellular matrix proteins, cell surface receptors, known as integrins, use multiple cytoplasmic signaling pathways to regulate G_1 phase cyclins and Cdks and to initiate re-arrangements in the actin cytoskeleton. This dynamic remodeling of the cytoskeleton is central to cell motility, invasion, and metastasis (Assoian, 1997; Reddig & Juliano, 2005; Schwartz & Assoian, 2001). Some of the most well known players in the integrin-mediated cell adhesion signaling pathways include members of the Src family of tyrosine kinases (SFKs), Rho family small GTPases, and focal adhesion complex-related proteins (Huveneers & Danen, 2009). Several independent researchers have now identified a relationship between PRL-1 and a variety of these integrin-responsive players. For example, up-regulation of PRL-1 leads to phosphorylation and activation of Src kinase and focal adhesion kinase (FAK), which results in phosphorylation/activation of the focal adhesion adaptor protein p130Cas and the mitogen activated protein kinase (MAPK) known as extracellular signal-regulated kinase (ERK). Src-induced ERK activation, in turn, can cause AP-1 and Sp1 mediated transcriptional up-regulation of the MMP2 and MMP9

metalloproteinases, which are able to facilitate invasion by degrading the basement membrane and extracellular matrix (Luo et al., 2009). Overexpression of PRL-1 can also lead to increased RhoA and RhoC activity (Fiordalisi et al., 2006; Nakashima & Lazo, 2010) and decreased expression of the adhesion molecules E-cadherin and vinculin (Nakashima & Lazo, 2010). In contrast, down-regulation of PRL-1 has been shown to cause a decrease in c-Src and p130Cas protein levels, a decrease in levels of the focal adhesion component paxillin, and decreased activation of the Rho family proteins Rac1 and Cdc42 (Achiwa & Lazo, 2007). Taken together, these data suggest that PRL-1 may, at least in part, regulate cell proliferation, invasion, motility, and metastasis through downstream effects on both the cell cycle and on mediators of actin cytoskeleton organization and cell adhesion.

1.3.5.2 PRL-2 Substrates and Signaling Pathways

To date, only one confirmed PRL-2 binding partner has been found. PRL-2 and not PRL-1 or PRL-3, can directly interact with the beta subunit of the Rab geranylgeranyltransferase GGTII (βGGTII) in a manner that is dependent both on PRL-2 farnesylation and on a region just upstream of the C-terminal CAAX box that differs in sequence from other PRL family members (Hardy et al., 2010; Si et al., 2001). GGTII functions as an α/β heterodimer and binding of αGGTII and PRL-2 to the β subunit are mutually exclusive events. PRL-2 binding causes displacement of the α subunit and decreases GGTII activity, suggesting that

GGTII function may be regulated by alterations in intracellular αGGTII/PRL-2 ratios (Si et al., 2001). Although PRL-2 can be weakly geranylgeranylated *in vitro*, it is normally farnesylated *in vivo* and is not a substrate of GGTII (Cates et al., 1996; Si et al., 2001). The only known GGTII substrates are the Rab proteins, monomeric G-proteins that are involved in regulation of membrane trafficking and vesicle movement (Stenmark & Olkkonen, 2001), therefore PRL-2 may indirectly function in control of Rab protein prenylation. Given that numerous Rab proteins are localized to endocytic pathways (Agola, Jim, Ward, Basuray, & Wandinger-Ness, 2011; Simpson & Jones, 2005), the presence of PRL-2 in the early endosome (Zeng et al., 2000) would position it well for a role in Rab protein regulation.

A large-scale protein-protein interaction mapping study by Ewing et al. (2007), used immunoprecipitation combined with mass spectrometry (MS) to identify several additional proteins as potential PRL-2 interaction partners. These included PRL-1; farnesyltransferase subunits α and β (FNTA, FNTB); Ephrin Type B Receptor 2 (EPHB2), a molecule involved in neuronal cell signaling; the negative regulator of apoptosis TNFAIP8; upstream transcription factor 2 (USF2), a helix-loop-helix transcription factor; cyclin M3 (CNNM3), a putative metal transporter; and cyclin M4 (CNNM4), another putative metal transporter, with a possible role in sensory neuron function or retinal function. The interaction of PRL-2 with a molecule thought to be involved in cell signaling

within the retina is especially intriguing given that the expression patterns of PRL-1 have also implicated it with a role in retinal cell signaling (Yarovinsky et al., 2000; Yu et al., 2007).

Various cellular changes that occur downstream, following alterations in PRL-2 expression, support the role for this family member in promoting cellular proliferation, cell survival and cell movement. Similar to PRL-1, PRL-2 is involved in cell cycle regulation by promoting the G_1 to S transition through down-regulation of $p21^{cip1/waf1}$, which subsequently results in up-regulation of Cdk2. However, unlike PRL-1, overexpression of PRL-2 does not influence expression of Cyclin A (Werner et al., 2003). Ectopic expression of PRL-2 in a murine pre-B-cell line (Baf3ER) increases expression of Bmi-1, a stem cell marker and promoter of cell survival and proliferation. In the same cell line, ectopic expression of PRL-2 augments phosphorylation of Stat5 in response to growth factor stimulation, suggesting that PRL-2 might provide cells with a heightened sensitivity to growth factors, thus allowing for a more rapid proliferative response (Akiyama et al., 2010). In HeLa and A549 cells, knockdown of PRL-2, using siRNA, causes down-regulation of total and phosphorylated p130Cas. This also leads to cleavage of p130Cas, generating a small fragment of the molecule that is capable of translocating to the nucleus where it functions as a transcriptional repressor and induces cell death (Daouti et al., 2008; Y. Wang & Lazo, 2012). In addition, knockdown of PRL-2 results in cleavage of FAK (Daouti et al., 2008), reduces expression of the focal adhesion component, vinculin, and increases phosphorylation (on Tyr146) of Ezrin, a cytoskeleton/plasma membrane linker

molecule with important roles in cell adhesion and migration (Y. Wang & Lazo, 2012). PRL-2 knockdown also leads to decreased phosphorylation, hence, activation of ERK, whereas ectopic overexpression of PRL-2 induces ERK activation and translocation of ERK to the nucleus where it can up-regulate transcription of target genes (Hardy et al., 2010; Y. Wang & Lazo, 2012). These data suggest a number of potential signaling pathways where PRL-2 may exert its effects; however no physiological substrates for PRL-2 have yet been identified.

1.3.5.3 PRL-3 Substrates and Signaling Pathways

There are several commonalities between the signaling pathways of PRL-3 and PRL-1/PRL-2, indicating at least some functional redundancy between family members. As with PRL-1, PRL-3 associates with α-tubulin (J. Wang et al., 2002), and also with FKBP38 (M. S. Choi et al., 2011). In addition, PRL-3 participates in a similar p53-driven negative feedback loop to PRL-1, where PRL-3 up-regulation by p53 ultimately results in p53 degradation, followed by down-regulation of p21 and culminating in enhanced cell proliferation and cell survival (Basak et al., 2008; Hwang et al., 2012; Min et al., 2010). Studies examining ectopic overexpression of PRL-3 (Basak et al., 2008) or down-regulation of PRL-3 using either RNAi (Jiang et al., 2011) or small molecule inhibitors (L. Wang et al., 2009) have revealed that PRL-3 mediated effects on the cell cycle can also

involve alterations in Akt, Cdk2, Cyclin D, p38 MAPK, the Cdk inhibitor p27, and Foxo3a, a transcriptional activator of p21 and p27.

As with PRL-1, PRL-3 appears to signal through several molecules involved in integrin-mediated cell adhesion signaling and cytoskeletal reorganization, including c-Src, FAK, paxillin, the Rho family GTPases, and the integrins themselves (Daouti et al., 2008; Fiordalisi et al., 2006; Ming et al., 2009; Mizuuchi et al., 2009; L. Wang et al., 2009; X. Wu et al., 2004). PRL-3 can interact directly with the α1 integrin subunit (ITGA1) and, possibly through this interaction, can decrease the tyrosine phosphorylation level of the integrin β1 (ITGB1) subunit (L. Peng et al., 2009). Dephosphorylation of ITGB1 enhances its ability to bind its effector molecules and leads to activation of downstream signal transduction pathways. For example, PRL-3 mediated dephosphorylation of ITGB1 leads to downstream activation of ERK, which promotes the increased expression and hydrolytic activity of MMP2. At the same time, PRL-3 overexpression and ITGB1 dephosphorylation leads to down-regulation of TIMP2, a negative regulator of MMP2 (L. Peng et al., 2009). Overexpression of PRL-3 also causes activation of Src kinase, leading to the phosphorylation and activation of ERK, p130Cas, and Stat3, all alterations which lead to promotion of cell proliferation and migration (Liang et al., 2007). Strikingly, PRL-3 up-regulates Src through an eIF2 (eukaryotic initiation factor 2)-mediated down-regulation of the negative Src regulator, Csk, leading to decreased Src phosphorylation at Tyr527, an inhibitory site (Liang et al., 2008). In contrast, PRL-1 activates Src by enhancing its phosphorylation at Tyr416, an activating

site (Luo et al., 2009), suggesting that, although the PRL family members might target similar molecules/pathways, the mechanisms they employ to control their targets may differ.

Similarities between the PRL-3 and PRL-2 signaling pathways can also be found. As with PRL-2, Ewing et al. (2007) found a direct interaction between PRL-3 and the farnesyltransferase subunits FNTA and FNTB, as well as with the metal transporters CNNM3 and CNNM4. Also, like PRL-2, the expression of PRL-3 is inversely correlated with the phosphorylation level of the cytoskeletal-membrane linker protein Ezrin (Forte et al., 2008; Orsatti, Forte, et al., 2009; Y. Wang & Lazo, 2012). Although a direct interaction between the two molecules has not yet been demonstrated, immunoprecipitated PRL-3 could effectively dephosphorylate immunoprecipitated Ezrin at its Thr567 residue (Forte et al., 2008), indicating that Ezrin may be a direct PRL-3 substrate. Ezrin is a member of the ERM (Ezrin, Radixin, Moesin) family of proteins whose primary role is to serve as an intracellular scaffold between the cell surface receptors and the actin cytoskeleton. ERM family members are capable of recruiting, among other molecules, RhoGEFs (positive Rho regulators) and RhoGDIs (negative Rho regulators) and thus are involved in control of Rho signaling. Phosphorylation of Ezrin at Thr567 is necessary for its activity, suggesting that dephosphorylation at this site by PRL-3 would have an inhibitory effect. Given this, it has been postulated that PRL-3-mediated down-regulation of Ezrin might ultimately lead to promotion of tumor progression through the deregulation of Rho signaling (Forte et al., 2008).

Other molecules which interact with PRL-3 and have been suggested as potential substrates include KRT8, Stathmin, nucleolin, and $PI(4,5)P_2$ (also known as PIP2). KRT8 (Keratin 8) is a cytoskeletal intermediate filament protein whose phosphorylation level at specific serine residues is inversely correlated to PRL-3 expression (Mizuuchi et al., 2009). Stathmin is a microtubule destabilizing protein that can promote cell proliferation and migration and whose expression is positively influenced by PRL-3 (Zheng et al., 2010). Nucleolin (NCL) is a major nucleolar protein involved in a variety of functions, including ribosome assembly, packaging of ribosomal RNA, and organization of nucleolar chromatin. PRL-3 overexpression leads to decreased NCL phosphorylation levels and promotes translocation of NCL to the nucleus where it participates in assembly of the nucleolus (Semba et al., 2010), a structure that is required for cell survival (Hernandez-Verdun, Roussel, & Gebrane-Younes, 2002).

Although direct dephosphorylation of KRT8, Stathmin, and NCL by PRL-3 has not been shown, the phosphatidylinositol phosphate PIP2 is a confirmed PRL-3 substrate. Evidence suggests that PRL-3 is a 5-phosphatase, responsible for removing the phosphate at the 5 position of the inositol ring in $PI(4,5)P_2$ and, to a lesser extent, $PI(3,4,5)P_3$ (McParland et al., 2011). Interestingly, Ezrin requires PIP2 binding to become active at the plasma membrane (Yonemura, Matsui, & Tsukita, 2002) and depletion of PIP2 increases cell motility (McParland et al., 2011), suggesting that PRL-3 also promotes metastatic effects through its lipid phosphatase activity.

A number of other PRL-3 interacting proteins, including CDH22, HDAC4, and EF2 have also been found. CDH22 is a member of the cadherin superfamily of proteins, which promote cell adhesion. PRL-3 overexpression reduces levels of CDH22, while knockdown of PRL-3 results in increased CDH22 levels (Y. Liu et al., 2009). HDAC4 is a histone deacetylase which functions as a negative regulator of transcriptional activity. PRL-3 specifically interacts with HDAC4 and not with other HDAC family members (Zhou et al., 2011), but the result of this interaction has not been studied. EF2 (elongation factor 2) is an actin-binding protein that is part of the translational machinery. Dephosphorylation of EF2, which can occur downstream of PRL-3, is required for its activation (Orsatti, Innocenti, Lo Surdo, Talamo, & Barbato, 2009; Zheng et al., 2010).

PRL-3 also exerts its influence on a diverse array of other signaling molecules. PRL-3 inhibits mobilization of intracellular calcium transients induced by angiotensin II (AngII) and may block AngII-mediated phosphorylation of p130Cas (Matter et al., 2001). PRL-3 overexpression up-regulates the $Ca2^{++}$ activated K^+ channel KCNN4 in an NF_KB-dependent manner, leading to KCNN4-regulated changes that support cellular proliferation (Lai et al., 2011). PRL-3 promotes vascular and lymphatic vessel formation by up-regulating pro-angiogenic factors such as VEGF and VEGF-C (Ming et al., 2009) and down-regulating anti-angiogenic factors like IL-4 (K. Guo et al., 2006). Furthermore, PRL-3 exerts its anti-apoptotic effects through alterations in expression of a number of pro-survival factors including Akt, mcl-1, cIAP1, and xIAP (Jiang et al., 2011; Min et al., 2010; Zhou et al., 2011).

Epithelial-mesenchymal transition (EMT) is an important process, during tumor progression, by which epithelial cells acquire mesenchymal fibroblast-like properties, exhibit reduced cell-cell adhesion, and display increased motility (Sipos & Galamb, 2012). The recognition that the phenotypic changes induced by stable expression of any of the three PRL molecules in non-tumorigenic epithelial cells are characteristic of EMT led to the theory that the PRL molecules may be major drivers of epithelial to mesenchymal transition. In support of this theory, overexpression of PRL-3 was found to initiate a chain of events involving down-regulation of PTEN, activation of PI3K/Akt signaling, and deactivation of GSK3β (glycogen synthase kinase 3β), leading to accumulation of the mesenchymal marker and transcription factor Snail concomitant with transcriptional repression of epithelial markers such as E-Cadherin, γ-catenin, cytokeratin, and integrin β3. Further supporting a role for PRL-3 in the initiation of EMT, PRL-3 overexpression also causes down-regulation of specific cell adhesion markers (e.g. paxillin and vinculin) and up-regulation of other mesenchymal markers (e.g. fibronectin and vimentin) in addition to Snail (Y. Liu et al., 2009; Mizuuchi et al., 2009; H. Wang et al., 2007).

Upstream effectors/regulators of PRL-3 signaling include FKBP38 (M. S. Choi et al., 2011), p53 (Fontemaggi et al., 2002; Min et al., 2010), and the PRL-3 family member p73α (Fontemaggi et al., 2002). Additionally, VEGF can promote the transcription of PRL-3 through the transcription factor MEF2C (J. Xu et al., 2011). Snail can also bind the PRL-3 promoter and up-regulate its activity (Zheng et al., 2011). TGFβ signaling promotes binding of Smad3 and Smad4 to

the PRL-3 promoter, suppressing PRL-3 promoter activity (Jiang et al., 2011). Lastly, poly(C)-RNA-binding protein 1 (PCBP1) was recently identified as a negative regulator of PRL-3 expression that can bind the 5’ UTR of PRL-3 mRNA and partially block protein translation (H. Wang et al., 2011).

CHAPTER 2. RESEARCH GOALS AND DISSERTATION FORMAT

An overwhelming amount of evidence suggests that the PRL phosphatases are multi-functional enzymes capable of signaling through a diverse number of interconnected pathways to trigger events that promote cellular proliferation, survival, and metastatic transformation. However, despite many recent advances in our understanding of the molecular players with which the PRL phosphatases interact, the specific functional roles of these enzymes and the underlying mechanisms by which they exert their effects are still poorly understood. This is true, in particular for PRL-1 and PRL-2, which have been much less studied than PRL-3. Therefore, I undertook the present study with the goal of expanding our knowledge about the cellular functions of the PRL family and the roles these enzymes play in the progression of human disease. Toward this goal, the specific aims of my dissertation research were to 1.) Characterize the tissue distribution and cell-type specific localization of PRL-1 and PRL-2 gene expression in normal human tissues, 2.) Compare the gene expression patterns of PRL-1 and PRL-2 between normal and diseased human tissues, and 3.) Globally identify and analyze possible signaling pathways in which the PRL-1 phosphatase may operate.

This dissertation includes three manuscripts that support each of my research goals. Two of these manuscripts are published and can be found in the 'Publications' section immediately preceding the introduction with supplementary material that supports these publications found in Chapter 4. The remaining manuscript, which is currently in preparation, can be found in its entirety in Chapter 7 with supporting information included in Chapters 5-6 and 8.

Goal 1: Examination of PRL Expression in Normal Human Tissues

The correlation of PRL expression with growth in some cellular systems and differentiation in others suggests that the PRL enzymes may have different roles depending on the tissue or cell type. Given this, characterization of the tissues and cell types that express the PRL genes is important to elucidating their physiological function and to providing a baseline for understanding their roles in the pathogenesis of disease.

While multi-tissue analysis revealed normal PRL-3 expression in humans to be largely confined to the heart and skeletal muscle (Matter et al., 2001; Zeng et al., 1998), PRL-1 and PRL-2 were reported to be more widely expressed (Diamond et al., 1994; K. Guo et al., 2006; Montagna et al., 1995). However, when I began my research, studies of normal PRL-1 or PRL-2 expression were largely limited to rodent tissues or to human cell lines and tissue northern blots (See Appendix Tables A.1 and A.2), which lack information on expression in specific microanatomical structures. Therefore, I sought to characterize the cellular localization and tissue distribution of PRL-1 and PRL-2 mRNA in a broad

range of normal adult human tissues using *in situ* hybridization (ISH). This technique provided the ability to pinpoint the exact cell-types which contribute to PRL-1 and -2 normal tissue expression

The results of this analysis were reported in a publication entitled: *Cellular localization of PRL-1 and PRL-2 gene expression in normal adult human tissues*. In addition, Chapter 4 of this dissertation contains supplemental information to support the reported work.

Goal 2: Comparison of PRL Expression in Normal and Diseased Tissues

There is clear evidence demonstrating that all three PRL enzymes can promote tumor progression *in vitro* and the literature now abounds with information regarding PRL-3 expression in human tumors and its positive correlation to increasing tumor aggressiveness and poor patient prognosis (Reviewed in: Bessette et al., 2008). Few studies, however, have examined the expression of PRL-1 or PRL-2 in human malignancies. In fact, at the onset of my research, there was only one other report examining either of these family members in human tumor samples (PRL-2; Q. Wang et al., 2002). Therefore, I sought to provide further insight into the role that PRL-1 and PRL-2 play in the development and progression of human disease by using ISH to examine expression of these molecules in a large panel (342 specimens) of human tissues of diverse tissue origin and to compare their expression profiles in normal versus diseased samples.

Provided that cell line and murine studies show an important role for PRL-1 and PRL-2 in tumor formation, invasion, and metastasis and given the abundant evidence linking PRL-3 to disease progression in multiple tumor types, I hypothesized that, like PRL-3, PRL-1 and PRL-2 expression would be up-regulated in a majority of human tumor tissues and might correlate with advanced stages of disease. Moreover, because PTPs, in general, have been connected to a variety of diseases other than cancer and PRL-3 over-expression in mouse models has been linked to cardiovascular disease, I hypothesized that aberrant expression of PRL-1 and PRL-2 may also be detected in human diseases other than cancer.

The results of this research were published in a manuscript entitled: *Tissue-specific alterations of PRL-1 and PRL-2 expression in cancer*. Additional supporting information is included in Chapter 4 of this dissertation.

Goal 3: Perform an Unbiased Examination of PRL Signaling Pathways

The normal physiological role of the PRL phosphatases remains an important, unanswered question. Their association with differentiation in some contexts and with proliferation in others raises the possibility that these enzymes may serve multiple functions within the cell. Their variable subcellular localization and the diverse array of signaling molecules to which they have now been connected seem to support this notion. An increased understanding of the signaling pathways in which the PRLs are involved and the substrates on which

they act will be required in order to elucidate both their normal functions and the processes by which they promote tumorigenesis and metastasis.

While knowledge surrounding PRL-mediated signaling events has been greatly enhanced through focused investigations on individual genes and isolated pathways, there is an increasing appreciation that cellular processes are governed by a complex interplay between multiple signaling networks. Moreover, what is known about PRL signaling to date suggests that we are unlikely to be successful in assigning these molecules to any single target pathway. "Omics" techniques offer the advantage of obtaining an unbiased and more global view of the changes that are occurring, as well as the opportunity to identify previously unforeseen players that are responding, with respect to a particular stimulus. Therefore, I used microarray gene expression profiling (transcriptomics) to more broadly examine the alterations that occur in response to PRL overexpression in HEK293 cells and to attempt to identify pathways and transcripts that might be responsive to changes in PRL levels. Additionally, because microRNAs (miRNAs) are emerging as key regulators of gene expression (Carthew, 2006), I also employed miRNA expression profiling to examine the effects of PRL overexpression on the miRNAome.

My primary interest for this portion of my studies was in the PRL-1 pathway, because this molecule displayed highly variable expression patterns in the ISH analysis of both normal and tumor tissues, while PRL-2 tended to be ubiquitously and heavily expressed in almost every tissue type examined and PRL-3 is known to have a limited expression profile. Therefore, I focused the

majority of my efforts on the transcriptional and miRNA profiling of PRL-1; however, because of its well known role in cancer progression, PRL-3 was also examined. Given prior knowledge of the PRL signaling pathways, I hypothesized that genes directly involved in cell movement, cell adhesion, and cell cycle regulation would be the primary targets influenced by PRL overexpression and that the use of Omics techniques would uncover previously undiscovered players involved in PRL-mediated signaling.

The analysis results for the PRL-1 expression profiling are included in a draft manuscript which is found in Chapter 7, with additional, supporting information included in Chapters 5-6 and 8 of this dissertation. The PRL-1 microRNA results are included in Chapter 9 and the PRL-3 results are presented in Chapters 10-11.

The potential involvement of all 3 PRLs in the progression of human malignancies makes them attractive targets for generation of novel anti-cancer therapeutics. The work described in this dissertation will contribute to the understanding of the biological functions of the PRL phosphatases and to the role they play in the development and progression of human disease.

CHAPTER 3. MATERIALS AND METHODS

3.1 Tissue Procurement

Human tissue samples were obtained from the Cooperative Human Tissue Network, National Disease Research Interchange, and Indiana University School of Medicine, Department of Pathology. Samples were collected in accordance with the guidelines of Indiana University with approval from the IUPUI Institutional Review Board. Specimens were fixed in 10% neutral buffered formalin, processed, and embedded in paraffin. Serial sections, 5μm thick, were cut and mounted on Fisherbrand Superfrost/Plus slides (Fisher Scientific, Pittsburgh, PA). Where available, the medical histories of the patients and pathological reports for each specimen were reviewed. Tissue sections of each specimen were then stained with Hematoxylin and Eosin and were examined by a pathologist (Dr. George E. Sandusky), with no prior knowledge of the available patient data, to confirm histopathologic diagnosis and tumor grading. For all cases, representative tissue sections were chosen for *in situ* hybridization (ISH).

3.2 Generation of Oligonucleotide Probes

Specific 45-mer, oligonucleotide probes for PRL-1 and PRL-2 mRNA were designed using the Hybridization Probes Search option of Oligo Primer Analysis Software (Molecular Biology Insights, Cascade, CO). The oligonucleotide sequences were verified using a BLAST search of EMBL and GenBank databases to ensure that there was no significant homology with other mRNA species. All chosen sequences showed a 100% homology with the target PRL-1 or PRL-2 sequence and no significant homology with any other known sequences. The PRL-1 probe mapped to PRL-1 with 100% identity over the full probe sequence ($E = 4 \times 10^{-17}$), while the first non-target sequence showed 100% identity over only 17 of the 45 nucleotides with an e-value of 8.3. The PRL-2 probe mapped to PRL-2 with 100% identity over the full probe sequence ($E = 4 \times 10^{-17}$) and the first non-target sequence displayed 95% identity over 20 nucleotides (E = 2.1).

Probes were custom synthesized by Midland Certified Reagent Company Inc. (Midland, TX) using cyanoethyl phosporamidite chemistry. Probes were labeled with fluorescein isothiocyanate (FITC) at both the 5' and 3' ends and were purified by Reversed Phase HPLC. The PRL-1 (5'-GGC CAA CAG AAA AGA AGT GCA CTG AGG TTT ACC CCA TCC AGG TCA-3') and PRL-2 (5'-TGG CAA ATA AAA AGT GTG AGC GTG CGT GTG AGT GTG ATG GGG AAA-3') antisense probes are complementary to nucleotides 150-194 and 19-63 of the human PRL-1 (GenBank U48296) and PRL-2 (GenBank U48297) mRNA

sequences, respectively. Corresponding control, sense oligonucleotides for PRL-1 and PRL-2 were also generated.

3.3 Slot Blot Hybridization

Slot blot hybridization was performed to verify the specificity of the oligonucleotide probes. PRL-1 cDNA and PRL-2 cDNA, both cloned in pUC19 vectors (Cates et al., 1996) and PRL-3 cDNA, in a pET-15b vector (a gift from Millenium Pharmaceuticals, Inc., Cambridge, MA), were linearized with BamHI (New England Biolabs, Beverly, MA). The resulting restriction fragments were analyzed on a 1% agarose gel, run at 75V (constant voltage) for 45-60 min in 1X TAE buffer (40mM Tris Acetate, pH 8.3, 10mM EDTA). Density profiling of the gel image was carried out with Scion Image Acquisition and Analysis Software, Beta 4.02 for Windows (Scion Corporation, Frederick, MD) and was used to estimate the amount of DNA in each lane for sample normalization.

Linearized DNA samples of 100ng, 50ng, 10ng, and 5ng each, were denatured by the addition of 0.4M NaOH and 10mM EDTA and by heating for 10 min at 100°C. Samples were then neutralized with an equal volume of cold 2M ammonium acetate, pH 7.0. Two-hundred microliters of each denatured DNA solution was spotted on a nitrocellulose membrane (Protran, Schleicher & Schuell Bioscience, Keene, NH) using a Bio-Dot SF Microfiltration Apparatus (BIO-RAD, Hercules, CA), according to the manufacturer's instructions. Samples were immobilized on the membrane using a Stratalinker Ultraviolet (UV) Crosslinker 1800 (Stratagene, La Jolla, CA). Slot-blots were prehybridized for 30

min at 37°C in pre-warmed Sigma PerfectHyb Plus hybridization buffer (Sigma-Aldrich, St. Louis, MO), followed by hybridization with FITC-labeled oligonucleotide antisense probes for PRL-1 and PRL-2, diluted to 100ng/ml in pre-warmed PerfectHyb Plus buffer. Hybridization was allowed to proceed overnight (16hr) at 37°C in a rotating hybridization oven (Hybridization Oven 640, Affymetrix, Santa Clara, CA). Post hybridization, membranes were washed two times for five minutes each in 2 X SSC (300mM NaCl, 30mM Sodium Citrate, pH 7.0) + 0.1% SDS at room temperature (RT), followed by one 20 min wash in 0.5X SSC (75mM NaCl, 7.5mM Sodium Citrate, pH 7.0) + 0.1% SDS at 37°C, and a five minute wash at RT in TBST (50mM Tris-HCL, 150mM NaCl, pH 7.6 plus 0.05% Tween-20). Prior to detection, membranes were blocked for two hours with 3% BSA in TBST and additionally, for 30 min with Serum Free Protein Block (DAKO Corporation, Carpenteria, CA). FITC-labeled probes were detected for 30 min using a mouse, anti-FITC primary antibody (DAKO) diluted 1:1000 in DAKO Antibody Diluent, followed by Peroxidase Link and Peroxidase-Conjugated Streptavidin Label (10 min each) from the DAKO Labeled Streptavidin-Biotin 2 (LSAB2) kit. Reactions were visualized using the DAKO 3, 3'-diaminobenzadine (DAB) substrate chromogen system. Development was allowed to occur for five minutes and the reactions were stopped by rinsing membranes in TBST, followed by distilled water. Membranes were washed three times, five minutes each, in TBST, between each step of the procedure.

3.4 Non-radioactive *In Situ* Hybridization

Paraffin sections were baked in a 60°C oven for four hours and subsequently dewaxed in xylene and rehydrated through a graded series of ethanol (100%, 95%, and 75%; two changes, five minutes each) to water. Slides were placed in an OmniSlide Slide Rack (ThermoHybaid, Ashford, Middlesex, UK) and tissue sections were encircled with a ImmEdge hydrophobic barrier pen (Vector Laboratories, Burlingame, CA), then covered with 1X PBS (D-PBS, Gibco BRL, Gaithersburg, MD).

Sections were permeabilized with 200μl of 10μg/ml, nuclease-free Proteinase K (Sigma-Aldrich) in 1X PBS at 37°C using an OmniSlide Thermal Cycler and Humidity Chamber (ThermoHybaid). The optimal length of time for Proteinase K digestion was determined empirically for each tissue type (see Chapter 4 for results). The deproteination reaction was stopped by washing slides two times, three minutes each in Nanopure (Chesterland, OH) ultrapure water. Slides were subsequently dehydrated by sequential washes in 95% and 100% ethanol (three minutes each) and allowed to air dry for one hour RT. Tissue sections were hybridized with 50μl of 750 ng/ml PRL-1, PRL-2, or control probe in PerfectHyb Plus hybridization buffer, sealed with parafilm, and hybridized 12-14 hr at 37°C in a humidity chamber. Coverslips were dislodged and non-specifically bound probe was removed by soaking slides for 5 min each in two changes of 2X SSC + 0.1% SDS at RT with gentle agitation. Slides were then washed stringently in pre-warmed 0.5X SSC + 0.1% SDS at 37°C for 20 min, followed by a 10 min rinse in TBS + 0.1% SDS at RT.

3.5 Histochemical Detection of Hybridized Probes

Detection of hybridized probe was performed by standard immunohistochemical techniques, using a catalyzed signal amplification procedure. All staining steps were performed on a DAKO Autostainer at room temperature and slides were rinsed for five minutes in TBST between each step of the procedure. Normal and diseased tissue sections from one organ type were always processed simultaneously.

Non-specific background staining was blocked by incubation with DAKO Serum-Free Protein Block for 30 min, followed by a 30 min incubation with mouse anti-FITC primary antibody (DAKO), diluted to 22 μg/ml in DAKO Antibody Diluent. Bound primary antibody was detected using the LSAB2 method combined with the Renaissance Tyramide Signal Amplification (TSA Biotin, PerkinElmer Life Sciences, Inc., Boston, MA) kit. Briefly, slides were incubated sequentially with DAKO LSAB2 Peroxidase Link for 30 min, DAKO LSAB2 Label for 10 min, Biotinyl Tyramide (TSA Biotin System) diluted 1:50 in the kit provided 1X Amplification Diluent for 10 min, and DAKO LSAB2 Label again for 10 min. The antibody complexes were visualized using DAB as the chromogenic substrate. Development was allowed to proceed for 2-5 minutes and was stopped by rinsing the slides in distilled water. Following immunohistochemical detection, sections were counterstained briefly with 1X Lerner's hematoxylin, dehydrated through graded alcohols (95%, 100%, two changes, one minute each), cleared in xylene (two changes, two minutes each), and coverslipped with permanent mounting media (Fisher Scientific).

3.6 Analysis of ISH Results

Evaluation of slides was performed under brightfield microscopy. All sections of a particular tissue type were stained and analyzed in a single run and are therefore directly comparable. The tissue distribution, localization pattern, intensity of staining, and the percentage of positive cells were evaluated with the aid of an experienced pathologist (Dr. George E. Sandusky), in a blinded fashion. The appearance of a brownish-red stain over the cells was used to indicate probe hybridization and thus reflect the cellular levels of PRL-1 and PRL-2 mRNA. The localization pattern was evaluated as cytoplasmic, nuclear, membranous, or a combination of these. Immunostaining was scored using established methods (Jackel, Mitteldorf, Schweyer, & Fuzesi, 2001; Nitadori et al., 2006). Briefly, staining intensity was classified according to the following scale: (-) absent, (+/-) barely detectable, (+) weak, (++) moderate, and (+++) strong. In cases of heterogeneous staining, the average intensity across the tissue was taken as the score. Also, in a few cases where a patient sample was stained twice, the case was given a mean score, based on evaluation of the two sections. The percentage of positive cells was estimated as the number of stained cells, per total number of cells counted. For semiquantitative analysis, the staining intensity was assigned an arbitrary value, on a scale of 0-3, as follows: (-) = 0, (+/-) = 0.5, (+) =1, (++) = 2, (+++) = 3. An overall staining score (SS) was calculated for each sample, by multiplying the staining intensity times the percentage of positive cells. After multiplication of both values, results were graded from 0 (negative) to 300 (almost all cells display strong staining).

To confirm the reproducibility of the analysis, 25% of the slides were randomly chosen and scored twice. Duplicate slides gave similar results. Images were acquired using a SPOT digital camera and imaging software (Diagnostic Instruments, Inc., Sterling Heights, MI).

Statistical calculations were executed by a qualified statistician (Dr. Han Weng Soo) using Statistical Analysis System software (SAS version 8.2, SAS Institute, Inc., Cary, NC). Analyses of differences in PRL expression between cancerous and noncancerous tissues were performed using a Student's paired t-test. Results are expressed as mean $\pm$ standard error of the mean (SEM) and $p < 0.05$ was considered statistically significant. For most samples, the medical histories of the patients and pathological reports for each specimen were also available. These were reviewed and correlations between PRL expression and patient clinicopathological features such as patient age and gender; tumor type, subtype, and grade; and presence of local or distant metastasis were calculated using a mixed model analysis of variance. Again, $p < 0.05$ was deemed statistically significant. GraphPad PRISM, version 5.0 (GraphPad Software Inc., La Jolla, CA) was used, by me, for visual representation of the results.

3.7 Cell Lines and Cell Culture

Human embryonic kidney 293 (HEK293) cells stably overexpressing PRL-1, PRL-3, empty pcDNA4 vector (PRL-1 control), or empty pcDNA3 vector (PRL-3 control) were generously provided by Dr. Zhong-Yin Zhang's laboratory (Department of Biochemistry and Molecular Biology, Indiana University School of

Medicine, Indianapolis, IN). Cells were grown in 100 mm plates in Dulbecco's Modified Eagle's Medium (DMEM) supplemented with 10% fetal bovine serum (Thermo Scientific HyClone, Logan, UT), 50units/ml penicillin (Mediatech, Inc., Manassas, VA), and 50μg/ml streptomycin (Mediatech).

H1299 human non-small cell lung carcinoma cells transiently transfected with PRL-3 or empty pcDNA3 vector were generated with the help of Dr. Martin L. Smith's laboratory at the Indiana University Melvin and Bren Simon Cancer Center (Indianapolis, IN). Plasmid DNA used for the transfections was provided by Dr. Zhong-Yin Zhang. H1299 cells were grown to 10-15% confluency in DMEM supplemented with 10% fetal bovine serum. Transfections were performed using FuGENE HD Transfection Reagent (Roche Diagnostics, Mannheim, Germany) as per the manufacturer's instructions. After 48hrs the media was removed, TRIzol reagent was added, and samples were stored frozen at -80°C until ready for RNA extraction.

3.8 RNA Extraction and RNA Quality Assessment

Total RNA was extracted from HEK293 cells stably transfected with PRL-1 (HEK293-PRL-1), PRL-3 (HEK293-PRL-3), or their respective empty vector controls (HEK293-vector), using the TRIzol reagent (Invitrogen Life Technologies, Carlsbad, CA). For microarray analysis and RT-PCR, the RNA was further purified with an RNeasy Mini Kit (Qiagen Inc., Valencia, CA), following manufacturer's instructions. For microRNA analysis, this column purification step was omitted. RNA integrity and yield were assessed by determining sample

absorbance at 260 and 280 nm on a DU640B spectrophotometer (Beckman Coulter, Brea, CA) and by subjecting samples to the Agilent 2100 Bioanalyzer (Agilent Technologies, Inc., Santa Clara, CA), using the Agilent RNA 6000 Nano LabChip Kit as directed.

3.9 Gene Expression Microarray

Gene expression profiling was carried out according to the protocol described in the Affymetrix GeneChip Expression Analysis Technical Manual. Briefly, 5μg of each cleaned, total RNA extracted from cultured HEK293-PRL-1, HEK293-PRL-3, and HEK293-vector control cells was used to generate double-stranded cDNA, by reverse transcription, using a Superscript Double-Stranded cDNA Synthesis Kit (Invitrogen Life Technologies) and a GeneChip T7-Oligo(dT) Promoter Primer Kit (Affymetrix). Following second-strand synthesis, cDNA was cleaned with a GeneChip Sample Cleanup Module (Affymetrix), and then used as a template for synthesis of biotinylated cRNA with the Enzo BioArray HighYield RNA Transcript Labeling Kit (Enzo Life Sciences, Farmingdale, NY). Labeled cRNA was cleaned with a GeneChip Sample Cleanup Module, fragmented, and hybridized overnight to HG-U133 Plus 2.0 GeneChip Human Genome Arrays (Affymetrix). Following hybridization, GeneChips were washed, stained with streptavidin phycoerythrin (Molecular Probes, a subsidiary of Life Technologies, Carlsbad, CA), and scanned using the Affymetrix GeneChip Scanner 3000 7G. Raw image (CEL file) generation and analysis was performed

using the Affymetrix GeneChip Operating System (GCOS). All RNA samples and arrays met Affymetrix recommendations for standard quality control metrics.

Microarray data analysis for the PRL-1 stable transfectants was performed by a bioinformatician (Dr. Boyd A. Steere). Data files were processed with R-project software (http://www.r-project.org/), version 2.13.1 through the RStudio interface version 0.94.92 (http://www.rstudio.org). The intensity values were read using the "affy" library of the Bioconductor package (Gentleman et al., 2004), version 2.8. Normalization and calls were made using the mas5 procedure under default parameters. After transformation into a $\log_2$ scale, mean normalized expression values were calculated for both of the experimental comparison groups (HEK293-PRL-1 and HEK293-vector). Differential expression between the two groups was determined for each probeset and assessed for significance in terms of p-value by the Student's t-test. Multiple-testing false discovery rate (FDR) correction values were calculated using the Benjamini-Hochberg procedure.

Data analysis for all other samples was carried out by myself, using multiple methods, including Bioconductor, as described above, Partek Genomics Suite version 6.11.1115 (Partek Inc., St. Louis, MO), and the MultiExperiment Viewer (MeV) data analysis application (Dana Farber Cancer Institute, Boston, MA). In all cases, raw data image files were normalized using the Robust Multichip Average (RMA) method and a student's paired t-test was performed to look for significant differences between groups. FDR correction values were calculated using both the Benjamini-Hochberg and the Bonferroni procedures.

The lists of significantly differentially expressed genes that were generated by each of the analysis tools were scrutinized for consistent changes.

3.10 Functional Profiling of Significantly Changing Transcripts

Functional/pathway profiling was performed to gain an understanding of the biological context behind genes whose mRNA expression was measured, by microarray, to be significantly altered with PRL-1 overexpression. This analysis was performed by Dr. Boyd A. Steere, using the significant gene lists from the microarray and miRNA analysis, in the following manner:

Two input data sets of the mRNA microarray results were prepared by applying significance cutoffs of $q \leq 0.20$ and $q \leq 0.50$ to the detected differentially-expressed probesets. These data sets, consisting of 58 and 2263 probesets respectively, included each probeset's Affymetrix ID, associated gene Entrez ID, fold change, and the p-value and FDR-corrected q-value of that change. Using both input data sets, enriched biological functions and pathways were determined using three systems: Ingenuity Pathway Analysis (IPA; Ingenuity Systems; www.ingenuity.com) core analysis, application build version 162820, content version 12710793 with default settings; the Enrichment and Interactome workflows of MetaCore from GeneGo, Inc. (www.genego.com/metacore.php) version 6.8 with default settings; and the Database for Annotation, Visualization, and Integrated Discovery (DAVID) functional annotation and gene function classification tools, version 6.7 (Dennis et al., 2003).

3.11 Quantitative RT-PCR for Selection of Endogenous Controls

Selection of endogenous controls for quantitative, real time, reverse transcription PCR (qRT-PCR) data analysis was performed using a TaqMan Low Density Endogenous Control Panel (Applied Biosystems, a subsidiary of Life Technologies, Carlsbad, CA), which contains 16 human control genes. Total RNA isolated from HEK293-PRL-1, HEK293-PRL-3, and HEK293-vector samples was treated with DNase I, using the Ambion TURBO DNA-free kit from Invitrogen Life Technologies and 1.5μg of each sample was reverse transcribed into cDNA with the SuperScript III First-Strand Synthesis System and random hexamer primers (Invitrogen Life Technologies), in accordance with the manufacturer's guidelines. The resulting cDNAs were combined with TaqMan Gene Expression Master Mix (Applied Biosystems) and 100ng cDNA was added to each well of a TaqMan Endogenous Control Array following the manufacturer's protocol. Samples were amplified by PCR on an Applied Biosystems 7900HT Fast Real-Time PCR System using universal cycling conditions (2 min at 50ºC, 10 min at 95°C and 40 cycles of 15 sec at 95°C for denaturation and 1 min at 60°C for annealing/extension). Raw threshold cycle (Ct) values were obtained using Sequence Detection System (SDS) Software v2.4 (Applied Biosystems; will be referred to in this document as SDSS to avoid confusion with Sodium Dodecyl Phosphate). C_t values ≥ 40 were set to 40 and were considered not detectable. DataAssist Software, v2.0 (Applied Biosystems) was used to examine the stability of the candidate endogenous controls across all samples. Microsoft Excel 2007 (Microsoft Corporation, Redmond, WA) was also used to calculate

the standard deviation across all measurements for each gene. The genes with the best stability scores and lowest standard deviation were selected as candidate endogenous controls for further qRT-PCR analysis. Data analysis for this section was performed fully by me.

3.12 Quantitative RT-PCR for detection of PRL-1 and PRL-3

Total RNA isolated from HEK293-PRL-1, HEK293-PRL-3, and HEK293-vector samples was treated with DNase I, using the Ambion TURBO DNA-free kit and 4μg of each sample was reverse transcribed into cDNA with the SuperScript III First-Strand Synthesis System and random hexamer primers, in accordance with the manufacturer's guidelines. The resulting cDNA was used as template for qRT-PCR using commercially available TaqMan Gene Expression Assays (Applied Biosystems,) for PRL-1 (Assay ID: Hs01109144_m1), PRL-3 (Hs02341134_m1), 18S (Hs99999901_s1), and UBC (Hs00824723_m1). For PRL-1 and UBC only, a pre-amplification step was performed using the TaqMan PreAmp Master Mix Kit (Applied Biosystems) according to the manufacturer's protocol. Briefly, 250ng of each cDNA was combined with 2X Taqman PreAmp Master Mix and a pooled mix of the PRL-1 and UBC TaqMan assays, each at 0.2X. Samples were pre-amplified using a GeneAmp PCR System 9700 (Applied Biosystems) and the following cycling conditions: 95°C for 10min, followed by 10 cycles of 95°C for 15 sec and 60°C for 4 min. Pre-amplified products were diluted 1:5 in 1X TE. Twenty-five microliters of diluted, pre-amplified product (for PRL-1 and UBC) or 100ng of non-amplified cDNA (for

PRL-3 and 18S) was combined with 2X TaqMan Gene Expression Master Mix and the corresponding 20X TaqMan Gene Expression Assay in triplicate wells of a 96-well PCR plate. PCR amplification and detection were carried out on an Applied Biosystems 7900HT Fast Real-Time PCR System under the universal cycling conditions. Raw Ct values were obtained using SDSS v2.4. Ct values ≥ 40 were set to 40 and were considered not detectable. DataAssist Software, v2.0 was used, by me, to verify the stability of the selected endogenous controls. Microsoft Excel 2007 was used to calculate relative fold change (FC) using the comparative Ct method ($\Delta\Delta$Ct) and either UBC (PRL-1) or 18S (PRL-3) as the endogenous control. GraphPad PRISM, version 5.0 was used for visual representation of the results.

3.13 Quantitative RT-PCR Custom Arrays

A set of 184 genes, identified by microarray as differentially regulated or associated in the literature with signaling pathways involved in integrin-mediated cell signaling, cytoskeletal remodeling, and/or cell motility, was chosen for validation of gene expression changes using qRT-PCR. Total RNA from HEK293-PRL-1 and HEK293-vector cell lines was treated with DNase I, using the Ambion TURBO DNA-free kit and 1μg of each sample was reverse transcribed into cDNA with the SuperScript III First-Strand Synthesis System and random hexamer primers, in accordance with the manufacturer's guidelines. The resulting cDNA was used as template for qRT-PCR using commercially available TaqMan Gene Expression Assays (Applied Biosystems) custom arrayed on 96-

well plates (92 experimental genes and 4 candidate endogenous controls: GAPDH, UBC, 18S, B2M per plate). See Chapter 7 for a full gene list and associated Assay IDs. As per the manufacturer's protocol, cDNAs were combined with TaqMan Gene Expression Master Mix and 100ng cDNA was added to each well of the custom TaqMan Array Plate and amplified by PCR on an Applied Biosystems 7900HT Fast Real-Time PCR System under the universal cycling conditions. Raw Ct values were obtained using SDSS v2.4. Ct values ≥ 40 were set to 40 and were considered not detectable. DataAssist Software, v2.0 was used to examine the stability of the candidate endogenous controls and the gene with the lowest stability score across all tested samples was chosen for use in data normalization.

Mean normalized Ct values for each assay over all biological replicates were calculated by Dr. Boyd A. Steere using Partek Genomics Suite version 6.11.1115 under default parameters. Differential expression between the two comparison groups was determined for each assay using the $\Delta\Delta$Ct method and was calculated by me, using Microsoft Excel. Comparative statistical analysis was then performed by Dr. Boyd A. Steere, in Partek Genomics Suite using the Student's t-test.

3.14 MicroRNA Profiling

MicroRNA (also called miRNA) expression was evaluated using TaqMan Array Human microRNA cards A and B, version 2.0 (Applied Biosystems), which measure the expression levels of 664 microRNAs. One thousand nanograms

each of total RNA from cultured HEK293-PRL-1, HEK293-PRL-3, and HEK293-vector control lines was subjected to reverse transcription using a TaqMan MicroRNA Reverse Transcription Kit (Applied Biosystems) with Megaplex Reverse Transcription Primers (Human Pools A and B v2.0; Applied Biosystems) following the manufacturer's protocol. Reverse transcription was carried out on an Applied Biosystems GeneAmp PCR System 9700 thermal cycler with the following conditions: 40 cycles of 16°C for 2 min, 42ºC for 1 min, and 50ºC for 1 sec, followed by an incubation at 85°C for 5 min to inactivate the reverse transcriptase. The resulting products were diluted with RNase-free water and combined with TaqMan Universal PCR Master Mix (Applied Biosystems), after which 100μl of each sample was loaded onto TaqMan Array Human MicroRNA Card Sets A and B v2.0 (Applied Biosystems). Per manufacturer's instructions, qRT-PCR was carried out on an Applied Biosystems 7900HT Fast Real-Time PCR System using the default thermal-cycling conditions for 384-well TaqMan Low Density Arrays. Raw Ct values were obtained using SDSS v2.4. Ct values ≥ 40 were set to 40 and were considered not detectable.

Raw miRNA data files were processed using Partek Genomics Suite version 6.11.1115 under default parameters. Expression levels of the small nuclear RNA MammU6 were used as the endogenous control for data normalization. Mean normalized Ct values for each of the 664 assays over all biological replicates for each of the experimental comparison groups were calculated. Differential expression between the two comparison groups was determined for each assay and assessed for significance in terms of p-value by

the Student's t-test. Multiple-testing FDR correction values were calculated using the Benjamini-Hochberg procedure. PRL-1 data analysis was carried out by Dr. Boyd A. Steere and PRL-3 data analysis was carried out by me.

3.15 miRNA Target Prediction

Prediction of mRNA targets for the assayed miRNAs was performed through the use of IPA and through use of the MiROR database (Friedman, Naamati, & Linial, 2010). Target prediction and analysis for the PRL-1 associated samples was performed by Dr. Boyd A. Steere and target prediction for the PRL-3 associated samples was performed by me.

3.16 Functional Profiling of miRNA Targets

The full list of predicted mRNA targets for each significantly differentially expressed miRNA was used as input for functional/pathway analysis using a combination of four systems: IPA software core analysis, application build version 162820, content version 12710793 with default settings; the Enrichment and Interactome workflows of MetaCore, version 6.8 with default settings; the PathWay Express tool from Wayne State University's Onto-Tools (Khatri, Draghici, Ostermeier, & Krawetz, 2002); and the DAVID Functional Annotation and Gene Function Classification tools version 6.7 (Dennis et al., 2003). These analyses were performed by both Dr. Boyd A. Steere and me.

3.17 miRNA/mRNA Data Integration

For the PRL-1 samples, integration of significant results from the mRNA and miRNA expression profiling studies was performed by Dr. Boyd A. Steere using the expression pairing function of the IPA software. For the PRL-3 samples, I used both IPA and Partek Genomics Suite Software to perform this analysis. Each data set was scrutinized to look for significantly changing mRNAs whose expression was inversely correlated to significantly changing miRNAs that are predicted to target them.

3.18 Western Blotting

HEK293-PRL-1 and HEK293-vector cells were grown to 80% confluency then rinsed with 1X PBS and lysed in RIPA Buffer (Thermo Scientific, Rockford, IL) plus 1X Halt Protease and Phosphatase Inhibitor Cocktail (Thermo Scientific). Cell lysates were sonicated for 5min at 4°C in a Branson 2510 sonicator (Thomas Scientific, Swedesboro, NJ), then centrifuged at 21,000 x g for 20 min at 4 C. Supernatant protein concentrations were determined using the Pierce BCA Protein Assay Kit (Thermo Scientific) and a SpectraMax Plus Microplate Spectrophotometer (Molecular Devices, Sunnyvale, CA), both according to the manufacturer's protocols. Samples were mixed 1:1 with 6X Laemmli reducing sample buffer (Boston Bioproducts, Ashland, MA) and 15μg of each sample was resolved using NuPAGE 4-12% Bis-Tris gels and NuPAGE 1X MOPS Running Buffer (Invitrogen Life Technologies). Samples were electro-transferred to nitrocellulose membranes using the iBlot Western Blotting System (Invitrogen

Life Technologies) and membranes were blocked for 1 hr in either 5% BSA or 5% nonfat dry milk (according to the manufacturer's instructions for each antibody) in 1X TBST. Blots were incubated in primary antibody at 4°C overnight, washed 4X, 2-3 min in TBST, incubated in secondary antibody for 1 hr at room temperature, and rinsed 4X, 2-3 min each in TBST again. Membranes were developed using the Pierce SuperSignal West Femto Maximum Sensitivity Substrate (Thermo Scientific) or Pierce SuperSignal West Pico Chemiluminescent Substrate (Thermo Scientific) depending on the primary antibody used. Images were captured using an ImageQuant LAS-4000 imager (GE Healthcare, Uppsala, Sweden). GAPDH was used as a loading control. Stripping of blots was performed using Pierce, Restore Western Blot Stripping Buffer (Thermo Scientific) according to the manufacturer's recommendations.

Antibodies (and the dilution used) included: RhoA (1:1000); Src (1:1000); Phospho-Src (Tyr527) (1:1000); Phospho-Src (Tyr416) (1:1000); Non-phospho-Src (Tyr527) (1:1000); Non-phospho-Src (Tyr416) (1:1000); p44/42 MAPK (ERK1/2, 1:1000); Phospho-p44/42 MAPK (Thr202/Tyr204) (1:1000); SAPK/JNK (1:1000); Phospho-SAPK/JNK (Thr183/Tyr185) (1:1000); PAK1 (1:1000); Phospho-PAK1 (Ser144)/PAK2 (Ser141) (1:1000); Anti-rabbit IgG, HRP-linked (1:1000); Anti-mouse IgG, HRP-linked (1:1000); GAPDH, HRP-linked (1:1000). All antibodies were purchased from Cell Signaling Technology (Danvers, MA). All primary antibodies have specificity for human sequences.

CHAPTER 4. IN SITU HYBRIDIZATON PROTOCOL OPTIMIZATION AND CONTROLS

4.1 Introduction

Most studies examining the tissue distribution of PRL-1 and PRL-2 have been conducted on rodent tissues, while reports on human samples have been largely limited to tissue northern blots. Tissue analysis performed at this level does distinguish between functionally different cell types in the tissue and, further, the results could reflect gene expression in contaminating cell types (e.g. stromal fibroblasts, inflammatory cells, or vascular cells) rather than the tissue proper. Therefore, I sought to characterize the cellular localization and tissue distribution of PRL-1 and PRL-2 in a large panel of normal and diseased human tissues of diverse origin using *in situ* hybridization. The results of this analysis are presented in my publications entitled *Cellular localization of PRL-1 and PRL-2 gene expression in normal adult human tissues* and *Tissue-specific alterations of PRL-1 and PRL-2 expression in cancer*. Additional information to support these two publications is included here.

Before beginning the ISH analysis, it was important to establish the appropriate assay conditions for each individual tissue type. Tissue samples used in this study were all obtained from archival, formalin-fixed, paraffin-embedded (FFPE) tissue blocks. While the process of formalin-fixation serves to

preserve tissue architecture, it leads to formation of biomolecular cross-links that can chemically mask proteins and nucleic acids (Gilbert et al., 2007). Due to this cross-linking, proteolytic digestion by an enzyme such as Proteinase K is often required to permeabilize the tissue and allow access of ISH probes and detection reagents to their target sites. Some tissue types are more sensitive to protease digestion than others; therefore, the appropriate Proteinase K digestion time for each tissue must be determined empirically such that a proper balance can be found to allow for increased permeability and signal enhancement without causing loss of tissue morphology. To determine the optimal Proteinase K incubation time for each tissue type, a time course of Proteinase K exposure was performed on two purchased multi-tissue arrays (Normal Tissue Checkerboard and Normal Sausage) from Biogenex (Fremont, CA) along with several self made tissue arrays (generated using the tissue samples described in the methods section). Protease treated samples were hybridized with the PRL-2 oligonucleotide probe or a poly d(T) probe (Novocastra Laboratories, New Castle upon Tyne, UK), detected using standard immunohistochemical procedures, and examined under brightfield microscopy to compare staining intensity and tissue integrity.

Besides assay optimization, it was also important to define suitable controls that could be used to verify the functionality and specificity of the assay. Therefore, a number of controls were selected and their performance was examined across multiple tissue types.

4.2 Results

As expected, different tissue types showed a large amount of variability in their susceptibility to Proteinase K digestion. Tissues such as lung, prostate, and gall bladder were particularly sensitive to proteolysis, while tissues such as uterus, ovary, brain, and cervix required the longest incubation times. Table 4.1 summarizes the optimal Proteinase K incubation times determined for each tissue type.

A variety of different tissues were examined to locate a sample that could be used as a good positive control for both PRL-1 and PRL-2 expression. While many tissues displayed variable expression patterns from specimen to specimen, particularly for PRL-1, the majority of normal and tumor tissues from the pancreas stained heavily for both markers. Therefore, select cases from this tissue type were chosen as positive controls to be run with each sample set and used in verification of the hybridization and detection procedure. Representative examples are shown in Figure 4.1A and B.

To verify the presence and examine the integrity of mRNA in each sample, a second positive control was used. This consisted of a fluorescein-conjugated poly d(T) probe, purchased from Novocastra Laboratories for the detection of total mRNA poly A tails. A weak or absent signal from this probe is an indication that the tissue RNA is heavily degraded. An example of this is shown in Figure 4.2.

A number of negative assay controls were also selected. These included: (a) omission of the oligonucleotide probes from the hybridization mixture and

incubation of the tissue specimens with hybridization buffer alone (Figure 4.1D), (b) substitution of the specific antisense probe with an equivalent concentration of labeled sense probe to examine the stringency of the assay (Figure 4.3), (c) hybridization using a cocktail of randomly generated, FITC-conjugated, oligonucleotide sequences (NCL-CONTROL, Novocastra), to assess binding of nonspecific sequences (Figure 4.1C), and (d) Pretreatment of tissue sections with 250μg/ml RNase A to demonstrate the specificity of the signal for single stranded RNA (Figure 4.4).

Throughout the remainder of the study, selected controls were run on serial sections of the same tissues as examined with the PRL-1 and PRL-2 probes, using the same detection procedures.

Table 4.1 Optimal incubation times for ISH tissue permeabilization
Incubation times were determined by performing a time course of Proteinase K exposure on several multi-tissue arrays then probing for PRL-2 and poly d(T) expression.

Tissue Type	Incubation Time (min)
Adrenal Gland	20
Appendix	7
Bladder	10
Brain	20
Breast	10
Cervix	20
Colon	10
Coronary Artery	15
Eye	5
Gall Bladder	5
Heart	7
Kidney	10
Liver	15
Lung	5
Lymph Node	20
Ovary	20
Pancreas	7
Parathyroid	20
Placenta	20
Prostate	5
Skeletal Muscle	5
Skin	10
Small Intestine	10
Spleen	10
Stomach	10
Testis	10
Thyroid	20
Tongue	20
Uterus	20

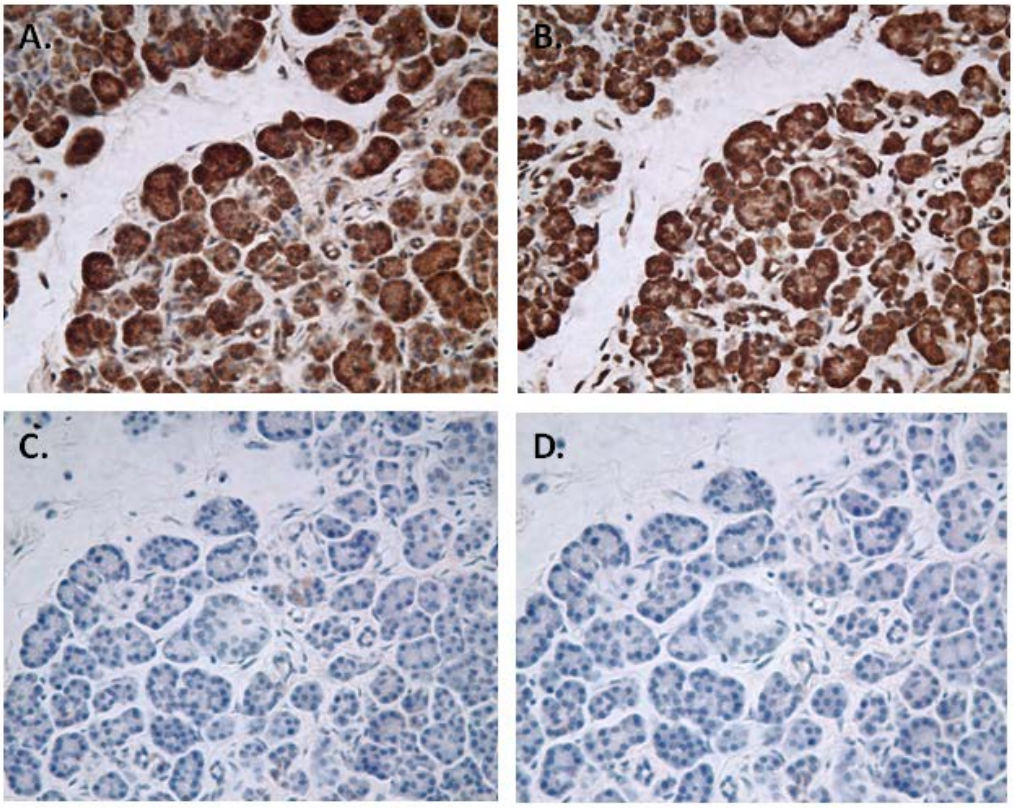

Figure 4.1 Positive and negative ISH controls
Serial sections of a normal human pancreas tissue (Case No. 2141) were hybridized with (A) PRL-1 antisense probe, (B) PRL-2 antisense probe, (C) random oligonucleotide sequences (NCL-CONTROL, Novocastra), or (D) hybridization buffer in the absence of any probe.

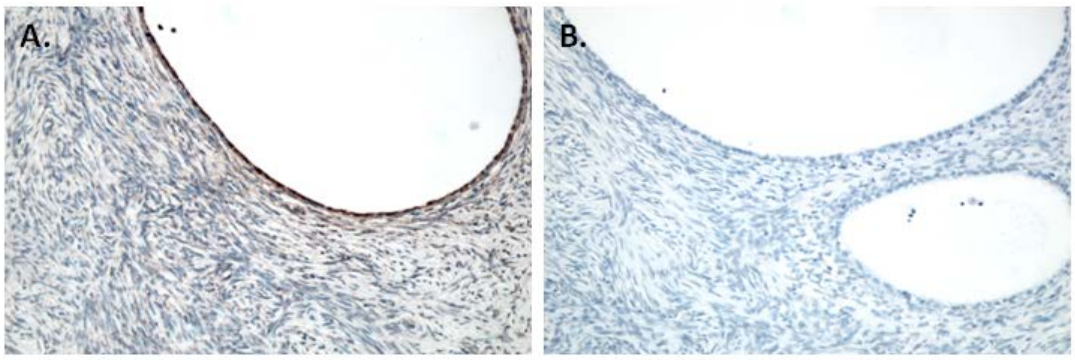

Figure 4.2 Poly d(T) control
(A) Hybridization of a poly d(T) probe to a normal ovarian tissue specimen (Case No. 9912C004) verifies the presence of mRNA in the sample. (B) Hybridization of the same poly d(T) probe to a normal ovarian tissue sample from another subject (Case No. 2242002) indicates that the RNA in this sample has been completely degraded, thus, this tissue would not be suitable for ISH analysis.

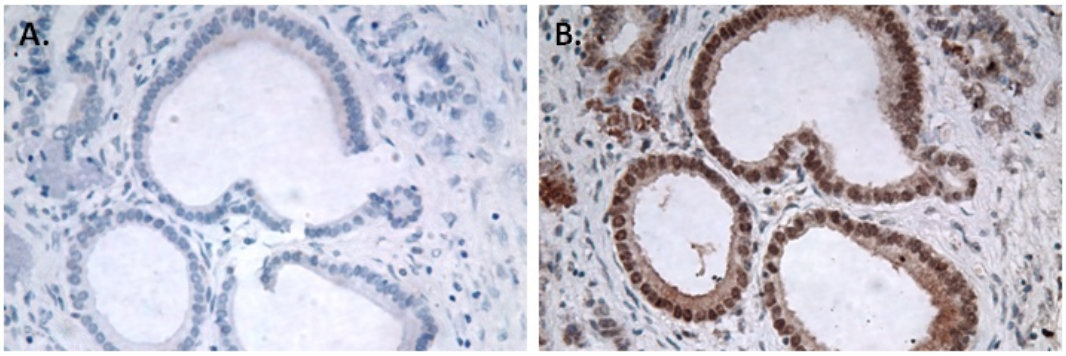

Figure 4.3 Sense and antisense hybridization probes
A pancreatic ductal adenocarcinoma tumor specimen (Case No. 2979B) was hybridized with (A) sense or (B) antisense oligonucleotide probe for PRL-1.

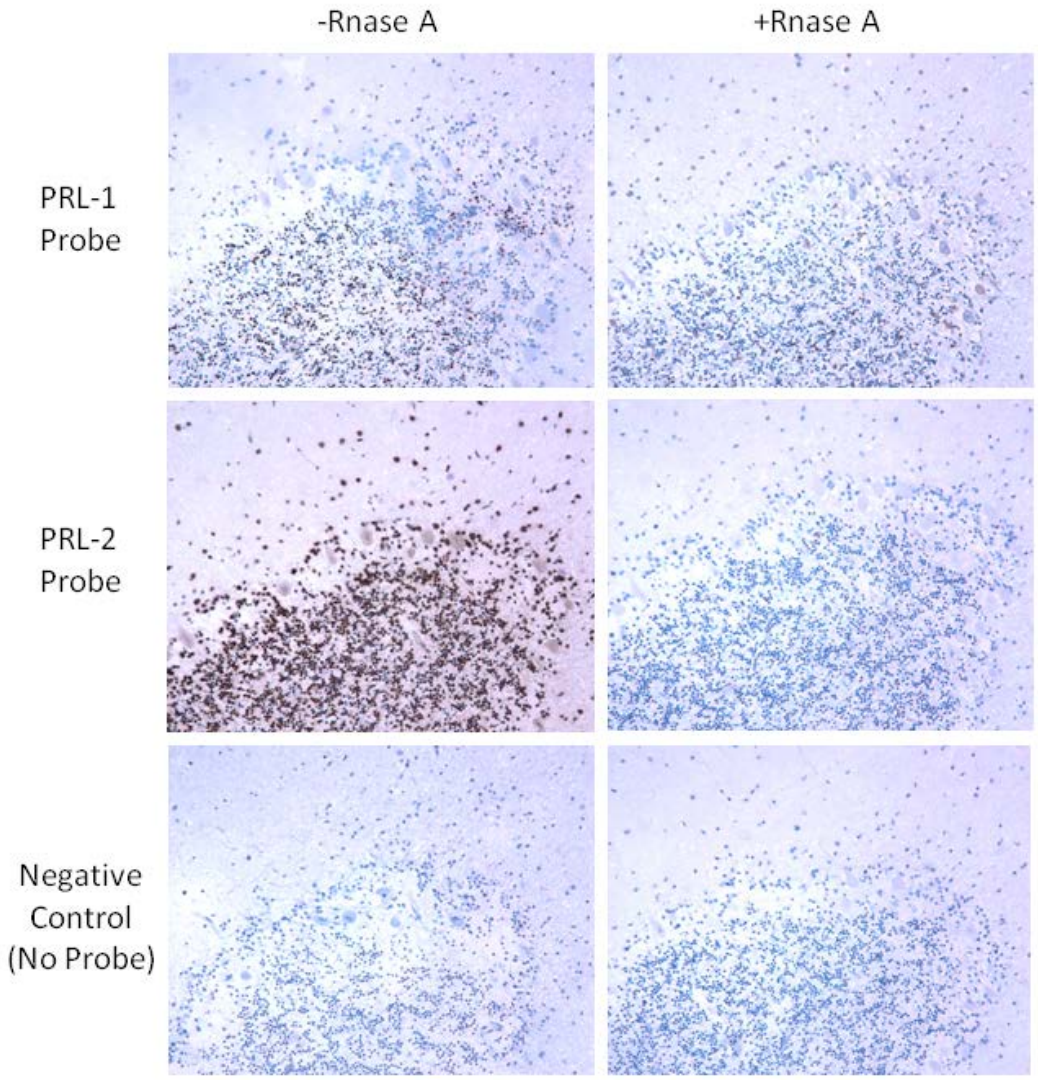

Figure 4.4 RNase pre-treatment
Pre-treatment of tissue samples with RNase A prior to hybridization of specific antisense probe results in near to complete abolishment of the hybridization signal. Serial sections taken from normal human cerebellum (Case No. 3011) are shown.

4.3 Discussion

Assay optimization and selection of appropriate assay controls are both central to establishing the validity of the *in situ* hybridization results. Here, we determined the optimal Proteinase K digestion time for each tissue type used in this study, in order to ensure maximum assay sensitivity with minimal disruption to tissue morphology. We also defined several positive and negative assay controls. Hybridization of a poly d(T) control probe confirmed the presence of mRNA in each sample, while pre-treatment of tissue sections with RNase A verified the specificity of the probes for RNA. The use of several negative controls, such as omission of probe, hybridization with a sense probe, or use of a random sequence "nonsense" probe, with each run further established the specificity of the staining results. Finally, inclusion of a positive control specimen that was known to be positive for PRL-1 and PRL-2 expression demonstrated that the assay and reagents were functioning as expected. In addition to the data shown here, slot blot hybridization on PRL-1, PRL-2, and PRL-3 cDNA targets was also carried out to ensure that the PRL-1 and PRL-2 probes were not cross-hybridizing with sequences from closely related family members (Dumaual et al., 2006). In combination, each of these factors helped to validate the specificity of the assay and increase our confidence in the staining results.

CHAPTER 5. QUALITY ASSESSMENT OF SAMPLES TO BE USED FOR MICROARRAY BASED TRANSCRIPTIONAL PROFILING

5.1 Introduction

In situ hybridization was used to examine the cellular localization and tissue distribution of PRL-1 and PRL-2 mRNA in a broad range of normal and diseased human tissues. This analysis revealed several significant, and highly tissue specific, differences in PRL-1 and PRL-2 expression between tumor tissues and their normal adjacent counterparts. Given that we already had an idea of the PRL-1 and -2 expression levels in the tissues analyzed by ISH, I was interested in learning what other genes were up- or down-regulated in concordance with the PRLs in these same tissues.

It is well known that thousands of genes in the body function through complex, combinatorial and interactive networks. However, traditional methods for quantitation of gene expression allow for interrogation of only a single or limited number of genes at a time, leading to low throughput and making the whole picture of gene function difficult to obtain. Techniques for multiplex gene expression analysis, such as DNA microarrays, have become increasingly widespread and provide an opportunity to simultaneously interrogate thousands of genes in a sample to provide a more global picture of transcriptional activity. Such investigations enable researchers, not only to better assess the behavior

and relationship of genes previously implicated in a given process, but also to identify novel, similarly regulated genes and complex interacting pathways. Given this, I felt that DNA microarrays would provide a powerful tool for examining the transcriptional profiles of some of the same matched normal and tumor tissues used in the ISH analysis. My primary interest was in the PRL-1 pathway, because it displayed the most highly variable expression patterns via ISH, while PRL-2 tended to be ubiquitously and heavily expressed and PRL-3 has previously been shown to have a limited expression profile. Based on information emerging in the literature, I hypothesized that PRL-1 expression in this sample set would correlate strongly with the expression of genes directly involved in cell movement, cell adhesion, and cell cycle regulation.

To begin the analysis, I first attempted to optimize a procedure for the isolation of RNA from microdissected, formalin-fixed, paraffin-embedded (FFPE) tissue sections. Microdissection provides an efficient method of extracting tissue samples from FFPE tissues for microarray analysis, because it enables the dissection of pure cell populations from a heterogeneous tissue specimen and allows for the screening of gene expression changes in the specific cell types of interest. However, efficient extraction and isolation of RNA from FFPE blocks is often limited by an inability to extract high quality and quantity genetic material from these samples. Several recent RNA extraction procedures advertise the ability to produce sufficient material for microarray profiling from FFPE samples, so I began by testing and comparing three different extraction protocols.

I first selected two tissue types with relatively high expression of PRL-1 in tumor as compared to matched normal tissue (stomach and liver) and two tissue types with significantly lower expression of PRL-1 in tumor as compared to matched normal tissue (breast and lung). For each case, 30 slides, each containing a single 5μm tissue section, were deparaffinized and rehydrated by passing slides through two changes of xylene for 5 minutes each, followed by incubation in a graded series of ethanols (100%, 95%, 70%) and two changes of nuclease-free water for 30 seconds each. Following rehydration, slides were briefly air dried (~3-5 minutes). Using a serial H&E stained section as a guide, the normal or tumor cells of interest were then scraped from each slide into a microfuge tube (10 slides per tube) using a sterile scalpel. Each tube was subjected to one of three different RNA extraction methods: TRIzol extraction; the Ambion RNAqueous Micro Kit (Invitrogen Life Technologies); or the Qiagen RNeasy Micro Kit. Each procedure was carried out according to the manufacturer's protocol. The quantity and quality of RNA produced by each method was then examined using spectrophotometry and the Agilent Bioanalyzer.

5.2 Results

RNA yields and 260/280 ratios from each of the three tested RNA extraction procedures are listed in Table 5.1. From this data, it can be seen that the TRIzol procedure provided the best total RNA yields. All RNA samples, though, showed signs of degradation, as evidenced by optical density 260/280 ratios less than 1.8. This sample degradation was confirmed by analysis on an Agilent Bioanalyzer (Figure 5.1). The Agilent Bioanalyzer has become the standard tool for RNA quality assessment of samples for microarray analysis. It uses electrophoretic separation on a microchip device, along with fluorescence detection, to reveal the size distribution of RNA fragments in a sample, represented in the form of a virtual gel or a chromatogram. Intact, electrophoretically separated eukaryotic RNA shows two distinct ribosomal peaks corresponding to 18S and 28S ribosomal RNA (rRNA), with the 28S band approximately twice as intense as the 18S band (2:1 ratio). As RNA degradation proceeds, the RNA begins to take on a smeared appearance in gel images and the 28S/18S rRNA ratio decreases. None of the RNA extracted from FFPE tissues in the current analysis displayed clear rRNA bands.

To ensure that this result was not specific to the four initial tissue samples analyzed, the TRIzol procedure was used to extract RNA from all of the FFPE tissues that were selected for microarray analysis. As before, the RNA yields were acceptable, but the RNA in each sample was heavily degraded. As an alternate approach, we next decided to examine RNA quality in a set of tissue samples that had been flash frozen in liquid nitrogen and stored frozen at -80°C

("fresh frozen") rather than fixed and embedded in paraffin. Case matched tumor and normal adjacent tissues were obtained for 6 breast and 6 stomach tissue specimens and RNA was extracted with TRIzol. As shown in Figure 5.2, the tumor sample RNAs were only partially degraded, but the RNA derived from the matched normal specimens was highly degraded and resembled the RNA quality obtained from the FFPE samples. Thus, it was determined that neither the FFPE nor the frozen tissue samples produced high enough quality RNA to proceed with standard microarray protocols.

As an alternative, we sought to obtain experimental cell lines that would allow the assessment of global changes in gene expression that might correlate with PRL-1 overexpression. Dr. Zhong-Yin Zhang's laboratory in the Indiana University School of Medicine, Department of Biochemistry and Molecular Biology, had already established HEK293 cell lines stably overexpressing PRL-1 (Luo et al., 2009) or PRL-3 (Liang et al., 2007) and graciously harvested and provided us cells from each of these lines, along with control HEK293 cells that were transfected only with empty vector. Total RNA was extracted from the cells using TRIzol and RNA quality was again assessed using the Agilent Bioanalyzer. The extracted RNA was of excellent quantity and quality as determined by the presence of clear 18S and 28S rRNA bands with the 28S band being roughly twice as intense as the 18S band (Figure 5.3). Based on these results, the cell line samples were selected for transcriptional profiling using Affymetrix microarrays.

Table 5.1 Comparison of methods for RNA extraction from FFPE tissues

Sample Number	Absorbance 260/280			RNA Yield (ng)		
	TRIzol	RNAqueous	RNeasy	TRIzol	RNAqueous	RNeasy
Tissue 1	1.68	1.71	1.87	259	216	133
Tissue 2	1.49	1.90	1.79	630	94	163
Tissue 3	1.53	1.52	1.68	1402	282	226
Tissue 4	1.52	1.70	1.84	1654	1101	133

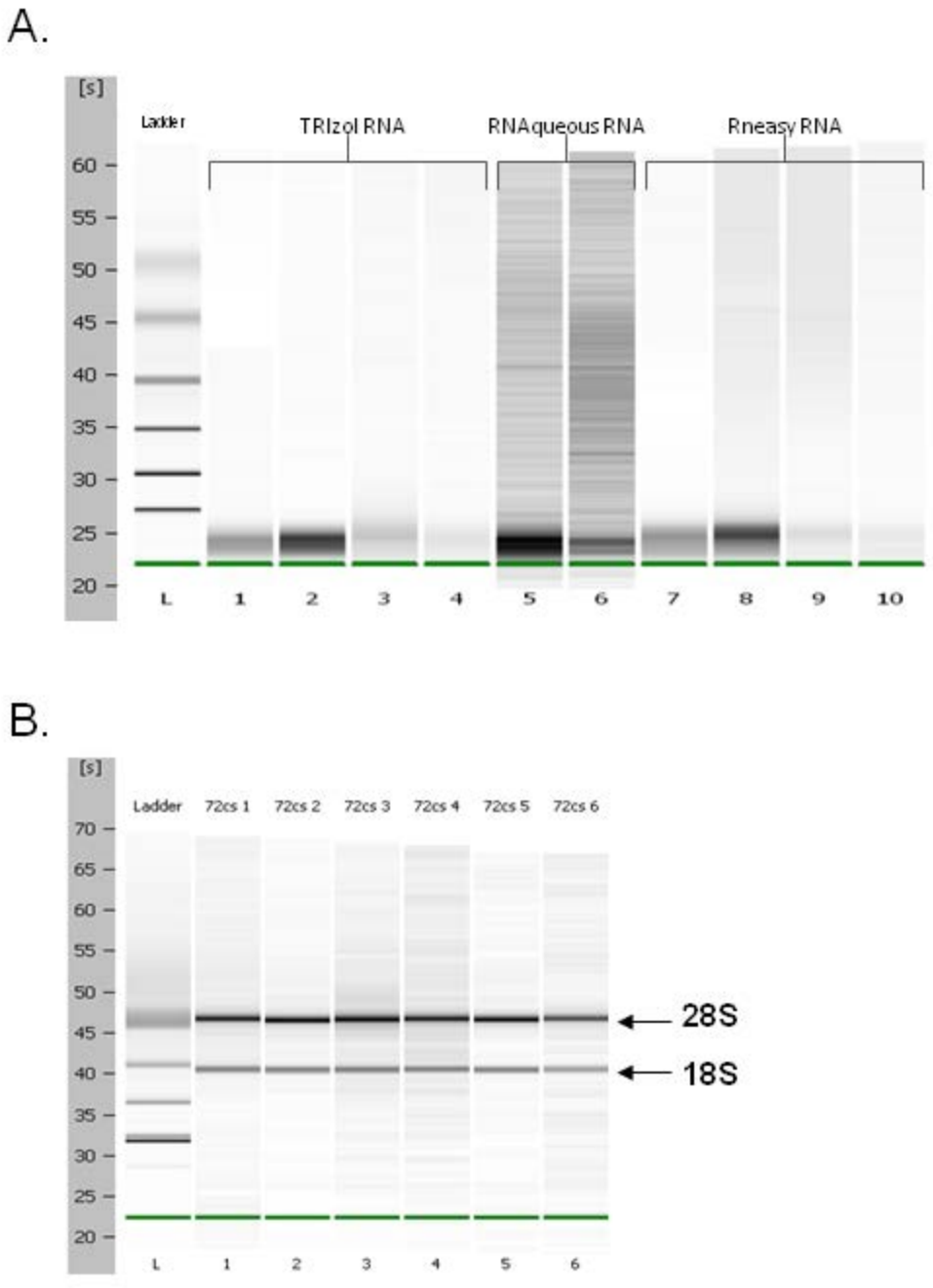

Figure 5.1 Agilent Bioanalyzer profile of RNA extracted from FFPE tissue
The virtual gel in (A) shows the poor quality of RNA derived from FFPE tissue blocks, as compared to an example gel (B), displaying high quality RNA derived from fresh, whole blood samples. The higher quality RNA in these samples is evidenced by the presence of clear 28S and 18S ribosomal RNA bands.

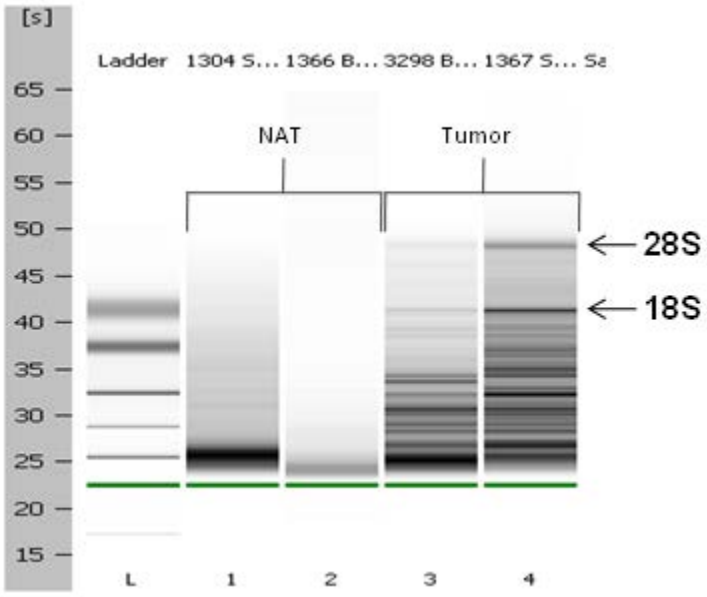

Figure 5.2 Representative Agilent Bioanalyzer profile of RNA extracted from fresh frozen tissues
Tumor tissues were only partially degraded and clearly retained 28S and 18S ribosomal RNA bands, whereas RNA from their matched Normal Adjacent Tissues (NAT) was heavily degraded.

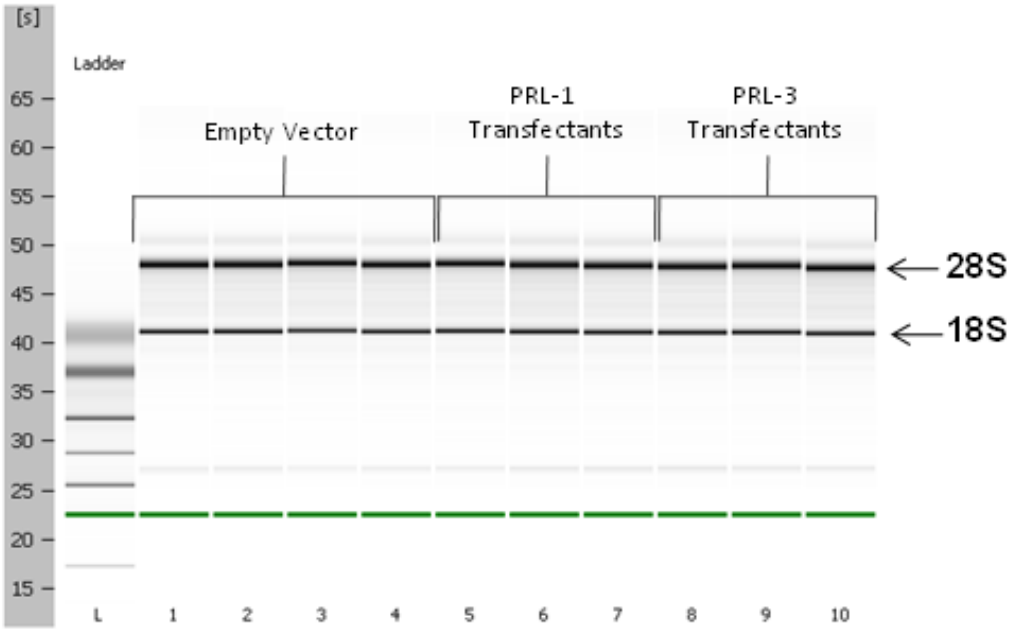

Figure 5.3 Agilent Bioanalyzer profile of cell line-derived RNA
RNA derived from HEK293 cells stably overexpressing PRL-1, PRL-3, or empty vector (control) displayed high quality, intact RNA, as indicated by the presence of distinct 28S and 18S ribosomal RNA bands on a virtual gel.

5.3 Discussion

The assessment of RNA integrity is a critical first step to obtaining meaningful gene expression data. Traditional microarray protocols rely on cDNA synthesized from the poly-A tail of RNA and therefore require well preserved, highly intact RNA in order to be successful. Older FFPE samples tend to yield particularly poor quality RNA, largely due to the handling practices that were used for collection of these specimens. In the past, less stringent collection procedures, supplying lower quality total RNA, were acceptable, because commonly used methods (e.g. ISH, PCR) examined only a small number of genes or did not require fully intact RNA. The advent of microarray analysis has led to the development of more stringent procedures for sample collection; however, archival FFPE sample blocks were typically not collected under these improved conditions. The tissue blocks used in our ISH experiments are more than a decade old at this point and a few years have passed even since they were used in the ISH analysis. Therefore, it is not surprising that the RNA in these samples exhibits a significant degree of degradation.

Due to the recent emergence of a number of protocols and kits that help overcome some of the technical limitations associated with microarray-based analysis of FFPE samples, it is possible that meaningful expression data could still be obtained from our FFPE-derived RNA. However the combinatorial effects of differential RNA degradation and inter-individual variability in PRL-1 expression between samples are likely to complicate and perhaps confound data interpretation, making it difficult to parse out the gene expression changes that

are directly correlated to PRL-1. The use of cell lines stably overexpressing PRL-1, on the other hand, will allow more direct analysis of the downstream changes related to altered PRL-1 transcript levels. In addition, use of the PRL-3 overexpressing lines will allow comparison of the downstream pathways affected by both of these genes and examination of any potential overlap in gene function between PRL family members.

CHAPTER 6. RT-PCR ENDOGENOUS CONTROL SELECTION AND ANALYSIS OF PRL EXPRESSION IN PRL TRANSFECTED HEK293 CELL LINES

6.1 Introduction

RT-PCR is considered the gold-standard method for quantifying gene expression and is often used to validate significant findings from microarray based data sets. Quantitative real-time PCR expression results are generally normalized using endogenous control genes to correct for potential biases in RNA input or reverse transcription efficiency. For accurate analysis, it is important to find control genes that are expressed at a constant level across all of the samples and experimental conditions that will be compared in a study. GAPDH and β-actin have historically been used as standard normalization controls for a number of RNA and protein assays, but it is now understood that levels of both of these genes can be modulated by a variety of conditions (Suzuki, Higgins, & Crawford, 2000). Hence, prior to running any qRT-PCR assay, it is important to first validate the selected control or set of controls in the study sample set. To this end, I used a TaqMan Endogenous Control Array to examine the stability of 16 candidate endogenous control genes in HEK293 cells transfected with PRL-1, PRL-3, or empty vector.

The HEK293 cell lines stably overexpressing PRL-1 and PRL-3 had previously been characterized and shown to exhibit at least two-fold higher levels of PRL-1 or PRL-3 expression compared to their respective empty vector-transfected cell lines (Liang et al., 2007; Luo et al., 2009). Despite this, using microarray analysis we were unable to detect a significant up-regulation of PRL expression in the PRL transfectants. It is not unheard of for cells to compensate and down-regulate expression of a transgene over time; therefore, I elected to use qRT-PCR to further examine the PRL-1 and PRL-3 expression levels in the same set of samples analyzed in the microarray studies, as well as to prospectively examine PRL levels in the samples used for other portions of this project (e.g. miRNA and RT-PCR custom arrays). Endogenous control genes selected from the above mentioned Endogenous Control Arrays were used for normalization of these data sets.

6.2 Results

The TaqMan DataAssist software was used to identify the most stably expressed transcripts on the endogenous control array. DataAssist is based on the GenNorm statistical algorithm (Vandesompele et al., 2002) which calculates an expression stability score for each candidate gene using pairwise comparisons of variability. Each gene is compared to every other gene to determine which genes display the least amount of variation in the sample set. The calculated scores are then used to rank the genes in order of stability. The resulting stability scores for the PRL-1 stable transfectants and controls are

displayed in Table 6.1. This analysis ranked UBC as the most stable gene in the PRL-1 sample set, followed closely by 18S.

In addition to the stability score comparison, the gene expression levels (expressed as Ct values) for each of the candidate endogenous controls were plotted (Figure 6.1) and a student's paired t-test was performed between the empty vector and PRL-1 transfectant groups. Expression of all 16 candidate genes was fairly consistent across the sample set. The standard deviation (SD) in Ct value across all samples was also examined individually for each gene (Figure 6.2). SD values ranged from 0.16 for UBC to 0.66 for HPRT1. The genes UBC, 18S, and IPO8, which were the top 3 genes ranked by stability score, all exhibited less than 0.2 standard deviations across samples.

In contrast to PRL-1, stable transfection of HEK293 cells with PRL-3 had a remarkable effect on the expression of almost all tested endogenous control genes. Genes that are not detected at a cycle threshold of 36-40 or above are often considered absent. From the DataAssist plot in Figure 6.3, it can be seen that each of the tested genes is expressed at detectable levels ($Ct < 36$) in the empty vector samples, but the bulk of these dramatically decrease in expression (Ct values increase, most to undetectable levels), in each of the PRL-3 transfectants. Only 18S displayed any degree of stability across the full sample set. Examination of the standard deviation in Ct values for this sample set revealed SD values greater than 3.5 for all genes except 18S, which had a standard deviation of 0.32 (Figure 6.4). A paired t-test comparing the mean Ct values between the empty vector and the PRL-3 transfectant groups revealed

significant differences between groups for all genes but 18S ($p = 0.35$), PGK1 ($p = 0.61$), and RPLP0 ($p = 0.11$). These results suggest that PRL-3 may exert effects on a broad range of signaling pathways and also underscore the importance of the endogenous control selection exercise for verifying consistent expression of candidate normalization controls. UBC was selected as a suitable normalization control for PRL-1, while 18S was deemed an acceptable control for either the PRL-1 or PRL-3 sample sets in this study.

Following endogenous control selection, qRT-PCR was performed to measure the levels of PRL-1 and PRL-3 in the study samples. Expression of PRL-1 in all samples was low and addition of a pre-amplification procedure to the qRT-PCR assay was required to measure it in either the HEK293-PRL-1 or HEK293-vector cell lines. This analysis revealed that two of the three stable PRL-1 transfectants used in the microarray analysis displayed PRL-1 transcript levels that were at least 4-fold higher than in the empty vector controls (Figure 6.5). The third PRL-1 transfectant did not exhibit increased levels of PRL-1 expression and so this sample was excluded from all downstream data analysis. A number of additional HEK293 stable transfectants were also examined and three of these, where the PRL-1 transfectants exhibited at least a 1.5-fold increase in expression over the vector controls (Figure 6.6), were selected for the miRNA and custom TaqMan array studies.

In the case of PRL-3, surprisingly, not only was PRL-3 not found to be overexpressed in the PRL-3 stably transfected cell lines, as compared to their empty vector controls, but PRL-3 expression was consistently decreased, by

greater than 50-fold, in the PRL-3 transfectants (Figure 6.7). These results are suggestive of a potential compensatory mechanism by which the stably transfected cells are down-regulating/silencing PRL-3 expression over time.

Table 6.1 Stability scores for candidate endogenous control genes in the PRL-1 sample set

The TaqMan DataAssist algorithm was used to calculate a stability value for expression of 16 candidate endogenous control genes in the HEK293 cells stably transfected with PRL-1 or empty vector that were used for microarray analysis. Genes were ranked in order of greatest stability (lowest stability score) to least stability (highest stability score). Using this algorithm, UBC was ranked as the most stably expressed gene in the PRL-1 sample set.

Rank	Gene Symbol	Stability Score
1	UBC	0.3346
2	18S	0.3356
3	IPO8	0.3392
4	POLR2A	0.3397
5	TBP	0.3686
6	PGK1	0.3843
7	HMBS	0.3847
8	TFRC	0.3913
9	PPIA	0.3947
10	B2M	0.4005
11	RPLP0	0.4145
12	YWHAZ	0.4392
13	GUSB	0.4898
14	GAPDH	0.6672
15	ACTB	0.6944
16	HPRT1	0.7111

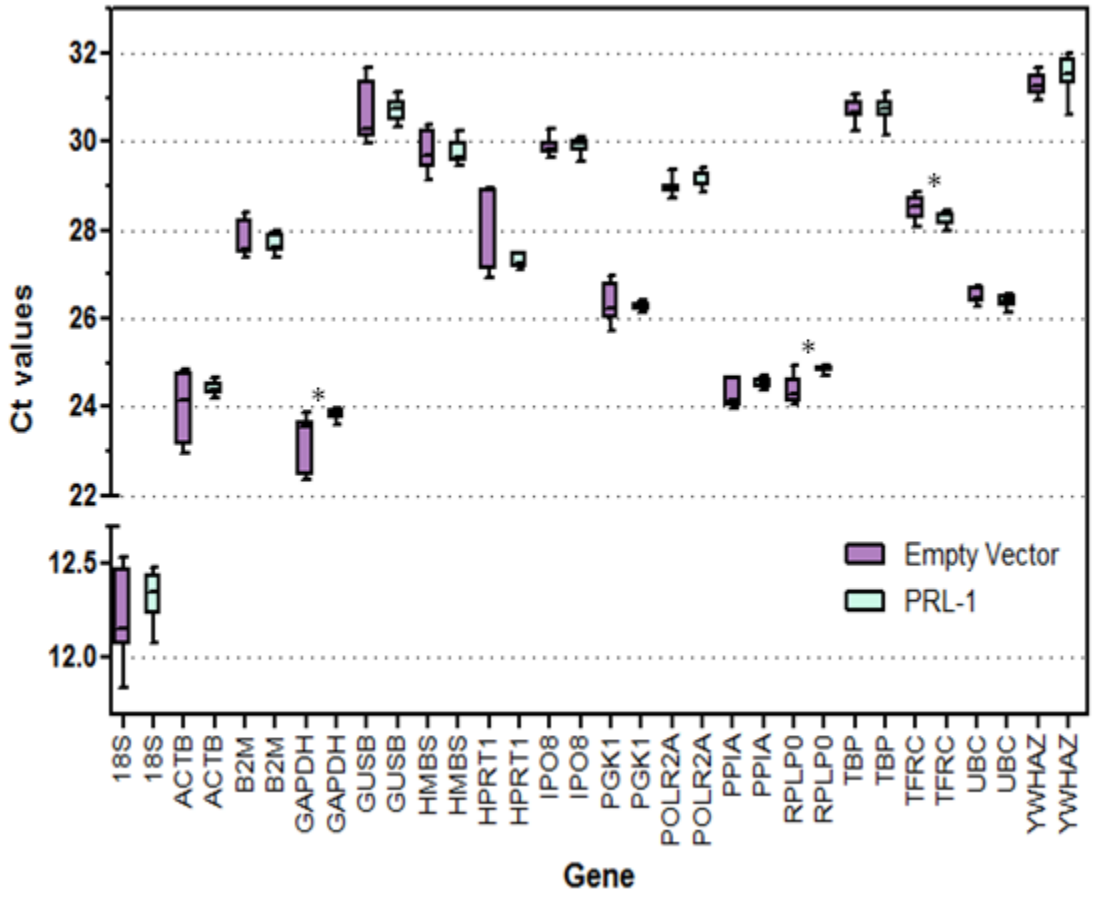

Figure 6.1 Expression levels of candidate endogenous control genes in the PRL-1 sample set

A TaqMan Endogenous Control Array was used to examine the expression of 16 candidate endogenous controls in the HEK293 cells stably transfected with PRL-1 or empty vector that were used for microarray analysis. Expression levels are represented by cycle threshold (Ct) values. Median Ct values are shown as the black line within each box plot and divide the plot into lower and upper quartile ranges. Whiskers illustrate the minimum and maximum sample values. An asterisk indicates a significant difference ($p < 0.05$) between sample groups, as determined by paired t-test.

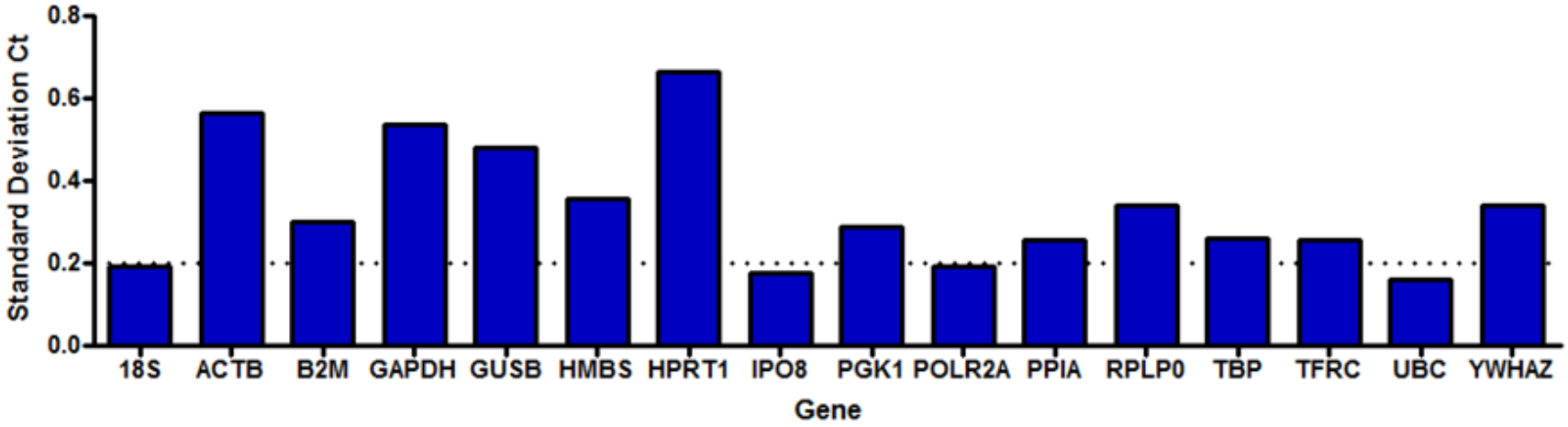

Figure 6.2 Standard deviation of candidate endogenous controls for PRL-1
A TaqMan Endogenous Control Array was used to examine the expression of 16 candidate endogenous controls in the HEK293 cells stably transfected with PRL-1 or empty vector that were used for microarray analysis. The standard deviation between Ct values for all samples was calculated using Microsoft Excel and plotted in GraphPad Prism. The genes UBC, 18S, and IPO8 exhibited the lowest standard deviation in Ct values for this sample set.

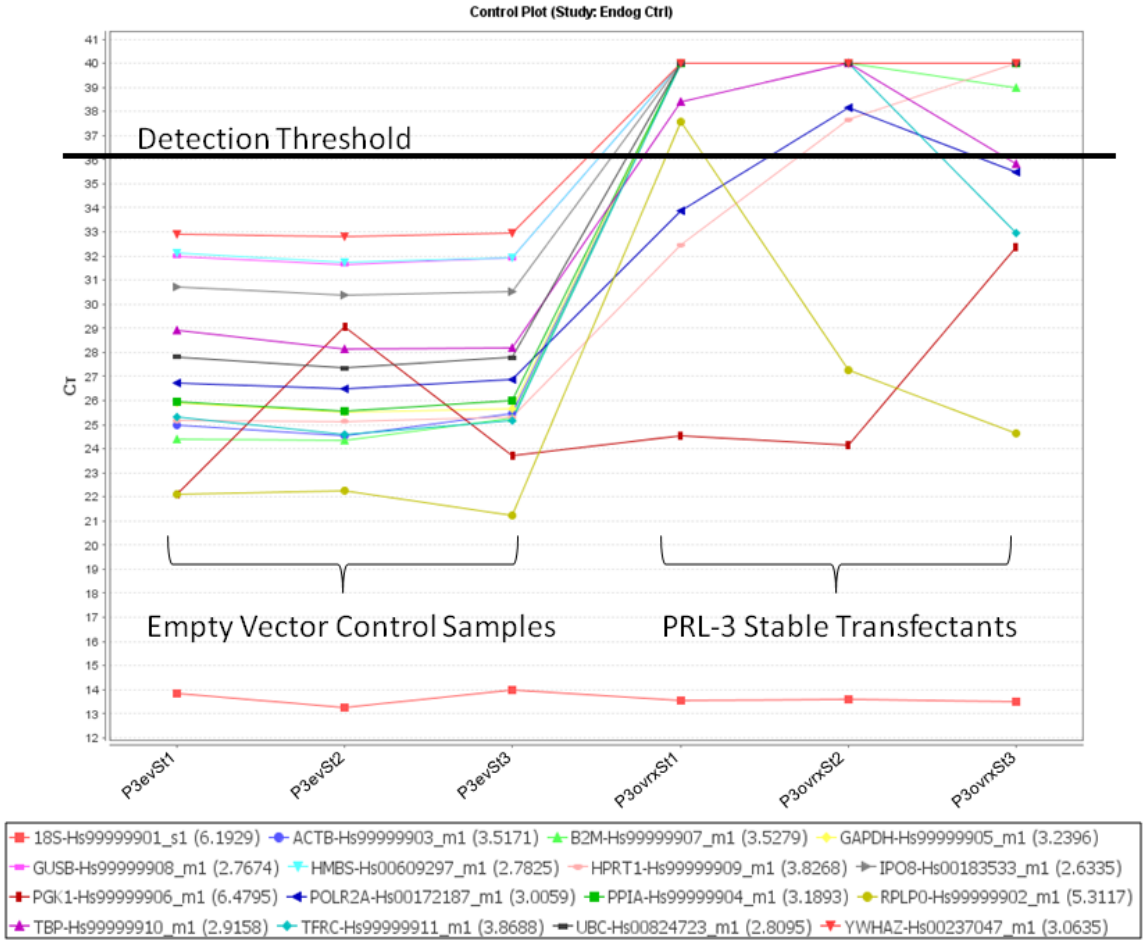

Figure 6.3 Endogenous control selection for PRL-3 in HEK293 cells
A TaqMan Endogenous Control Array was used to examine the expression of 16 candidate endogenous controls in the HEK293 cell lines stably transfected with PRL-3 or empty vector that were used for microarray analysis. Examination of the expression values with DataAssist revealed that only the 18S gene is expressed at constant levels across all samples. In contrast, stable transfection of PRL-3 leads to a significant decrease in expression of most other candidate genes, as evidenced by Ct values that are well within the detection range of the assay in the vector control samples, but increase beyond the level of detection in the stable PRL-3 transfectants.

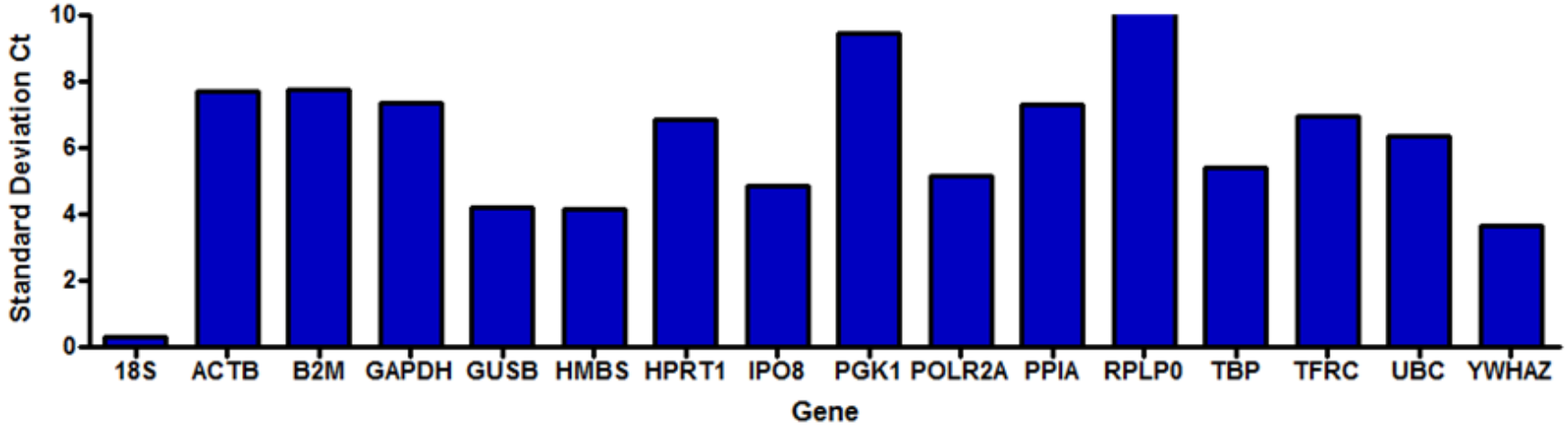

Figure 6.4 Standard deviation of candidate endogenous controls for PRL-3
A TaqMan Endogenous Control Array was used to examine the expression of 16 candidate endogenous controls in the HEK293 cells stably transfected with PRL-3 or empty vector that were used for microarray analysis. The standard deviation between Ct values for all samples was calculated using Microsoft Excel and plotted in GraphPad Prism. The 18S gene exhibited the lowest standard deviation in Ct values for this sample set.

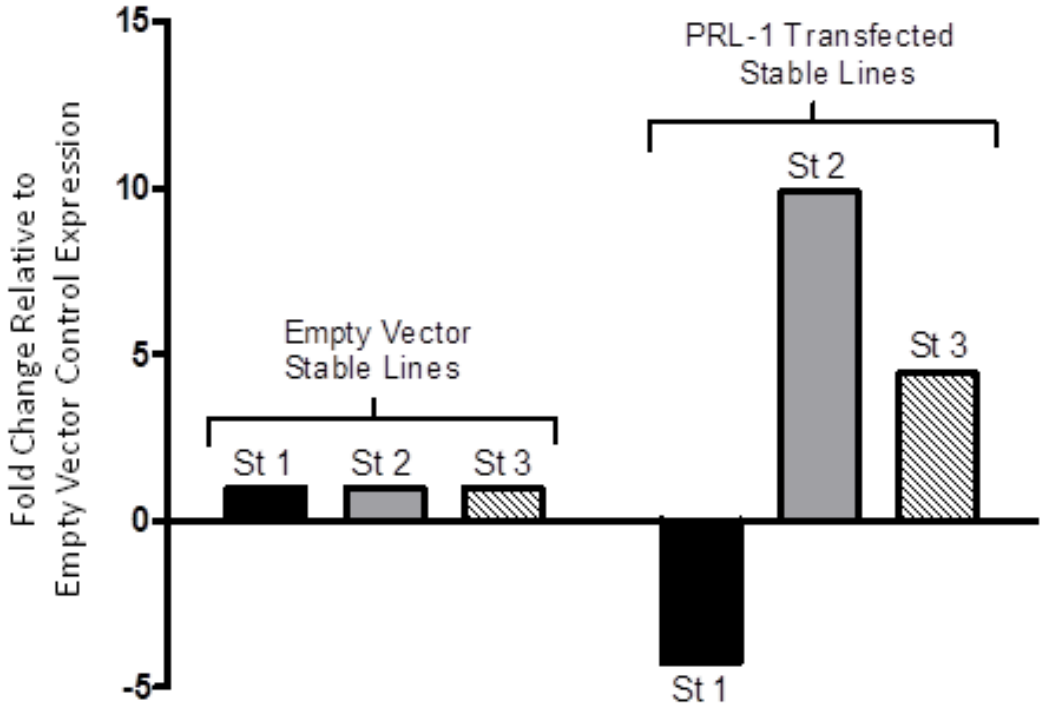

Figure 6.5 PRL-1 expression in cell lines used for microarray experiments

The fold change differences in PRL-1 mRNA transcript levels in HEK293 cells stably transfected with PRL-1 or empty vector were determined by qRT-PCR. A single PRL-1 stable transfectant (St1) did not exhibit enhanced levels of PRL-1 compared to the empty vector controls and was removed from microarray data analysis.

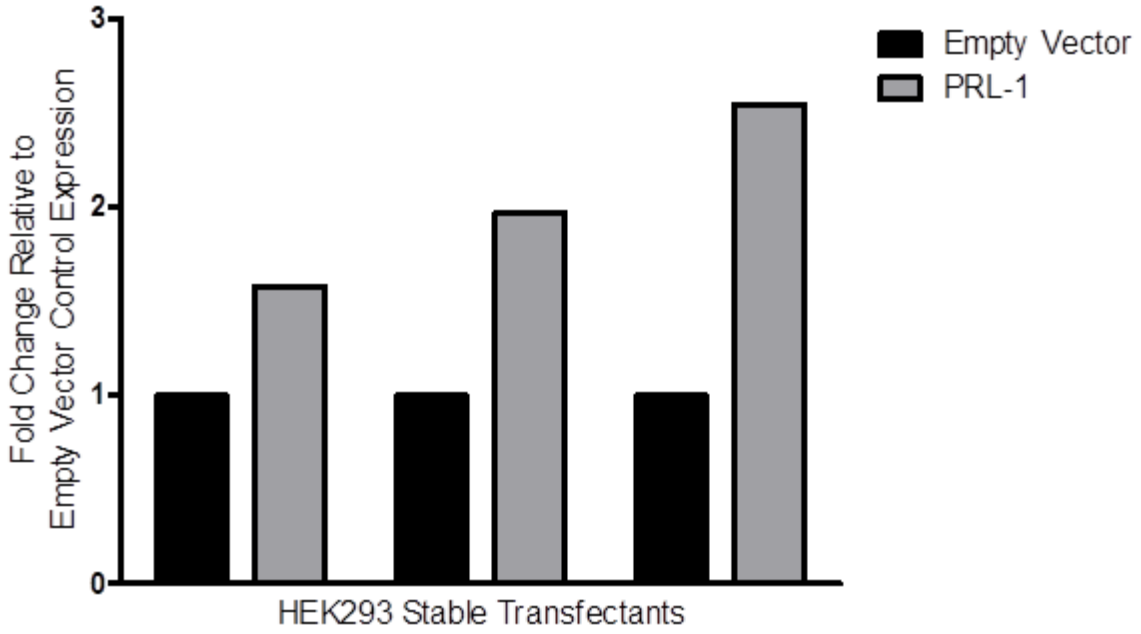

Figure 6.6 PRL-1 expression in samples used for miRNA and RT-PCR custom array analysis
Quantitative RT-PCR analysis confirmed at least a 1.5-fold up-regulation of PRL-1 in HEK293 cells stably transfected with PRL-1 compared to cells transfected with empty vector. These samples were utilized to examine the effects of PRL-1 overexpression on miRNA expression and on expression of a custom array of genes related to cytoskeletal rearrangement and cell motility.

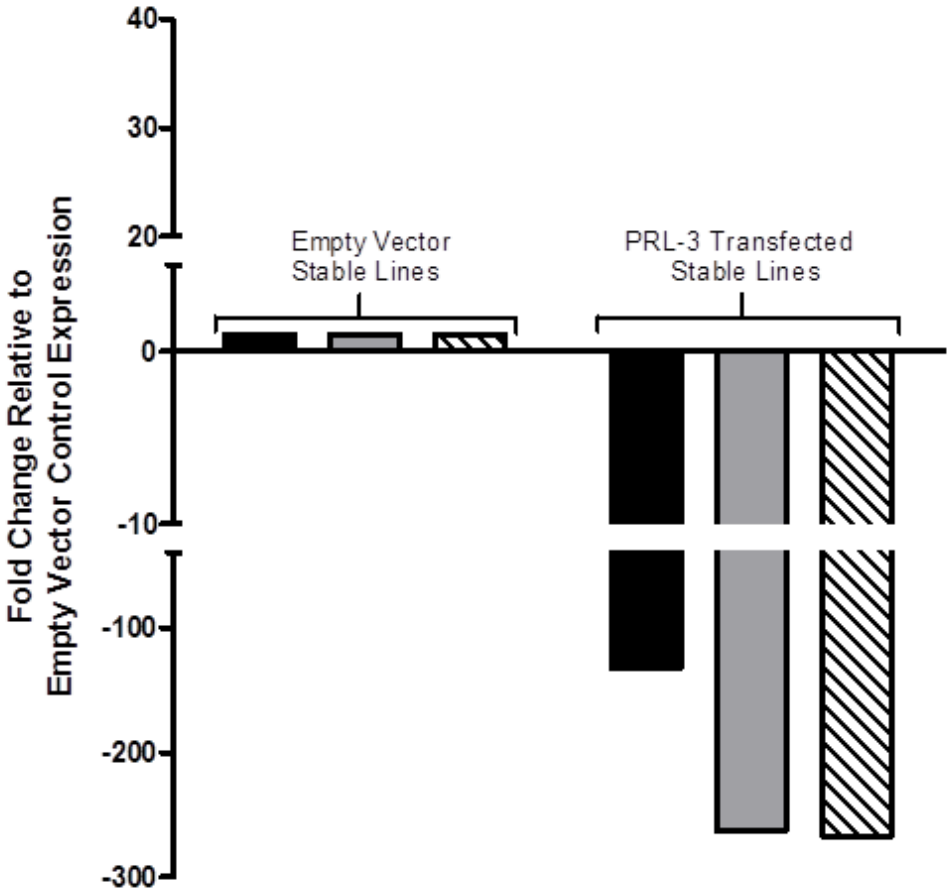

Figure 6.7 PRL-3 expression in cell lines used for microarray experiments

The fold change differences in PRL-3 mRNA transcript levels in HEK293 cells stably transfected with PRL-1 or with empty vector were determined by qRT-PCR. All PRL-3 transfected cells, unexpectedly, displayed lower levels of PRL-3 than in the respective empty vector controls.

6.3 Discussion

The fact that PRL-1 transcripts are present at such low levels as to require pre-amplification, even with the more sensitive method of qRT-PCR, explains why changes in PRL-1 mRNA levels could not be detected using microarrays. Moreover, this could suggest that maintenance of basal PRL-1 expression levels is tightly regulated within the cell. Expression of PRL-3 also appears to be carefully controlled, given that HEK293 cells stably transfected with PRL-3 were initially confirmed to overexpress the transgene, but after multiple passages exhibit a down-regulation of PRL-3 expression. It is possible that the cells recognize high levels of PRL-3 and undergo a protective mechanism (e.g. gene silencing) to compensate. This would not be entirely surprising as Basak et al. (2008) previously reported the effects of PRL-3 expression on cell-cycle progression to be highly dose-sensitive.

The primary goal of my microarray studies was to identify signaling pathways and molecules that are responsive to PRL overexpression; however there is clearly additional biology that is occurring in the stably transfected PRL-3 lines that could confound this analysis. We are unlikely to be able to confidently select candidate PRL-3 effectors from transcriptional profiling of the HEK293 stable cell lines alone. A number of commonalities between the PRL-1 and PRL-3 signaling pathways have now been discovered though, so molecular changes

occurring in response to PRL-1 overexpression may provide useful clues that promote our understanding of PRL-3 signaling and the cellular response to PRL-3 up-regulation.

CHAPTER 7. NOVEL INSIGHTS TO PRL-1 SIGNALING GAINED THROUGH INTEGRATED ANALYSIS OF mRNA AND PROTEIN EXPRESSION DATA

7.1 Chapter Introduction

To improve our understanding of PRL-1-mediated cellular signaling, I performed transcriptional profiling via microarray on triplicate biological replicates of the HEK293-PRL-1 and HEK293-vector stable transfectants described in Chapters 5 and 6. The results of this analysis were then integrated with a set of proteomic (mass spectrometry) data generated and kindly made available to us by Chad Walls in Dr. Zhong-Yin Zhang's laboratory (Department of Biochemistry and Molecular Biology, Indiana University School of Medicine, Indianapolis, IN). These combined data sets have been incorporated into a manuscript that is currently in preparation to be submitted for publication and is included, in its entirety below. An 'Author Contributions' section included at the end of the manuscript specifies the portions of this work that were completed by me and also details the specific contributions of each co-author.

7.2 Manuscript Title Page

Novel insights to PRL-1 signaling gained through integrated analysis of mRNA and protein expression data

Carmen M. Dumaual[1*§], Boyd A. Steere[2*§], Chad D. Walls[3], Zhong-Yin Zhang[3], Stephen K. Randall[1*]

[1]Department of Biology, Indiana University-Purdue University Indianapolis, 723 West Michigan St., Room SL306, Indianapolis, Indiana, 46202, USA

[2]Lilly Research Laboratories, Eli Lilly and Company, Lilly Corporate Center, Indianapolis, Indiana, 46285, USA

[3]Department of Biochemistry and Molecular Biology, Indiana University School of Medicine, 635 Barnhill Drive, Indianapolis, Indiana, 46202, USA

[§]These authors contributed equally to this work.

7.3 Abstract

7.3.1 Background

The protein tyrosine phosphatase PRL-1 represents a putative oncogene with wide-ranging cellular effects. Overexpression of PRL-1 can promote cell proliferation, survival, migration, invasion, and metastasis, but the underlying mechanisms by which it influences these processes remain poorly understood.

7.3.2 Methodology

To increase our comprehension of PRL-1 mediated signaling events, we employed transcriptional profiling (DNA microarray) and proteomics (mass spectrometry) to perform a thorough characterization of the global molecular changes in gene expression that occur in response to stable PRL-1 overexpression in a relevant model system (HEK293).

7.3.3 Principle Findings

Overexpression of PRL-1 led to several significant changes in the mRNA and protein expression profiles of HEK293 cells. The differentially expressed gene set was highly enriched in genes involved in cytoskeletal remodeling, integrin-mediated cell-matrix adhesion, and RNA recognition and splicing. In particular, members of the Rho signaling pathway and molecules that converge on this pathway were heavily influenced by PRL-1 overexpression, supporting observations from previous studies that link PRL-1 to the Rho GTPase signaling

network. In addition, several genes not previously connected to PRL-1 were found to be significantly altered by its expression. Most notable among these were Filamin A, RhoGDIα, SPARC, hnRNPH2, and PRDX2.

7.3.4 Conclusions and Significance

This systems-level approach sheds new light on the molecular networks underlying PRL-1 action and presents several novel directions for future, hypothesis-based studies.

7.4 Introduction

The PRL family of enzymes has recently emerged as potential tumor biomarkers and novel anti-cancer therapeutic targets. Evidence suggests that the three PRL family members (PRL-1, PRL-2, and PRL-3) may be multi-faceted molecules involved in a number of diverse biological processes [1-5], however recent attention to these enzymes revolves around their relationship to cellular proliferation and tumor progression.

PRL-1, the first family member identified, was initially characterized and named Phosphatase of Regenerating Liver for its role as an immediate early gene induced in mitogen-stimulated cells and in proliferating rat liver during hepatic regeneration [6,7]. Accumulating evidence now indicates that up-regulation of PRL-1 expression may play a causal role in cellular transformation and tumor advancement. Overexpression of PRL-1 in non-tumorigenic cells leads to rapid cellular growth and a transformed phenotype [6,8,9]. Moreover,

cells that stably overexpress PRL-1 exhibit enhanced cell motility and invasive activity and are capable of forming metastatic tumors in nude mice [6,10-13]. Conversely, knockdown of endogenous PRL-1 in tumor cells has the opposite effect, reducing proliferation and suppressing cell migration and invasion [10,12,14-16]. An association between PRL-1 expression and tumor promotion has also been found in human tumor tissues where we previously showed that PRL-1 was significantly up-regulated in 100% of hepatocellular and gastric carcinomas compared to matched normal tissues from the same patients [17]. Collectively, these results suggest that the PRL-1 phosphatase regulates key pathways involved in tumorigenesis and metastasis. However, the mechanisms of PRL-1 action and regulation are poorly understood and the exact biological function of this molecule remains unknown.

Examination of individual molecules and pathways reveals that PRL-1 may be involved in multiple different signaling cascades. PRL-1 up-regulation may enhance cell proliferation by coordinately decreasing expression of negative cell cycle regulators ($p21^{cip1/waf1}$, p53) and increasing expression of positive cell cycle regulators (Cyclin A, Cdk2), thus promoting unscheduled entry into S phase [9,18]. PRL-1 might also augment cell motility and invasion by signaling through the Rho family small GTPases, focal adhesion complex-associated proteins, and the ERK1/2 mitogen-activated protein kinase (MAPK) cascade to induce the alterations in the actin cytoskeleton required for cell movement and to up-regulate matrix metalloproteinases capable of breaking down the extracellular matrix and permitting cell invasion and migration [10-12,14]. A direct physical

interaction between PRL-1 and the Rho GTPase activating protein (GAP), p115 RhoGAP may promote some of these effects by preventing p115 RhoGAP from deactivating RhoA as well as blocking its inhibitory binding of the ERK activator MEKK1 [19].

To date, PRL-1 shows the strongest activity as an autophosphatase [6], but it can also bind and partially dephosphorylate the pro-survival transcription factor ATF-7 (a.k.a. ATF-5) [20]. PRL-1 interacts directly with several phosphoinositide lipids [16], the cytoskeletal component α-tubulin [21], the suppressor of TNF-mediated apoptosis TNFAIP8 (tumor necrosis factor alpha-induced protein 8) [22], and with FKBP38 (peptidylprolyl cis/trans isomerase FK506-binding protein 38), whose binding may target PRL-1 for proteosomal degradation [23]. PRL-1 induction in mitogen stimulated cells and regenerating liver can largely be attributed to its up-regulation by the transcriptional activator EGR-1 [24]. Additionally, PRL-1 is subject to redox regulation and has been suggested to play a role in the photo-oxidative stress response in the retina, where it relies on the glutathione system for constant regeneration of its enzymatic activity [5,25].

While knowledge surrounding PRL-1-mediated signaling events has been greatly enhanced through focused investigations on individual genes and isolated pathways, it is clear that PRL-1 signaling is a multi-dimensional process. Moreover, there is an increasing appreciation that all cellular processes are governed by the complex interplay between multiple signaling networks. “Omics” techniques offer the advantage of an unbiased and global view of the changes

that are occurring as well as the opportunity to identify previously unforeseen players that are responding with respect to a particular stimulus. Therefore, in the current study, we utilized microarray profiling of gene expression (transcriptomics) and mass spectrometry (proteomics) to more broadly examine the gene and protein level alterations occurring in human embryonic kidney 293 (HEK293) cells stably overexpressing PRL-1. This integrated, systems-level approach provides an unprecedented, comprehensive dataset that helps shed light on the molecular networks underlying PRL-1 action and also presents new possible directions for future, hypothesis-driven research.

7.5 Methods

7.5.1 Stable Cell Lines and Cell Culture

Human embryonic kidney 293 cells stably overexpressing PRL-1 (HEK293-PRL-1) or empty pcDNA4 vector (HEK293-vector) were previously generated and described [11,16]. Cells were grown in 100 mm plates in Dulbecco's Modified Eagle's Medium (DMEM) supplemented with 10% (v/v) fetal bovine serum (Thermo Scientific HyClone, Logan, UT), 50units/ml penicillin (Mediatech, Inc., Manassas, VA), and 50μg/ml streptomycin (Mediatech).

7.5.2 Mass Spectrometry

Seven 100mm plates each of HEK293-PRL-1 and HEK293-vector cells were grown to 95% confluency, the culture medium was aspirated and the cell

monolayers were washed once in 1X PBS, then frozen at -80°C until use. Upon thawing the cells, protein samples were prepared and analyzed as previously described [26]. Briefly, cells were treated with 100μl of a hypotonic lysis buffer containing 8M urea, 10mM DTT and 1mM sodium orthovanadate (Sigma-Alrich, St. Louis, MO). The resulting cell lysates were reduced by triethylphosphine (Sigma-Aldrich), alkylated by iodoethanol (Sigma-Aldrich) and subsequently digested using trypsin (Promega, Madison, WI). Peptide concentration was determined using the Bradford Protein Assay.

Mass spectrometry (MS) and MS data analysis were carried out at Monarch Life Sciences (Indianapolis, IN) using previously described methods [26-29]. Tryptic digests were analyzed using a linear ion-trap mass spectrometer (LTQ) coupled to a Surveyor HPLC system (Thermo Scientific, Waltham, MA). Tryptic peptides (~20μg/injection) were injected in random order onto a microbore, C18 reversed-phase column (Zorbax 300SB0C18, 1mm x 5cm) with a flow rate of 50μl/min and eluted with a gradient from 5 to 45% acetonitrile (Honeywell Burdick & Jackson, Morristown, NJ) developed over 120 min. The effluent was electrosprayed into the LTQ mass spectrometer and data were collected in triple-play mode (MS scan, zoom scan, MS/MS scan). The acquired data were filtered and analyzed using algorithms developed and described by Higgs et al. [27-29]. For peptide identification, database searches were carried out against the IPI (International Protein Index) human database and the non-redundant Homo sapiens database using both the X!Tandem and SEQUEST algorithms [30,31]. Identified proteins were categorized into tier groups (1-4)

based on the quality of the peptide identification and the number of unique peptides identified. Proteins assigned to Tier 1 had high (>90%) peptide confidence and multiple sequences identified; Tier 2 had high peptide confidence with only a single sequence identified; Tier 3 had moderate (75-89%) peptide confidence and multiple sequences; Tier 4 had moderate peptide confidence and a single sequence. Estimation of confidence levels was based on a random forest recursive partition supervised learning algorithm [27]. Peptides assigned to proteins with a confidence level of less than 90% (Tier 3 and Tier 4 peptides) were filtered out of this study. For protein quantification, raw files were acquired from the LTQ mass spectrometer and all extracted chromatograms (XIC) were aligned by retention time. To be used in the protein quantification procedure, each aligned peak must match parent ion, charge state, daughter ions (MS/MS data) and retention time (within a one-minute window). After alignment, the area-under-the-curve (AUC) for each individually aligned peak from each sample was measured, quantile normalized, and compared for relative abundance. All peak intensities were transformed to a $\log_2$ scale before quantile normalization. If multiple peptides had the same protein identification, then their quantile normalized $\log_2$ intensities were averaged to obtain $\log_2$ protein intensities. Analysis of Variance (ANOVA) was used to detect significant changes in protein expression between the HEK293-PRL-1 and HEK293-vector groups. The p-value threshold was fixed to control the false discovery rate at 5% (≤ 0.05). The inverse $\log_2$ of each sample mean was calculated to determine the fold change between samples.

IPI identifiers and NCBI (National Center for Biotechnology Information) GenInfo Identifiers (GIs) were mapped to NCBI gene symbols using the Biobase Biological Database (http://www.biobase-international.com/) and the National Center for Biotechnology Information (NCBI) database (http://www.ncbi.nlm.nih.gov/gquery). This mapping of proteins to their coding genes serves as the basis for integrating the protein mass-spectrometry results with the mRNA data sets described below.

7.5.3 Gene Expression Microarray

Total RNA was extracted from three independent cultures each of HEK293-PRL-1 and HEK293-vector cells using the TRIzol reagent (Invitrogen Life Technologies, Carlsbad, CA) and further purified with an RNeasy Mini Kit (Qiagen Inc., Valencia, CA), following manufacturer's instructions. RNA integrity and yield were assessed by determining sample absorbance at 260 and 280 nm on a DU640B spectrophotometer (Beckman Coulter, Brea, CA) and by subjecting samples to the Agilent 2100 Bioanalyzer (Agilent Technologies, Inc., Santa Clara, CA), using the Agilent RNA 6000 Nano LabChip Kit as directed.

Gene expression profiling was carried out according to the protocol described in the Affymetrix GeneChip Expression Analysis Technical Manual. Briefly, 5μg of each cleaned, total RNA was used to generate double-stranded cDNA, by reverse transcription, using a Superscript Double-Stranded cDNA Synthesis Kit (Invitrogen Life Technologies) and a GeneChip T7-Oligo(dT) Promoter Primer Kit (Affymetrix, Santa Clara, CA). Following second-strand

synthesis, cDNA was cleaned with a GeneChip Sample Cleanup Module (Affymetrix), and then used as a template for synthesis of biotinylated cRNA with the Enzo BioArray HighYield RNA Transcript Labeling Kit (Enzo Life Sciences, Farmingdale, NY). Labeled cRNA was cleaned with a GeneChip Sample Cleanup Module (Affymetrix), fragmented, and hybridized overnight to HG-U133 Plus 2.0 GeneChip Human Genome Arrays (Affymetrix), which analyze the expression level of more than 47,000 RNA transcripts and variants. Following hybridization, GeneChips were washed, stained with streptavidin phycoerythrin (Molecular Probes, a subsidiary of Life Technologies, Carlsbad, CA), and scanned using the Affymetrix GeneChip Scanner 3000 7G. Raw image (CEL file) generation and analysis was performed using the Affymetrix GeneChip Operating System (GCOS). All RNA samples and arrays met Affymetrix recommendations for standard quality control metrics.

Microarray data files were processed with R-project software (http://www.r-project.org/), version 2.13.1 through the RStudio interface version 0.94.92 (http://www.rstudio.org). The intensity values were read using the “affy” library of the Bioconductor package, version 2.8 [32,33]. Normalization and calls were made using the mas5 procedure under default parameters. Probesets were scored for hybridization reliability as “High”, “Medium”, or “Low” by the method described in [34]. One of the chips that was hybridized with a HEK293-PRL-1 sample was removed from the analysis, after quantitative real-time reverse transcription PCR (qRT-PCR) confirmation revealed that this sample did not express PRL-1 differently from the controls, leaving 2 biological replicates in

the PRL-1 overexpressing group and 3 biological replicates in the vector control group. Probesets that were not called as 'present' by mas5 in at least four out of the five remaining chips were removed from the analysis, save for cases where a probeset was present in both members of the PRL-1 overexpressing group but absent in all of the vector controls. 15,967 probesets of the original 54,675 passed this presence filter.

After transformation into a $\log_2$ scale, mean normalized expression values were calculated for each of the 15,967 probesets over all biological replicates for both of the experimental comparison groups (HEK293-PRL-1 and HEK293-vector). Differential expression between the two groups was determined for each probeset and assessed for significance in terms of p-value by the Student's t-test. Multiple-testing false discovery rate (FDR) correction values were calculated using the Benjamini-Hochberg procedure [35].

7.5.4 Quantitative RT-PCR

A set of 184 genes, identified by microarray and/or proteomic analyses as differentially regulated or associated in the literature with signaling pathways involved in integrin-mediated cell signaling, cytoskeletal remodeling, and/or cell motility, was chosen for validation of gene expression changes using qRT-PCR. Total RNA was isolated as described for the microarray experiments, but using independent biological replicates of HEK293-PRL-1 and HEK293-vector cells. Isolated total RNA was treated with DNase I, using the Ambion TURBO DNA-free kit from Invitrogen Life Technologies and 1μg of each sample was reverse

transcribed into cDNA with the SuperScript III First-Strand Synthesis System and random hexamer primers (Invitrogen Life Technologies), in accordance with the manufacturer's guidelines. The resulting cDNA was used as template for qRT-PCR using commercially available TaqMan Gene Expression Assays (Applied Biosystems, a subsidiary of Life Technologies, Carlsbad, CA) custom arrayed on 96-well plates. Supplemental Table S1 contains the full list of TaqMan assays that were examined.

As per the manufacturer's protocol, cDNAs were combined with TaqMan Gene Expression Master Mix (Applied Biosystems) and 100ng cDNA was added to each well of the custom TaqMan Array Plate and amplified by PCR on an Applied Biosystems 7900HT Fast Real-Time PCR System under the recommended cycling conditions: 2 min at 50°C, 10 min at 95°C and 40 cycles of 15 sec at 95°C for denaturation and 1 min at 60°C for annealing/extension. Raw threshold cycle (C_t) values were obtained using Sequence Detection System (SDS) software v2.4 (Applied Biosystems). C_t values ≥ 40 were set to 40 and were considered not detectable. Among 4 reference genes tested, B2M, 18S ribosomal RNA, GAPDH, and UBC, 18S was found to be the most stable according to analysis with DataAssist Software, v2.0 (Applied Biosystems) and therefore was chosen as the reference gene for normalization of all gene expression results.

For comparative statistics, mRNA data files were processed with Partek Genomics Suite version 6.11.1115 (http://www.partek.com) using default parameters and 18S as the endogenous control. Mean normalized C_t values for

each assay over all biological replicates (n = 2) for both of the experimental comparison groups (HEK293-PRL-1 and HEK293-vector) were calculated. Differential expression between the two comparison groups was determined for each assay using the comparative C_t method ($\Delta\Delta C_t$) and assessed for significance in terms of p-value by the Student's t-test.

7.5.5 Functional, Network, and Pathway Analysis

Two input data sets for functional and pathway analysis of the protein mass-spectrometry results were prepared by applying significance cutoffs of $q \leq 0.20$ and $q \leq 0.50$ to the detected Tier-1 differentially-expressed proteins. These data sets, consisting of 81 and 152 proteins respectively, included each protein's Entrez Gene ID, fold change under the experimental conditions described in the mass-spectrometry section above, and the p-value and FDR-corrected q-value of that change.

Two input data sets for functional and pathway analysis of the mRNA microarray results were prepared by applying significance cutoffs of $q \leq 0.20$ and $q \leq 0.50$ to the detected differentially-expressed probesets. These data sets, consisting of 58 and 2263 probesets respectively, included each probeset's Affymetrix ID, associated gene Entrez ID, fold change under the experimental conditions described in the mass-spectrometry section above, and the p-value and FDR-corrected q-value of that change.

For each of the four above input data sets, enriched biological functions and pathways were determined using three systems: Ingenuity Pathway Analysis

(IPA) software core analysis (Ingenuity Systems, http://www.ingenuity.com), application build version 162820, content version 12710793 with default settings; the Enrichment and Interactome workflows of MetaCore from GeneGo, Inc. version 6.8 with default settings; and the DAVID Functional Annotation and Gene Function Classification tools version 6.7 [36,37].

7.6 Results

To investigate the signaling pathways through which PRL-1 mediates its biological effects, we previously established and characterized a HEK293 cell line stably overexpressing PRL-1 and confirmed that both the mRNA and protein levels of PRL-1 in this line are at least 2-fold higher than that of endogenous PRL-1 in the associated vector control cells [11,16]. The stable overexpression of PRL-1 in the HEK293 cells produces significant changes in the patterns of expression of mRNA transcripts and proteins. In the first part of this section, we examine these changes at the level of the individual nucleic acid and protein experiments. In the second part, we examine these changes using data sets constructed from the integration of the results of nucleic acid and protein experiments.

7.6.1 Mass Spectrometry

To identify proteins whose expression is specifically altered in response to PRL-1, protein lysates from seven independent cultures each of HEK293-PRL-1 and HEK293-vector cells were subjected to MS analysis. Proteomic analysis

resulted in the identification, coding gene annotation, and relative quantification of 763 Tier 1 (high peptide confidence; multiple hits) and 571 Tier 2 (high peptide confidence; single hit) proteins. Of these, there were 45 Tier 1 and 15 Tier 2 proteins that were subtly, but significantly differentially expressed (FDR ≤ 0.05) between the HEK293-PRL-1 and HEK293- vector cell lines. 23 Tier 1 and 5 Tier 2 proteins were up-regulated in the HEK293-PRL-1 lines and 22 Tier 1 and 10 Tier 2 proteins were down-regulated in these lines with respect to the vector controls. A list of significantly differentially expressed Tier 1 proteins is provided in Table 7.1.

7.6.2 Microarray

Expression changes at the mRNA level were simultaneously analyzed using Affymetrix Human Genome U133 Plus 2.0 microarrays on HEK293 cells that were cultured independently from those utilized in the proteomic analysis. Of the 15,967 microarray probesets that were assayed for mRNA expression and found to be present in one or both comparison groups of HEK293 cells, 25 were found to show significant (q ≤ 0.10) differential expression between PRL-1 overproducing and control vector groups after adjustment for FDR. Of these probesets, 11 showed a decrease of expression and 14 showed an increase of expression in the presence of overproduced PRL-1. Table 7.2 lists these probesets along with their corresponding genes.

7.6.3 Quantitative RT-PCR Validation

The protein coded by the top up-regulated transcript by microarray, SPARC (secreted protein, acidic, cysteine-rich), was not detected in the proteomic data, therefore, to further validate the microarray result for this gene, SPARC expression was evaluated by quantitative RT-PCR, using two HEK293-PRL-1 and two HEK293-empty-vector samples that were independent from those used for the microarray analysis. As shown in Table 7.3, qRT-PCR validation confirmed that SPARC mRNA is significantly (q-value = 5.83×10^{-03}, fold-change = 226) up-regulated in response to PRL-1 overexpression.

Previous studies have shown a relationship between PRL-1 and various components of integrin-mediated cell signaling pathways. These integrin-responsive players can promote re-arrangements in the actin cytoskeleton that are central to promotion of cell motility, invasion, and metastasis. Therefore, a total of 184 genes (including SPARC) known to be associated with integrin-mediated signaling pathways or cytoskeletal remodeling were arrayed on Taqman custom 96-well plates and assayed for differential expression in response to PRL-1 up-regulation. Of the 177 qRT-PCR assays that yielded mRNA expression signals, 58 were found to have significant differential expression at a Fold Change > 2, $p \leq 0.02$, and FDR q-value ≤ 0.05. Table 7.3 lists these assays along with their corresponding genes. The full list of qRT-PCR results can be found in Table S1. Most significantly up-regulated genes represented positive regulators of epithelial-mesenchymal transition (EMT), cell proliferation, survival, and migration, for example, HIF1A, ZEB1, H-RAS, N-RAS,

K-RAS, ROCK 1/2, Arp 2/3 (ACTR2/3) and phosphoinositide 3-kinase (PIK3CA and PIK3R1). Only seven genes were significantly down-regulated. Among these were HNF4A, a suppressor of EMT; IGFBP7, a stimulator of cell adhesion and inhibitor of cell growth; and, interestingly, PRL-3 (PTP4A3).

7.6.4 Microarray and protein data integration

Approximately 825 of the 918 Tier-1 proteins detected by mass spectrometry were mapped to a least one probe set on the HG-U133 Plus 2.0 array by coding gene name matching. After accounting for multiple protein products associated with the same coding gene, the final count of unique Tier 1 proteins that were mapped to microarray probesets was 763. Although other groups have demonstrated that some microarray probesets can be associated with the specific mRNA transcripts of particular protein isoforms [38], all protein-mRNA mapping in this study was performed at the more conservative level of the coding gene. Of the 1202 probesets mapped to Tier-1 proteins, 1089 (91%) had detectable gene expression as defined by their presence or absence in either comparison group, demonstrating a high level of co-detection.

Further evidence of the alignment of the mRNA microarray and protein experimental results is provided by a comparison of the distributions of the expression signals of those mRNA probesets that were matched to coding genes of detected proteins and those that were not. Figure 7.1 shows that the proteins associated with higher mRNA expression levels were preferentially detected in the mass-spectrometry experiment in both the empty-vector (EV) and the PRL-1-

overproducing (P1) groups. The medians of the distributions for the protein-matched and non-protein-matched probeset expression values differ by a factor of approximately 4-fold, which is consistent with values reported by other paired protein and mRNA studies [39]. The median expression level for the mRNA's associated with proteins that were detected under PRL-1-overproducing conditions was approximately 5% higher than that observed in the empty vector group.

We also observed a positive directional correlation between the expression levels of 63 significantly-changed ($q \leq 0.10$) proteins and their associated microarray mRNA probesets, as illustrated by the annotated volcano plot in Figure 7.2. Of the 63 proteins with significant differential expression, 52 were mapped to detected microarray probesets and 30 (48%) had corresponding mRNA level changes at a p-value ≤ 0.2. The total number mRNA transcripts with $p \leq 0.2$ that mapped to these 30 proteins was 43. Of these 43 changing transcripts, 39 (91%) demonstrated fold changes in the same direction as the protein and only 4 (mapped to the genes EEF1A1, ELAVL1, FASN, and HSP1A1) changed in the opposite direction.

7.6.5 Functional and Pathway Analysis

7.6.5.1 Functional annotation enrichment

To address the biological relevance of the significantly differentially regulated proteins and mRNA signals under PRL-1 overproducing conditions, we

first used functional annotation enrichment analysis to associate the data with specific biological themes and canonical pathways. Three different tool systems were used: IPA, MetaCore, and DAVID (see Methods).

The enrichment results from the protein data set indicated an over-representation of coding genes related to high-level (more broad) ontology database annotations of cellular proliferation, tumorigenesis, regulation of cell death, and protein folding (p-value range from 1E-11 to 1E-06). The most enriched low-level (more detailed) annotations were spliceosome components and RNA recognition *via* RRM domains, nucleotide binding and metabolism (purines in general and GTP in particular), cytoskeletal remodeling (notably actin and intermediate filaments), and integrin-mediated cell-matrix adhesion (p-value range from 1E-12 to 1E-05).

At the mRNA microarray level, the top functional annotation results follow those for the protein data set in most of the categories described above, including cellular proliferation, tumorigenesis, RNA recognition and splicing, and cytoskeletal remodeling (p-value range from 1E-07 to 1E-03). As an exception, the mRNA data indicate an enrichment in transcriptional regulation terms that is not seen in the protein data, which follows given the greater sensitivity of nucleic acid assays over global protein mass-spectrometry methods when detecting low-abundance regulatory gene products.

7.6.5.2 Pathway analysis

The interactions among the proteins that were differentially-expressed under PRL-1 overexpressing conditions were evaluated in light of previous studies that described PRL-1-associated changes in Rho-mediated signaling pathways [10,12,14], the direct interaction between PRL-1 and Rho-regulator ARHGAP4 [19], and the prominence of Rho-regulating proteins in the mass-spectrometry results of this study (e.g. ARHGDIA, GDI2).

We observe broad changes in cytoskeletal remodeling signaling proteins in the presence of overexpressed PRL-1. These changes are illustrated in **Error! Reference source not found.** using a diagram of selected direct influences of Rho-regulating proteins on cytoskeleton remodeling that was adapted from the Rho-mediated signaling canonical pathways published in the IPA and GeneGo MetaCore databases. Specifically, we observe a decrease in the expression of the Tier-1 Rho guanine nucleotide dissociation inhibitor RhoGDIα (ARHGDIA, foldchange = -1.17, p = 6.8E-12). RhoGDIα binds to the ezrin-radixin-moesin (ERM) proteins, which regulate membrane-cytoskeletal interactions and maintain membrane tension [40]. All three ERM proteins were detected at Tier-1 and show a non-significant but co-directional decrease in expression [41]. RhoGDIα also binds to RhoA. This interaction not only blocks nucleotide exchange and sequesters RhoA away from its substrates, but additionally protects RhoA from proteosomal degradation [42]. Consequently, RhoA protein expression levels tend to mimic the expression of RhoGDIα [42,43]. Consistent with this, RhoA protein levels were decreased in the PRL-1 transfectants compared to the empty

vector controls and this result was confirmed by western blotting (data shown in dissertation Chapter 8). We also observed non-significant, but consistent changes in proteins that drive actin polymerization (e.g. actin-related protein 2 or ACTR2 and other members of the ARP2/3 complex), actin disassembly (e.g. destrin, cofilin-1, and cofilin-2), and myosin light chain components. The direct interaction between PRL-1 (PTP4A1) and ARHGAP4 is shown in **Error! Reference source not found.**, but the indirect influences of PRL-1 on the pathway components (e.g. via ERK1/2) are not shown here.

7.7 Discussion

The identification of genes that are affected by PRL-1 up-regulation may provide important clues regarding the biology of this protein and shed light on the mechanism underlying PRL-1 induced tumorigenesis and metastasis. However, there is an expanding repertoire of genes thought to be under PRL-1 control and no single, linear signaling pathway can be attributed to its effects. Therefore, we took a systems level approach to globally characterize the molecular changes in expression that occur upon sustained exposure to PRL-1 at the transcriptome and proteome levels using DNA microarray and mass spectrometry technology. The HEK293 epithelial cell line was chosen to investigate the effects of PRL-1 overexpression because we had previously characterized the phenotypic alterations, including enhanced cell growth and increased migratory and invasive capacity, associated with stable PRL-1 overexpression in this system [11,16]. Through use of these highly complementary technologies, we have identified

several new genes as being responsive to PRL-1 signaling and provide evidence strengthening the notion that PRL-1 leverages signaling pathways which exert effects mainly on the cell cycle, cytoskeleton, and cellular adhesions to promote cell proliferation and cell survival and to favor the acquisition of invasive and metastatic properties.

7.7.1 Most genes display coordinate regulation at the mRNA and protein levels

Overall, there was good directional correspondence between the RNA and protein data with 91% of mRNA microarray probesets changing in the same direction as the significantly differentially expressed proteins to which they map. This correspondence implies that the levels of these proteins are driven directly by the abundance of their cognate transcripts. There were also instances, however, where the changes at the RNA and protein levels did not parallel one another. There were a small number of instances where one of either the RNA or protein, was changing significantly while the other was not. In addition, there were four genes, ELAVL1 (embryonic lethal, abnormal vision, drosophila-like 1), HSPA1A (heat shock 70kDa protein 1A), EEF1A1 (eukaryotic translation elongation factor 1, alpha 1), and FASN (fatty acid synthase) where the protein and RNA showed opposite expression patterns. A lack of correlation between RNA and protein could be due to multiple factors, including differential turnover rates or the presence of post-transcriptional or post-translational control mechanisms. The established thresholds or differential sensitivities and biases between the microarray and proteomics assays could also be a factor. For one,

proteomics datasets tend to display a systematic bias favoring more abundant proteins over low abundant, transiently expressed or unstable molecules [44-46]. In support of this, an examination of the RNA expression levels revealed that the signal distribution was approximately four times higher for genes whose products were detected in the proteomic survey as compared to those that were not, suggesting that some changes may simply not have been detected due to low protein abundance.

Despite these discrepancies, the combined proteomic and transcriptomic data sets are highly complementary to one another and provide a more complete picture of PRL-1-mediated signaling events, in HEK293 cells, than could be gleaned from either technique in isolation. These data suggest that, in many cases, transcript levels trend the same as protein levels and can be used as a general indicator of protein abundance in this system, but that both transcription-dependent and transcription-independent pathways contribute to PRL-1-induced signaling responses.

7.7.2 FLNA, HNRNPH2, and PRDX2 are among the most significantly changing gene products in both the microarray and proteomics datasets

A total of 17 genes were identified (those marked with an asterisk in Figure 7.2) that exhibited statistically significant changes in expression at both the RNA and protein levels and each of these is revealed here, for the first time, to be responsive to alterations in PRL-1 expression. Three of these genes, FLNA, HNRNPH2, and PRDX2 continued to reach significance at both the RNA

and protein levels, even after multiple testing correction was applied to both data sets and therefore make highly promising candidates for downstream components of the PRL-1 signaling pathway.

FLNA (Filamin A) represents the most robustly and highly up-regulated protein in the proteomic analysis. In addition, all three probesets for FLNA on the Affymetrix microarray showed approximately 2-fold up-regulation in response to PRL-1 ($p < 0.05$). The FLNA gene encodes the most abundant and widely expressed member of a family of three filamin proteins (FLNa, FLNb, FLNc) [47]. It is a large, homodimeric, actin binding protein that plays important roles in remodeling the cytoskeleton to influence cell shape and cell motility [47-49]. Cells deficient in FLNa exhibit defects in both cell spreading and initiation of migration [50].

Filamin A also serves as a versatile molecular scaffold, connecting and coordinating the intracellular signaling partners from a wide variety of cellular processes. It directly interacts with more than 90 different proteins including transmembrane receptors, ion channels, intracellular signaling molecules, and transcription factors [51]. Among these are several members of the integrin and Rho GTPase families which play central roles in actin cytoskeletal reorganization, cell adhesion, cell migration, invasion, and control of cell cycle progression [52-54]. FLNa can bind the Rho GTPases Rho, Rac, and Cdc42, the Rac guanine nucleotide exchange factor (GEF) Trio, the RhoGEF Lbc, the Rho GTPase activating protein p190RhoGAP, the Rac GAP FilGAP, and the Rho GTPase effectors PAK and ROCK [48]. These interactions make FLNa an ideal integrator

of the Rho GTPase signaling cascade. Changes in PRL-1 expression have previously been shown to alter the downstream activity (amount bound to GTP) of RhoA, RhoC, Rac1, and Cdc42 [10,12]. Moreover, PRL-1 overexpression in the current study led to down-regulation of RhoGDIα and RhoA expression levels. The strong up-regulation of FLNa in the PRL-1 transfectants, combined with its known relationship to the Rho pathways make it an attractive subject for future examination as a potential link between PRL-1 and control of Rho GTPase-mediated signaling.

Besides having an influence on various mediators of cell cycle and cell migration, FLNa has been implicated in regulation of a multitude of other wide-ranging processes. Among these, regulation of potassium ion channel function [55-57], vascular function and angiogenesis [58-61], TGFβ-mediated signaling [62-64], and integrin receptor recycling [65] are particularly intriguing, given that PRL family member PRL-3 has previously been linked to each of these processes [10,66-69]. Furthermore, FLNa has been found to directly interact with and control the surface expression levels of the 2.1 subunit (also known as KCNJ2) of the inwardly rectifying K^+ 2 (Kir2) subfamily of potassium channel [57]. In the current study, we did not detect significant changes in Kir2.1 levels, however we did find that PRL-1 overexpression led to significantly elevated (1.6 fold) transcript levels of the Kir2.2 subunit (KCNJ12), which can heterotetramerize with Kir2.1 to form active Kir channels [70]. FLNa thus has the potential to serve as a link between PRL-1 and a wide variety of downstream signaling pathways, which may, in part, overlap with the functions of closely

related family member PRL-3. Interestingly, expression of PRL-3 mRNA was decreased in the PRL-1 transfectants.

HNRNPH2 was also significantly up-regulated at both the mRNA and protein levels in response to PRL-1. This molecule belongs to the heterogenous nuclear ribonucleoprotein (hnRNP) family of RNA-binding proteins which heavily influence pre-mRNA processing as well as other aspects of mRNA metabolism and transport [71,72]. The hnRNPH2 protein is part of a subfamily of hnRNP whose members (H1, H2, H3, and F) are best known for their key roles in the regulation of alternative splicing. Splice site selection is controlled by the orchestrated effects of multiple splicing factors that bind to specific RNA elements and either promote or impede the assembly of the splicing machinery [73,74]. In addition to the HNRNP family, other gene families with well known roles in alternative splice site selection include the serine/arginine-rich splicing factor (SRSF) family [74] and the embryonic lethal, abnormal vision, *Drosophila*-like (ELAVL) family [75,76]. Notably, in our study, members of each of these three families of splice site regulators (HNRNPH1, HNRNPH2, HNRNPF, HNRNPA3, SRSF2, SRSF3, and ELAVL1) exhibited significant changes in expression, at least at the protein level, upon PRL-1 overexpression. Alternative splicing increases the functional complexity of gene expression and, in tumors, it generates variants that can contribute to multiple aspects of tumor establishment, progression, and maintenance. Observations suggest that genes involved in cell morphology, movement, adhesion, growth, proliferation, and cytoskeletal organization are particularly prone to alternative splicing events [77]. Genes

involved in each of these processes have been shown, both here and in other studies, to be modulated by PRL-1 raising the possibility that changing alternative splicing patterns may be one mechanism by which PRL-1 contributes to cancer cell plasticity.

In contrast to FLNA and HNRNPH2, the gene products of PRDX2 were significantly down-regulated upon PRL-1 overexpression. PRDX2 is a member of the peroxiredoxin (Prdx) family of ubiquitously expressed antioxidant enzymes with important functions in maintaining cellular redox homeostasis [78]. Additional roles have also been found for the Prdx enzymes in signal transduction, protection from tissue injury and infection, and tumorigenesis [79,80]. Family member Prdx1 (also decreasing with PRL-1 expression in our study) has been described as a tumor suppressor, because it binds c-myc, suppressing its oncogenic signaling potential [81], binds to the tumor suppressor PTEN, protecting it from oxidative inactivation, and suppresses H-Ras and ErbB-2-induced cellular transformation and tumor formation [82]. Studies have also shown that inactivation of Prdx1 or Prdx2 may be necessary for hydrogen peroxide mediated cellular signaling in response to growth factor stimulation and for cell survival signaling under conditions of oxidative stress [83,84]. However, elevated levels of each Prdx family member have been found in a variety of cancer cell lines and tissues [79,85-87] and both Prdx1 and Prdx2 can directly suppress the activity of several pro-apoptotic factors [79]. Therefore, the functional consequences of Prdx activity and/or inhibition remain an active area of study.

Taken together, the consistent and robust changes between RNA and protein for FLNA, HNRNPH2, and PRDX2, provides strong confidence that these alterations can be attributed to PRL-1 overexpression and make these attractive candidates for further investigation.

7.7.3 The matrix associated gene SPARC (osteonectin) is the most significantly up-regulated gene at the mRNA level

Most PRL-1-induced differences in expression were less than two-fold in magnitude, however, SPARC transcripts were shown by the Affymetrix microarray to be up-regulated 20-fold ($p = 5.86E-05$) in the PRL-1 transfectants compared to vector control cells. SPARC (also known as osteonectin) is a non-structural, extracellular matrix (matricellular) glycoprotein that is involved in matrix remodeling and influences a diverse array of biological processes [Reviewed in 88,89-91]. SPARC influences cell-cell and cell-matrix interactions; promotes extracellular matrix remodeling; regulates integrin expression and activity; alters focal adhesions; and modulates the activity of growth factors, cell cycle regulators, matrix metalloproteinases, and molecules involved in cytoskeletal rearrangement. It thereby controls a wide range of cellular functions, including cell cycle progression, cell proliferation, cell survival, angiogenesis, migration, invasion and metastasis. However its effects on these processes are highly context and cell type dependent [88].

Although qRT-PCR validation, in an independent sample set, reproducibly confirmed the significant up-regulation of SPARC message in the HEK293-PRL-1

transfectants, no protein product was detected for this gene in either the PRL-1 overexpressing or the control cell lines. However, SPARC is a secreted protein and internalized SPARC is thought to be quickly re-released outside the cell [92], which could explain our inability to detect SPARC protein in whole cell lysates. Differential RNA and protein stability could also play a role given that SPARC message has been found to be stable for more than 38 hours [93], while SPARC protein has a half-life of less than two hours [94]. Limitations described in the previous section, regarding low abundance proteins, could also be a factor. Nevertheless, overexpression of PRL-1 in HEK293 cells clearly leads to enhanced levels of SPARC mRNA transcripts, which could play a role in mediating the signaling events downstream of PRL-1. Further supporting this notion, qRT-PCR analysis revealed that FAK (PTK2), SHC, and the Ras pathway, all which lie immediately downstream of SPARC, were also up-regulated in response to PRL-1 overexpression. A proposed diagram of SPARC-mediated signaling is included in Figure 7.4.

Several parallels exist between SPARC and PRL-1 signaling. When overexpressed in epithelial cells, both genes induce morphological and biological changes consistent with an EMT-like transition [11,12,95]. Each has pleiotropic functions with the capacity to enhance cellular proliferation and metastatic potential, but also playing important roles in cellular differentiation [1,96]. Both molecules display similar tumor type specific influences on human tumor tissues [17,88,89,97-100]. Both can also exert similar effects on downstream signaling pathways and molecules such as E-Cadherin [12,101], Src [11,102], FAK

[11,101], ERK1/2 [11,103], MMP2 [11,104], Akt, p53, $p21^{cip1/waf1}$ [18,105,106], and the Rho GTPase family members [12,102]. Moreover, both genes have been implicated in maintenance of retinal function [5,107,108]. Both display age-dependent changes in expression with an inverse correlation to age in the skeletal muscle [17,109] and a positive correlation to age in structures of the brain [17,110]. And finally, both genes exhibit cell cycle dependent localization of expression [21,111]. During mitosis, PRL-1 interacts directly with α-tubulin and localizes to the centrosomes, where it has been suggested to play a role in modulating spindle dynamics [21]. Interestingly, the integrin-linked kinase (ILK), which is a SPARC interaction partner and a known effector of SPARC signaling [112], also localizes to the centrosome in mitotic cells, where it binds to the RuvB-like proteins 1 and 2 (RUVBL1, RUVBL2), which were both significantly up-regulated in the HEK293-PRL-1 cells. Together, ILK, RUVBL1, and RUVBL2 regulate microtubule dynamics and mitotic spindle organization [113]. ILK also connects to Filamin A through the Filamin binding protein Migfilin. These many commonalities between the PRL-1 and SPARC signaling pathways, along with the up-regulation of SPARC transcripts in response to PRL-1, make SPARC an attractive candidate as a mediator of PRL-1 function.

7.7.4 Altered levels of gene products involved in cytoskeletal rearrangements are a common theme with PRL-1 overexpression

Dynamic reorganization of the cytoskeleton is the primary mechanism by which cells generate the protrusive structures and contractile forces necessary

for cell movement [114-117]. Cytoskeletal changes also play a crucial role in the orchestration of cell division [118,119]. In this study, transcriptomic and proteomic analysis revealed that stable overexpression of PRL-1 significantly alters the RNA and/or protein levels of a number of molecules with roles in the assembly, organization, and regulation of each of the three main structural components of the cytoskeleton. PRL-1 overexpression led to significant up-regulation of actin-binding and cross-linking proteins such as FLNA, transgelin-2 (TAGLN2), and the alpha-actinin isoforms ACTN1, ACTN2, and ACTN4. Conversely, overexpression of PRL-1 caused the significant down-regulation of tubulin isoforms (TUBA1A, TUBA4A, TUBA1C, TUBA3C), the microtubule regulators RAN and stathmin (STMN1 and STMN2), the intermediate filament protein vimentin (VIM), and the regulator of Rho signaling RhoGDIα. These data suggest that PRL-1 can modulate cytoskeletal changes at multiple levels. Moreover, the known interaction between PRL-1 and α-tubulin [21] suggests that the influence of PRL-1 on the various isoforms of α-tubulin may be direct.

It deserves mention that up-regulation of vimentin is one of the hallmarks of conversion from an epithelial to a mesenchymal phenotype and expression of vimentin is typically correlated with enhanced cell migration and invasive activity [120]. Thus, we were surprised to find that both vimentin RNA and protein were slightly down-regulated in the PRL-1 transfectants, especially considering that PRL-1 overexpression visibly alters the morphology of HEK293 cells, causing them to elongate and take on a more fibroblast-like appearance and also results in a gain of invasive motility, both changes that are consistent with EMT [121].

Vimentin expression levels have also previously been reported to positively correlate with the expression of FLNA [122] and SPARC [95], hence the mechanisms leading to down-regulation of vimentin in the present study are currently unclear. In some cell types, down-regulation of vimentin has been proposed to inhibit apoptosis, contributing to cell survival and resistance to various anti-cancer agents [123-125]. Therefore it is plausible that PRL-1-mediated down-regulation of vimentin could provide HEK293 cells with a survival advantage.

Further supporting the ability of PRL-1 to exert strong influences on the cytoskeleton, members of the Rho signaling pathway and molecules that feed into this pathway were highly over-represented among both significant and non-significant differentially expressed gene products. Alterations in several molecules downstream of the Rho GTPases that mediate actin polymerization and disassembly are consistent with the occurrence of active cytoskeletal remodeling in these cells. Many other molecules with known or suspected roles in the regulation of cytoskeletal reorganization and cell migration also displayed significantly altered expression in response to PRL-1, including SPARC [102,126], ELAVL1 [127], HSPA1A (Hsp70) [128], EIF6 [129], EEF1A1 [130], IGF2BP1 [131], NME1 [132], NME2 [133], SEPT11 [134], LGALS3BP [135], SPINT2 [136], VCAN [137], MYADM [138], RAB35 [139], FLRT1 [140], and FAM84B [141]. Accordingly, functional enrichment analysis showed an over-representation of genes related to cytoskeletal remodeling and cell adhesion. Up-regulation of gene products involved in nucleotide, nucleic acid, protein, and lipid biosynthesis

was also a common theme, consistent with an increased rate of proliferation in the PRL-1 overexpressing cells.

Taken together, all of the above data support a role for PRL-1 in modulation of cytoskeletal components and cytoskeletal regulators to influence cell proliferation, survival, invasion, and migration. Given that PRL-1 significantly up-regulates Filamin A and down-regulates RhoGDIα and RhoA in this system; that Filamin A is known to control the early phases of cell spreading and migration initiation [50]; and that an initial inhibition of RhoA is necessary early on to allow membrane extension during cell spreading [52]; the current evidence may implicate a role for PRL-1 in the very early stages of cell spreading and migration, at least in HEK293 cells.

7.8 Conclusions

The use of two highly complementary technologies (microarray and mass spectrometry) has expanded our knowledge of the repertoire of signaling molecules and pathways effected by PRL-1 and allowed the identification of several novel candidates for downstream mediators of PRL-1 function. In particular, Filamin A, RhoGDIα, and SPARC are attractive subjects of future study given their established relationships with a number of signaling molecules (e.g. the Rho GTPase family) known to be influenced by PRL-1 expression. PRL-1 was also found to significantly alter the expression of multiple other genes with roles in regulation of cell shape, adhesion, motility, and the cell cycle, supporting prior evidence that PRL-1 may control cytoskeletal dynamics and cell

division. In particular, members of the Rho signaling pathway appear to be heavily influenced by PRL-1 overexpression. PRL-1 also has strong influence on the expression of genes involved in alternative splicing, presenting another possible mechanism by which PRL-1 may contribute to the acquisition of a tumorigenic and/or metastatic phenotype. This study represents the first comprehensive overview of the biological impact of PRL-1 overexpression on cellular mRNA or protein levels. It is clear from these results that the effects of PRL-1 are much broader than we currently understand. Although further studies will be required to characterize and examine the consequences of the interactions between PRL-1 and the PRL-1 responsive molecules identified here, these results provide a rich resource of information that should serve as a starting point to open up new lines of investigation into the role of this important oncogene.

7.9 Abbreviations Not Defined in Manuscript Text

ARHGDIA, Rho GDP dissociation inhibitor alpha; ARP, actin-related protein; ATF-7, activating transcription factor 7; B2M, beta-2 microglobulin; Cdk2, cyclin-dependent kinase 2; cDNA, complementary DNA; DNA, deoxyribonucleic acid; DTT, Dithiothreitol; Egr-1, early growth response 1; EIF6, eukaryotic translation initiation factor 6; ERK, extracellular signal-regulated kinase; FAK, focal adhesion kinase; FAM84B, family with sequence similarity 84, member B; FLRT1, fibronectin leucine rich transmembrane protein 1; GAPDH, glyceraldehyde-3-phosphate dehydrogenase; GDP, guanosine 5’-diphosphate;

GTP, guanosine 5’-triphosphate; HIF1A, hypoxia inducible factor 1, alpha subunit; HNF4A, hepatocyte nuclear factor 4, alpha; HPLC, high-performance liquid chromatography; ID, identification; IGFBP7, insulin-like growth factor 2 binding protein 7; IGF2BP1, insulin-like growth factor 2 mRNA binding protein 1; KCNJ, potassium inwardly rectifying channel, subfamily J; LGALS3BP, lectin, galactoside-binding, soluble, 3 binding protein; Mas5, Microarray Analysis Suite 5.0; MEKK1, mitogen-activated protein kinase kinase kinase 1 (Gene Symbol MAP3K1); MMP, matrix metalloproteinase; MYADM, myeloid-associated differentiation marker; NME, non-metastatic cells; PAK, p21 protein (Cdc42/Rac)-activated kinase 1; PBS, phosphate buffered saline; RAB35, ras-related (ras analog in brain) protein 35; RAN, ras-related nuclear protein; RAS, Rous sarcoma kinase; RNA, ribonucleic acid; ROCK, Rho-associated, coiled-coil containing protein kinase; RRM, RNA recognition motif; SEPT, septin; SHC, Src homology 2 domain containing transforming protein; SPINT2, serine peptidase inhibitor, Kunitz type 2; Src, v-src sarcoma (Schmidt-Ruppin A-2) viral oncogene homolog; TGFβ, transforming growth factor, beta 1; TNF, tumor necrosis factor; UBC, ubiquitin C; VCAN, versican; ZEB1, zinc finger E-box binding homeobox 1.

7.10 Authors’ Contributions

CMD designed and performed the microarray, RT-PCR, and western blot experiments, wrote the manuscript and participated in the analysis and tabulation of the RT-PCR data. CDW cultured the cells for all experiments, prepared the samples for mass spectrometry analysis, and designed and oversaw the MS

experiments. BAS performed all data integration and analysis, created most figures and tables, and co-wrote the results portion of the manuscript. SKR and ZYZ assisted in the design and coordination of and supervised all experiments. ZYZ provided the cell lines. All authors participated in the review of this manuscript and reviewed and approved the final document.

7.11 Manuscript References

1. Diamond RH, Peters C, Jung SP, Greenbaum LE, Haber BA, et al. (1996) Expression of PRL-1 nuclear PTPase is associated with proliferation in liver but with differentiation in intestine. Am J Physiol 271: G121-129.

2. Guo K, Li J, Wang H, Osato M, Tang JP, et al. (2006) PRL-3 initiates tumor angiogenesis by recruiting endothelial cells in vitro and in vivo. Cancer Res 66: 9625-9635.

3. Guo S, Russo IH, Russo J (2003) Difference in gene expression profile in breast epithelial cells from women with different reproductive history. Int J Oncol 23: 933-941.

4. Takano S, Fukuyama H, Fukumoto M, Kimura J, Xue JH, et al. (1996) PRL-1, a protein tyrosine phosphatase, is expressed in neurons and oligodendrocytes in the brain and induced in the cerebral cortex following transient forebrain ischemia. Brain Res Mol Brain Res 40: 105-115.

5. Yu L, Kelly U, Ebright JN, Malek G, Saloupis P, et al. (2007) Oxidative stress-induced expression and modulation of Phosphatase of Regenerating Liver-1 (PRL-1) in mammalian retina. Biochim Biophys Acta 1773: 1473-1482.

6. Diamond RH, Cressman DE, Laz TM, Abrams CS, Taub R (1994) PRL-1, a unique nuclear protein tyrosine phosphatase, affects cell growth. Mol Cell Biol 14: 3752-3762.

7. Mohn KL, Laz TM, Hsu JC, Melby AE, Bravo R, et al. (1991) The immediate-early growth response in regenerating liver and insulin-stimulated H-35 cells: comparison with serum-stimulated 3T3 cells and identification of 41 novel immediate-early genes. Mol Cell Biol 11: 381-390.

8. Cates CA, Michael RL, Stayrook KR, Harvey KA, Burke YD, et al. (1996) Prenylation of oncogenic human PTP(CAAX) protein tyrosine phosphatases. Cancer Lett 110: 49-55.

9. Werner SR, Lee PA, DeCamp MW, Crowell DN, Randall SK, et al. (2003) Enhanced cell cycle progression and down regulation of p21(Cip1/Waf1) by PRL tyrosine phosphatases. Cancer Lett 202: 201-211.

10. Fiordalisi JJ, Keller PJ, Cox AD (2006) PRL tyrosine phosphatases regulate rho family GTPases to promote invasion and motility. Cancer Res 66: 3153-3161.

11. Luo Y, Liang F, Zhang ZY (2009) PRL1 promotes cell migration and invasion by increasing MMP2 and MMP9 expression through Src and ERK1/2 pathways. Biochemistry 48: 1838-1846.

12. Nakashima M, Lazo JS (2010) Phosphatase of regenerating liver-1 promotes cell migration and invasion and regulates filamentous actin dynamics. J Pharmacol Exp Ther 334: 627-633.

13. Zeng Q, Dong JM, Guo K, Li J, Tan HX, et al. (2003) PRL-3 and PRL-1 promote cell migration, invasion, and metastasis. Cancer Res 63: 2716-2722.

14. Achiwa H, Lazo JS (2007) PRL-1 tyrosine phosphatase regulates c-Src levels, adherence, and invasion in human lung cancer cells. Cancer Res 67: 643-650.

15. Stephens B, Han H, Hostetter G, Demeure MJ, Von Hoff DD (2008) Small interfering RNA-mediated knockdown of PRL phosphatases results in altered Akt phosphorylation and reduced clonogenicity of pancreatic cancer cells. Mol Cancer Ther 7: 202-210.

16. Sun JP, Luo Y, Yu X, Wang WQ, Zhou B, et al. (2007) Phosphatase activity, trimerization, and the C-terminal polybasic region are all required for PRL1-mediated cell growth and migration. J Biol Chem 282: 29043-29051.

17. Dumaual CM, Sandusky GE, Soo HW, Werner SR, Crowell PL, et al. (2012) Tissue-specific alterations of PRL-1 and PRL-2 expression in cancer. Am J Transl Res 4: 83-101.

18. Min SH, Kim DM, Heo YS, Kim YI, Kim HM, et al. (2009) New p53 target, phosphatase of regenerating liver 1 (PRL-1) downregulates p53. Oncogene 28: 545-554.

19. Bai Y, Luo Y, Liu S, Zhang L, Shen K, et al. (2011) PRL-1 protein promotes ERK1/2 and RhoA protein activation through a non-canonical interaction with the Src homology 3 domain of p115 Rho GTPase-activating protein. J Biol Chem 286: 42316-42324.

20. Peters CS, Liang X, Li S, Kannan S, Peng Y, et al. (2001) ATF-7, a novel bZIP protein, interacts with the PRL-1 protein-tyrosine phosphatase. J Biol Chem 276: 13718-13726.

21. Wang J, Kirby CE, Herbst R (2002) The tyrosine phosphatase PRL-1 localizes to the endoplasmic reticulum and the mitotic spindle and is required for normal mitosis. J Biol Chem 277: 46659-46668.

22. Ewing RM, Chu P, Elisma F, Li H, Taylor P, et al. (2007) Large-scale mapping of human protein-protein interactions by mass spectrometry. Mol Syst Biol 3: 89.

23. Choi MS, Min SH, Jung H, Lee JD, Lee TH, et al. (2011) The essential role of FKBP38 in regulating phosphatase of regenerating liver 3 (PRL-3) protein stability. Biochem Biophys Res Commun 406: 305-309.

24. Peng Y, Du K, Ramirez S, Diamond RH, Taub R (1999) Mitogenic up-regulation of the PRL-1 protein-tyrosine phosphatase gene by Egr-1. Egr-1 activation is an early event in liver regeneration. J Biol Chem 274: 4513-4520.

25. Skinner AL, Vartia AA, Williams TD, Laurence JS (2009) Enzyme activity of phosphatase of regenerating liver is controlled by the redox environment and its C-terminal residues. Biochemistry 48: 4262-4272.

26. Hale JE, Butler JP, Gelfanova V, You JS, Knierman MD (2004) A simplified procedure for the reduction and alkylation of cysteine residues in proteins prior to proteolytic digestion and mass spectral analysis. Anal Biochem 333: 174-181.

27. Higgs RE, Knierman MD, Freeman AB, Gelbert LM, Patil ST, et al. (2007) Estimating the statistical significance of peptide identifications from shotgun proteomics experiments. J Proteome Res 6: 1758-1767.

28. Higgs RE, Knierman MD, Gelfanova V, Butler JP, Hale JE (2005) Comprehensive label-free method for the relative quantification of proteins from biological samples. J Proteome Res 4: 1442-1450.

29. Higgs RE, Knierman MD, Gelfanova V, Butler JP, Hale JE (2008) Label-free LC-MS method for the identification of biomarkers. Methods Mol Biol 428: 209-230.

30. Craig R, Beavis RC (2004) TANDEM: matching proteins with tandem mass spectra. Bioinformatics 20: 1466-1467.

31. Yates JR, 3rd, Eng JK, McCormack AL, Schieltz D (1995) Method to correlate tandem mass spectra of modified peptides to amino acid sequences in the protein database. Anal Chem 67: 1426-1436.

32. Gautier L, Cope L, Bolstad BM, Irizarry RA (2004) affy--analysis of Affymetrix GeneChip data at the probe level. Bioinformatics 20: 307-315.

33. Gentleman RC, Carey VJ, Bates DM, Bolstad B, Dettling M, et al. (2004) Bioconductor: open software development for computational biology and bioinformatics. Genome Biol 5: R80.

34. Helvering LM, Adrian MD, Geiser AG, Estrem ST, Wei T, et al. (2005) Differential effects of estrogen and raloxifene on messenger RNA and matrix metalloproteinase 2 activity in the rat uterus. Biol Reprod 72: 830-841.

35. Benjamini Y, Hochberg Y (1995) Controlling the False Discovery Rate: a practical and powerful approach to multiple testing. J R Statist Soc B 57: 289-300.

36. Huang da W, Sherman BT, Lempicki RA (2009) Bioinformatics enrichment tools: paths toward the comprehensive functional analysis of large gene lists. Nucleic Acids Res 37: 1-13.

37. Huang da W, Sherman BT, Lempicki RA (2009) Systematic and integrative analysis of large gene lists using DAVID bioinformatics resources. Nat Protoc 4: 44-57.

38. Li Q, Birkbak NJ, Gyorffy B, Szallasi Z, Eklund AC (2011) Jetset: selecting the optimal microarray probe set to represent a gene. BMC Bioinformatics 12: 474.

39. Mootha VK, Bunkenborg J, Olsen JV, Hjerrild M, Wisniewski JR, et al. (2003) Integrated analysis of protein composition, tissue diversity, and gene regulation in mouse mitochondria. Cell 115: 629-640.

40. Liu Y, Belkina NV, Park C, Nambiar R, Loughhead SM, et al. (2012) Constitutively active ezrin increases membrane tension, slows migration, and impedes endothelial transmigration of lymphocytes in vivo in mice. Blood 119: 445-453.

41. Takahashi K, Sasaki T, Mammoto A, Takaishi K, Kameyama T, et al. (1997) Direct interaction of the Rho GDP dissociation inhibitor with ezrin/radixin/moesin initiates the activation of the Rho small G protein. J Biol Chem 272: 23371-23375.

42. Boulter E, Garcia-Mata R, Guilluy C, Dubash A, Rossi G, et al. (2010) Regulation of Rho GTPase crosstalk, degradation and activity by RhoGDI1. Nat Cell Biol 12: 477-483.

43. Giang Ho TT, Stultiens A, Dubail J, Lapiere CM, Nusgens BV, et al. (2011) RhoGDIalpha-dependent balance between RhoA and RhoC is a key regulator of cancer cell tumorigenesis. Mol Biol Cell 22: 3263-3275.

44. Chandramouli K, Qian PY (2009) Proteomics: challenges, techniques and possibilities to overcome biological sample complexity. Hum Genomics Proteomics 2009.

45. Cho WC (2007) Proteomics technologies and challenges. Genomics Proteomics Bioinformatics 5: 77-85.

46. Piruzian E, Bruskin S, Ishkin A, Abdeev R, Moshkovskii S, et al. (2010) Integrated network analysis of transcriptomic and proteomic data in psoriasis. BMC Syst Biol 4: 41.

47. Stossel TP, Condeelis J, Cooley L, Hartwig JH, Noegel A, et al. (2001) Filamins as integrators of cell mechanics and signalling. Nat Rev Mol Cell Biol 2: 138-145.

48. Zhou AX, Hartwig JH, Akyurek LM (2010) Filamins in cell signaling, transcription and organ development. Trends Cell Biol 20: 113-123.

49. Glogauer M, Arora P, Chou D, Janmey PA, Downey GP, et al. (1998) The role of actin-binding protein 280 in integrin-dependent mechanoprotection. J Biol Chem 273: 1689-1698.

50. Baldassarre M, Razinia Z, Burande CF, Lamsoul I, Lutz PG, et al. (2009) Filamins regulate cell spreading and initiation of cell migration. PLoS One 4: e7830.

51. Nakamura F, Stossel TP, Hartwig JH (2011) The filamins: organizers of cell structure and function. Cell Adh Migr 5: 160-169.

52. Huveneers S, Danen EH (2009) Adhesion signaling - crosstalk between integrins, Src and Rho. J Cell Sci 122: 1059-1069.

53. Schwartz MA, Assoian RK (2001) Integrins and cell proliferation: regulation of cyclin-dependent kinases via cytoplasmic signaling pathways. J Cell Sci 114: 2553-2560.

54. Villalonga P, Ridley AJ (2006) Rho GTPases and cell cycle control. Growth Factors 24: 159-164.

55. Cantiello HF, Prat AG, Bonventre JV, Cunningham CC, Hartwig JH, et al. (1993) Actin-binding protein contributes to cell volume regulatory ion channel activation in melanoma cells. J Biol Chem 268: 4596-4599.

56. Petrecca K, Miller DM, Shrier A (2000) Localization and enhanced current density of the Kv4.2 potassium channel by interaction with the actin-binding protein filamin. J Neurosci 20: 8736-8744.

57. Sampson LJ, Leyland ML, Dart C (2003) Direct interaction between the actin-binding protein filamin-A and the inwardly rectifying potassium channel, Kir2.1. J Biol Chem 278: 41988-41997.

58. Armstrong LJ, Heath VL, Sanderson S, Kaur S, Beesley JF, et al. (2008) ECSM2, an endothelial specific filamin a binding protein that mediates chemotaxis. Arterioscler Thromb Vasc Biol 28: 1640-1646.

59. Falet H, Pollitt AY, Begonja AJ, Weber SE, Duerschmied D, et al. (2010) A novel interaction between FlnA and Syk regulates platelet ITAM-mediated receptor signaling and function. J Exp Med 207: 1967-1979.

60. Kakita A, Hayashi S, Moro F, Guerrini R, Ozawa T, et al. (2002) Bilateral periventricular nodular heterotopia due to filamin 1 gene mutation: widespread glomeruloid microvascular anomaly and dysplastic cytoarchitecture in the cerebral cortex. Acta Neuropathol 104: 649-657.

61. Yu N, Erb L, Shivaji R, Weisman GA, Seye CI (2008) Binding of the P2Y2 nucleotide receptor to filamin A regulates migration of vascular smooth muscle cells. Circ Res 102: 581-588.

62. Castoria G, D'Amato L, Ciociola A, Giovannelli P, Giraldi T, et al. (2011) Androgen-induced cell migration: role of androgen receptor/filamin A association. PLoS One 6: e17218.

63. Loy CJ, Sim KS, Yong EL (2003) Filamin-A fragment localizes to the nucleus to regulate androgen receptor and coactivator functions. Proc Natl Acad Sci U S A 100: 4562-4567.

64. Sasaki A, Masuda Y, Ohta Y, Ikeda K, Watanabe K (2001) Filamin associates with Smads and regulates transforming growth factor-beta signaling. J Biol Chem 276: 17871-17877.

65. Kim H, McCulloch CA (2011) Filamin A mediates interactions between cytoskeletal proteins that control cell adhesion. FEBS Lett 585: 18-22.

66. Jiang Y, Liu XQ, Rajput A, Geng L, Ongchin M, et al. (2011) Phosphatase PRL-3 is a direct regulatory target of TGFbeta in colon cancer metastasis. Cancer Res 71: 234-244.

67. Krndija D, Munzberg C, Maass U, Hafner M, Adler G, et al. (2012) The phosphatase of regenerating liver 3 (PRL-3) promotes cell migration via Arf-activity dependent stimulation of integrin alpha5 recycling. J Cell Sci.

68. Lai W, Chen S, Wu H, Guan Y, Liu L, et al. (2011) PRL-3 promotes the proliferation of LoVo cells via the upregulation of KCNN4 channels. Oncol Rep 26: 909-917.

69. Ming J, Liu N, Gu Y, Qiu X, Wang EH (2009) PRL-3 facilitates angiogenesis and metastasis by increasing ERK phosphorylation and up-regulating the levels and activities of Rho-A/C in lung cancer. Pathology 41: 118-126.

70. Panama BK, McLerie M, Lopatin AN (2010) Functional consequences of Kir2.1/Kir2.2 subunit heteromerization. Pflugers Arch 460: 839-849.

71. McCloskey A, Taniguchi I, Shinmyozu K, Ohno M (2012) hnRNP C tetramer measures RNA length to classify RNA polymerase II transcripts for export. Science 335: 1643-1646.

72. Weighardt F, Biamonti G, Riva S (1996) The roles of heterogeneous nuclear ribonucleoproteins (hnRNP) in RNA metabolism. Bioessays 18: 747-756.

73. Black DL (2003) Mechanisms of alternative pre-messenger RNA splicing. Annu Rev Biochem 72: 291-336.

74. Busch A, Hertel KJ (2012) Evolution of SR protein and hnRNP splicing regulatory factors. Wiley Interdiscip Rev RNA 3: 1-12.

75. Izquierdo JM (2008) Hu antigen R (HuR) functions as an alternative pre-mRNA splicing regulator of Fas apoptosis-promoting receptor on exon definition. J Biol Chem 283: 19077-19084.

76. Antic D, Keene JD (1997) Embryonic lethal abnormal visual RNA-binding proteins involved in growth, differentiation, and posttranscriptional gene expression. Am J Hum Genet 61: 273-278.

77. Germann S, Gratadou L, Dutertre M, Auboeuf D (2012) Splicing programs and cancer. J Nucleic Acids 2012: 269570.

78. Rhee SG, Chae HZ, Kim K (2005) Peroxiredoxins: a historical overview and speculative preview of novel mechanisms and emerging concepts in cell signaling. Free Radic Biol Med 38: 1543-1552.

79. Ishii T, Warabi E, Yanagawa T (2012) Novel roles of peroxiredoxins in inflammation, cancer and innate immunity. J Clin Biochem Nutr 50: 91-105.

80. Neumann CA, Cao J, Manevich Y (2009) Peroxiredoxin 1 and its role in cell signaling. Cell Cycle 8: 4072-4078.

81. Mu ZM, Yin XY, Prochownik EV (2002) Pag, a putative tumor suppressor, interacts with the Myc Box II domain of c-Myc and selectively alters its biological function and target gene expression. J Biol Chem 277: 43175-43184.

82. Cao J, Schulte J, Knight A, Leslie NR, Zagozdzon A, et al. (2009) Prdx1 inhibits tumorigenesis via regulating PTEN/AKT activity. EMBO J 28: 1505-1517.

83. Day AM, Brown JD, Taylor SR, Rand JD, Morgan BA, et al. (2012) Inactivation of a peroxiredoxin by hydrogen peroxide is critical for thioredoxin-mediated repair of oxidized proteins and cell survival. Mol Cell 45: 398-408.

84. Woo HA, Yim SH, Shin DH, Kang D, Yu DY, et al. (2010) Inactivation of peroxiredoxin I by phosphorylation allows localized H(2)O(2) accumulation for cell signaling. Cell 140: 517-528.

85. Basu A, Banerjee H, Rojas H, Martinez SR, Roy S, et al. (2011) Differential expression of peroxiredoxins in prostate cancer: consistent upregulation of PRDX3 and PRDX4. Prostate 71: 755-765.

86. Kim JH, Bogner PN, Baek SH, Ramnath N, Liang P, et al. (2008) Up-regulation of peroxiredoxin 1 in lung cancer and its implication as a prognostic and therapeutic target. Clin Cancer Res 14: 2326-2333.

87. Noh DY, Ahn SJ, Lee RA, Kim SW, Park IA, et al. (2001) Overexpression of peroxiredoxin in human breast cancer. Anticancer Res 21: 2085-2090.

88. Arnold SA, Brekken RA (2009) SPARC: a matricellular regulator of tumorigenesis. J Cell Commun Signal 3: 255-273.

89. Chlenski A, Cohn SL (2010) Modulation of matrix remodeling by SPARC in neoplastic progression. Semin Cell Dev Biol 21: 55-65.

90. Clark CJ, Sage EH (2008) A prototypic matricellular protein in the tumor microenvironment--where there's SPARC, there's fire. J Cell Biochem 104: 721-732.

91. Rivera LB, Bradshaw AD, Brekken RA (2011) The regulatory function of SPARC in vascular biology. Cell Mol Life Sci 68: 3165-3173.

92. Chlenski A, Guerrero LJ, Salwen HR, Yang Q, Tian Y, et al. (2011) Secreted protein acidic and rich in cysteine is a matrix scavenger chaperone. PLoS One 6: e23880.

93. Vial E, Perez S, Castellazzi M (2000) Transcriptional control of SPARC by v-Jun and other members of the AP1 family of transcription factors. Oncogene 19: 5020-5029.

94. Beck KF, Walpen S, Eberhardt W, Pfeilschifter J (2001) Downregulation of integrin-linked kinase mRNA expression by nitric oxide in rat glomerular mesangial cells. Life Sci 69: 2945-2955.

95. Robert G, Gaggioli C, Bailet O, Chavey C, Abbe P, et al. (2006) SPARC represses E-cadherin and induces mesenchymal transition during melanoma development. Cancer Res 66: 7516-7523.

96. Bradshaw AD, Sage EH (2001) SPARC, a matricellular protein that functions in cellular differentiation and tissue response to injury. J Clin Invest 107: 1049-1054.

97. Tai IT, Tang MJ (2008) SPARC in cancer biology: its role in cancer progression and potential for therapy. Drug Resist Updat 11: 231-246.

98. Liu YQ, Li HX, Lou X, Lei JY (2008) Expression of phosphatase of regenerating liver 1 and 3 mRNA in esophageal squamous cell carcinoma. Arch Pathol Lab Med 132: 1307-1312.

99. Reich R, Hadar S, Davidson B (2011) Expression and clinical role of protein of regenerating liver (PRL) phosphatases in ovarian carcinoma. Int J Mol Sci 12: 1133-1145.

100. Wang Y, Li ZF, He J, Li YL, Zhu GB, et al. (2007) Expression of the human phosphatases of regenerating liver (PRLs) in colonic adenocarcinoma and its correlation with lymph node metastasis. Int J Colorectal Dis 22: 1179-1184.

101. Smit DJ, Gardiner BB, Sturm RA (2007) Osteonectin downregulates E-cadherin, induces osteopontin and focal adhesion kinase activity stimulating an invasive melanoma phenotype. Int J Cancer 121: 2653-2660.

102. Bhoopathi P, Gondi CS, Gujrati M, Dinh DH, Lakka SS (2011) SPARC mediates Src-induced disruption of actin cytoskeleton via inactivation of small GTPases Rho-Rac-Cdc42. Cell Signal 23: 1978-1987.

103. Pavasant P, Yongchaitrakul T (2008) Secreted protein acidic, rich in cysteine induces pulp cell migration via alphavbeta3 integrin and extracellular signal-regulated kinase. Oral Dis 14: 335-340.

104. McClung HM, Thomas SL, Osenkowski P, Toth M, Menon P, et al. (2007) SPARC upregulates MT1-MMP expression, MMP-2 activation, and the secretion and cleavage of galectin-3 in U87MG glioma cells. Neurosci Lett 419: 172-177.

105. Fenouille N, Puissant A, Tichet M, Zimniak G, Abbe P, et al. (2011) SPARC functions as an anti-stress factor by inactivating p53 through Akt-mediated MDM2 phosphorylation to promote melanoma cell survival. Oncogene 30: 4887-4900.

106. Fenouille N, Robert G, Tichet M, Puissant A, Dufies M, et al. (2011) The p53/p21Cip1/ Waf1 pathway mediates the effects of SPARC on melanoma cell cycle progression. Pigment Cell Melanoma Res 24: 219-232.

107. Yarovinsky TO, Rickman DW, Diamond RH, Taub R, Hageman GS, et al. (2000) Expression of the protein tyrosine phosphatase, phosphatase of regenerating liver 1, in the outer segments of primate cone photoreceptors. Brain Res Mol Brain Res 77: 95-103.

108. Rodriguez IR, Moreira EF, Bok D, Kantorow M (2000) Osteonectin/SPARC secreted by RPE and localized to the outer plexiform layer of the monkey retina. Invest Ophthalmol Vis Sci 41: 2438-2444.

109. Scime A, Desrosiers J, Trensz F, Palidwor GA, Caron AZ, et al. (2010) Transcriptional profiling of skeletal muscle reveals factors that are necessary to maintain satellite cell integrity during ageing. Mech Ageing Dev 131: 9-20.

110. Yan Q, Sage EH, Hendrickson AE (1998) SPARC is expressed by ganglion cells and astrocytes in bovine retina. J Histochem Cytochem 46: 3-10.

111. Gooden MD, Vernon RB, Bassuk JA, Sage EH (1999) Cell cycle-dependent nuclear location of the matricellular protein SPARC: association with the nuclear matrix. J Cell Biochem 74: 152-167.

112. Barker TH, Baneyx G, Cardo-Vila M, Workman GA, Weaver M, et al. (2005) SPARC regulates extracellular matrix organization through its modulation of integrin-linked kinase activity. J Biol Chem 280: 36483-36493.

113. Fielding AB, Dedhar S (2009) The mitotic functions of integrin-linked kinase. Cancer Metastasis Rev 28: 99-111.

114. Goldman RD, Cleland MM, Murthy SN, Mahammad S, Kuczmarski ER (2012) Inroads into the structure and function of intermediate filament networks. J Struct Biol 177: 14-23.

115. Ballestrem C, Wehrle-Haller B, Hinz B, Imhof BA (2000) Actin-dependent lamellipodia formation and microtubule-dependent tail retraction control-directed cell migration. Mol Biol Cell 11: 2999-3012.

116. Ridley AJ, Schwartz MA, Burridge K, Firtel RA, Ginsberg MH, et al. (2003) Cell migration: integrating signals from front to back. Science 302: 1704-1709.

117. Watanabe T, Noritake J, Kaibuchi K (2005) Regulation of microtubules in cell migration. Trends Cell Biol 15: 76-83.

118. Chou YH, Khuon S, Herrmann H, Goldman RD (2003) Nestin promotes the phosphorylation-dependent disassembly of vimentin intermediate filaments during mitosis. Mol Biol Cell 14: 1468-1478.

119. Fededa JP, Gerlich DW (2012) Molecular control of animal cell cytokinesis. Nat Cell Biol 14: 440-447.

120. Mendez MG, Kojima S, Goldman RD (2010) Vimentin induces changes in cell shape, motility, and adhesion during the epithelial to mesenchymal transition. FASEB J 24: 1838-1851.

121. Guarino M, Rubino B, Ballabio G (2007) The role of epithelial-mesenchymal transition in cancer pathology. Pathology 39: 305-318.

122. Jackson WM, Jaasma MJ, Tang RY, Keaveny TM (2008) Mechanical loading by fluid shear is sufficient to alter the cytoskeletal composition of osteoblastic cells. Am J Physiol Cell Physiol 295: C1007-1015.

123. Kanakkanthara A, Rawson P, Northcote PT, Miller JH (2012) Acquired Resistance to Peloruside A and Laulimalide is Associated with Downregulation of Vimentin in Human Ovarian Carcinoma Cells. Pharm Res.

124. Penuelas S, Noe V, Ciudad CJ (2005) Modulation of IMPDH2, survivin, topoisomerase I and vimentin increases sensitivity to methotrexate in HT29 human colon cancer cells. FEBS J 272: 696-710.

125. Wilson KS, Roberts H, Leek R, Harris AL, Geradts J (2002) Differential gene expression patterns in HER2/neu-positive and -negative breast cancer cell lines and tissues. Am J Pathol 161: 1171-1185.

126. Baldini G, Ponti C, Bortul R, Narducci P, Grill V, et al. (2008) Sparc localizes to the blebs of hobit cells and human primary osteoblasts. J Cell Biochem 104: 2310-2323.

127. Dormoy-Raclet V, Menard I, Clair E, Kurban G, Mazroui R, et al. (2007) The RNA-binding protein HuR promotes cell migration and cell invasion by stabilizing the beta-actin mRNA in a U-rich-element-dependent manner. Mol Cell Biol 27: 5365-5380.

128. Simard JP, Reynolds DN, Kraguljac AP, Smith GS, Mosser DD (2011) Overexpression of HSP70 inhibits cofilin phosphorylation and promotes lymphocyte migration in heat-stressed cells. J Cell Sci 124: 2367-2374.

129. Benelli D, Cialfi S, Pinzaglia M, Talora C, Londei P (2012) The translation factor eIF6 is a Notch-dependent regulator of cell migration and invasion. PLoS One 7: e32047.

130. Gross SR, Kinzy TG (2005) Translation elongation factor 1A is essential for regulation of the actin cytoskeleton and cell morphology. Nat Struct Mol Biol 12: 772-778.

131. Stohr N, Kohn M, Lederer M, Glass M, Reinke C, et al. (2012) IGF2BP1 promotes cell migration by regulating MK5 and PTEN signaling. Genes Dev 26: 176-189.

132. Boissan M, De Wever O, Lizarraga F, Wendum D, Poincloux R, et al. (2010) Implication of metastasis suppressor NM23-H1 in maintaining adherens junctions and limiting the invasive potential of human cancer cells. Cancer Res 70: 7710-7722.

133. Polanski R, Maguire M, Nield PC, Jenkins RE, Park BK, et al. (2011) MDM2 interacts with NME2 (non-metastatic cells 2, protein) and suppresses the ability of NME2 to negatively regulate cell motility. Carcinogenesis 32: 1133-1142.

134. Mostowy S, Cossart P (2012) Septins: the fourth component of the cytoskeleton. Nat Rev Mol Cell Biol 13: 183-194.

135. Grassadonia A, Tinari N, Iurisci I, Piccolo E, Cumashi A, et al. (2004) 90K (Mac-2 BP) and galectins in tumor progression and metastasis. Glycoconj J 19: 551-556.

136. Parr C, Sanders AJ, Jiang WG (2010) Hepatocyte growth factor activation inhibitors - therapeutic potential in cancer. Anticancer Agents Med Chem 10: 47-57.

137. Rahmani M, Wong BW, Ang L, Cheung CC, Carthy JM, et al. (2006) Versican: signaling to transcriptional control pathways. Can J Physiol Pharmacol 84: 77-92.

138. Aranda JF, Reglero-Real N, Kremer L, Marcos-Ramiro B, Ruiz-Saenz A, et al. (2011) MYADM regulates Rac1 targeting to ordered membranes required for cell spreading and migration. Mol Biol Cell 22: 1252-1262.

139. Chua CE, Lim YS, Tang BL (2010) Rab35--a vesicular traffic-regulating small GTPase with actin modulating roles. FEBS Lett 584: 1-6.

140. Wheldon LM, Haines BP, Rajappa R, Mason I, Rigby PW, et al. (2010) Critical role of FLRT1 phosphorylation in the interdependent regulation of FLRT1 function and FGF receptor signalling. PLoS One 5: e10264.

141. Adam PJ, Boyd R, Tyson KL, Fletcher GC, Stamps A, et al. (2003) Comprehensive proteomic analysis of breast cancer cell membranes reveals unique proteins with potential roles in clinical cancer. J Biol Chem 278: 6482-6489.

7.11.1 List of Websites

BioBase Biological Database. Accessed March 2012 from http://www.biobase-international.com/

Ingenuity Pathway Analysis (Version 162820). Available from http://www.ingenuity.com

National Center for Biotechnology Information Database. Accessed March 2012 from http://www.ncbi.nlm.nih.gov/gquery

Partek Genomics Suite (Version 6.11.1115). Available from http://www.partek.com

R-project software (Version 2.13.1). Available from http://www.r-project.org/

RStudio (Version 0.94.92). Available from http://www.rstudio.org

Table 7.1 Significant (q ≤ 0.05) differentially-expressed Tier-1 proteins from mass-spectrometry analysis of PRL-1-overexpressing HEK293 cells

Protein ID	Coding Gene Symbol	Entrez Gene ID	HEK293-vector Average Signal	HEK293-PRL-1 Average Signal	Fold Change	p-value	FDR
IPI00302592.2	**FLNA**	2316	14630	18061	1.23	1.28E-15	1.2E-12
IPI00550363.2	**TAGLN2**	8407	28555	25728	1.21	2.77E-11	8.5E-09
IPI00026230.1	**HNRNPH2**	3188	18665	22688	1.14	2.68E-04	9.8E-03
IPI00010204.1	**SRSF3**	6428	36303	24669	1.14	8.64E-04	2.2E-02
IPI00010105.1	**EIF6**	3692	13685	19513	1.13	3.36E-04	1.1E-02
IPI00005978.7	**SRSF2**	6427	27477	25050	1.13	2.73E-03	4.8E-02
IPI00465439.4	**ALDOA**	226	26307	15255	1.12	1.34E-03	2.9E-02
IPI00021700.3	**PCNA**	5111	22571	18349	1.11	8.51E-08	8.7E-06
IPI00029079.5	**GMPS**	8833	15137	27233	1.11	3.06E-05	1.4E-03
IPI00009104.6	**RUVBL2**	10856	19000	20909	1.10	1.17E-05	6.3E-04
IPI00021187.3	**RUVBL1**	8607	17014	38789	1.09	4.68E-05	2.0E-03
28935	**ACLY**	47	18448	16848	1.09	9.83E-04	2.4E-02
IPI00017617.1	**DDX5**	1655	24037	25907	1.08	2.88E-04	1.0E-02
IPI00011134.1	**HSPA6**	3310	48728	19488	1.08	8.22E-04	2.2E-02
IPI00012007.5	**AHCY**	191	19038	20153	1.08	1.32E-03	2.9E-02
IPI00014424.1	**EEF1A2**	1917	31227	21229	1.08	2.53E-03	4.6E-02
IPI00645907.2	**FASN**	2194	25369	26014	1.07	3.15E-07	2.6E-05
IPI00301936.3	**ELAVL1**	1994	18210	30686	1.07	1.76E-04	6.7E-03
IPI00304925.3	**HSPA1A**	3303	35223	20761	1.07	2.16E-03	4.1E-02
IPI00027442.4	**AARS**	16	13358	12750	1.06	4.79E-04	1.4E-02
IPI00186290.5	**EEF2**	1938	35443	14098	1.06	6.80E-04	1.8E-02
IPI00013808.1	**ACTN4**	81	20245	41484	1.05	1.05E-03	2.5E-02
IPI00013508.5	**ACTN1**	87	17101	21325	1.04	1.61E-03	3.4E-02
IPI00003881.5	**HNRNPF**	3185	25884	24858	-1.04	1.09E-03	2.6E-02
IPI00645078.1	**UBA1**	7317	21758	29386	-1.05	3.54E-04	1.2E-02
IPI00024067.3	**CLTC**	1213	15241	20481	-1.05	1.28E-03	2.9E-02
IPI00166768.2	**TUBA1C**	84790	53528	50481	-1.06	1.88E-03	3.8E-02
IPI00220644.7	**PKM**	5315	32867	37698	-1.07	3.80E-04	1.2E-02
IPI00643041.2	**RAN**	5901	58484	11372	-1.07	2.53E-03	4.6E-02
IPI00479997.3	**STMN1**	3925	24430	18787	-1.09	4.41E-04	1.3E-02
IPI00329801.11	**ANXA5**	308	16450	30922	-1.09	1.41E-03	3.0E-02
438069	**PRDX2**	7001	21747	42207	-1.09	2.57E-03	4.6E-02
IPI00015018.1	**PPA1**	5464	28822	18988	-1.11	8.25E-05	3.4E-03
IPI00643920.2	**TKT**	7086	25307	9141	-1.12	8.51E-09	1.1E-06
IPI00008557.3	**IGF2BP1**	10642	20573	29331	-1.12	3.51E-06	2.1E-04
IPI00015947.4	**DNAJB1**	3337	22598	41893	-1.12	1.24E-04	4.9E-03
IPI00031461.1	**GDI2**	2665	21957	36925	-1.13	7.64E-08	8.7E-06
5822569	**GSTP1**	2950	17205	27309	-1.13	1.66E-07	1.5E-05
IPI00012048.1	**NME1**	4830	43955	35961	-1.13	1.94E-05	9.9E-04
IPI00291510.3	**IMPDH2**	3615	18005	14479	-1.13	3.03E-05	1.4E-03
IPI00019376.5	**SEPT11**	55752	12830	10236	-1.13	2.05E-03	4.0E-02
IPI00218667.2	**STMN2**	11075	14649	31947	-1.15	6.73E-04	1.8E-02
IPI00217143.2	**SDHA**	6389	11687	19318	-1.15	1.75E-03	3.6E-02
IPI00003815.2	**ARHGDIA**	396	30071	28853	-1.17	6.79E-12	3.1E-09
IPI00418471.5	**VIM**	7431	28883	24494	-1.17	9.93E-11	2.3E-08

Table 7.2 Significant (q ≤ 0.10) differentially-expressing mRNA signals from microarray analysis of PRL-1 overexpressing HEK293 cells

Probeset ID	Gene Symbol	Entrez Gene ID	HEK293-vector Average Signal	HEK293-PRL-1 Average Signal	Fold Change	p-value	FDR
200665_s_at	**SPARC**	6678	32	632	20	5.86E-05	0.068
210715_s_at	**SPINT2**	10653	486	2389	4.9	2.46E-05	0.068
213746_s_at	**FLNA**	2316	1080	2402	2.2	6.44E-05	0.068
200859_x_at	**FLNA**	2316	1750	3459	2.0	4.05E-05	0.068
201132_at	**HNRPH2**	3188	2008	3824	1.9	1.04E-04	0.079
203689_s_at	**FMR1**	2332	1961	3603	1.8	1.19E-04	0.083
219569_s_at	**SLC35G2**	80723	868	1556	1.8	4.07E-05	0.068
206546_at	**SYCP2**	10388	68	114	1.7	4.12E-05	0.068
232289_at	**KCNJ12**	3768	192	309	1.6	5.39E-05	0.068
225673_at	**MYADM**	91663	858	1203	1.4	9.79E-05	0.079
1553122_s_at	**RBAK**	57786	177	232	1.3	4.65E-05	0.068
215646_s_at	**VCAN**	1462	1538	2007	1.3	9.03E-05	0.079
219326_s_at	**B3GNT2**	10678	365	455	1.2	1.13E-04	0.082
200874_s_at	**NOP56**	10528	1352	1617	1.2	1.38E-05	0.068
223125_s_at	**C1orf21**	81563	1186	1059	-1.1	4.20E-05	0.068
221194_s_at	**RNFT1**	51136	636	503	-1.3	1.37E-04	0.091
221819_at	**RAB35**	11021	1098	834	-1.3	9.64E-05	0.079
211658_at	**PRDX2**	7001	5648	4248	-1.3	1.45E-04	0.092
217780_at	**WDR830S**	51398	4568	3218	-1.4	3.78E-05	0.068
227590_at	**C22orf40**	150383	566	375	-1.5	6.00E-05	0.068
219029_at	**C5orf28**	64417	750	418	-1.8	6.86E-05	0.068
210414_at	**FLRT1**	23769	232	101	-2.3	3.65E-05	0.068
208966_x_at	**IFI16**	3428	1317	394	-3.3	6.85E-05	0.068
239352_at	**SLC6A15**	55117	447	38	-12	6.28E-05	0.068
225864_at	**FAM84B**	157638	3361	11	-300	1.01E-04	0.079

Table 7.3 Genes confirmed by qRT-PCR to be significantly differentially expressed in HEK293 cells overexpressing PRL-1

Significance was defined as Fold Change > 2, p-value ≤ 0.02, and FDR ≤ 0.05

Assay ID	Gene Symbol	Entrez Gene ID	HEK293-vector Average ΔCt	HEK293-PRL-1 Average ΔCt	Fold Change	p-value	FDR
Hs00234160_m1	**SPARC**	6678	22.9	15.1	225.7	1.08E-04	5.83E-03
Hs00181051_m1	**APC**	324	20.6	15.9	25.2	2.07E-03	9.33E-03
Hs00153074_m1	**ROCK2**	9475	19.6	14.9	24.7	6.02E-04	8.12E-03
Hs00180679_m1	**PIK3CA**	5290	23.7	19.3	21.0	1.06E-02	1.50E-02
Hs00232783_m1	**ZEB1**	6935	21.3	17.0	20.0	4.13E-03	1.24E-02
Hs00179099_m1	**MAP3K2**	10746	20.0	15.8	18.6	6.69E-03	1.34E-02
Hs00936371_m1	**HIF1A**	3091	19.2	15.1	17.1	5.29E-03	1.19E-02
Hs00362308_m1	**SOS1**	6654	20.7	16.6	16.8	5.24E-03	1.23E-02
Hs00989507_m1	**CHUK**	1974	20.9	16.9	16.7	1.72E-02	1.69E-02
Hs00182099_m1	**PPP1R12A**	4659	19.9	15.9	15.9	1.03E-02	1.50E-02
Hs00169257_m1	**DUSP6**	1848	22.8	18.9	15.0	1.70E-02	1.70E-02
Hs00855199_g1	**ACTR2**	10097	19.4	15.5	14.5	8.67E-03	1.46E-02
Hs01110394_m1	**ITGB8**	3696	24.7	21.0	13.7	4.50E-03	1.21E-02
Hs00180035_m1	**NRAS**	4893	17.9	14.1	13.3	9.27E-03	1.43E-02
Hs01127699_m1	**ROCK1**	6093	19.5	15.8	13.1	1.07E-02	1.45E-02
Hs00828586_m1	**ACTR3**	10096	17.4	13.8	12.7	6.56E-03	1.36E-02
Hs01039896_m1	**MAP3K5**	4217	22.1	18.6	11.5	1.91E-03	9.38E-03
Hs00270666_m1	**KRAS**	6407	19.4	15.9	11.4	1.82E-02	1.75E-02
Hs00381459_m1	**PIK3R1**	5295	20.8	17.3	11.3	7.33E-03	1.41E-02
Hs00248373_m1	**TAB2**	23118	18.9	15.4	10.8	1.40E-02	1.54E-02
Hs00168433_m1	**ITGA4**	3676	19.1	15.7	10.8	3.65E-03	1.31E-02
Hs00601957_m1	**CSNK2A1**	1457	20.0	16.7	10.2	1.17E-02	1.44E-02
Hs00559595_m1	**ITGB1**	3688	17.8	14.4	10.2	1.96E-02	1.74E-02
Hs00243196_m1	**RYK**	6259	18.6	15.3	10.0	1.53E-02	1.62E-02
Hs00177373_m1	**MAP3K7**	6885	18.0	14.7	9.9	3.82E-03	1.29E-02
Hs01041011_m1	**ITGA6**	3655	18.7	15.5	9.6	1.84E-02	1.74E-02
Hs00243115_m1	**RASA1**	5921	20.1	16.8	9.6	1.44E-02	1.55E-02
Hs00237216_m1	**NCK1**	4690	20.9	17.6	9.4	1.21E-03	9.37E-03
Hs00375042_m1	**SHC3**	53358	23.4	20.2	8.8	8.88E-03	1.45E-02
Hs00187614_m1	**WASL**	8976	19.9	16.8	8.6	1.10E-02	1.45E-02
Hs00180418_m1	**CRK**	1398	18.2	15.1	8.6	6.08E-03	1.31E-02
Hs00235006_m1	**ITGA1**	3672	20.9	17.9	8.3	1.92E-02	1.72E-02
Hs00394890_m1	**MAP3K1**	4214	20.3	17.3	7.9	1.22E-02	1.43E-02
Hs00377415_m1	**MAP4K4**	9448	18.1	15.2	7.8	1.37E-02	1.54E-02
Hs00427259_m1	**PPP2CA**	5515	16.0	13.0	7.6	1.20E-02	1.44E-02
Hs00177150_m1	**MAP2K6**	5608	21.1	18.3	7.2	1.68E-02	1.71E-02
Hs01047719_m1	**GSK3B**	2932	17.5	14.7	7.1	1.86E-02	1.71E-02

Table 7.3 Cont.

Assay ID	Gene Symbol	Entrez Gene ID	HEK293-vector Average ΔCt	HEK293-PRL-1 Average ΔCt	Fold Change	p-value	FDR
Hs00387426_m1	**MAP2K4**	6416	19.6	16.9	6.5	3.96E-03	1.26E-02
Hs01124081_m1	**LAMA2**	3908	26.1	23.5	5.8	8.67E-04	7.80E-03
Hs00169407_m1	**RIPK1**	8737	21.4	19.0	5.5	1.53E-02	1.59E-02
Hs00177102_m1	**MAPK9**	5601	17.2	14.8	5.5	8.44E-03	1.47E-02
Hs00300550_m1	**LAMA1**	284217	17.1	14.8	4.8	1.85E-02	1.72E-02
Hs00560189_m1	**PPM1E**	22843	18.9	16.7	4.8	1.00E-02	1.50E-02
Hs00177083_m1	**MAPK8**	5599	17.8	15.5	4.8	4.22E-03	1.20E-02
Hs00373461_m1	**MAPK10**	5602	25.0	22.9	4.4	1.24E-02	1.43E-02
Hs00183311_m1	**SOS2**	6655	19.0	16.8	4.4	3.19E-03	1.23E-02
Hs00180269_m1	**BAX**	581	12.8	10.8	4.1	2.15E-03	8.91E-03
Hs00169777_m1	**PECAM1**	5175	26.0	24.5	3.0	7.53E-03	1.40E-02
Hs00237119_m1	**MMP14**	4323	21.2	19.7	2.8	1.16E-02	1.46E-02
Hs00266332_m1	**COL15A1**	1306	25.2	23.9	2.4	1.31E-03	8.85E-03
Hs00610483_m1	**HRAS**	3265	15.8	14.7	2.1	8.49E-04	9.17E-03
Hs00365167_m1	**COL6A2**	1292	14.9	16.1	-2.2	1.14E-02	1.46E-02
Hs00242448_m1	**COL6A1**	1291	14.7	16.1	-2.7	8.39E-03	1.51E-02
Hs00266026_m1	**IGFBP7**	3490	17.1	18.9	-3.4	1.37E-04	3.71E-03
Hs00609088_m1	**COL5A1**	1289	19.5	21.6	-4.2	1.71E-03	9.23E-03
Hs02341135_m1	**PTP4A3**	11156	16.3	19.0	-6.4	5.10E-03	1.31E-02
Hs00174009_m1	**ITGB4**	3691	19.5	22.5	-8.0	5.86E-04	1.05E-02
Hs00230853_m1	**HNF4A**	3172	22.6	25.9	-9.7	1.06E-02	1.47E-02

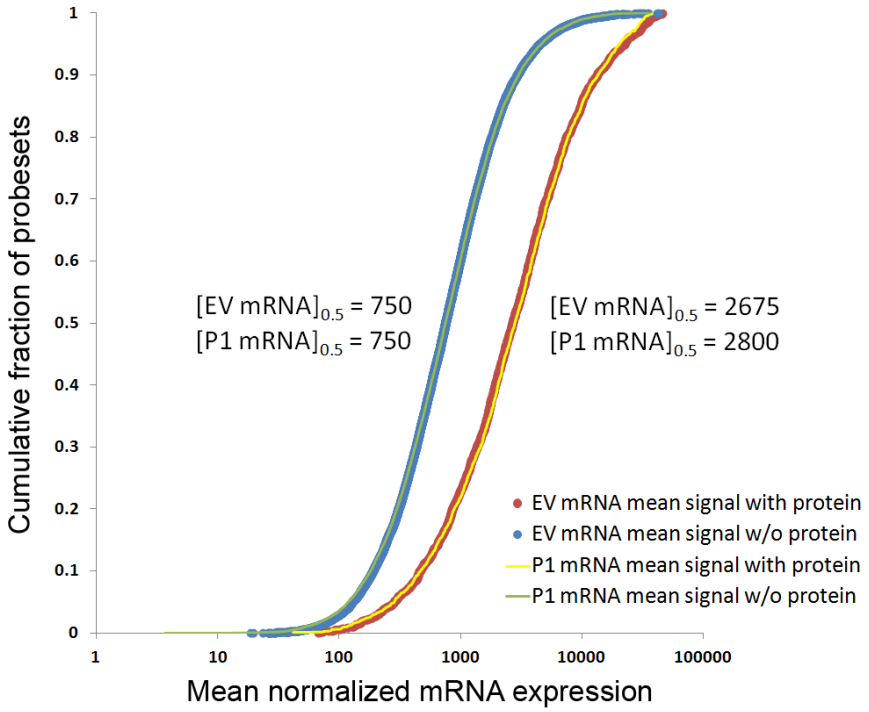

Figure 7.1 Cumulative distributions of mRNA expression levels for microarray probesets

The cumulative distributions of the expression levels of mRNA probesets that were associated with the coding genes of detected and non-detected proteins are respectively shown in blue and red for the empty-vector (EV) group, and in green and yellow for the PRL-1-overexpressing (P1) group.

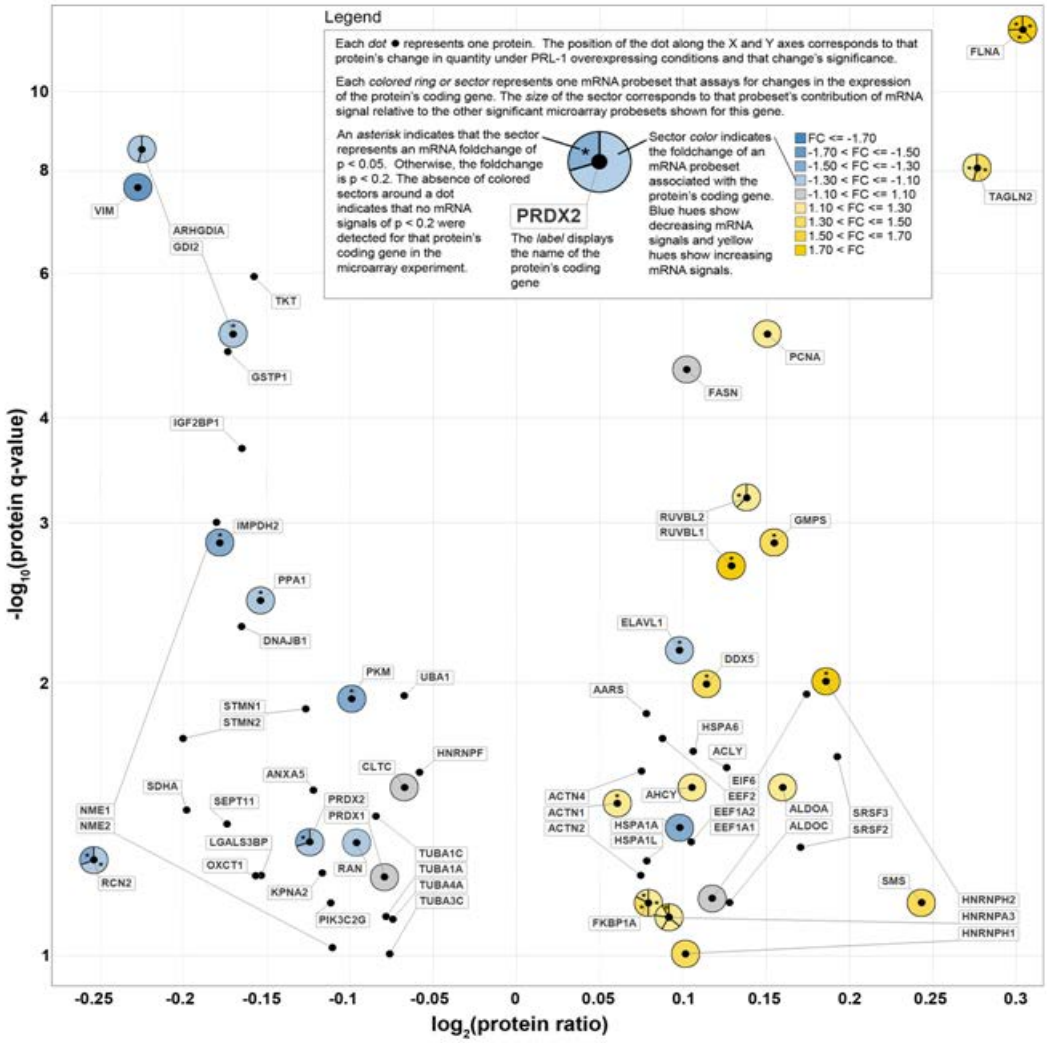

Figure 7.2 Volcano plot of significant (q ≤ 0.10) differentially-expressed proteins integrated with changes in corresponding mRNA signals
The dot (●) symbols represent the Tier-1 proteins that were observed to be differentially expressed in HEK293-PRL-1 cells. These protein data are plotted along the X- and Y-axes according to the log of the protein expression ratio and FDR-corrected significance respectively. A positive log2(protein ratio) value indicates an up-regulation of protein expression in the PRL-1 transients as compared to controls, while a negative value indicates down-regulation of protein expression. Each protein's corresponding mRNA data is represented by colored circle around that protein's dot symbol. Each probeset in the microarray experiment that was 1) mapped to a plotted protein's coding gene and was 2) differentially expressed with a significance of p ≤ 0.20 is represented by a colored region. An asterisk (*) indicates an mRNA signal with a significance of p ≤ 0.05. In cases where multiple detected probesets were mapped to the same protein's coding gene, the colored circle is divided into sectors according to the relative contribution that each probeset had to the total mRNA signal. Yellow colors represent an up-regulation of mRNA expression and blue colors indicate a down-regulation at the mRNA level.

Figure 7.3 Protein changes in the Rho-signaling canonical pathway resulting from PRL-1 overexpression in HEK293 cells

Selected proteins that conduct signals to remodel the cytoskeleton through RhoA, Rac1, and CDC42 are represented by their coding gene names in a canonical pathway diagram adapted from IPA. The symbols of proteins that were detected in the mass-spectrometry experiment at Tier-1 or Tier-2 levels are colored according to the direction of their expression change under PRL-1-overexpressing conditions as compared to the empty vector group, with yellow hues indicating an increased quantity of protein and blue hues indicating a decrease. An asterisk (*) indicates that a protein expression change is significant at a level of $p \leq 0.05$. Tier-1 proteins are noted with bold font labels. Groups of related or complex-forming proteins are illustrated with double-outlined symbols. Connecting lines with arrowheads indicate an activating, de-activating, or translocating influence, and the absence of an arrowhead indicates a protein-protein binding interaction or group membership. Solid connecting lines show direct interactions while dashed lines show indirect interactions. The direct interaction of PRL-1 (PTP4A1) with ARHGAP4 is represented here, but indirect connections between PRL-1 and the components of this pathway are not shown.

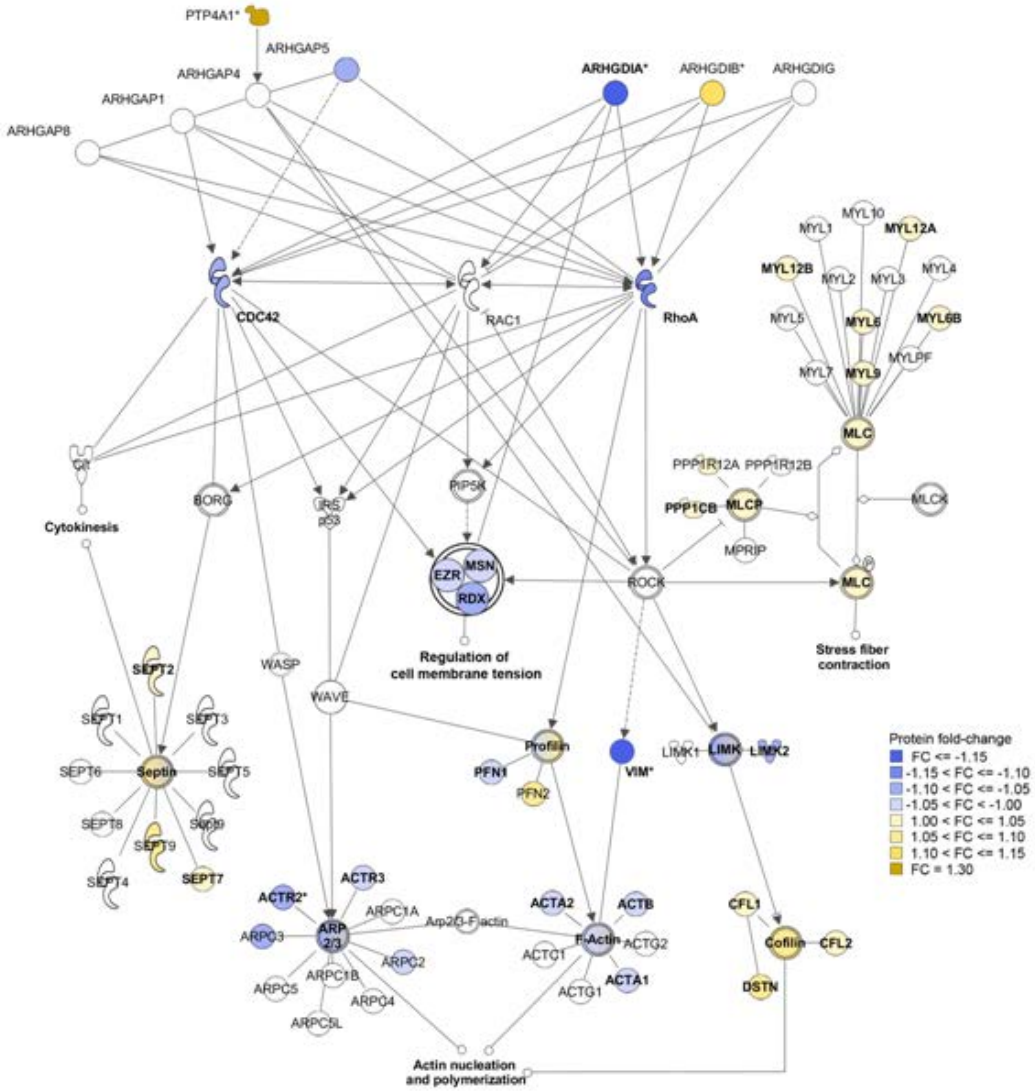
PTP4A1*
ARHGAP5
ARHGAP4
ARHGAP1
ARHGAP8
ARHGDIA*
ARHGDIB*
ARHGDIG
CDC42
RAC1
RhoA
MYL10
MYL1
MYL12A
MYL12B
MYL2
MYL3
MYL4
MYL5
MYL6
MYL6B
MYL7
MYL9
MYLPF
MLC
PPP1R12A
PPP1R12B
PPP1CB
MLCP
MLCK
MPRIP
GR
Cytokinesis
BORG
IRS
p53
PIP5K
EZR
MSN
RDX
ROCK
MLC
Regulation of cell membrane tension
Stress fiber contraction
SEPT2
SEPT1
SEPT3
SEPT6
Septin
SEPT5
SEPT8
SEPT9
SEPT4
SEPT7
WASP
WAVE
Profilin
PFN1
PFN2
VIM*
LIMK1
LIMK
LIMK2
ACTR3
ACTR2*
ARPC1A
ARP 2/3
ARPC3
ARPC2
ARPC1B
ARPC5
ARPC4
ARPC5L
Arp2/3-F actin
ACTA2
ACTB
F-Actin
ACTG2
ACTC1
ACTG1
ACTA1
CFL1
Cofilin
CFL2
DSTN
Actin nucleation and polymerization
Protein fold-change
FC <= -1.15
-1.15 < FC <= -1.10
-1.10 < FC <= -1.05
-1.05 < FC < -1.00
1.00 < FC <= 1.05
1.05 < FC <= 1.10
1.10 < FC <= 1.15
FC = 1.30

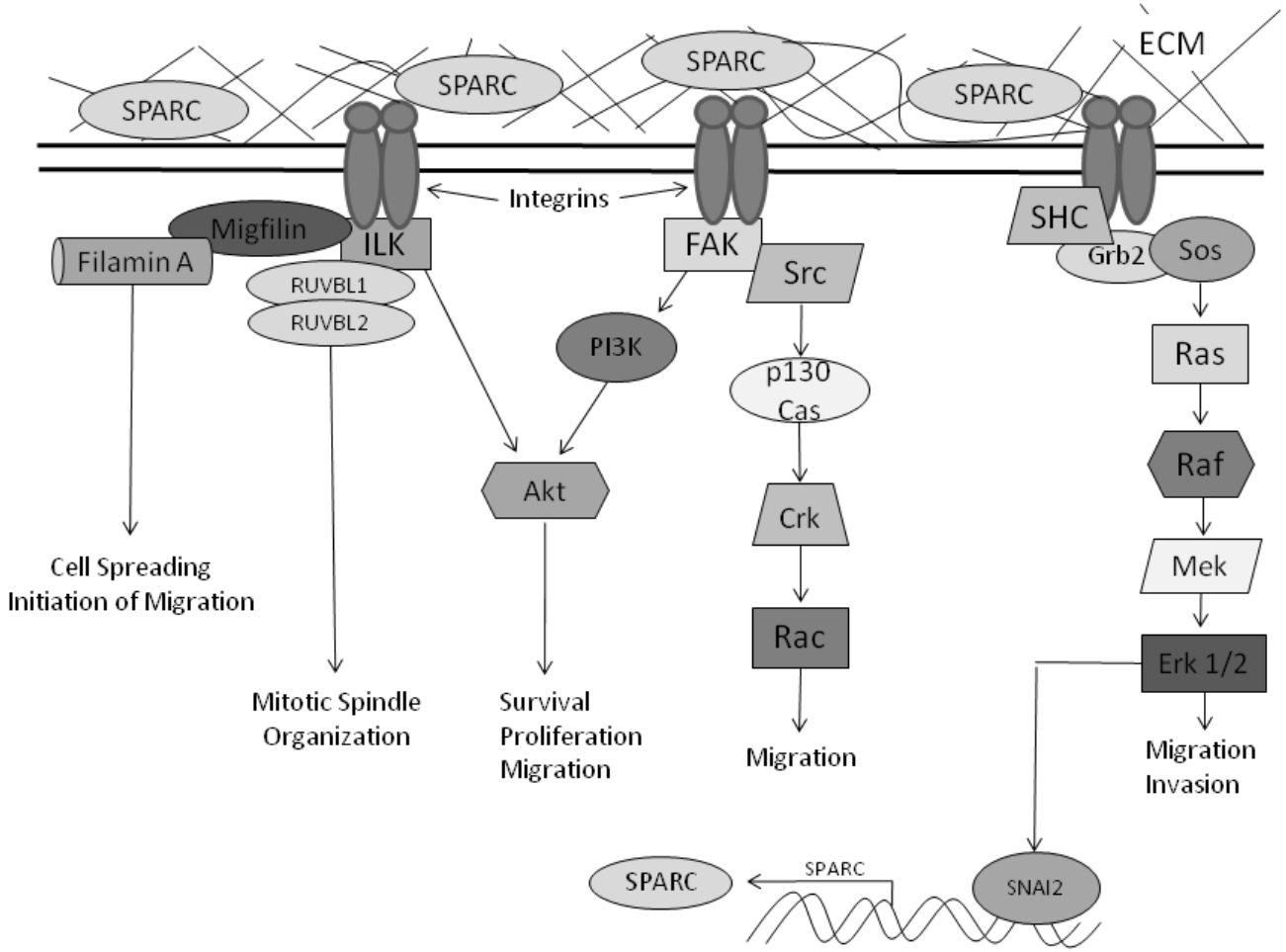

Figure 7.4 SPARC-mediated signaling pathways

Table S1 Full list of qRT-PCR assays and results

A value of Not Applicable (N/A) indicates that the gene was undetectable (Ct ≥ 40) in all assayed samples.

Assay ID	Gene Symbol	HEK293-vector Average ΔCt	HEK293-PRL-1 Average ΔCt	Fold Change	p-value	FDR
Hs00855199_g1	ACTR2	19.4	15.5	14.5	8.67E-03	1.46E-02
Hs00828586_m1	ACTR3	17.4	13.8	12.7	6.56E-03	1.36E-02
Hs00178289_m1	AKT1	12.2	12.6	-1.3	1.23E-01	4.80E-02
Hs00181051_m1	APC	20.6	15.9	25.2	2.07E-03	9.33E-03
Hs00869394_s1	ARHGAP5	24.5	19.6	29.3	3.53E-02	2.17E-02
Hs00241801_m1	ARHGAP6	N/A	N/A	N/A	N/A	N/A
Hs00976924_g1	ARHGDIA	9.6	9.6	1.0	9.94E-01	2.83E-01
Hs00180327_m1	ARHGEF1	15.3	15.4	-1.1	4.11E-01	1.36E-01
Hs00153179_m1	ATF2	20.1	15.7	20.9	4.38E-02	2.39E-02
Hs00247172_m1	ATF5	12.3	12.7	-1.3	5.95E-01	1.92E-01
Hs00180269_m1	BAX	12.8	10.8	4.1	2.15E-03	8.91E-03
Hs00183953_m1	BCAR1	14.6	13.9	1.6	5.82E-02	2.73E-02
Hs99999018_m1	BCL2	21.6	16.3	38.4	2.33E-02	1.85E-02
Hs00197982_m1	BCL2L11	17.5	16.3	2.4	6.73E-02	2.98E-02
Hs00269944_m1	BRAF	21.6	15.4	75.8	3.00E-01	1.02E-01
Hs00965092_m1	CAPN2	16.1	13.5	6.0	2.97E-02	1.96E-02
Hs00174575_m1	CCL5	24.4	24.6	-1.2	5.17E-03	1.27E-02
Hs00765553_m1	CCND1	15.1	13.1	3.8	2.41E-02	1.83E-02
Hs00236949_m1	CCND3	14.2	14.1	1.0	5.30E-01	1.74E-01
Hs00854939_g1	CDC42	18.3	15.7	5.7	2.22E-02	1.85E-02
Hs01013953_m1	CDH1	19.3	18.9	1.4	2.16E-01	7.54E-02
Hs00355782_m1	CDKN1A	12.8	13.0	-1.2	9.59E-02	3.95E-02
Hs00989507_m1	CHUK	20.9	16.9	16.7	1.72E-02	1.69E-02
Hs01058288_g1	CKB	9.4	9.6	-1.1	2.27E-02	1.86E-02
Hs00355024_m1	CNTN1	19.9	20.7	-1.7	1.12E-01	4.49E-02
Hs00266273_m1	COL11A1	N/A	N/A	N/A	N/A	N/A
Hs00189184_m1	COL12A1	22.4	17.8	24.5	4.76E-02	2.50E-02
Hs00385388_m1	COL14A1	15.9	14.6	2.6	6.22E-02	2.80E-02
Hs00266332_m1	COL15A1	25.2	23.9	2.4	1.31E-03	8.85E-03
Hs00156876_m1	COL16A1	N/A	N/A	N/A	N/A	N/A
Hs00164004_m1	COL1A1	21.6	23.2	-3.0	2.70E-02	1.84E-02
Hs01098873_m1	COL4A2	12.0	12.0	-1.0	9.69E-01	2.78E-01
Hs00609088_m1	COL5A1	19.5	21.6	-4.2	1.71E-03	9.23E-03
Hs00242448_m1	COL6A1	14.7	16.1	-2.7	8.39E-03	1.51E-02
Hs00365167_m1	COL6A2	14.9	16.1	-2.2	1.14E-02	1.46E-02
Hs00164310_m1	COL7A1	21.1	20.2	1.8	4.88E-02	2.53E-02
Hs00156669_m1	COL8A1	24.8	24.8	-1.0	9.81E-01	2.80E-01

Table S1 Cont.

Assay ID	Gene Symbol	HEK293-vector Average ΔCt	HEK293-PRL-1 Average ΔCt	Fold Change	p-value	FDR
Hs00180418_m1	CRK	18.2	15.1	8.6	6.08E-03	1.31E-02
Hs00177843_m1	CSK	18.1	18.2	-1.1	8.33E-01	2.46E-01
Hs00601957_m1	CSNK2A1	20.0	16.7	10.2	1.17E-02	1.44E-02
Hs00176268_m1	CSNK2B	10.4	10.1	1.3	4.24E-02	2.36E-02
Hs00355045_m1	CTNNB1	15.1	12.4	6.7	2.44E-02	1.80E-02
Hs00946556_m1	DIAPH1	16.0	14.6	2.6	4.75E-02	2.51E-02
Hs00169192_m1	DOCK1	18.3	15.3	7.9	2.71E-02	1.83E-02
Hs00169257_m1	DUSP6	22.8	18.9	15.0	1.70E-02	1.70E-02
Hs00152928_m1	EGR1	16.0	15.9	1.1	6.47E-01	2.02E-01
Hs01052961_m1	FLT1	20.4	17.9	5.9	3.18E-02	2.02E-02
Hs01549976_m1	FN1	16.5	16.6	-1.1	6.88E-01	2.10E-01
Hs00941600_m1	FYN	14.6	13.7	1.9	9.96E-02	4.05E-02
Hs00157817_m1	GRB2	15.2	14.2	2.0	2.69E-02	1.86E-02
Hs00534180_m1	GRLF1	17.6	15.0	6.0	3.38E-02	2.12E-02
Hs01047719_m1	GSK3B	17.5	14.7	7.1	1.86E-02	1.71E-02
Hs00356079_m1	GSTM3	18.7	17.5	2.4	9.92E-02	4.06E-02
Hs00168310_m1	GSTP1	11.0	11.6	-1.5	4.09E-02	2.30E-02
Hs00936371_m1	HIF1A	19.2	15.1	17.1	5.29E-03	1.19E-02
Hs00230853_m1	HNF4A	22.6	25.9	-9.7	1.06E-02	1.47E-02
Hs00610483_m1	HRAS	15.8	14.7	2.1	8.49E-04	9.17E-03
Hs03044127_g1	HSPB1	10.7	10.3	1.3	2.01E-01	7.06E-02
Hs00164932_m1	ICAM1	23.8	23.8	1.0	7.44E-01	2.24E-01
Hs00153126_m1	IGF1	N/A	N/A	N/A	N/A	N/A
Hs00609566_m1	IGF1R	14.4	13.4	2.0	5.81E-02	2.75E-02
Hs00266026_m1	IGFBP7	17.1	18.9	-3.4	1.37E-04	3.71E-03
Hs00233287_m1	IKBKB	17.5	16.5	2.0	8.72E-02	3.74E-02
Hs00415849_m1	IKBKG	15.5	15.7	-1.1	5.01E-01	1.65E-01
Hs00174092_m1	IL1A	25.7	23.3	5.2	3.65E-02	2.14E-02
Hs00178563_m1	IRS1	21.4	19.1	4.8	3.78E-02	2.15E-02
Hs00192713_m1	ISG15	24.8	25.0	-1.1	6.10E-01	1.94E-01
Hs00235006_m1	ITGA1	20.9	17.9	8.3	1.92E-02	1.72E-02
Hs00158127_m1	ITGA2	20.9	18.2	6.3	2.57E-02	1.83E-02
Hs01076873_m1	ITGA3	18.5	19.5	-2.1	3.56E-02	2.16E-02
Hs00168433_m1	ITGA4	19.1	15.7	10.8	3.65E-03	1.31E-02
Hs01547673_m1	ITGA5	13.1	13.2	-1.1	6.08E-01	1.94E-01
Hs01041011_m1	ITGA6	18.7	15.5	9.6	1.84E-02	1.74E-02
Hs00174397_m1	ITGA7	18.2	19.2	-2.0	1.22E-01	4.82E-02
Hs00233321_m1	ITGA8	18.7	16.8	3.8	2.46E-02	1.77E-02
Hs00559595_m1	ITGB1	17.8	14.4	10.2	1.96E-02	1.74E-02

Table S1 Cont.

Assay ID	Gene Symbol	HEK293-vector Average ΔCt	HEK293-PRL-1 Average ΔCt	Fold Change	p-value	FDR
Hs00164957_m1	ITGB2	24.3	24.9	-1.5	6.71E-01	2.07E-01
Hs01001478_m1	ITGB3	22.8	23.0	-1.1	8.69E-01	2.54E-01
Hs00174009_m1	ITGB4	19.5	22.5	-8.0	5.86E-04	1.05E-02
Hs00174435_m1	ITGB5	16.2	15.7	1.4	1.13E-01	4.50E-02
Hs01110394_m1	ITGB8	24.7	21.0	13.7	4.50E-03	1.21E-02
Hs00270666_m1	KRAS	19.4	15.9	11.4	1.82E-02	1.75E-02
Hs00300550_m1	LAMA1	17.1	14.8	4.8	1.85E-02	1.72E-02
Hs01124081_m1	LAMA2	26.1	23.5	5.8	8.67E-04	7.80E-03
Hs00165042_m1	LAMA3	18.7	16.9	3.4	3.00E-02	1.95E-02
Hs01055971_m1	LAMB1	16.5	14.2	5.1	5.43E-02	2.62E-02
Hs00165078_m1	LAMB3	22.6	21.2	2.8	3.65E-02	2.16E-02
Hs00267056_m1	LAMC1	15.6	13.9	3.3	5.04E-02	2.54E-02
Hs00605615_mH	MAP2K1	15.2	13.6	3.1	2.05E-02	1.76E-02
Hs00360961_m1	MAP2K2	13.8	13.7	1.1	2.88E-01	9.89E-02
Hs00177127_m1	MAP2K3	13.5	12.9	1.5	5.06E-02	2.53E-02
Hs00387426_m1	MAP2K4	19.6	16.9	6.5	3.96E-03	1.26E-02
Hs00177134_m1	MAP2K5	15.2	15.1	1.1	6.77E-01	2.08E-01
Hs00177150_m1	MAP2K6	21.1	18.3	7.2	1.68E-02	1.71E-02
Hs00178198_m1	MAP2K7	15.2	15.1	1.0	9.59E-01	2.78E-01
Hs00394890_m1	MAP3K1	20.3	17.3	7.9	1.22E-02	1.43E-02
Hs00176759_m1	MAP3K11	14.1	14.0	1.1	8.23E-01	2.44E-01
Hs01089753_m1	MAP3K14	17.3	16.5	1.7	3.18E-02	2.04E-02
Hs00179099_m1	MAP3K2	20.0	15.8	18.6	6.69E-03	1.34E-02
Hs00176747_m1	MAP3K3	15.9	15.8	1.0	6.47E-01	2.01E-01
Hs00245958_m1	MAP3K4	20.2	17.4	7.0	3.71E-02	2.15E-02
Hs01039896_m1	MAP3K5	22.1	18.6	11.5	1.91E-03	9.38E-03
Hs00177373_m1	MAP3K7	18.0	14.7	9.9	3.82E-03	1.29E-02
Hs00178297_m1	MAP3K8	20.2	19.4	1.7	2.92E-01	9.98E-02
Hs00377415_m1	MAP4K4	18.1	15.2	7.8	1.37E-02	1.54E-02
Hs01046830_m1	MAPK1	17.1	14.5	6.1	2.29E-02	1.84E-02
Hs00373461_m1	MAPK10	25.0	22.9	4.4	1.24E-02	1.43E-02
Hs00176247_m1	MAPK14	16.3	14.5	3.5	2.60E-02	1.82E-02
Hs00385075_m1	MAPK3	12.9	12.9	-1.0	7.55E-01	2.25E-01
Hs00177079_m1	MAPK7	15.5	15.1	1.3	4.52E-02	2.44E-02
Hs00177083_m1	MAPK8	17.8	15.5	4.8	4.22E-03	1.20E-02
Hs00177102_m1	MAPK9	17.2	14.8	5.5	8.44E-03	1.47E-02
Hs00250126_m1	MARK2	15.5	15.2	1.2	1.69E-01	6.29E-02
Hs00237119_m1	MMP14	21.2	19.7	2.8	1.16E-02	1.46E-02
Hs01548727_m1	MMP2	19.5	19.2	1.2	8.98E-03	1.43E-02

Table S1 Cont.

Assay ID	Gene Symbol	HEK293-vector Average ΔCt	HEK293-PRL-1 Average ΔCt	Fold Change	p-value	FDR
Hs00957555_m1	MMP9	N/A	N/A	N/A	N/A	N/A
Hs00364926_m1	MYLK	21.6	20.0	3.1	6.89E-02	3.03E-02
Hs00294850_m1	MYLK3	24.1	23.7	1.3	8.39E-01	2.46E-01
Hs00941830_m1	NCAM1	18.1	16.8	2.4	3.41E-01	1.14E-01
Hs00237216_m1	NCK1	20.9	17.6	9.4	1.21E-03	9.37E-03
Hs00765730_m1	NFKB1	18.4	16.7	3.2	5.26E-02	2.56E-02
Hs00174517_m1	NFKB2	14.6	15.4	-1.9	5.49E-02	2.62E-02
Hs00180035_m1	NRAS	17.9	14.1	13.3	9.27E-03	1.43E-02
Hs00176815_m1	PAK1	17.2	16.4	1.7	6.16E-02	2.82E-02
Hs00605586_m1	PAK2	19.6	16.8	6.8	3.62E-02	2.17E-02
Hs00176828_m1	PAK3	25.8	23.7	4.3	1.35E-01	5.23E-02
Hs00178686_m1	PAK4	14.5	14.2	1.2	9.42E-02	3.94E-02
Hs00205457_m1	PCDH17	22.7	25.4	-6.4	2.45E-02	1.78E-02
Hs00964426_m1	PDGFA	16.5	16.8	-1.2	1.25E-01	4.85E-02
Hs00966522_m1	PDGFB	18.6	19.1	-1.4	3.23E-01	1.09E-01
Hs00998018_m1	PDGFRA	25.1	21.9	9.2	5.93E-02	2.76E-02
Hs01019589_m1	PDGFRB	22.1	23.2	-2.2	1.39E-01	5.32E-02
Hs00169777_m1	PECAM1	26.0	24.5	3.0	7.53E-03	1.40E-02
Hs00180679_m1	PIK3CA	23.7	19.3	21.0	1.06E-02	1.50E-02
Hs00381459_m1	PIK3R1	20.8	17.3	11.3	7.33E-03	1.41E-02
Hs00560189_m1	PPM1E	18.9	16.7	4.8	1.00E-02	1.50E-02
Hs00182099_m1	PPP1R12A	19.9	15.9	15.9	1.03E-02	1.50E-02
Hs00427259_m1	PPP2CA	16.0	13.0	7.6	1.20E-02	1.44E-02
Hs00925195_m1	PRKCA	16.0	14.9	2.1	1.08E-01	4.33E-02
Hs01920652_s1	PTEN	23.6	16.1	171.1	9.46E-02	3.93E-02
Hs00178587_m1	PTK2	18.6	15.6	8.0	2.42E-02	1.82E-02
Hs00140)69444_m1	PTK2B	19.5	20.1	-1.5	1.53E-01	5.76E-02
Hs01109144_m1	PTP4A1**	N/A	N/A	N/A	N/A	N/A
Hs00754750_s1	PTP4A2	17.3	14.5	6.6	2.91E-02	1.94E-02
Hs02341135_m1	PTP4A3	16.3	19.0	-6.4	5.10E-03	1.31E-02
Hs00236064_m1	PXN	12.1	12.0	1.1	5.35E-01	1.74E-01
Hs00251654_m1	RAC1	16.0	15.3	1.7	8.00E-02	3.46E-02
Hs00234119_m1	RAF1	18.5	17.3	2.3	6.16E-02	2.84E-02
Hs00243115_m1	RASA1	20.1	16.8	9.6	1.44E-02	1.55E-02
Hs01042010_m1	RELA	12.2	11.4	1.8	5.03E-02	2.56E-02
Hs00357608_m1	RHOA	11.0	10.8	1.2	1.42E-01	5.39E-02
Hs00747110_s1	RHOC	14.5	14.4	1.1	6.34E-01	1.99E-01
Hs00169407_m1	RIPK1	21.4	19.0	5.5	1.53E-02	1.59E-02

Table S1 Cont.

Assay ID	Gene Symbol	HEK293-vector Average ΔCt	HEK293-PRL-1 Average ΔCt	Fold Change	p-value	FDR
Hs01127699_m1	ROCK1	19.5	15.8	13.1	1.07E-02	1.45E-02
Hs00153074_m1	ROCK2	19.6	14.9	24.7	6.02E-04	8.12E-03
Hs00243196_m1	RYK	18.6	15.3	10.0	1.53E-02	1.62E-02
Hs00174057_m1	SELE	N/A	N/A	N/A	N/A	N/A
Hs01384744_m1	SGK1	N/A	N/A	N/A	N/A	N/A
Hs00427539_m1	SHC1	14.5	14.4	1.1	6.28E-01	1.98E-01
Hs01044374_m1	SHC2	15.3	16.2	-1.9	2.37E-02	1.85E-02
Hs00375042_m1	SHC3	23.4	20.2	8.8	8.88E-03	1.45E-02
Hs00950344_m1	SNAI2	25.4	24.8	1.6	6.07E-01	1.95E-01
Hs00362308_m1	SOS1	20.7	16.6	16.8	5.24E-03	1.23E-02
Hs00183311_m1	SOS2	19.0	16.8	4.4	3.19E-03	1.23E-02
Hs00234160_m1	SPARC	22.9	15.1	225.7	1.08E-04	5.83E-03
Hs00178494_m1	SRC	14.4	14.4	-1.1	7.12E-01	2.16E-01
Hs01047580_m1	STAT3	16.2	15.2	2.1	6.67E-02	2.98E-02
Hs00194572_m1	SYT1	20.8	25.3	-23.7	3.40E-02	2.11E-02
Hs00980604_m1	SYT2	21.1	20.6	1.4	3.78E-01	1.26E-01
Hs00196143_m1	TAB1	14.4	15.0	-1.5	1.50E-01	5.66E-02
Hs00248373_m1	TAB2	18.9	15.4	10.8	1.40E-02	1.54E-02
Hs00194578_m1	TAF12	16.1	14.8	2.4	7.62E-02	3.32E-02
Hs00234278_m1	TIMP2	14.4	14.1	1.2	5.24E-02	2.60E-02
Hs00196775_m1	TLN1	13.3	13.0	1.3	2.36E-01	8.17E-02
Hs00377558_m1	TRAF6	N/A	N/A	N/A	N/A	N/A
Hs01003372_m1	VCAM1	N/A	N/A	N/A	N/A	N/A
Hs00243320_m1	VCL	14.1	12.7	2.8	4.91E-02	2.53E-02
Hs00900054_m1	VEGFA	15.9	15.9	-1.0	9.63E-01	2.78E-01
Hs01591751_m1	WASF1	17.6	15.7	3.8	4.74E-02	2.53E-02
Hs00746309_s1	WASF2	14.9	15.0	-1.0	7.49E-01	2.25E-01
Hs00187614_m1	WASL	19.9	16.8	8.6	1.10E-02	1.45E-02
Hs00219183_m1	WNK1	14.9	12.8	4.2	3.73E-02	2.14E-02
Hs00998537_m1	WNT5A	17.0	15.2	3.5	2.18E-02	1.84E-02
Hs00232783_m1	ZEB1	21.3	17.0	20.0	4.13E-03	1.24E-02

**Note that no pre-amplification step was performed as part of this analysis and pre-amplification is known to be required for PRL-1 (PTP4A1) detection using this TaqMan assay.

CHAPTER 8. PRL-1 INDUCTION ALTERS RHOA AND PHOSPHO-SRC LEVELS

8.1 Introduction

The combined analysis of transcript and protein level changes that occur in response to stable overexpression of PRL-1 in HEK293 cells identified several novel candidates for mediators of PRL-1 function and provided evidence strengthening the notion that PRL-1 can leverage signaling pathways which regulate cellular adhesions and cytoskeletal rearrangement. Given that cell migration occurs through a multi-step cycle that requires continuous remodeling of both the actin cytoskeleton and cell-matrix adhesions (Ridley, Vincente-Manzanares); the ability of PRL-1 to influence each of these structures likely plays a role in its capacity to promote cell motility and metastasis.

The integration of microarray and proteomics data sets considerably expanded our knowledge of the signaling molecules and pathways influenced by PRL-1. Nevertheless, due to mechanisms such as alternative splicing and post-translational modification, the level of transcription of a protein-coding RNA does not always correspond to the level of expression or, moreover, to the level of activity of the coded protein. For example, PRL-1 signaling has previously been shown to cause activation of c-Src, through increased phosphorylation at Tyr416,

without any change in the levels of total c-Src (Luo et al., 2009). This relationship between c-Src and PRL-1 would not be possible to observe through analysis of RNA or protein abundance alone. Therefore, I used western blotting with total and phospho-specific antibodies to further examine the influence of PRL-1 on the expression and activity levels of select molecules with crucial roles in cell adhesion, cytoskeletal remodeling, cell motility, and cell invasion.

8.2 Results

Downstream of integrin activation, Src kinase is a crucial mediator of adhesion-related signaling and cell motility. It localizes to cell-matrix adhesions where it augments adhesion turnover and regulates activity of the Rho GTPases, which are the primary drivers of cytoskeletal reorganization for cell migration (Huveneers & Danen, 2009; Parri & Chiarugi, 2010). Src activity is regulated by tyrosine phosphorylation at two sites, each having opposing effects: phosphorylation at Tyr416 up-regulates enzyme activity, while phosphorylation at Tyr527 has an inhibitory effect (Hunter, 1987). Luo et al. (2009) previously demonstrated that stable overexpression of PRL-1 in HEK293 cells enhances c-Src activity through increased phosphorylation at its activating Tyr416 residue. SPARC, which was determined by microarray to be the mostly highly up-regulated transcript in response to stable PRL-1 expression in the current study, is also known to increase Tyr416 phosphorylation of c-Src (Bhoopathi, Gondi, Gujrati, Dinh, & Lakka, 2011). Based on this evidence, I expected that c-Src Tyr416 phosphorylation would be enhanced in the HEK293 lines used for the

current study. To determine if this was the case, I performed western blotting, on duplicate biological replicates of HEK293 cells stably transfected with PRL-1 or with empty vector, using antibodies against several forms of phosphorylated and non-phosporylated-Src. The National Institute of Health's ImageJ program (Schneider, Rasband, & Eliceiri, 2012) was then used to quantify the blots and compare expression levels between samples. This analysis revealed that, in line with previous reports, the level of c-Src phosphorylation at Tyr416 was dramatically increased (approximately 5-fold) in response to stable PRL-1 overexpression in HEK293 cells (Figure 8.1; First row). Moreover, this increase in Tyr416 phosphorylation was accompanied by a concomitant decrease in levels of non-phospho-Tyr416 Src (Figure 8.1; Second row). In contrast, no appreciable changes were seen in the levels of phosphorylated or unphosphorylated Src at Tyr527 (Figure 8.1; Third and Fourth rows) or in the levels of total Src protein (Figure 8.1; Fifth row).

Rho family GTPases act as molecular switches that cycle between an active, GTP-bound state and an inactive, GDP-bound, state. They are key regulators of actin cytoskeletal dynamics associated with cell motility and are also important regulators of cell cycle progression, survival, and invasion (Parri & Chiarugi, 2010; Ridley, 2004). Among the best characterized of the Rho proteins are RhoA, Rac, and Cdc42. Rac and Cdc42 regulate the formation of membrane protrusions, while RhoA regulates the assembly of the contractile filaments that are required to move the cell body forward and retract the trailing edge (Raftopoulou & Hall, 2004). A reciprocal relationship has previously been

reported between SPARC and RhoA, where overexpression of RhoA leads to repression of SPARC and RhoA silencing by siRNA causes SPARC up-regulation (Giang Ho et al., 2011). Given that PRL-1 overexpression led to up-regulated SPARC expression and SPARC and RhoA are known to be inversely correlated, I was interested in determining the effect of increased PRL-1 levels on RhoA. A closer look at the microarray and MS data sets revealed that RhoA transcript levels were unaltered with PRL-1 up-regulation. In contrast, the abundance of RhoA protein was lower in the PRL-1 transfectants compared to the empty vector lines, though this difference failed to meet the significance thresholds set for the MS data analysis. To further examine the effect of PRL-1 overexpression on RhoA protein levels, I used western blotting to assess the amount of total RhoA in an independent set of HEK293 samples stably transfected with PRL-1 or empty vector. This analysis confirmed that stable PRL-1 overexpression in HEK293 leads to decreased expression of RhoA protein (Figure 8.2; First row).

The levels of total and phosphorylated PAK1 (p21-activated kinase 1), ERK1/2, and SAPK/JNK (stress-activated protein kinase/c-Jun N-terminal kinase) were also measured by western blot. PAK1 is a downstream effector of Rac1 and Cdc42 that is activated by the actin crosslinking and Rho GTPase scaffolding protein FLNA (Vadlamudi et al., 2002), a molecule which was determined by both microarray and MS to be highly up-regulated in response to PRL-1. FLNA also directly interacts with the MAPK kinases MEK1 and MKK4 which are upstream activators of ERK and SAPK/JNK respectively. Besides

FLNA, several other signaling molecules/pathways that control cell migration and/or invasion, including the Rho GTPase and Src signaling pathways ultimately converge at ERK or SAPK/JNK. However, neither the phosphorylation status nor total protein level of PAK1 (Figure 8.3), ERK1/2 (Figure 8.2), or SAPK/JNK (Figure 8.4) were notably altered in the HEK293 cells stably transfected with PRL-1 compared to those transfected with empty vector.

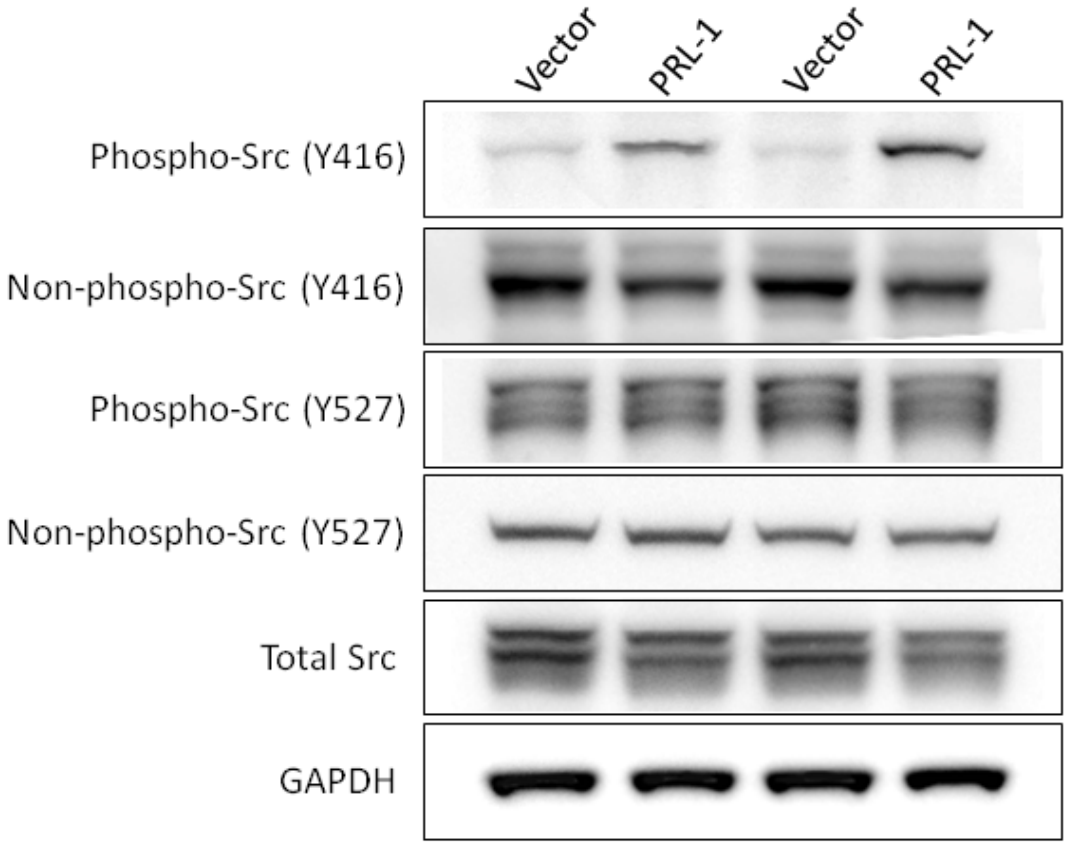

Figure 8.1 PRL-1 expression enhances Src phosphorylation at Tyr416
HEK293 cells stably transfected with PRL-1 or empty vector were subject to western blot analysis using antibodies against phospho, non-phospho, and total Src. An approximately 5-fold increase in Tyr416 (Y416) phosphorylation, concomitant with a decrease in non-phosphorylated Tyr416 was observed in PRL-1 transfectants compared to the vector controls. After accounting for differences in sample loading, no appreciable changes were seen in phosphorylation of Src at Tyr527 or in the levels of total Src. GAPDH was utilized as a loading control.

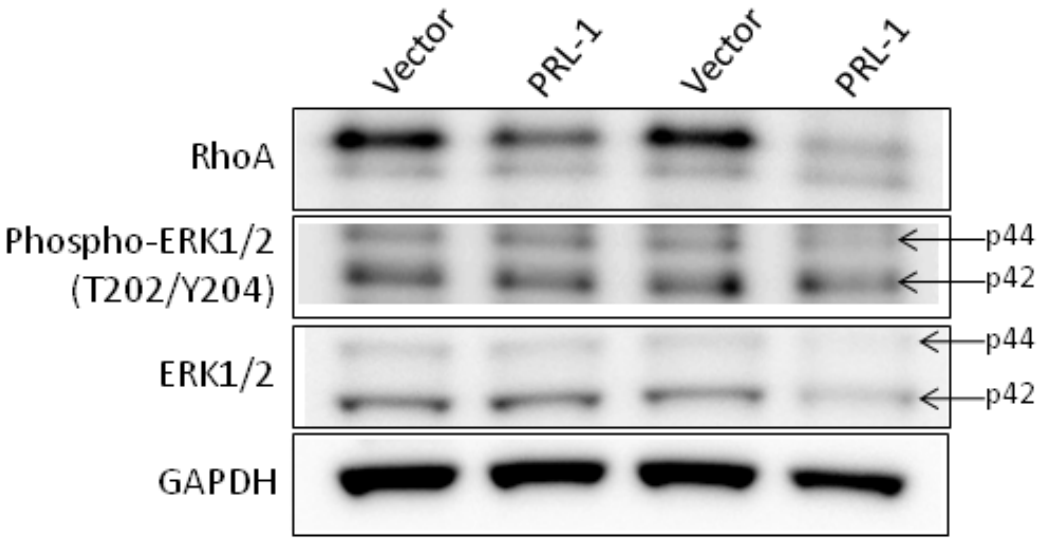

Figure 8.2 PRL-1 expression down-regulates RhoA protein levels
HEK293 cells stably transfected with PRL-1 or empty vector were subject to western blot analysis using antibodies against total RhoA, phosphorylated ERK1/2, or total ERK1/2. Expression of RhoA was heavily decreased in the PRL-1 transfectants compared to the vector controls, while the expression of total and phospho-ERK was unvaried. GAPDH was used as the loading control.

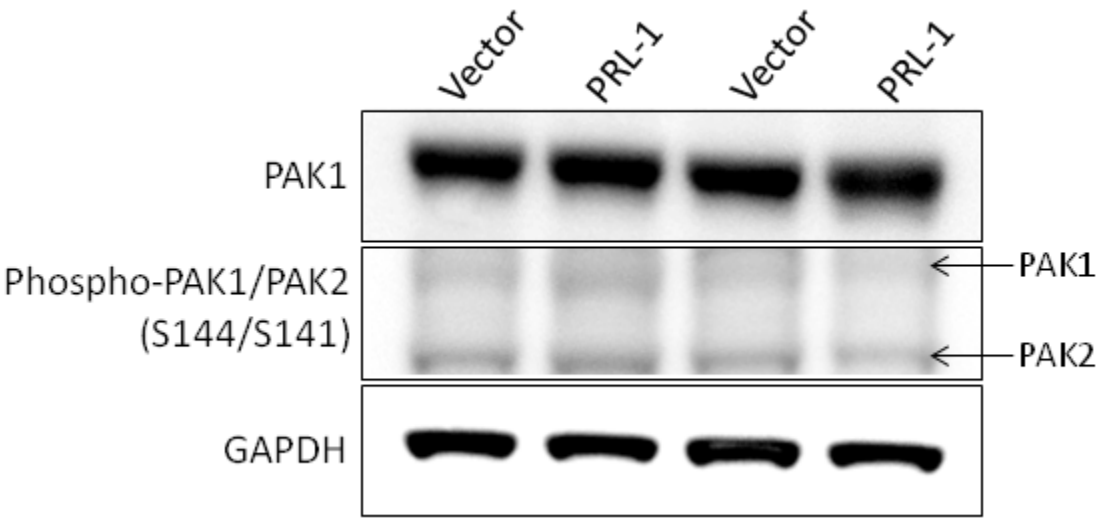

Figure 8.3 PRL-1 expression has no effect on PAK1 expression or phosphorylation at serine 144
HEK293 cells stably transfected with PRL-1 or empty vector were subject to western blot analysis using antibodies against total PAK1 or phosphorylated PAK1/PAK2 (Ser144/Ser141). No differences were observed between samples in either total PAK1 expression or phosphorylation state. GAPDH was used as a loading control.

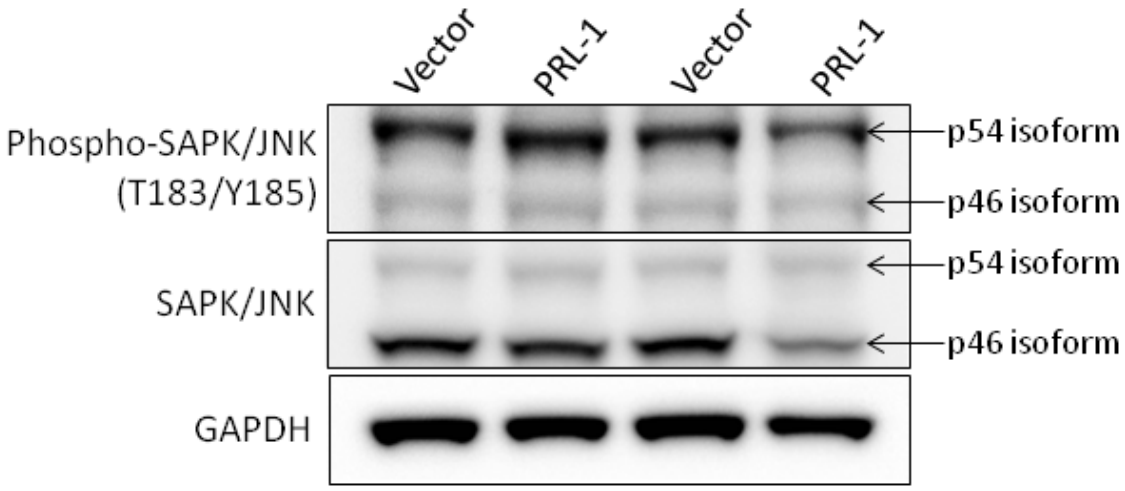

Figure 8.4 PRL-1 expression does not alter the levels of total or phospho-SAPK/JNK
HEK293 cells stably transfected with PRL-1 or empty vector were subject to western blot analysis using antibodies against total SAPK/JNK or SAPK/JNK phosphorylated at Thr183 (T183) and Tyr185 (Y185). No apparent differences were observed between samples in either total SAPK/JNK expression or phosphorylation state. GAPDH was used as a loading control.

8.3 Discussion

Cell movement is a multistep process that involves turnover of cell-matrix adhesions and dynamic reorganization of the actin cytoskeleton. Through the ability to effect the necessary changes in both the actin cytoskeleton and cell adhesions, small GTPases of the Rho family, such as RhoA, Cdc42, and Rac, have been identified as essential regulators of cell motility. Rac and Cdc42 both stimulate formation of protrusions at the leading edge of the cell, while RhoA controls retraction of the rear of the cell (Raftopoulou & Hall, 2004). Although the Rho GTPases work coordinately to influence cell movement, their activity must be precisely controlled, both spatially and temporally, for efficient cell migration to occur. For example, while RhoA expression and activity are crucial for tail retraction, high levels of RhoA activity can block the formation of membrane protrusions and result in inhibition of cell movement (Arthur & Burridge, 2001). Studies have suggested that an initial inhibition of RhoA is necessary to relieve cytoskeletal tension and allow membrane extension during cell spreading. As spreading ends, RhoA activity then gradually increases, allowing the formation of stress fibers and promoting cell contractility. Finally, RhoA activity decreases to a low basal level (Arthur & Burridge, 2001; X. D. Ren, Kiosses, & Schwartz, 1999).

The initial, transient down-regulation of RhoA activity during cell spreading occurs, at least in part, through the actions of Src, which activates the Rho GTPase activating protein p190RhoGAP, leading to Rho GTP hydrolysis and inactivation (Arthur, Petch, & Burridge, 2000). The current results suggest that,

in addition to increasing the levels of active c-Src, which has the capacity to down-regulate RhoA enzyme activity, ectopic overexpression of PRL-1 in HEK293 cells can also down-regulate RhoA protein abundance. One mechanism by which this might occur is through the control of another Rho regulator, RhoGDIα (gene symbol ARHGDIA). Most Rho family proteins are post-translationally modified by prenylation, enhancing their interaction with membranes. Rho guanine nucleotide dissociation inhibitors (RhoGDIs) can bind Rho proteins via their prenyl group, blocking Rho nucleotide exchange, extracting the Rho proteins from the membrane, and sequestering them away from their substrates (Dovas & Couchman, 2005). The interaction between Rho and RhoGDI can also protect the Rho proteins from proteosomal degradation (Boulter et al., 2010). Consequently, exogenous expression of RhoGDIα is accompanied by increased levels of RhoA protein, while silencing of endogenous RhoGDIα corresponds with decreased levels of RhoA protein (Boulter et al., 2010; Giang Ho et al., 2011). In the current study, microarray and mass spectrometry analysis revealed that PRL-1 overexpression leads to significantly decreased levels of RhoGDIα at both the mRNA and protein levels. Therefore, it is possible that PRL-1 down-regulates RhoA expression by decreasing the amount of RhoGDIα available for RhoA protein stabilization. Such post-translational control of Rho protein stability would explain the fact that ectopic overexpression of PRL-1 leads to decreased expression of RhoA protein without influencing RhoA transcript levels. Collectively, the microarray, mass spectrometry, and western blotting results support prior evidence suggesting that PRL-1 regulates focal

adhesion turnover and cytoskeletal rearrangement, through control of molecules such as Src and the RhoGTPases, to promote cell motility and metastasis.

An established link also exists between PRL-1 expression and increased cell invasion (Achiwa & Lazo, 2007; Fiordalisi et al., 2006; Luo et al., 2009; Zeng et al., 2003). Luo et al. (2009) showed that ectopic overexpression of PRL-1 in HEK293 cells leads to increased phosphorylation (hence activation) of ERK1/2 at Thr202/Tyr204 and to increased expression of the matrix metalloproteinases MMP2 and MMP9. They proposed that PRL-1-mediated activation of Src signaling leads to the downstream phosphorylation/activation of ERK1/2, which in turn causes activation of the transcription factors AP-1 and Sp1, leading to up-regulation of MMP2 and MMP9 expression which can cause degradation of the extracellular matrix, contributing to increased invasive activity. In the current analysis, we did not see any notable changes in either the expression or activity levels of ERK1/2 in response to PRL-1. The reasons for this are unclear; however alterations in ERK1/2 activity are often rapid and transient in order to precisely fine tune the cellular response. Moreover, RhoA activity may be required for establishing sustained ERK activation (Renshaw, Ren, & Schwartz, 1997; Welsh et al., 2001) and we have shown that RhoA expression in these cells is down-regulated. Given that Rho has been implicated in controlling the duration of ERK signaling and that Rho activity is known to fluctuate in a cyclical manner, it is likely that the detection of changes in phospho-ERK levels is dependent on the time of cell collection. It would be interesting, in future experiments, to generate HEK293 cell lines transiently expressing PRL-1 and to

examine the response of ERK, as well as other players involved in integrin-mediated cell signaling, to PRL-1 expression over a time course. Regardless, the current and previously reported results all suggest that PRL-1 can heavily influence Rho GTPase signaling. Provided that the Rho GTPases have been tied to all stages of cancer progression, including cell growth, proliferation, migration, invasion, and metastasis, it is possible that many or all of the phenotypic effects resulting from aberrant PRL-1 expression could be linked to PRL-1-mediated control of the Rho GTPase signaling pathways.

CHAPTER 9. PRL-1 OVEREXPRESSION ALTERS THE MICRORNA EXPRESSION PROFILE OF HEK293 CELLS AND LEADS TO DOWN-REGULATION OF MICRORNAS THAT TARGET PRL-1 AND ITS DOWNSTREAM PATHWAYS

9.1 Introduction

MicroRNAs (miRNAs; miRs) have recently emerged as central post-transcriptional regulators of gene expression. These small, non-coding RNA molecules are capable of influencing many biological processes and are increasingly recognized as having critical roles in malignant transformation (Stahlhut Espinosa & Slack, 2006; E. Wang, 2008). MicroRNAs bind to complementary mRNA targets and, generally, inhibit protein synthesis by inducing mRNA degradation or sterically hindering protein translation (Bartel, 2004; Eulalio, Huntzinger, & Izaurralde, 2008), but translational up-regulation by miRNA's has also been observed (Place, Li, Pookot, Noonan, & Dahiya, 2008; Vasudevan, 2012). Interestingly, while examining the effects of the PRL-1 phosphatase on global gene expression, we found that overexpression of PRL-1 in HEK293 cells led to up-regulation of the mRNA and/or protein products for several genes with important roles in microRNA biogenesis and function (see Chapter 7). Two of these (HNRNPH1 and DDX5) are part of the DGCR8 recognition complex that directs the RNase III enzyme Drosha to primary miRNA targets (pri-miRNAs) to carry out the first step in generation of mature

miRNA transcripts (Shiohama, Sasaki, Noda, Minoshima, & Shimizu, 2007). Another gene, FMR1, is a component of the microRNA RNA induced silencing complex (miRISC) that mediates inhibition of miRNA targets (Ishizuka, Siomi, & Siomi, 2002). Finally, a fourth gene, ELAVL1, can bind mRNA target sequences and either facilitate or counteract miRNA-mediated repression in a gene-specific manner (Meisner & Filipowicz, 2011).

Given that PRL-1 signaling can up-regulate the expression of such key molecules related to miRNA processing and behavior, I hypothesized that PRL-1 could, either directly or indirectly, regulate miRNA expression and/or function. The relationship between PRL-1 and microRNAs had not previously been explored; therefore, I used TaqMan Low Density Human MicroRNA arrays to compare the miRNA expression profiles of HEK293 cells stably transfected with PRL-1 or with empty vector control.

9.2 Results

Expression levels of 664 microRNAs were evaluated in triplicate biological replicates of HEK293-PRL-1 and HEK293-vector cells using TaqMan Human MicroRNA arrays. The resulting data set was then filtered to retain the 268 miRNA measurements that had consistent present or not-present calls in all 3 replicates of each comparison group. Of these 268 miRNAs, there were 50 that displayed differential expression below a p-value threshold of 0.1, but only 5 of these retained significance below an FDR of 10% (Table 9.1). The miRNA's hsa-miR-154* and hsa-miR-886-5p were significantly up-regulated, while the miRNA's

hsa-miR-339-5p, hsa-miR-801, and hsa-miR-616 were significantly down-regulated in the PRL-1-overexpressing cells compared to the empty vector controls.

A combination of different software tools were used to determine which functional categories and signaling pathways were most over-represented by those mRNAs that were either experimental proven or predicted with high confidence, by at least two prediction algorithms, to be targets of the 5 miRs that showed significantly altered expression with increased exposure to PRL-1. Each tool gave similar results. Figure 9.1 and Figure 9.2 display the top 30 functions/pathways that are over-represented by mRNA targets of the up-regulated and down-regulated miRs respectively. MicroRNA targets were commonly involved in cancer, cell adhesion, actin cytoskeletal rearrangement, and MAPK signaling, indicating that the miRNAs that change significantly with PRL-1 overexpression are influencing many of the same pathways where significant changes in mRNA and protein expression were also seen. Other highly over-represented pathways included those related to neuronal signaling, Wnt signaling, Jak-STAT signaling, calcium signaling, and immune signaling.

Given that many of the targets of significantly altered miRNAs were genes involved in actin cytoskeletal rearrangement and cell adhesion and that qRT-PCR analysis confirmed significant changes in mRNA expression of several genes involved in these same processes, we choose to perform a direct comparison of the qRT-PCR (significantly changing genes only) and miRNA (all miRs) data sets. Since miRNAs are best known as negative regulators of gene

expression, the data sets were scrutinized for negative correlations between the expression of a particular miRNA and the expression levels of its predicted and/or known mRNA targets. As can be seen in the volcano plot in Figure 9.3, most of the transcripts that were significantly up-regulated in the PRL-1 transfectants corresponded to miRNAs whose expression was down-regulated in those same samples. In contrast, none of the miRs for three of four significantly down-regulated mRNAs were differentially expressed between the HEK293-PRL-1 and HEK293-vector samples. In addition, we found that the two miRNAs (miR-339-5p and miR-30-c-5p), which are consistently reported, by all examined prediction algorithms, to target PRL-1 were down-regulated in the PRL-1 overexpressing cells compared to the controls (Figure 9.4). Therefore, overexpression of PRL-1 leads to down-regulation of microRNAs that target PRL-1 as well as down-regulation of microRNAs that target signaling molecules having increased mRNA expression in response to PRL-1.

Table 9.1 MicroRNAs with differential expression in HEK293-PRL-1 cells compared to HEK293-vector cells
A total of 664 microRNAs were assessed for differential expression using TaqMan Array Human microRNA Cards. Significance was determined based on an FDR threshold of 10% (i.e. FDR < 0.10).

Assay ID	Associated IPA mature RNA ID	Empty vector Average ΔC_t	PRL-1 transfectant Average ΔC_t	Fold Change	p-value	FDR
hsa-miR-886-5p	Vault RNA 2-1	10.2	6.5	12.8	6.8E-04	6.3E-02
hsa-miR-154*	miR-154-3p	22.4	19	10.6	9.5E-04	6.3E-02
hsa-miR-339-5p	miR-339-5p	11.0	11.2	-1.2	7.2E-04	6.3E-02
hsa-miR-801	RNU11	12.8	14.8	-3.8	1.2E-03	6.3E-02
hsa-miR-616	miR-616-3p	17.3	20.5	-9.3	8.1E-04	6.3E-02

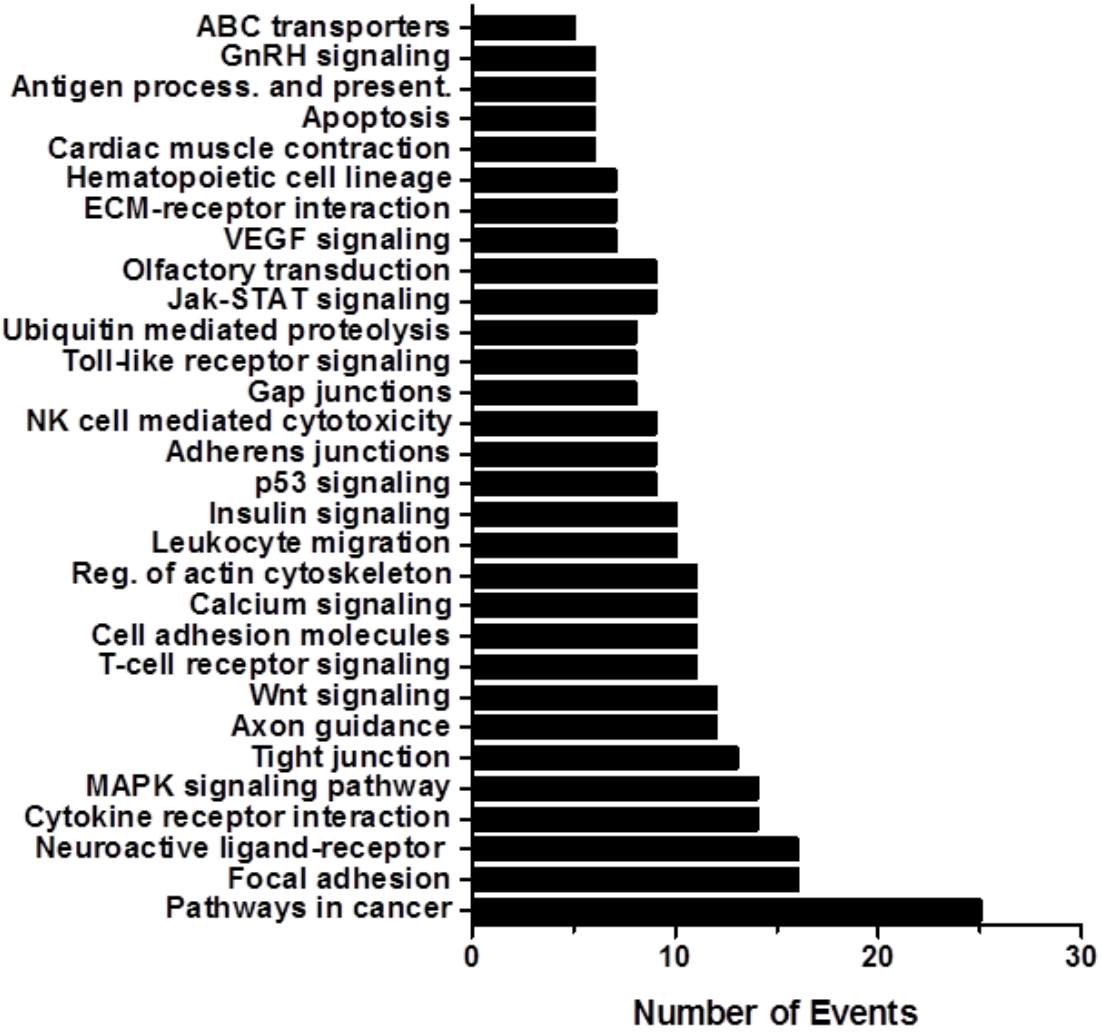

Figure 9.1 Functional categories/pathways over-represented by predicted and known targets of the miRNAs that were significantly up-regulated by PRL-1

Number of events refers to the number of genes in each category. Abbreviations: ABC, ATP-binding cassette; ECM, extracellular matrix; GnRH, gonadotropin-releasing hormone; Jak-STAT, Janus-activated kinase-signal transducer and activator of transcription; MAPK, mitogen-activated protein kinase; NK, natural killer; Present, presentation; Process, processing; Reg, regulation; VEGF, vascular endothelial growth factor.

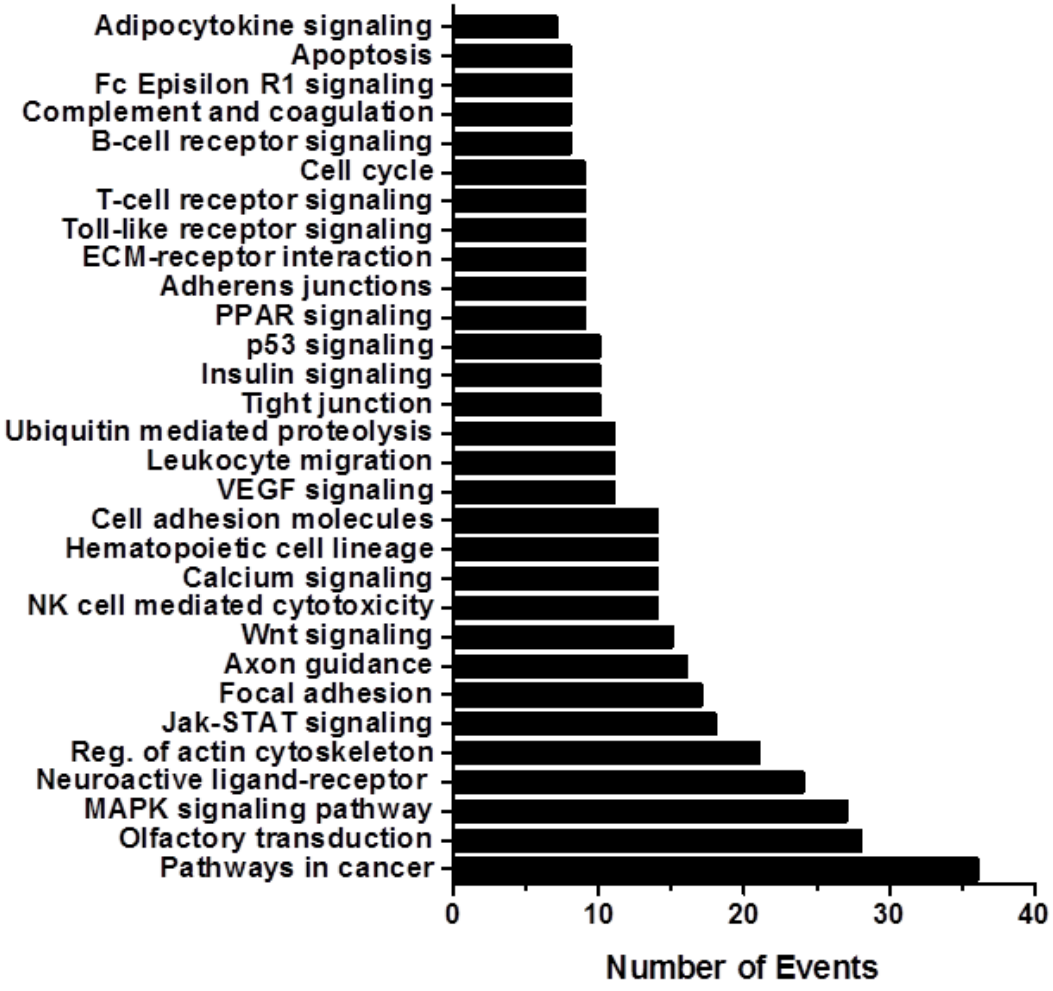

Figure 9.2 Functional categories/pathways over-represented by predicted and known targets of the miRNAs that were significantly down-regulated by PRL-1

Number of events refers to the number of genes in each category. Abbreviations: ECM, extracellular matrix; Fc Epsilon R1, fragment crystallizable region, epsilon, receptor 1; Jak-STAT, Janus-activated kinase-signal transducer and activator of transcription; MAPK, mitogen-activated protein kinase; NK, natural killer; PPAR, peroxisome proliferator-activated receptor; Reg, regulation; VEGF, vascular endothelial growth factor.

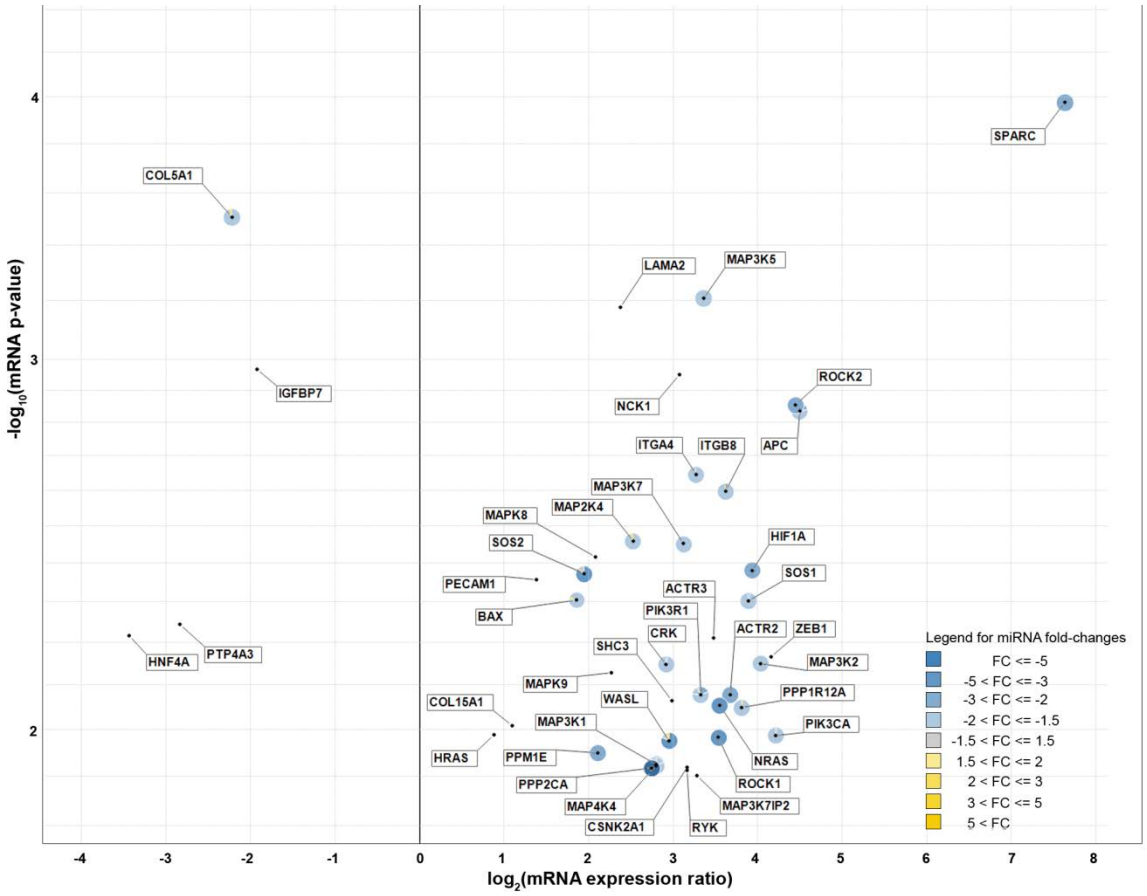

Figure 9.3 Significantly differentially expressed mRNA transcripts integrated with changes in corresponding miRNA signals
Each black dot represents a gene whose transcripts were confirmed by qRT-PCR to be differentially expressed between HEK293-PRL-1 and HEK293-vector cells. A positive $\log_2$(mRNA expression ratio) value on the x-axis indicates an up-regulation of mRNA expression, while a negative value indicates a down-regulation of mRNA expression. The $-\log_{10}$ of the p-value for the mRNA expression data is plotted on the y-axis such that the higher the number, the better the p-value. Colored circles surrounding the dots represent miRNAs known or predicted with moderate- to high-confidence to target each mRNA and having expression data from the TaqMan MicroRNA Arrays. In instances where more than one miRNA with expression data targets the same mRNA, the colored circle is divided into sectors where each sector represents a single miRNA sequence and the size of the sector represents that miRNA's contribution to the total signal for all miRNAs targeting that gene. The various shades of color represent different fold change (FC) thresholds for the miRNA data, as defined in the inset legend.

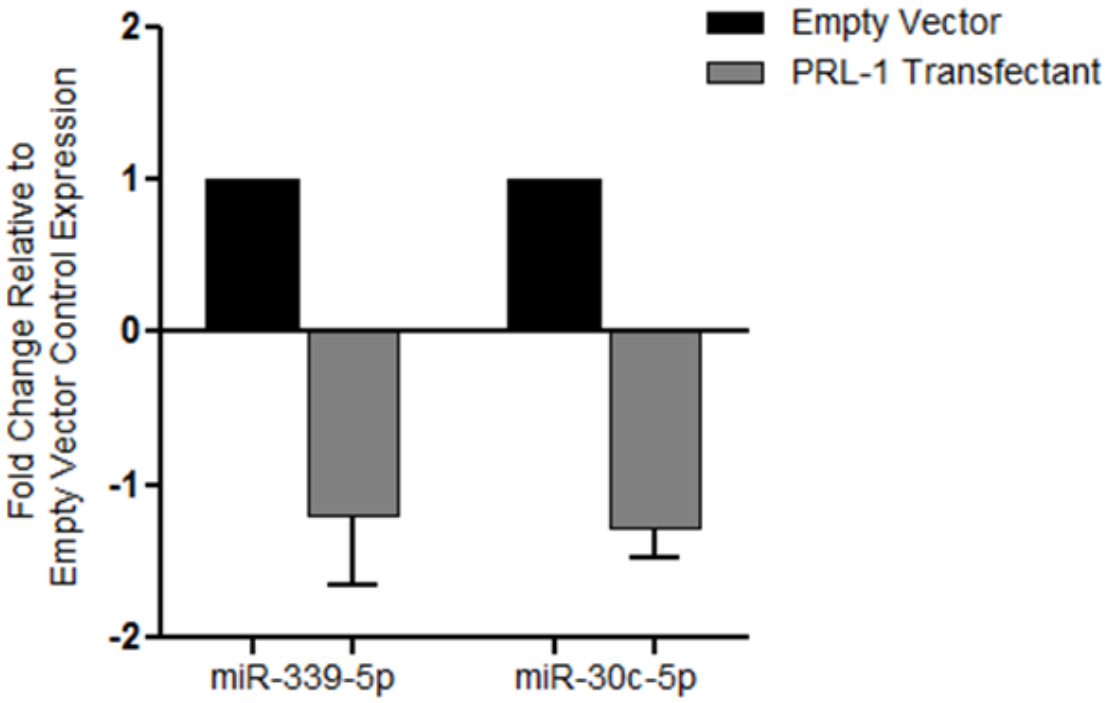

Figure 9.4 Expression of miRs targeting PRL-1
The fold change in expression for each miRNA in HEK293 cells stably transfected with PRL-1 is shown relative to the expression of the miR in cells transfected with empty vector. The mean ± SEM for three independent biological replicates are shown.

9.3 Discussion

To begin to investigate the role of microRNAs in regulation of gene expression downstream of PRL-1, we used TaqMan Low Density Human MicroRNA arrays to compare the miRNA expression profiles of PRL-1 transfected to empty vector transfected HEK293 cells. In this analysis, five miRNAs were identified whose expression was significantly ($q \leq 0.10$) altered in the PRL-1 transfectants. Of these, two (miR-886-5p and miR-154*) were significantly up-regulated and three (miR-339-5p, miR-801, and miR-616) were significantly down-regulated.

MicroRNA-886-5p was the most significantly up-regulated miRNA (up 13-fold) in the HEK293-PRL-1 transfectants. The classification of the miR-886 sequence as a microRNA is actually a topic of some debate. In 2009, Nandy et al. proposed that, based on structural resemblance and a similar expression profile to vault RNAs (vtRNAs), miR-886 might instead be a component of the hollow, barrel-shaped ribonucleoprotein complex known as the vault complex. Accordingly, miR-886 was officially renamed vtRNA2-1. More recently, however, K. Lee et al. (2011) provided evidence suggesting that 886 is not part of the vault complex, nor is it a canonical miRNA. Instead, this sequence may represent a new, as yet uncharacterized, class of non-coding RNA (ncRNA). The biological significance of miR-886/vt2-1 is just beginning to be explored, but it appears to have the capacity to both promote and suppress malignant transformation in a cell-type dependent manner (Gao, Shen, Liu, Xu, & Shu, 2011; Han et al., 2012; K. Lee et al., 2011; J. H. Li et al., 2011; Xiao et al., 2012). It is predicted to target

the genes FLNA, TAGLN2, and EF2, all which were significantly increasing in our PRL-1 transfectants, and is also predicted to target RhoGDIα and COL5A1, which were both significantly decreasing in the PRL-1 transfectants. Not enough is known yet about the relationship of miR-886/vtRNA2-1 to these molecules to say whether its effects on each are normally synergistic or antagonistic.

Two instances where the effect of miRNA-886/vtRNA2-1 is experimentally shown to have an inhibitory effect are on the pro-apoptotic molecule Bax (J. H. Li et al., 2011) and the RNA-dependent protein kinase PKR (K. Lee et al., 2011). Interestingly, miR-616, which was the most significantly down-regulated miRNA (down 9-fold) in the PRL-1 transfectants, is also predicted to target both Bax and PKR. The differential regulation of two ncRNAs with similar targets underscores the complexity of both PRL-1 signaling and miRNA regulation and suggests that opposing forces may be at work in an attempt to regain balance within in the system, following perturbation by PRL-1. Given that alterations in PKR activity can have profound effects on the cell, it is not surprising that the activity of this molecule would be tightly controlled. PKR is a versatile signaling molecule that has both pro-survival and pro-apoptotic effects (Cho et al., 2011; Kazemi et al., 2007; K. Lee et al., 2011; von Roretz & Gallouzi, 2010; Yoon, Miah, Kim, & Bae, 2010). It is known to promote increased mRNA expression of HNRNPH1 and TAGLN2 (Guerra, Lopez-Fernandez, Garcia, Zaballos, & Esteban, 2006), which were both significantly increased in the PRL-1 transfectants. Nonetheless, PKR is best known for its regulation of the eukaryotic translation initiation factor eIF2A. In response to cellular stress, active PKR can phosphorylate and inhibit eIF2A,

resulting in a shutdown of global protein synthesis (Garcia et al., 2006). Sustained inhibition of protein synthesis can lead to cell death, however, more transient inhibition can selectively regulate the translation of specific mRNAs that have a higher requirement for eIF2A activity. Notably, Liang et al. (2008) previously showed that ectopic expression of PRL-3 in HEK293 cells leads to enhanced phosphorylation and inactivation of eIF2A and proposed this as the mechanism by which PRL-3 is able to down-regulate the expression of the Src inhibitor Csk, leading to increased Src activity. The current results suggest that, as with PRL-3, ectopic expression of PRL-1 in HEK293 can also influence the expression of molecules which regulate downstream eIF2A activity.

In addition to miR-886/vtRNA2-1, miR-154* was also up-regulated (11-fold) in the HEK293-PRL-1 lines. This miR is predicted to target HNRNPH2, ACTN4, and ALDOA, all genes whose products were significantly up-regulated in those samples. Up-regulation of miR-154* has also been associated with cancer. It is known to be highly expressed in a subset of acute myeloid leukemia patient samples (Dixon-McIver et al., 2008) and in primary Ewing's sarcoma xenografts (Mosakhani et al., 2012); however it is found at lower levels in the associated metastatic tumors from the Ewing's sarcomas.

MiR-339-5p and miR-801 were significantly down-regulated (1.2- and 3.8-fold respectively) in the PRL-1 transfectants. MiR-339-5p is predicted to target PRL-1 itself and is also predicted to target Mdm2, a molecule that is known to function downstream of PRL-1 promoting p53 degradation and apoptosis inhibition (Min et al., 2009). This miR appears to have a tumor suppressive effect

on cells, as it has been found at significantly lower levels in breast cancer tissue compared to benign tissue and is capable of decreasing migration and invasion of breast cancer cell lines (Z. S. Wu et al., 2010). As with miR-886, miR-801 is another molecule that was originally thought to be a microRNA and was included on the Applied Biosystems TaqMan miRNA Arrays, but has recently been reclassified. This molecule was originally identified based on its ability to associate with the AIN-1 and AIN-2 proteins that form part of the RNA induced silencing complex (RISC) (L. Zhang et al., 2007). However, the sequence was later determined to be a fragment of the small nuclear ribonucleoprotein (snRNP) U11 (www.mirbase.org). The snRNP U11 (a.k.a. RNU11) functions as a component of the minor spliceosome (noncanonical splicing pathway) that is responsible for catalyzing the removal of a small (~0.1% of all introns) class of atypical intron (Tarn & Steitz, 1996). Known targets of the minor spliceosome that are relevant to PRL-1-biology include PTEN and PRDX1 (The U12 Intron Database: genome.crg.es/cgi-bin/u12db/u12db.cgi). Microarray and proteomic analysis revealed that PRL-1 overexpression in HEK293 cells caused alterations in the mRNA and protein expression levels of a number of molecules with important roles in alternative splicing, including members of the HNRNP, SRSF, and ELAVL1 gene families. The down-regulation of RNU11 in response to PRL-1 further implicates PRL-1 with a potential role in altering alternative splicing patterns to influence downstream gene expression.

Altogether, the full list of predicted and known targets for all five significantly differentiated ncRNAs show an over-representation of genes

involved in cell adhesion and cytoskeletal rearrangement. This result is in close agreement with the mRNA and protein results for this sample set. Focusing in further on these pathways, we found a down-regulation of almost all assayed miRs, which target mRNA transcripts that were confirmed by qRT-PCR to be significantly up-regulated in response to PRL-1, in the PRL-1 transfectants (i.e. expression of these miRs was inversely correlated to the expression of their targets). Moreover, both miRNAs which are thought to directly target PRL-1 were also down-regulated in the PRL-1 transfectants. These findings indicate that PRL-1 signaling has the capacity to indirectly affect downstream gene expression through alteration of microRNA levels. Moreover, up-regulation of PRL-1 may initiate a positive feedback loop leading to inhibition of PRL-1 targeting miRNA's and thus increased PRL-1 mRNA stability or protein translation. Further characterization will be required to understand the roles of each of the differentially expressed miRNAs and other ncRNAs in PRL-1 signaling and their relationship to PRL-1 induced malignant transformation. Nevertheless, this study is the first to show that PRL-1 signaling can lead to altered patterns of miRNA expression.

CHAPTER 10. STABLE TRANSFECTION OF PRL-3 IN HEK293 CELLS LEADS TO DOWN-REGULATION OF GLOBAL TRANSCRIPTION

10.1 Introduction

A growing number of studies have implicated PRL-3 in the progression and metastasis of a wide array of tumor types (Reviewed in: Bessette et al., 2008), calling attention to the PRL family as potential novel targets for cancer therapy. However, despite much emerging evidence surrounding PRL-3 binding partners and the downstream consequences of exogenous PRL-3 expression or endogenous PRL-3 knockdown by RNAi, the normal biological function of this molecule remains unknown and the signaling pathways through which it exerts its effects are poorly understood. Although the primary focus of my research project was PRL-1, because we were also able to obtain HEK293 cells stably transfected with PRL-3 and because many questions surrounding PRL-3 signaling events still remain unanswered, I also attempted to examine the global transcriptional profiles of HEK293 cells transfected with PRL-3 using microarray analysis.

For this analysis, total RNA was extracted from triplicate biological replicates of HEK293 cells stably transfected with PRL-3 and HEK293 cells transfected with empty vector. Transcriptional profiling of each RNA sample was performed, using Affymetrix microarrays, as described in the methods section.

10.2 Results

The Affymetrix GeneChip Operating System (GCOS) was used to generate an “Expression Report” for each sample hybridized to a microarray and an initial quality check of each sample was performed by evaluating the Expression Report metrics. Typically, in a given sample, at any one time, somewhere between 40-50% of all transcripts represented on the microarray are being expressed. This value is measured by the GCOS Software and is referred to as the Percent Present call or %P in the Expression Report. Although, in some tissue types or cell lines, fewer than 40% or greater than 50% of the transcripts can be expressed, the %P is almost always consistent between samples of the same origin (e.g. same cell type). Table 10.1 lists the %P calls that were reported for all samples examined by microarray in the current study. As expected, the % Present calls for the PRL-1 transfected samples and their pcDNA4 empty vector control samples ranged from 44-50%. In addition, all other quality control (QC) parameters (e.g. background level, scale factor, 3’/5’ ratios of β-actin and GAPDH) for these samples were within normal ranges, suggesting high quality RNA as starting material and consistent performance of the assay. Likewise, all report values for the PRL-3 empty vector (pcDNA3) controls were within expected ranges and these lines displayed %P values ranging from 45 to 48%. Unexpectedly, however, in all biological replicates of the HEK293 lines stably transfected with PRL-3, the %P values were between 11 and 12%. Normally, such a result would suggest poor sample quality, which would also be evident in the values of other QC parameters within the report, but in this case,

all other report values were normal. In addition, evaluation of the RNA using the Agilent Bioanalyzer had indicated the presence of high quality RNA in these samples (see Chapter 5 results). Since all evidence indicates that the RNA sample quality was good and the assay was performing correctly, these data suggest that stable overexpression of PRL-3 may lead to down-regulation of transcription on a global level.

To further examine the PRL-3 microarray results, Partek Genomics Suite was used to perform a statistical comparison of the genes that were expressed in the PRL-3 transfectants compared to those expressed in the corresponding empty vector samples. In this analysis, the large scale alterations in overall gene expression caused by stable PRL-3 transfection were even more apparent. Of the 47,400 total RNA transcripts represented on the Affymetrix U133 Plus 2.0 microarrays, 22,123 (47%) of these displayed more than a 2-fold change in expression between the PRL-3 stable cell lines and the empty vector control lines. Even when far more stringent cut-off criteria were applied, for example a fold change threshold of 10 in combination with a false discovery rate threshold of 10%, there were still almost 2,300 transcripts exhibiting significant differences in expression between the two groups (Figure 10.1). Interestingly, PRL-3 did not appear among the list of genes that displayed significantly increased expression in the PRL-3 transfectants. To confirm this result, we elected to examine PRL-3 expression in the microarray samples using qRT-PCR. As shown in Chapter 6 of this dissertation, RT-PCR analysis revealed that PRL-3 expression was actually

several orders of magnitude lower in the PRL-3 transfectants than in the empty vector controls.

One possible explanation for the large scale alterations in gene expression observed in the PRL-3 stable transfectants is that these lines, which have a significantly enhanced doubling time compared to the control lines may have been overgrown, with a large proportion of cells dead or dying at the time of sample collection. To test this theory, a new batch of cells, which had more recently been taken out of frozen storage (had been through fewer passages) than the initial set of samples used in the microarray experiments, was grown and cells were collected at various stages of growth, ranging from 20% to 90% confluency. RNA was extracted and reverse transcribed, then analyzed by qRT-PCR using an ABI Endogenous Control Array. Quantitative RT-PCR analysis with the same Endogenous Control Array and the samples from the microarray experiments, had already revealed that stable transfection of PRL-3 could dramatically reduce the expression of a number of genes typically considered to be housekeeping controls (see Chapter 6 results); thus, use of the same array with this new batch of samples allowed a direct comparison of the results. Despite marked differences in the confluency at which the new cells were harvested and careful consideration as to the conditions under which they were harvested, the results of this endogenous control experiment were the same as with the previous batch of cells. With the exception of 18S rRNA, the expression of all 15 other control genes on the array was down-regulated in the PRL-3 transfectants compared to the empty vector samples. As can be seen by plotting

the Ct values for the samples using DataAssist (Figure 10.2), genes which were expressed at low, moderate, or even high levels in the vector only control lines became low to undetectable in the PRL-3 overexpressing cells regardless of the confluency at which they were collected. These data indicate that the observed alterations in global gene expression, upon stable PRL-3 transfection in HEK293 cells are not simply a factor of the conditions under which the cells were harvested. Taken together with Agilent Bioanalyzer results and the quality review of the microarrays, these data suggest that the global changes in gene expression observed with exogenous expression of PRL-3 in HEK293 cells is a real biological phenomenon and not the result of poor sample quality, sample handling error, or technical/assay error.

The expression of PRL-3 itself was also examined by RT-PCR in the samples that were collected at various stages of confluency. As with the previous sample set, PRL-3 expression was again lower in the cells stably transfected with PRL-3 than in the lines transfected with empty vector (Figure 10.3). Compellingly, PRL-3 expression declined as the cells grew more confluent, suggesting that PRL-3 transgene expression is influenced by cell density.

The large scale decreases of PRL-3 expression in the PRL-3 stable transfectants compared to the vector controls raised the question of whether these stably transfected HEK293 lines may have undergone some sort of adaptive response over time, leading to transgene silencing. This, along with the presence of such numerous changes in gene expression that it is difficult to filter the microarray data down to a reasonable and meaningful level, is likely to

preclude our ability to use these stable HEK293 PRL-3 transfectants to identify alterations in gene expression that are directly influenced by PRL-3. Instead, cells transiently transfected with PRL-3 might be more useful in that capacity. To evaluate whether we could successfully generate cell lines transiently overexpressing pcDNA3-PRL-3, a human non small cell lung carcinoma cell line (H1299) was transiently transfected with either PRL-3 or empty vector (n =1 each). RNA was extracted from the cells and was subjected to both RT-PCR and microarray analysis. Quantitation of PRL-3 levels in these samples revealed that PRL-3 was expressed at more than 30-fold higher levels in the PRL-3 transfected H1299 cells than in the cells transfected with empty vector (Figure 10.4). Moreover, evaluation of the QC report metrics for these samples after hybridization to microarrays revealed %P values for the empty vector and PRL-3 transfectants of 43.9% and 43.6% respectively. Based on these results, the H1299 transient transfectants may be a viable alternative to the HEK293 stable transfectants for use in future examination of the signaling events downstream of PRL-3.

Table 10.1 Percentage of total transcripts called present (%P) for samples assayed by microarray

RNA derived from HEK293 cells that were stably transfected with PRL-1, PRL-3 or their respective empty vectors were hybridized to Affymetrix U133A Plus 2.0 microarrays and the Affymetrix GCOS software was used to determine the number of transcripts on the array that were called present in each sample. Values between 40-50%, such as seen for the PRL-1 transfectants and all empty vector controls are typical. Transfection of HEK293 cells with PRL-3, on the other hand, led to a large scale decrease in global transcription as indicated by the unusually low %P values for all biological replicates of these samples on the microarray.

Cell Line	Sample	%P
HEK293	Empty Vector 1 (PRL-1)	43.6
HEK293	Empty Vector 2 (PRL-1)	44.1
HEK293	Empty Vector 3 (PRL-1)	44.4
HEK293	PRL-1 Transfectant 1	46.5
HEK293	PRL-1 Transfectant 2	45.1
HEK293	PRL-1 Transfectant 3	50.0
HEK293	Empty Vector 1 (PRL-3)	47.7
HEK293	Empty Vector 1 (PRL-3)	47.6
HEK293	Empty Vector 1 (PRL-3)	45.0
HEK293	PRL-3 Transfectant 1	11.9
HEK293	PRL-3 Transfectant 2	11.5
HEK293	PRL-3 Transfectant 3	10.7

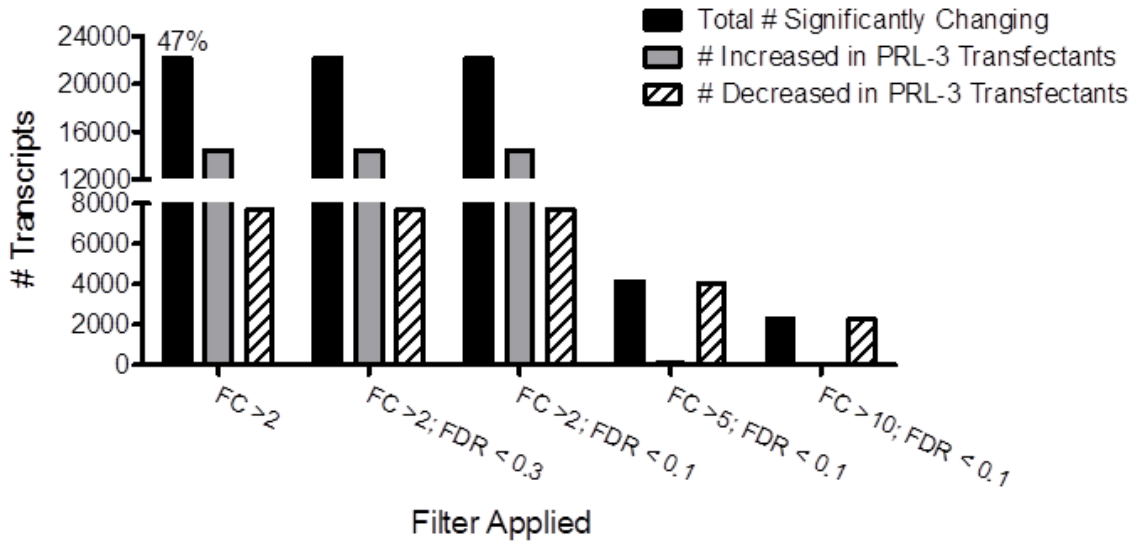

Figure 10.1 Number of transcripts significantly differentially expressed in HEK293 cells stably transfected with PRL-3

Global gene expression in HEK293 cells stably transfected with PRL-3 or empty vector was assessed using Affymetrix microarrays and Partek Genomics Suite software was used to identify genes that were significantly different between the two sample groups (PRL-3 vs. empty vector) using various significance thresholds to filter the data. FC = Fold Change; FDR = False Discovery Rate.

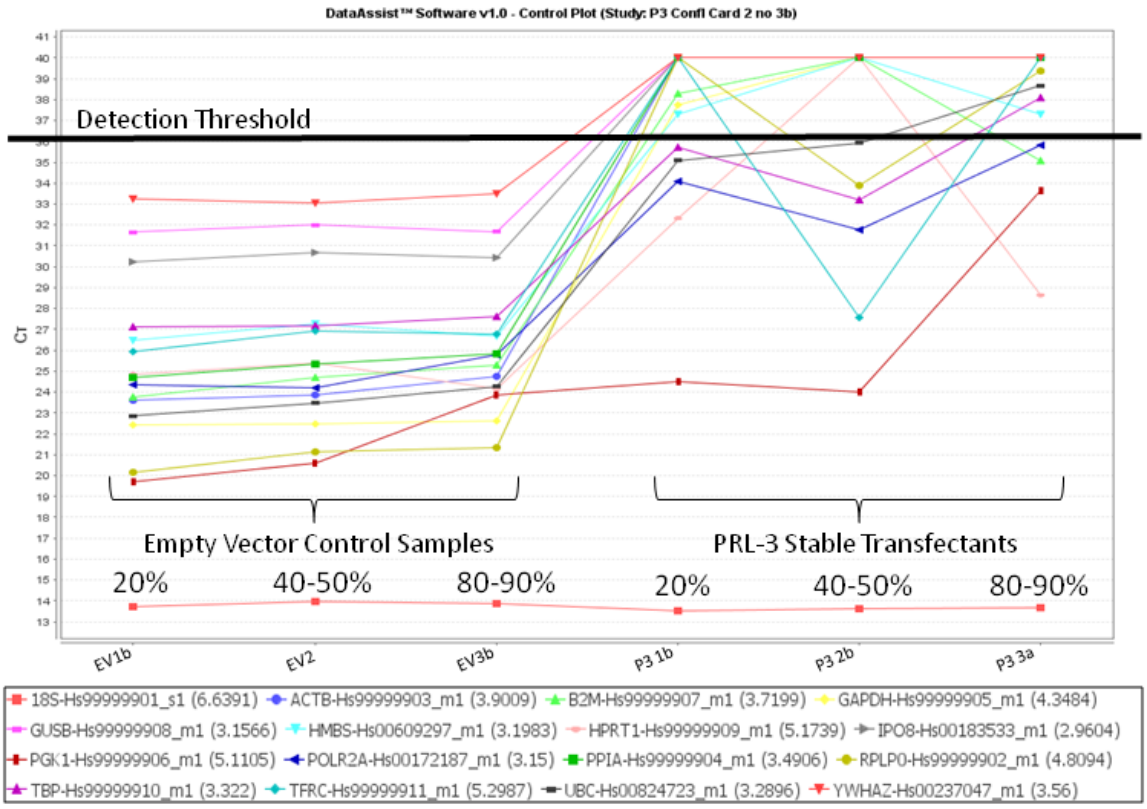

Figure 10.2 Influence of PRL-3 transfection on global gene expression is independent of cell confluency

A TaqMan Endogenous Control Array was used to examine the expression of 16 classical endogenous control genes in HEK293 cells stably transfected with PRL-3 or with empty vector. Cells were grown to confluencies of 20%, 40-50%, and 80-90% prior to cell collection and RNA extraction. Gene expression was then examined using qRT-PCR. Visualization of the resulting cycle threshold (Ct) values revealed that stable transfection of the PRL-3 containing vector leads to a significant decrease in expression (increase in Ct value) of most housekeeping genes, regardless of cell confluency.

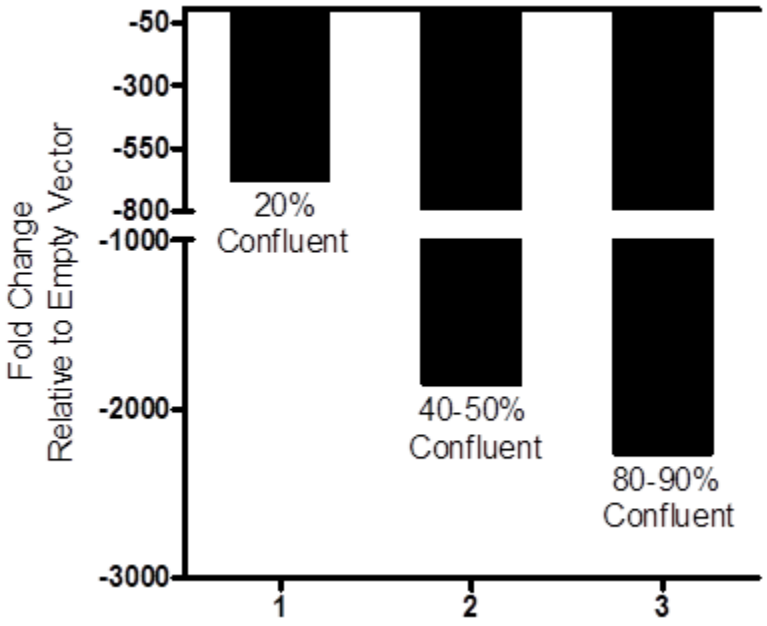

Figure 10.3 PRL-3 transgene expression is influenced by cell density
HEK293 cells stably transfected with PRL-3 or empty vector were grown to various stages of cell confluency, then RNA was extracted and PRL-3 expression was evaluated using qRT-PCR. PRL-3 transcript levels, which were found to be down-regulated in the PRL-3 transfectants compared to the empty vector controls, declined to lower and lower levels as cell confluency (density) increased.

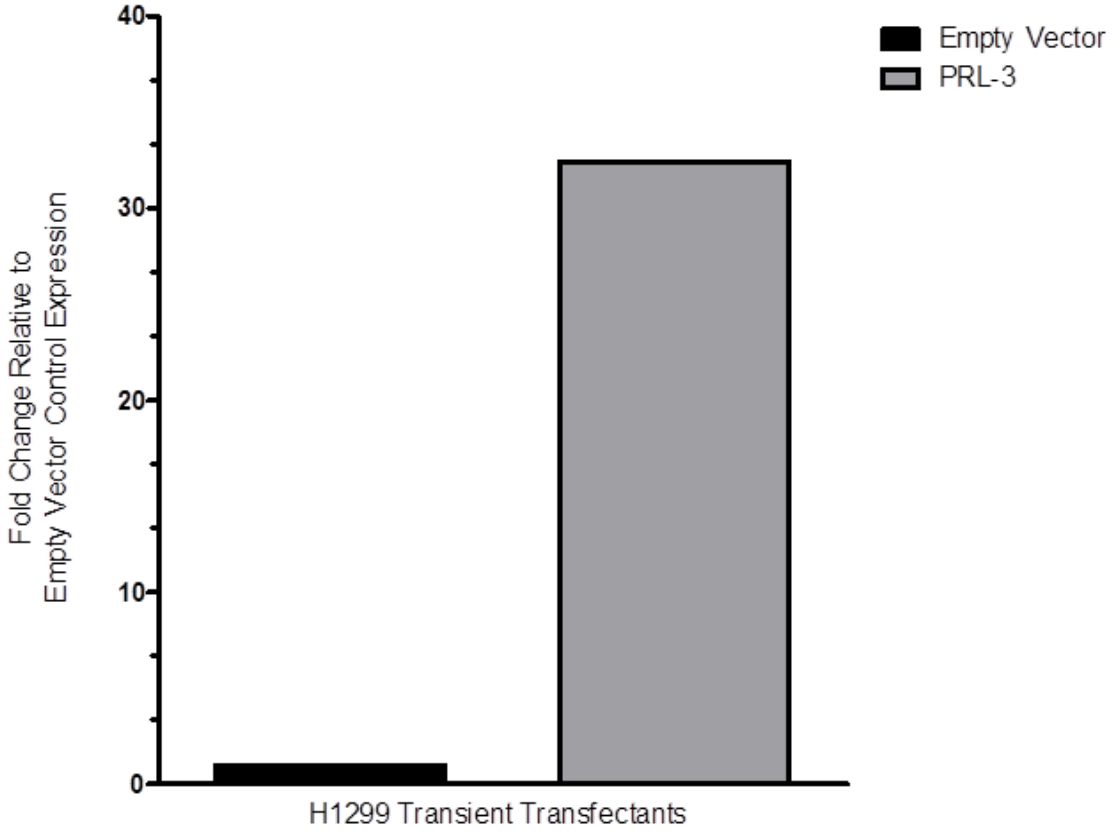

Figure 10.4 PRL-3 expression in H1299 transient transfectants
The fold change differences in PRL-3 mRNA transcript levels in H1299 cells transiently transfected with PRL-3 or with empty vector (n=1 each) were determined by qRT-PCR. The PRL-3 transient transfectants successfully overexpressed PRL-3 at more than 30-fold higher levels than in the empty vector control lines.

10.3 Discussion

HEK293 cells stably transfected with PRL-3 appear to undergo some form of transgene silencing over time, where the degree of silencing is tied to the density, or possibly the rate of proliferation, of the cells in culture. The PRL-3 transgene was under the control of the cytomegalovirus (CMV) immediate-early promoter on the pcDNA3 expression vector. Due to its potent activity, the CMV promoter is one of the most commonly used promoters, *in vitro* and *in vivo*, for driving expression of transgenes in mammalian cells. However, CMV promoter-driven expression is strongly affected by cellular context and, thus, can be highly cell type specific (Mao et al., 2008; Radhakrishnan, Basma, Klinkebiel, Christman, & Cheng, 2008; Wiederkehr & Caroni, 1995). It has been documented that, in some stably transfected cells, CMV promoter activity is vulnerable to silencing and is gradually suppressed over the course of time in culture (K. H. Choi, Basma, Singh, & Cheng, 2005; Norrman et al., 2010). It is possible that this is the reason for the eventual down-regulation of PRL-3 in the HEK293 stable transfectants.

The mechanisms involved in silencing the CMV and other transgene promoters are poorly understood, particularly in cultured mammalian cells, but DNA methylation (Brooks et al., 2004; K. H. Choi et al., 2005), histone hypoacetylation (K. H. Choi et al., 2005), and RNAi (Ketting & Plasterk, 2000) have all been implicated. The specific mechanisms used can vary from cell type to cell type, but generally result in either gene inactivation by blocking transcription or inhibition of mRNA accumulation following transcription. When

transcription is blocked, this is referred to as transcriptional gene silencing or TGS. When transcription occurs, but mRNA accumulation is inhibited, it is known as post-transcriptional gene silencing or PTGS (Stam, Mol, & Kooter, 1997). Studies in developing tobacco plants have shown that PTGS can be released with synthesis of DNA in proliferating cells and again reactivated when proliferation is complete (Mitsuhara et al., 2002). It is therefore plausible that the decline in PRL-3 expression with increasing cell confluency is related to a partial release of gene silencing when the cells are rapidly proliferating and a reactivation of gene silencing when proliferation slows as the cells approach confluency or begin to exceed the capacity of the medium to support growth. However, further studies would be required to determine the exact mechanisms of gene silencing in these cell lines and the factors by which they are controlled.

Not only is PRL-3 expression reduced in the PRL-3 stable transfectants, but there appears to be a global down-regulation of transcription in these cell lines. Again, the mechanisms for this are unclear. They could be similar to those affecting PRL-3 expression, although the decreases in expression seen for other genes seem to be less dependent on cell density than those observed for PRL-3. The goal of the microarray analysis on the HEK293 stable transfectants was to elucidate the pathways in which the PRL enzymes act and to identify new candidates for possible PRL effectors and/or substrates, but there is clearly additional biology occurring in the PRL-3 stable transfectants that would interfere with this goal. The use of transient transfectants instead may avoid any issues of transgene silencing over time because, unlike stable transfection, the transgene

is not integrated into the genome and its expression is not dependent on the site of integration or influenced by the surrounding chromosomal elements. We show here, proof of concept that PRL-3 transcripts can be successfully overexpressed in transiently transfected H1299 cells compared to cells transfected only with pcDNA3 vector and that no apparent down-regulation of global transcription occurs in these transient lines. In future studies, biological replicates of the H1299 transient transfectants should be generated, which could then be used to assess alterations in gene expression that occur more directly as a result of PRL-3 overexpression.

CHAPTER 11. MICRORNA EXPRESSION IS NOT THE PRIMARY CAUSE OF DECREASED GLOBAL TRANSCRIPTION IN HEK293 CELLS STABLY TRANSFECTED WITH PRL-3

11.1 Introduction

MicroRNAs are now known to play key roles in the post-transcriptional regulation of gene expression through the destabilization of their mRNA targets or inhibition of protein translation (Eulalio et al., 2008). Given their ability to regulate the expression levels of target mRNAs, I theorized that alterations in microRNA abundance might partially explain the profound effect we observed of stable PRL-3 transfection on global mRNA levels in HEK293 cells. To begin to investigate this, TaqMan Low Density Human MicroRNA arrays were used to examine the differences in microRNA expression profiles between HEK293 cells stably transfected with PRL-3 and those transfected with empty vector.

11.2 Results

Triplicate biological replicates of HEK293 cells stably transfected with PRL-3 or with empty vector were assayed using TaqMan Human MicroRNA arrays and Partek Genomics Suite was used to compare the resulting miRNA expression profiles. This analysis revealed that approximately 222 (33%) of the 664 miRNAs on the TaqMan array were altered by more than 2-fold in the PRL-3

transfectants compared to the empty vector controls. 162 (73%) of these were down-regulated and only 60 were up-regulated. Despite the large number of changes that were observed, no miRs met an initial significance threshold set at a fold change (FC) >2 with FDR < 5% and only two miRs (miR-509-5p and miR-624*) met a cutoff of FC > 2 and FDR <10%. Increasing the FDR cutoff to 30% generated a list of 35 significantly changing miRs, which are displayed in Table 11.1. Twenty-eight of these were increasing and 7 of these were decreasing in the PRL-3 transfectants.

Ingenuity Pathway Analysis was next used to perform a direct comparison of the lists of miRNAs and mRNAs that were significantly changing in the PRL-3 transfectants. Of the greater than 2,000 mRNA transcripts most significantly (FC > 100; FDR < 10%) differentially expressed between the stable HEK293 PRL-3 transfectants and empty vector controls, 54 were predicted, based on either experimental evidence or moderate to high confidence predictions, to be targets of at least one of 26 out of the 35 miRs that were also significantly (FC > 2; FDR < 30%) changing. Due to its size, the table listing these predicted miR-mRNA interactions has been placed in the appendix as Table B.

Although microRNAs can positively regulate their mRNA targets (Vasudevan, 2012), they are best known for their ability to function as negative regulators of gene expression; therefore the generated list of 26 miRs and 54 mRNAs was scrutinized to look for negative correlations in miRNA and mRNA target expression. We found that all of the 54 mRNAs were significantly down-regulated in the PRL-3 transfectants compared to the empty vector samples,

therefore miRs that were significantly down-regulated tended to be moving in the same direction as their targets, while miRs that were significantly up-regulated were all inversely correlated to the expression of their targets.

Table 11.1 MicroRNAs displaying differential expression between HEK293 cells stably transfected with PRL-3 or empty vector
A total of 664 microRNAs were examined for differential expression, using TaqMan Array Human microRNA cards. Significance was determined based on a threshold of Fold Change > 2 and FDR < 30%. Data is sorted from lowest (best) to highest FDR.

miR	FDR	Fold Change
hsa-miR-509-5p	0.054	20.48
hsa-miR-624*	0.091	4.91
hsa-miR-98	0.103	-14.02
hsa-miR-519a	0.118	15.14
hsa-miR-375	0.120	25.84
hsa-miR-346	0.121	10.80
hsa-miR-190b	0.126	-4.25
hsa-miR-642	0.129	24.04
hsa-miR-129-3p	0.131	9.01
hsa-miR-576-3p	0.132	21.15
hsa-miR-671-3p	0.145	21.63
hsa-miR-372	0.151	9.00
hsa-miR-519e	0.166	4.19
hsa-miR-19a*	0.172	-13.38
hsa-miR-423-5p	0.176	10.95
hsa-miR-33a*	0.180	12.96
hsa-miR-526b*	0.192	-4.86
hsa-miR-128	0.197	16.52
hsa-miR-133a	0.211	6.17
hsa-miR-210	0.214	-2.59
hsa-miR-605	0.215	24.04
hsa-miR-34b*	0.231	9.81
hsa-miR-570	0.232	3.01
hsa-miR-512-3p	0.232	3.03
hsa-miR-219-1-3p	0.234	5.20
hsa-miR-622	0.241	29.65
hsa-miR-518d-3p	0.251	4.37
hsa-miR-614	0.262	-6.31
hsa-miR-672	0.265	5.63
hsa-miR-517c	0.267	4.25
hsa-miR-150	0.276	2.94
hsa-miR-141	0.278	-4.22
hsa-miR-487a	0.285	5.31
hsa-miR-215	0.295	3.83
hsa-miR-515-3p	0.296	5.12

11.3 Discussion

Blocking translation was initially thought to be the predominant means by which miRNAs inhibit protein synthesis, however there is now much evidence supporting the idea that microRNAs can inhibit protein production by lowering mRNA levels (Bagga et al., 2005; Lim et al., 2005). Although a topic of much debate, some researchers have recently provided evidence that down-regulation of mRNA expression may even be the primary mechanism by which miRNAs exert their effects (Baek et al., 2008; H. Guo, Ingolia, Weissman, & Bartel, 2010). HEK293 cells stably transfected with PRL-3 appear to have undergone silencing of the PRL-3 transgene over time. However, not only is PRL-3 expression down-regulated, but global mRNA levels in these cells are much lower than those in HEK293 cells transfected with empty vector. To examine any changes in miRNA expression levels that might help to explain the large scale decreases in mRNA expression observed in the PRL-3 transfectants, I used TaqMan microRNA arrays to evaluate and compare the miRNA expression profiles of the PRL-3 and empty vector transfected HEK293 cell lines.

Approximately 33% of the 664 microRNAs on the TaqMan arrays exhibited at least a 2-fold change in expression between the PRL-3 transfectants and the empty vector controls, however most (73%) of these had lower expression levels in the PRL-3 transfected lines than in the controls. These results are not, therefore, consistent with the hypothesis that increased expression of miRNAs is causing a global down-regulation of mRNA expression levels.

Although miRNA up-regulation does not appear to be the major mechanism by which mRNA transcript levels are decreased in the PRL-3 transfectants, some significant alterations in miRNA abundance in these lines do exist and all of the significantly up-regulated miRNAs show an inverse correlation of expression to their predicted and/or known targets. It is important to note that the changes in miRNA expression are relatively small (< 30-fold increases) compared to the changes in expression of their target genes (100-300-fold decreases); however 34 (63%) of the 54 significantly altered mRNAs are targeted by multiple significantly up-regulated miRNAs, indicating the possibility that the degree of the change at the mRNA level could be due to the combined effects of multiple miRNAs acting in unison. Nevertheless, the possibility of additional mechanisms contributing to decreased mRNA expression, even when the expression of miRs targeting those transcripts is increasing, cannot be ruled out.

Other possible explanations for the widespread and high magnitude changes of mRNA expression, that could be examined in future studies, include increases in global DNA methylation, decreases in global histone acetylation, up-regulation of siRNA expression, or altered phosphorylation of the C-terminal domain (CTD) of RNA polymerase II, leading to inhibition of its activity.

CHAPTER 12. CONCLUSIONS AND FUTURE DIRECTIONS

Elucidation of the mechanisms governing tumor formation and metastasis is crucial to enhancing our understanding of the oncogenic process and to providing effective tools for cancer diagnosis, prognosis, and optimal patient therapy. The results presented in this dissertation helped to define the basal gene expression of the PRL-1 and PRL-2 phosphatases in adult human tissues and provided a foundation for the recognition and interpretation of the changes in these expression patterns that are associated with cancer and/or other disease states. We found that PRL-1 and PRL-2 are nearly ubiquitously expressed in normal human tissues and thus are likely to play an important role in maintaining normal tissue homeostasis. This role may be tissue and/or cell-type specific, because each molecule is widely expressed in cell types from a variety of different molecular backgrounds and functions, including cells with different proliferation and differentiation potentials. In human cancers, we showed that alterations of PRL-1 and PRL-2 expression are a common event, but that the nature of these alterations are also highly tissue-type specific. In some tissues, such as the stomach and liver, PRL-1 and PRL-2 expression appear to have a tumor promoting effect, while in other tissue types, like the ovary and lung, expression of these molecules may normally serve a protective function. The

frequent deregulation of these molecules in human neoplasms suggests that they may be useful markers for cancer diagnosis. They may also serve as indicators of disease severity and/or as valuable therapeutic targets for disease treatment in some tumor types.

To fully realize the potential of the PRL phosphatases as molecular targets for cancer therapy, researchers must first understand the mechanisms that govern their function, the signaling pathways and substrates on which they act, their normal biological roles, and the basis of their transforming activity. In order to enhance our understanding of PRL-1-mediated signaling events, I performed a global, unbiased analysis of the changes in mRNA and miRNA expression that occur in response to stable PRL-1 overexpression in HEK293 cells and correlated these results to changes occurring at the protein level. This analysis significantly expanded on the current knowledge surrounding PRL-1 signaling and allowed identification of several novel candidates for mediators of PRL-1 function. Future studies should focus on further validation and functional characterization of the identified targets (e.g. by perturbation of the potential targets to determine the effect on PRL-1-mediated cellular response). In particular, the relationship between PRL-1 and SPARC, RhoGDIα, and Filamin A should be further examined. Moreover, the role of PRL-1 in regulating the Rho GTPase signaling pathways should be explored in greater depth.

Analysis of the PRL-2 and PRL-3 signaling pathways might also benefit from a broad, integrated, systems-level approach such as that taken here. This would allow a direct comparison of the gene expression profiles of each of the

three PRL family members. Although HEK293 cells stably transfected with PRL-3, under the control of a CMV promoter, appear to undergo transgene silencing over time, we have shown that PRL-3 can be successfully overexpressed in a transiently transfected H1299 lung carcinoma cell line. Using a transient transfection approach for all three PRL genes could provide a quick and straightforward method by which the effects of exogenous PRL expression could be examined over a time course, allowing separation of early events from those occurring further downstream. Since PRL-mediated signaling events, particularly those for PRL-1, may be profoundly dependent on cellular context, a variety of cell types should ultimately be examined.

Although additional studies will be required to clarify the biological function of the PRL phosphatases and the exact mechanisms by which they mediate their effects, as well as to establish their utility as targets for anti-cancer therapy, the results presented here provide novel insights into the biology of these enzymes that should open up new lines of investigation for future study.

REFERENCES

REFERENCES

Achiwa, H., & Lazo, J. S. (2007). PRL-1 Tyrosine Phosphatase Regulates c-Src Levels, Adherence, and Invasion in Human Lung Cancer Cells. *Cancer Research, 67*(2), 643-650.

Agola, J., Jim, P., Ward, H., Basuray, S., & Wandinger-Ness, A. (2011). Rab GTPases as regulators of endocytosis, targets of disease and therapeutic opportunities. *Clinical Genetics*.

Ahn, J. H., Kim, S. J., Park, W. S., Cho, S. Y., Ha, J. D., Kim, S. S., . . . Choi, J. K. (2006). Synthesis and biological evaluation of rhodanine derivatives as PRL-3 inhibitors. *Bioorganic & Medicinal Chemistry Letters, 16*(11), 2996-2999.

Akiyama, S., Dhavan, D., & Yi, T. (2010). PRL-2 increases Epo and IL-3 responses in hematopoietic cells. *Blood Cells Molecules and Diseases, 44*(4), 209-214.

Alioto, T. (January 24, 2007). U12-type Intron Database. Retrieved July, 2012 from genome.crg.es/cgi-bin/u12db/u12db.cgi

Alonso, A., Sasin, J., Bottini, N., Friedberg, I., Osterman, A., Godzik, A., . . . Mustelin, T. (2004). Protein tyrosine phosphatases in the human genome. *Cell, 117*(6), 699-711.

Aricescu, A. R., Hon, W. C., Siebold, C., Lu, W., van der Merwe, P. A., & Jones, E. Y. (2006). Molecular analysis of receptor protein tyrosine phosphatase mu-mediated cell adhesion. *The EMBO Journal, 25*(4), 701-712.

Arthur, W. T., & Burridge, K. (2001). RhoA inactivation by p190RhoGAP regulates cell spreading and migration by promoting membrane protrusion and polarity. *Molecular Biology of the Cell, 12*(9), 2711-2720.

Arthur, W. T., Petch, L. A., & Burridge, K. (2000). Integrin engagement suppresses RhoA activity via a c-Src-dependent mechanism. *Current Biology, 10*(12), 719-722.

Assoian, R. K. (1997). Anchorage-dependent cell cycle progression. *Journal of Cell Biology, 136*(1), 1-4.

Baek, D., Villen, J., Shin, C., Camargo, F. D., Gygi, S. P., & Bartel, D. P. (2008). The impact of microRNAs on protein output. *Nature, 455*(7209), 64-71.

Bagga, S., Bracht, J., Hunter, S., Massirer, K., Holtz, J., Eachus, R., & Pasquinelli, A. E. (2005). Regulation by let-7 and lin-4 miRNAs results in target mRNA degradation. *Cell, 122*(4), 553-563.

Bai, Y., Luo, Y., Liu, S., Zhang, L., Shen, K., Dong, Y., . . . Zhang, Z. Y. (2011). PRL-1 protein promotes ERK1/2 and RhoA protein activation through a non-canonical interaction with the Src homology 3 domain of p115 Rho GTPase-activating protein. *Journal of Biological Chemistry, 286*(49), 42316-42324.

Bardelli, A., Saha, S., Sager, J. A., Romans, K. E., Xin, B., Markowitz, S. D., . . . Vogelstein, B. (2003). PRL-3 expression in metastatic cancers. *Clinical Cancer Research, 9*(15), 5607-5615.

Barford, D. (1996). Molecular mechanisms of the protein serine/threonine phosphatases. *Trends in Biochemical Sciences, 21*(11), 407-412.

Bartel, D. P. (2004). MicroRNAs: genomics, biogenesis, mechanism, and function. *Cell, 116*(2), 281-297.

Basak, S., Jacobs, S. B., Krieg, A. J., Pathak, N., Zeng, Q., Kaldis, P., . . . Attardi, L. D. (2008). The metastasis-associated gene Prl-3 is a p53 target involved in cell-cycle regulation. *Molecular Cell, 30*(3), 303-314.

Bayon, Y., & Alonso, A. (2010). Atypical DUSPS: 19 Phosphatases in Search of a Role. In P. A. Lazo (Ed.), *Emerging Signaling Pathways in Tumor Biology* (pp. 185-208). Kerala, India: Transworld Research Network.

Bermudez, O., Pages, G., & Gimond, C. (2010). The dual-specificity MAP kinase phosphatases: critical roles in development and cancer. *American Journal of Physiology - Cell Physiology, 299*(2), C189-202.

Bessette, D. C., Qiu, D., & Pallen, C. J. (2008). PRL PTPs: mediators and markers of cancer progression. *Cancer and Metastasis Reviews, 27*(2), 231-252.

Bhoopathi, P., Gondi, C. S., Gujrati, M., Dinh, D. H., & Lakka, S. S. (2011). SPARC mediates Src-induced disruption of actin cytoskeleton via inactivation of small GTPases Rho-Rac-Cdc42. *Cellular Signalling, 23*(12), 1978-1987.

Blanchetot, C., Tertoolen, L. G., Overvoorde, J., & den Hertog, J. (2002). Intra- and intermolecular interactions between intracellular domains of receptor protein-tyrosine phosphatases. *Journal of Biological Chemistry, 277*(49), 47263-47269.

Boulter, E., Garcia-Mata, R., Guilluy, C., Dubash, A., Rossi, G., Brennwald, P. J., & Burridge, K. (2010). Regulation of Rho GTPase crosstalk, degradation and activity by RhoGDI1. *Nature Cell Biology, 12*(5), 477-483.

Bourdeau, A., Dube, N., & Tremblay, M. L. (2005). Cytoplasmic protein tyrosine phosphatases, regulation and function: the roles of PTP1B and TC-PTP. *Current Opinion in Cell Biology, 17*(2), 203-209.

Braithwaite, S. P., Voronkov, M., Stock, J. B., & Mouradian, M. M. (2012). Targeting phosphatases as the next generation of disease modifying therapeutics for Parkinson's disease. *Neurochemistry International*, In press. Epub ahead of print. Retrieved April 27, 2012 doi:10.1016/j.neuint.2012.01.031

Brooks, A. R., Harkins, R. N., Wang, P., Qian, H. S., Liu, P., & Rubanyi, G. M. (2004). Transcriptional silencing is associated with extensive methylation of the CMV promoter following adenoviral gene delivery to muscle. *Journal of Gene Medicine, 6*(4), 395-404.

Burroughs, A. M., Allen, K. N., Dunaway-Mariano, D., & Aravind, L. (2006). Evolutionary genomics of the HAD superfamily: understanding the structural adaptations and catalytic diversity in a superfamily of phosphoesterases and allied enzymes. *Journal of Molecular Biology, 361*(5), 1003-1034.

Cans, C., Mangano, R., Barila, D., Neubauer, G., & Superti-Furga, G. (2000). Nuclear tyrosine phosphorylation: the beginning of a map. *Biochemical Pharmacology, 60*(8), 1203-1215.

Carter, D. A. (1998). Expression of a novel rat protein tyrosine phosphatase gene. *Biochimica et Biophysica Acta, 1442*(2-3), 405-408.

Carthew, R. W. (2006). Gene regulation by microRNAs. *Current Opinion in Genetics & Development, 16*(2), 203-208.

Cates, C. A., Michael, R. L., Stayrook, K. R., Harvey, K. A., Burke, Y. D., Randall, S. K., . . . Crowell, D. N. (1996). Prenylation of oncogenic human PTP(CAAX) protein tyrosine phosphatases. *Cancer Letters, 110*(1-2), 49-55.

Cheng, A., Uetani, N., Lampron, C., & Tremblay, M. L. (2005) Protein Tyrosine Phosphatases as Therapeutic Targets. L. A. Pinna & P. T. W. Cohen (Vol. Ed.), *Handbook of Experimental Pharmacology: Vol. 167. Inhibitors of Protein Kinases and Protein Phosphatases* (pp. 191-214). Berlin Heidelberg: Springer.

Chiarugi, P., Taddei, M. L., Cirri, P., Talini, D., Buricchi, F., Camici, G., . . . Ramponi, G. (2000). Low molecular weight protein-tyrosine phosphatase controls the rate and the strength of NIH-3T3 cells adhesion through its phosphorylation on tyrosine 131 or 132. *Journal of Biological Chemistry, 275*(48), 37619-37627.

Cho, H., Mukherjee, S., Palasuberniam, P., Pillow, L., Bilgin, B., Nezich, C., . . . Chan, C. (2011). Molecular mechanism by which palmitate inhibits PKR autophosphorylation. *Biochemistry, 50*(6), 1110-1119.

Choi, K. H., Basma, H., Singh, J., & Cheng, P. W. (2005). Activation of CMV promoter-controlled glycosyltransferase and beta -galactosidase glycogenes by butyrate, tricostatin A, and 5-aza-2'-deoxycytidine. *Glycoconjugate Journal, 22*(1-2), 63-69.

Choi, M. S., Min, S. H., Jung, H., Lee, J. D., Lee, T. H., Lee, H. K., & Yoo, O. J. (2011). The essential role of FKBP38 in regulating phosphatase of regenerating liver 3 (PRL-3) protein stability. *Biochemical and Biophysical Research Communications, 406*(2), 305-309.

Cismasiu, V. B., Denes, S. A., Reilander, H., Michel, H., & Szedlacsek, S. E. (2004). The MAM (meprin/A5-protein/PTPmu) domain is a homophilic binding site promoting the lateral dimerization of receptor-like protein-tyrosine phosphatase mu. *Journal of Biological Chemistry, 279*(26), 26922-26931.

Cohen, P. (2004) Overview of protein serine/threonine phosphatases. J. Ariño & D. Alexander (Vol. Ed.), *Topics in Current Genetics: Vol. 5. Protein Phosphatases* (pp. 1-20). Berlin Heidelberg: Springer.

Columbano, A., Ledda-Columbano, G. M., Pibiri, M., Piga, R., Shinozuka, H., De Luca, V., . . . Tripodi, M. (1997). Increased expression of c-fos, c-jun and LRF-1 is not required for in vivo priming of hepatocytes by the mitogen TCPOBOP. *Oncogene, 14*(7), 857-863.

Cuevas, I. C., Rohloff, P., Sanchez, D. O., & Docampo, R. (2005). Characterization of farnesylated protein tyrosine phosphatase TcPRL-1 from Trypanosoma cruzi. *Eukaryotic Cell, 4*(9), 1550-1561.

Dai, N., Lu, A. P., Shou, C. C., & Li, J. Y. (2009). Expression of phosphatase regenerating liver 3 is an independent prognostic indicator for gastric cancer. *World Journal of Gastroenterology, 15*(12), 1499-1505.

Daouti, S., Li, W. H., Qian, H., Huang, K. S., Holmgren, J., Levin, W., . . . Niu, H. (2008). A selective phosphatase of regenerating liver phosphatase inhibitor suppresses tumor cell anchorage-independent growth by a novel mechanism involving p130Cas cleavage. *Cancer Research, 68*(4), 1162-1169.

den Hertog, J. (2003). Regulation of protein phosphatases in disease and behaviour. *EMBO Reports, 4*(11), 1027-1032.

den Hertog, J., Ostman, A., & Bohmer, F. D. (2008). Protein tyrosine phosphatases: regulatory mechanisms. *FEBS Journal, 275*(5), 831-847.

Dennis, G., Jr., Sherman, B. T., Hosack, D. A., Yang, J., Gao, W., Lane, H. C., & Lempicki, R. A. (2003). DAVID: Database for Annotation, Visualization, and Integrated Discovery. *Genome Biology, 4*(5), P3.

Denu, J. M., & Dixon, J. E. (1998). Protein tyrosine phosphatases: mechanisms of catalysis and regulation. *Current Opinion in Chemical Biology, 2*(5), 633-641.

Deshpande, T., Takagi, T., Hao, L., Buratowski, S., & Charbonneau, H. (1999). Human PIR1 of the protein-tyrosine phosphatase superfamily has RNA 5'-triphosphatase and diphosphatase activities. *Journal of Biological Chemistry, 274*(23), 16590-16594.

Diamond, R. H., Cressman, D. E., Laz, T. M., Abrams, C. S., & Taub, R. (1994). PRL-1, a unique nuclear protein tyrosine phosphatase, affects cell growth. *Molecular and Cellular Biology, 14*(6), 3752-3762.

Diamond, R. H., Peters, C., Jung, S. P., Greenbaum, L. E., Haber, B. A., Silberg, D. G., . . . Taub, R. (1996). Expression of PRL-1 nuclear PTPase is associated with proliferation in liver but with differentiation in intestine. *American Journal of Physiology, 271*(1 Pt 1), G121-129.

Dixon-McIver, A., East, P., Mein, C. A., Cazier, J. B., Molloy, G., Chaplin, T., . . . Debernardi, S. (2008). Distinctive patterns of microRNA expression associated with karyotype in acute myeloid leukaemia. *PLoS ONE, 3*(5), e2141.

Dovas, A., & Couchman, J. R. (2005). RhoGDI: multiple functions in the regulation of Rho family GTPase activities. *Biochemical Journal, 390*(Pt 1), 1-9.

Ducruet, A. P., Vogt, A., Wipf, P., & Lazo, J. S. (2005). Dual specificity protein phosphatases: therapeutic targets for cancer and Alzheimer's disease. *Annual Review of Pharmacology and Toxicology, 45*, 725-750.

Dumaual, C. M., Sandusky, G. E., Crowell, P. L., & Randall, S. K. (2006). Cellular localization of PRL-1 and PRL-2 gene expression in normal adult human tissues. *Journal of Histochemistry and Cytochemistry, 54*(12), 1401-1412.

Dumaual, C. M., Sandusky, G. E., Soo, H. W., Werner, S. R., Crowell, P. L., & Randall, S. K. (2011). Tissue-specific alterations of PRL-1 and PRL-2 expression in cancer. *American Journal of Translational Research, 4*(1), 83-101.

Eulalio, A., Huntzinger, E., & Izaurralde, E. (2008). Getting to the root of miRNA-mediated gene silencing. *Cell, 132*(1), 9-14.

Ewing, R. M., Chu, P., Elisma, F., Li, H., Taylor, P., Climie, S., . . . Figeys, D. (2007). Large-scale mapping of human protein-protein interactions by mass spectrometry. *Molecular Systems Biology, 3*, 89.

Fagerli, U. M., Holt, R. U., Holien, T., Vaatsveen, T. K., Zhan, F., Egeberg, K. W., . . . Borset, M. (2008). Overexpression and involvement in migration by the metastasis-associated phosphatase PRL-3 in human myeloma cells. *Blood, 111*(2), 806-815.

Fiordalisi, J. J., Keller, P. J., & Cox, A. D. (2006). PRL tyrosine phosphatases regulate rho family GTPases to promote invasion and motility. *Cancer Research, 66*(6), 3153-3161.

Fontemaggi, G., Kela, I., Amariglio, N., Rechavi, G., Krishnamurthy, J., Strano, S., . . . Blandino, G. (2002). Identification of direct p73 target genes combining DNA microarray and chromatin immunoprecipitation analyses. *Journal of Biological Chemistry, 277*(45), 43359-43368.

Forte, E., Orsatti, L., Talamo, F., Barbato, G., De Francesco, R., & Tomei, L. (2008). Ezrin is a specific and direct target of protein tyrosine phosphatase PRL-3. *Biochimica et Biophysica Acta, 1783*(2), 334-344.

Friedman, Y., Naamati, G., & Linial, M. (2010). MiRror: a combinatorial analysis web tool for ensembles of microRNAs and their targets. *Bioinformatics, 26*(15), 1920-1921.

Fu, H. W., & Casey, P. J. (1999). Enzymology and biology of CaaX protein prenylation. *Recent Progress in Hormone Research, 54*, 315-342; discussion 342-313.

Ganem, C., Devaux, F., Torchet, C., Jacq, C., Quevillon-Cheruel, S., Labesse, G., . . . Faye, G. (2003). Ssu72 is a phosphatase essential for transcription termination of snoRNAs and specific mRNAs in yeast. *EMBO Journal, 22*(7), 1588-1598.

Gao, W., Shen, H., Liu, L., Xu, J., & Shu, Y. (2011). MiR-21 overexpression in human primary squamous cell lung carcinoma is associated with poor patient prognosis. *Journal of Cancer Research and Clinical Oncology, 137*(4), 557-566.

Garcia, M. A., Gil, J., Ventoso, I., Guerra, S., Domingo, E., Rivas, C., & Esteban, M. (2006). Impact of protein kinase PKR in cell biology: from antiviral to antiproliferative action. *Microbiology and Molecular Biology Reviews, 70*(4), 1032-1060.

Gentleman, R. C., Carey, V. J., Bates, D. M., Bolstad, B., Dettling, M., Dudoit, S., . . . Zhang, J. (2004). Bioconductor: open software development for computational biology and bioinformatics. *Genome Biology, 5*(10), R80.

Giang Ho, T. T., Stultiens, A., Dubail, J., Lapiere, C. M., Nusgens, B. V., Colige, A. C., & Deroanne, C. F. (2011). RhoGDIalpha-dependent balance between RhoA and RhoC is a key regulator of cancer cell tumorigenesis. *Molecular Biology of the Cell, 22*(17), 3263-3275.

Gilbert, M. T., Haselkorn, T., Bunce, M., Sanchez, J. J., Lucas, S. B., Jewell, L. D., . . . Worobey, M. (2007). The isolation of nucleic acids from fixed, paraffin-embedded tissues-which methods are useful when? *PLoS ONE, 2*(6), e537.

Gjorloff-Wingren, A., Saxena, M., Han, S., Wang, X., Alonso, A., Renedo, M., . . . Mustelin, T. (2000). Subcellular localization of intracellular protein tyrosine phosphatases in T cells. *European Journal of Immunology, 30*(8), 2412-2421.

Gohla, A., Birkenfeld, J., & Bokoch, G. M. (2005). Chronophin, a novel HAD-type serine protein phosphatase, regulates cofilin-dependent actin dynamics. *Nature Cell Biology, 7*(1), 21-29.

Goldstein, B. J. (2002). Protein-tyrosine phosphatases: emerging targets for therapeutic intervention in type 2 diabetes and related states of insulin resistance. *Journal of Clinical Endocrinology & Metabolism, 87*(6), 2474-2480.

Guerra, S., Lopez-Fernandez, L. A., Garcia, M. A., Zaballos, A., & Esteban, M. (2006). Human gene profiling in response to the active protein kinase, interferon-induced serine/threonine protein kinase (PKR), in infected cells. Involvement of the transcription factor ATF-3 IN PKR-induced apoptosis. *Journal of Biological Chemistry, 281*(27), 18734-18745.

Guo, H., Ingolia, N. T., Weissman, J. S., & Bartel, D. P. (2010). Mammalian microRNAs predominantly act to decrease target mRNA levels. *Nature, 466*(7308), 835-840.

Guo, K., Li, J., Tang, J. P., Koh, V., Gan, B. Q., & Zeng, Q. (2004). Catalytic domain of PRL-3 plays an essential role in tumor metastasis: formation of PRL-3 tumors inside the blood vessels. *Cancer Biology and Therapy, 3*(10), 945-951.

Guo, K., Li, J., Wang, H., Osato, M., Tang, J. P., Quah, S. Y., . . . Zeng, Q. (2006). PRL-3 Initiates Tumor Angiogenesis by Recruiting Endothelial Cells In vitro and In vivo. *Cancer Research, 66*(19), 9625-9635.

Guo, K., Tang, J. P., Tan, C. P., Wang, H., & Zeng, Q. (2008). Monoclonal antibodies target intracellular PRL phosphatases to inhibit cancer metastases in mice. *Cancer Biology and Therapy, 7*(5), 750-757.

Guo, S., Russo, I. H., & Russo, J. (2003). Difference in gene expression profile in breast epithelial cells from women with different reproductive history. *International Journal of Oncology, 23*(4), 933-941.

Guzinska-Ustymowicz, K., Pryczynicz, A., & Kemona, A. (2009). PTP4A3 expression increases strongly in lymph node metastases from colorectal carcinoma. *Anticancer Research, 29*(10), 3913-3916.

Haber, B., Naji, L., Cressman, D., & Taub, R. (1995). Coexpression of liver-specific and growth-induced genes in perinatal and regenerating liver: attainment and maintenance of the differentiated state during rapid proliferation. *Hepatology, 22*(3), 906-914.

Han, Z. B., Zhong, L., Teng, M. J., Fan, J. W., Tang, H. M., Wu, J. Y., . . . Peng, Z. H. (2012). Identification of recurrence-related microRNAs in hepatocellular carcinoma following liver transplantation. *Molecular Oncology, 6*(4), 445-457.

Hao, R. T., Zhang, X. H., Pan, Y. F., Liu, H. G., Xiang, Y. Q., Wan, L., & Wu, X. L. (2010). Prognostic and metastatic value of phosphatase of regenerating liver-3 in invasive breast cancer. *Journal of Cancer Research and Clinical Oncology, 136*(9), 1349-1357.

Hardy, S., Wong, N. N., Muller, W. J., Park, M., & Tremblay, M. L. (2010). Overexpression of the protein tyrosine phosphatase PRL-2 correlates with breast tumor formation and progression. *Cancer Research, 70*(21), 8959-8967.

Hatate, K., Yamashita, K., Hirai, K., Kumamoto, H., Sato, T., Ozawa, H., . . . Watanabe, M. (2008). Liver metastasis of colorectal cancer by protein-tyrosine phosphatase type 4A, 3 (PRL-3) is mediated through lymph node metastasis and elevated serum tumor markers such as CEA and CA19-9. *Oncology Reports, 20*(4), 737-743.

Hernandez-Verdun, D., Roussel, P., & Gebrane-Younes, J. (2002). Emerging concepts of nucleolar assembly. *Journal of Cell Science, 115*(Pt 11), 2265-2270.

Hofmann, K., Bucher, P., & Kajava, A. V. (1998). A model of Cdc25 phosphatase catalytic domain and Cdk-interaction surface based on the presence of a rhodanese homology domain. *Journal of Molecular Biology, 282*(1), 195-208.

Hubbard, M. J., & Cohen, P. (1993). On target with a new mechanism for the regulation of protein phosphorylation. *Trends in Biochemical Sciences, 18*(5), 172-177.

Hunter, T. (1987). A tail of two src's: mutatis mutandis. *Cell, 49*(1), 1-4.

Hunter, T. (1998). The Croonian Lecture 1997. The phosphorylation of proteins on tyrosine: its role in cell growth and disease. *Philosophical Transactions of the Royal Society of London. Series B, Biological Sciences, 353*(1368), 583-605.

Hunter, T. (2004). Protein Phosphorylation: What does the future hold? In E. Keinan, I. Schechter & M. Sela (Eds.), *Life Sciences for the 21st Century* (pp. 191-223). Hoboken, NJ: Wiley.

Huveneers, S., & Danen, E. H. (2009). Adhesion signaling - crosstalk between integrins, Src and Rho. *Journal of Cell Science, 122*(Pt 8), 1059-1069.

Hwang, J. J., Min, S. H., Sin, K. H., Heo, Y. S., Kim, K. D., Yoo, O. J., & Lee, S. H. (2012). Altered expression of phosphatase of regenerating liver gene family in non-small cell lung cancer. *Oncology Reports, 27*(2), 535-540.

Ingenuity Pathway Analysis (Version 162820). Available from www.ingenuity.com

Ishizuka, A., Siomi, M. C., & Siomi, H. (2002). A Drosophila fragile X protein interacts with components of RNAi and ribosomal proteins. *Genes & Development, 16*(19), 2497-2508.

Jackel, M. C., Mitteldorf, C., Schweyer, S., & Fuzesi, L. (2001). Clinical relevance of Fas (APO-1/CD95) expression in laryngeal squamous cell carcinoma. *Head & Neck, 23*(8), 646-652.

Jeong, D. G., Kim, S. J., Kim, J. H., Son, J. H., Park, M. R., Lim, S. M., . . . Ryu, S. E. (2005). Trimeric structure of PRL-1 phosphatase reveals an active enzyme conformation and regulation mechanisms. *Journal of Molecular Biology, 345*(2), 401-413.

Jiang, Y., Liu, X. Q., Rajput, A., Geng, L., Ongchin, M., Zeng, Q., . . . Wang, J. (2011). Phosphatase PRL-3 is a direct regulatory target of TGFbeta in colon cancer metastasis. *Cancer Research, 71*(1), 234-244.

Johnson, L. N. (2009). The regulation of protein phosphorylation. *Biochemical Society Transactions, 37*(Pt 4), 627-641.

Julien, S. G., Dube, N., Hardy, S., & Tremblay, M. L. (2011). Inside the human cancer tyrosine phosphatome. *Nature Reviews Cancer, 11*(1), 35-49.

Kato, H., Semba, S., Miskad, U. A., Seo, Y., Kasuga, M., & Yokozaki, H. (2004). High expression of PRL-3 promotes cancer cell motility and liver metastasis in human colorectal cancer: a predictive molecular marker of metachronous liver and lung metastases. *Clinical Cancer Research, 10*(21), 7318-7328.

Kazemi, S., Mounir, Z., Baltzis, D., Raven, J. F., Wang, S., Krishnamoorthy, J. L., . . . Koromilas, A. E. (2007). A novel function of eIF2alpha kinases as inducers of the phosphoinositide-3 kinase signaling pathway. *Molecular Biology of the Cell, 18*(9), 3635-3644.

Kerk, D., & Moorhead, G. B. (2010). A phylogenetic survey of myotubularin genes of eukaryotes: distribution, protein structure, evolution, and gene expression. *BMC Evolutionary Biology, 10*, 196.

Ketting, R. F., & Plasterk, R. H. (2000). A genetic link between co-suppression and RNA interference in C. elegans. *Nature, 404*(6775), 296-298.

Khatri, P., Draghici, S., Ostermeier, G. C., & Krawetz, S. A. (2002). Profiling gene expression using onto-express. *Genomics, 79*(2), 266-270.

Khoury, G. A., Baliban, R. C., & Floudas, C. A. (2011). Proteome-wide post-translational modification statistics: frequency analysis and curation of the swiss-prot database. *Sci Rep, 1*.

Kim, K. A., Song, J. S., Jee, J., Sheen, M. R., Lee, C., Lee, T. G., . . . Cheong, C. (2004). Structure of human PRL-3, the phosphatase associated with cancer metastasis. *FEBS Letters, 565*(1-3), 181-187.

Kong, L., Li, Q., Wang, L., Liu, Z., & Sun, T. (2007). The value and correlation between PRL-3 expression and matrix metalloproteinase activity and expression in human gliomas. *Neuropathology, 27*(6), 516-521.

Kong, W., Swain, G. P., Li, S., & Diamond, R. H. (2000). PRL-1 PTPase expression is developmentally regulated with tissue-specific patterns in epithelial tissues. *American Journal of Physiology - Gastrointestinal and Liver Physiology, 279*(3), G613-621.

Kozlov, G., Cheng, J., Ziomek, E., Banville, D., Gehring, K., & Ekiel, I. (2004). Structural insights into molecular function of the metastasis-associated phosphatase PRL-3. *Journal of Biological Chemistry, 279*(12), 11882-11889.

Krueger, N. X., Reddy, R. S., Johnson, K., Bateman, J., Kaufmann, N., Scalice, D., . . . Saito, H. (2003). Functions of the ectodomain and cytoplasmic tyrosine phosphatase domains of receptor protein tyrosine phosphatase Dlar in vivo. *Molecular and Cellular Biology, 23*(19), 6909-6921.

Lai, W., Chen, S., Wu, H., Guan, Y., Liu, L., Zeng, Y., . . . Chu, Z. (2011). PRL-3 promotes the proliferation of LoVo cells via the upregulation of KCNN4 channels. *Oncology Reports, 26*(4), 909-917.

Lee, J. O., Yang, H., Georgescu, M. M., Di Cristofano, A., Maehama, T., Shi, Y., . . . Pavletich, N. P. (1999). Crystal structure of the PTEN tumor suppressor: implications for its phosphoinositide phosphatase activity and membrane association. *Cell, 99*(3), 323-334.

Lee, K., Kunkeaw, N., Jeon, S. H., Lee, I., Johnson, B. H., Kang, G. Y., . . . Lee, Y. S. (2011). Precursor miR-886, a novel noncoding RNA repressed in cancer, associates with PKR and modulates its activity. *RNA, 17*(6), 1076-1089.

Leslie, N. R., & Downes, C. P. (2004). PTEN function: how normal cells control it and tumour cells lose it. *Biochemical Journal, 382*(Pt 1), 1-11.

Li, J., Guo, K., Koh, V. W., Tang, J. P., Gan, B. Q., Shi, H., . . . Zeng, Q. (2005). Generation of PRL-3- and PRL-1-specific monoclonal antibodies as potential diagnostic markers for cancer metastases. *Clinical Cancer Research, 11*(6), 2195-2204.

Li, J. H., Xiao, X., Zhang, Y. N., Wang, Y. M., Feng, L. M., Wu, Y. M., & Zhang, Y. X. (2011). MicroRNA miR-886-5p inhibits apoptosis by down-regulating Bax expression in human cervical carcinoma cells. *Gynecologic Oncology, 120*(1), 145-151.

Li, Z., Zhan, W., Wang, Z., Zhu, B., He, Y., Peng, J., . . . Ma, J. (2006). Inhibition of PRL-3 gene expression in gastric cancer cell line SGC7901 via microRNA suppressed reduces peritoneal metastasis. *Biochemical and Biophysical Research Communications, 348*(1), 229-237.

Li, Z. R., Wang, Z., Zhu, B. H., He, Y. L., Peng, J. S., Cai, S. R., . . . Zhan, W. H. (2007). Association of tyrosine PRL-3 phosphatase protein expression with peritoneal metastasis of gastric carcinoma and prognosis. *Surgery Today, 37*(8), 646-651.

Liang, F., Liang, J., Wang, W. Q., Sun, J. P., Udho, E., & Zhang, Z. Y. (2007). PRL3 promotes cell invasion and proliferation by down-regulation of Csk leading to Src activation. *Journal of Biological Chemistry, 282*(8), 5413-5419.

Liang, F., Luo, Y., Dong, Y., Walls, C. D., Liang, J., Jiang, H. Y., . . . Zhang, Z. Y. (2008). Translational control of C-terminal Src kinase (Csk) expression by PRL3 phosphatase. *Journal of Biological Chemistry, 283*(16), 10339-10346.

Lim, L. P., Lau, N. C., Garrett-Engele, P., Grimson, A., Schelter, J. M., Castle, J., . . . Johnson, J. M. (2005). Microarray analysis shows that some microRNAs downregulate large numbers of target mRNAs. *Nature, 433*(7027), 769-773.

Liu, Y., Zhou, J., Chen, J., Gao, W., Le, Y., Ding, Y., & Li, J. (2009). PRL-3 promotes epithelial mesenchymal transition by regulating cadherin directly. *Cancer Biology and Therapy, 8*(14), 1352-1359.

Liu, Y. Q., Li, H. X., Lou, X., & Lei, J. Y. (2008). Expression of phosphatase of regenerating liver 1 and 3 mRNA in esophageal squamous cell carcinoma. *Archives of Pathology & Laboratory Medicine, 132*(8), 1307-1312.

Lou, X., Liu, Y., Guo, K., Lei, J., & Li, H. (2012). Overexpression of phosphatase regenerating liver 3 in esophageal squamous cell carcinoma associated with metastasis and its comparison with phosphatase regenerating liver 1. *Cell Biology International*.

Luo, Y., Liang, F., & Zhang, Z. Y. (2009). PRL1 promotes cell migration and invasion by increasing MMP2 and MMP9 expression through Src and ERK1/2 pathways. *Biochemistry, 48*(8), 1838-1846.

Ma, Y., & Li, B. (2011). Expression of phosphatase of regenerating liver-3 in squamous cell carcinoma of the cervix. *Medical Oncology, 28*(3), 775-780.

Maehama, T., & Dixon, J. E. (1998). The tumor suppressor, PTEN/MMAC1, dephosphorylates the lipid second messenger, phosphatidylinositol 3,4,5-trisphosphate. *Journal of Biological Chemistry, 273*(22), 13375-13378.

Mao, G., Marotta, F., Yu, J., Zhou, L., Yu, Y., Wang, L., & Chui, D. (2008). DNA context and promoter activity affect gene expression in lentiviral vectors. *Acta Biomed, 79*(3), 192-196.

Matsukawa, Y., Semba, S., Kato, H., Koma, Y., Yanagihara, K., & Yokozaki, H. (2010). Constitutive suppression of PRL-3 inhibits invasion and proliferation of gastric cancer cell in vitro and in vivo. *Pathobiology, 77*(3), 155-162.

Matter, W. F., Estridge, T., Zhang, C., Belagaje, R., Stancato, L., Dixon, J., . . . Vlahos, C. J. (2001). Role of PRL-3, a human muscle-specific tyrosine phosphatase, in angiotensin-II signaling. *Biochemical and Biophysical Research Communications, 283*(5), 1061-1068.

McLean, D. J., Friel, P. J., Pouchnik, D., & Griswold, M. D. (2002). Oligonucleotide microarray analysis of gene expression in follicle-stimulating hormone-treated rat Sertoli cells. *Molecular Endocrinology, 16*(12), 2780-2792.

McParland, V., Varsano, G., Li, X., Thornton, J., Baby, J., Aravind, A., . . . Kohn, M. (2011). The metastasis-promoting phosphatase PRL-3 shows activity toward phosphoinositides. *Biochemistry, 50*(35), 7579-7590.

Meisner, N. C., & Filipowicz, W. (2011). Properties of the Regulatory RNA-Binding Protein HuR and its Role in Controlling miRNA Repression. *Advances in Experimental Medicine and Biology, 700*, 106-123.

MetaCore (Version 6.8). Available from www.genego.com/metacore.php

Min, S. H., Kim, D. M., Heo, Y. S., Kim, H. M., Kim, I. C., & Yoo, O. J. (2010). Downregulation of p53 by phosphatase of regenerating liver 3 is mediated by MDM2 and PIRH2. *Life Sciences, 86*(1-2), 66-72.

Min, S. H., Kim, D. M., Heo, Y. S., Kim, Y. I., Kim, H. M., Kim, J., . . . Yoo, O. J. (2009). New p53 target, phosphatase of regenerating liver 1 (PRL-1) downregulates p53. *Oncogene, 28*(4), 545-554.

Ming, J., Liu, N., Gu, Y., Qiu, X., & Wang, E. H. (2009). PRL-3 facilitates angiogenesis and metastasis by increasing ERK phosphorylation and up-regulating the levels and activities of Rho-A/C in lung cancer. *Pathology, 41*(2), 118-126.

Miskad, U. A., Semba, S., Kato, H., Matsukawa, Y., Kodama, Y., Mizuuchi, E., . . . Yokozaki, H. (2007). High PRL-3 expression in human gastric cancer is a marker of metastasis and grades of malignancies: an in situ hybridization study. *Virchows Archiv, 450*(3), 303-310.

Miskad, U. A., Semba, S., Kato, H., & Yokozaki, H. (2004). Expression of PRL-3 phosphatase in human gastric carcinomas: close correlation with invasion and metastasis. *Pathobiology, 71*(4), 176-184.

Mitsuhara, I., Shirasawa-Seo, N., Iwai, T., Nakamura, S., Honkura, R., & Ohashi, Y. (2002). Release from post-transcriptional gene silencing by cell proliferation in transgenic tobacco plants: possible mechanism for noninheritance of the silencing. *Genetics, 160*(1), 343-352.

Mizuuchi, E., Semba, S., Kodama, Y., & Yokozaki, H. (2009). Down-modulation of keratin 8 phosphorylation levels by PRL-3 contributes to colorectal carcinoma progression. *International Journal of Cancer, 124*(8), 1802-1810.

Mocciaro, A., & Schiebel, E. (2010). Cdc14: a highly conserved family of phosphatases with non-conserved functions? *Journal of Cell Science, 123*(Pt 17), 2867-2876.

Mohn, K. L., Laz, T. M., Hsu, J. C., Melby, A. E., Bravo, R., & Taub, R. (1991). The immediate-early growth response in regenerating liver and insulin-stimulated H-35 cells: comparison with serum-stimulated 3T3 cells and identification of 41 novel immediate-early genes. *Molecular and Cellular Biology, 11*(1), 381-390.

Mollevi, D. G., Aytes, A., Padulles, L., Martinez-Iniesta, M., Baixeras, N., Salazar, R., . . . Villanueva, A. (2008). PRL-3 is essentially overexpressed in primary colorectal tumours and associates with tumour aggressiveness. *British Journal of Cancer, 99*(10), 1718-1725.

Montagna, M., Serova, O., Sylla, B. S., Feunteun, J., & Lenoir, G. M. (1995). A 100-kb physical and transcriptional map around the EDH17B2 gene: identification of three novel genes and a pseudogene of a human homologue of the rat PRL-1 tyrosine phosphatase. *Human Genetics, 96*(5), 532-538.

Montagna, M., Serova, O., Sylla, B. S., Mattei, M. G., & Lenoir, G. M. (1996). Localization of the human phosphotyrosine phosphatase-related genes (h-PRL-1) to chromosome bands 1p35-p34, 17q12-q21, 11q24-q25 and 12q24. *Human Genetics, 98*(6), 738-740.

Moorhead, G. B., De Wever, V., Templeton, G., & Kerk, D. (2009). Evolution of protein phosphatases in plants and animals. *Biochemical Journal, 417*(2), 401-409.

Moorhead, G. B., Trinkle-Mulcahy, L., & Ulke-Lemee, A. (2007). Emerging roles of nuclear protein phosphatases. *Nature Reviews Molecular Cell Biology, 8*(3), 234-244.

Mosakhani, N., Guled, M., Leen, G., Calabuig-Farinas, S., Niini, T., Machado, I., . . . Knuutila, S. (2012). An integrated analysis of miRNA and gene copy numbers in xenografts of Ewing's sarcoma. *Journal of Experimental and Clinical Cancer Research, 31*, 24.

Mustelin, T. (2007). A brief introduction to the protein phosphatase families. *Methods in Molecular Biology, 365*, 9-22.

Mustelin, T., Brockdorff, J., Rudbeck, L., Gjorloff-Wingren, A., Han, S., Wang, X., . . . Saxena, M. (1999). The next wave: protein tyrosine phosphatases enter T cell antigen receptor signalling. *Cellular Signalling, 11*(9), 637-650.

Nakashima, M., & Lazo, J. S. (2010). Phosphatase of regenerating liver-1 promotes cell migration and invasion and regulates filamentous actin dynamics. *Journal of Pharmacology and Experimental Therapeutics, 334*(2), 627-633.

Nandy, C., Mrazek, J., Stoiber, H., Grasser, F. A., Huttenhofer, A., & Polacek, N. (2009). Epstein-barr virus-induced expression of a novel human vault RNA. *Journal of Molecular Biology, 388*(4), 776-784.

Nitadori, J., Ishii, G., Tsuta, K., Yokose, T., Murata, Y., Kodama, T., . . . Ochiai, A. (2006). Immunohistochemical differential diagnosis between large cell neuroendocrine carcinoma and small cell carcinoma by tissue microarray analysis with a large antibody panel. *American Journal of Clinical Pathology, 125*(5), 682-692.

Norrman, K., Fischer, Y., Bonnamy, B., Wolfhagen Sand, F., Ravassard, P., & Semb, H. (2010). Quantitative comparison of constitutive promoters in human ES cells. *PLoS ONE, 5*(8), e12413.

Olsen, J. V., Blagoev, B., Gnad, F., Macek, B., Kumar, C., Mortensen, P., & Mann, M. (2006). Global, in vivo, and site-specific phosphorylation dynamics in signaling networks. *Cell, 127*(3), 635-648.

Ooki, A., Yamashita, K., Kikuchi, S., Sakuramoto, S., Katada, N., Waraya, M., . . . Watanabe, M. (2011). Therapeutic potential of PRL-3 targeting and clinical significance of PRL-3 genomic amplification in gastric cancer. *BMC Cancer, 11*, 122.

Ooki, A., Yamashita, K., Kikuchi, S., Sakuramoto, S., Katada, N., & Watanabe, M. (2009). Phosphatase of regenerating liver-3 as a prognostic biomarker in histologically node-negative gastric cancer. *Oncology Reports, 21*(6), 1467-1475.

Ooki, A., Yamashita, K., Kikuchi, S., Sakuramoto, S., Katada, N., & Watanabe, M. (2010). Phosphatase of regenerating liver-3 as a convergent therapeutic target for lymph node metastasis in esophageal squamous cell carcinoma. *International Journal of Cancer, 127*(3), 543-554.

Orsatti, L., Forte, E., Tomei, L., Caterino, M., Pessi, A., & Talamo, F. (2009). 2-D Difference in gel electrophoresis combined with Pro-Q Diamond staining: a successful approach for the identification of kinase/phosphatase targets. *Electrophoresis, 30*(14), 2469-2476.

Orsatti, L., Innocenti, F., Lo Surdo, P., Talamo, F., & Barbato, G. (2009). Mass spectrometry study of PRL-3 phosphatase inactivation by disulfide bond formation and cysteine into glycine conversion. *Rapid Communications in Mass Spectrometry, 23*(17), 2733-2740.

Ostman, A., Frijhoff, J., Sandin, A., & Bohmer, F. D. (2011). Regulation of protein tyrosine phosphatases by reversible oxidation. *Journal of Biochemistry, 150*(4), 345-356.

Ostman, A., Hellberg, C., & Bohmer, F. D. (2006). Protein-tyrosine phosphatases and cancer. *Nature Reviews Cancer, 6*(4), 307-320.

Parker, B. S., Argani, P., Cook, B. P., Liangfeng, H., Chartrand, S. D., Zhang, M., . . . Madden, S. L. (2004). Alterations in vascular gene expression in invasive breast carcinoma. *Cancer Research, 64*(21), 7857-7866.

Parri, M., & Chiarugi, P. (2010). Rac and Rho GTPases in cancer cell motility control. *Cell Commun Signal, 8*, 23.

Pascaru, M., Tanase, C., Vacaru, A. M., Boeti, P., Neagu, E., Popescu, I., & Szedlacsek, S. E. (2009). Analysis of molecular determinants of PRL-3. *Journal of Cellular and Molecular Medicine, 13*(9B), 3141-3150.

Patterson, K. I., Brummer, T., O'Brien, P. M., & Daly, R. J. (2009). Dual-specificity phosphatases: critical regulators with diverse cellular targets. *Biochemical Journal, 418*(3), 475-489.

Paul, S., & Lombroso, P. J. (2003). Receptor and nonreceptor protein tyrosine phosphatases in the nervous system. *Cellular and Molecular Life Sciences, 60*(11), 2465-2482.

Pawson, T., & Scott, J. D. (1997). Signaling through scaffold, anchoring, and adaptor proteins. *Science, 278*(5346), 2075-2080.

Peng, L., Ning, J., Meng, L., & Shou, C. (2004). The association of the expression level of protein tyrosine phosphatase PRL-3 protein with liver metastasis and prognosis of patients with colorectal cancer. *Journal of Cancer Research and Clinical Oncology, 130*(9), 521-526.

Peng, L., Xing, X., Li, W., Qu, L., Meng, L., Lian, S., . . . Shou, C. (2009). PRL-3 promotes the motility, invasion, and metastasis of LoVo colon cancer cells through PRL-3-integrin beta1-ERK1/2 and-MMP2 signaling. *Molecular Cancer, 8*, 110.

Peng, Y., Genin, A., Spinner, N. B., Diamond, R. H., & Taub, R. (1998). The gene encoding human nuclear protein tyrosine phosphatase, PRL-1. Cloning, chromosomal localization, and identification of an intron enhancer. *Journal of Biological Chemistry, 273*(27), 17286-17295.

Peters, C. S., Liang, X., Li, S., Kannan, S., Peng, Y., Taub, R., & Diamond, R. H. (2001). ATF-7, a novel bZIP protein, interacts with the PRL-1 protein-tyrosine phosphatase. *Journal of Biological Chemistry, 276*(17), 13718-13726.

Place, R. F., Li, L. C., Pookot, D., Noonan, E. J., & Dahiya, R. (2008). MicroRNA-373 induces expression of genes with complementary promoter sequences. *Proceedings of the National Academy of Sciences of the United States of America, 105*(5), 1608-1613.

Polato, F., Codegoni, A., Fruscio, R., Perego, P., Mangioni, C., Saha, S., . . . Broggini, M. (2005). PRL-3 phosphatase is implicated in ovarian cancer growth. *Clinical Cancer Research, 11*(19 Pt 1), 6835-6839.

Poon, R. Y., & Hunter, T. (1995). Dephosphorylation of Cdk2 Thr160 by the cyclin-dependent kinase-interacting phosphatase KAP in the absence of cyclin. *Science, 270*(5233), 90-93.

Pryczynicz, A., Guzinska-Ustymowicz, K., Chang, X. J., Kisluk, J., & Kemona, A. (2010). PTP4A3 (PRL-3) expression correlate with lymphatic metastases in gastric cancer. *Folia Histochemica et Cytobiologica, 48*(4), 632-636.

Pulido, R., & Hooft van Huijsduijnen, R. (2008). Protein tyrosine phosphatases: dual-specificity phosphatases in health and disease. *FEBS Journal, 275*(5), 848-866.

Qian, F., Li, Y. P., Sheng, X., Zhang, Z. C., Song, R., Dong, W., . . . Xu, Q. (2007). PRL-3 siRNA inhibits the metastasis of B16-BL6 mouse melanoma cells in vitro and in vivo. *Molecular Medicine, 13*(3-4), 151-159.

R-Project software (Version 2.13.1). Available from http://www.r-project.org/

Radhakrishnan, P., Basma, H., Klinkebiel, D., Christman, J., & Cheng, P. W. (2008). Cell type-specific activation of the cytomegalovirus promoter by dimethylsulfoxide and 5-aza-2'-deoxycytidine. *International Journal of Biochemistry & Cell Biology, 40*(9), 1944-1955.

Radke, I., Gotte, M., Kersting, C., Mattsson, B., Kiesel, L., & Wulfing, P. (2006). Expression and prognostic impact of the protein tyrosine phosphatases PRL-1, PRL-2, and PRL-3 in breast cancer. *British Journal of Cancer, 95*(3), 347-354.

Raftopoulou, M., & Hall, A. (2004). Cell migration: Rho GTPases lead the way. *Developmental Biology, 265*(1), 23-32.

Rayapureddi, J. P., Kattamuri, C., Steinmetz, B. D., Frankfort, B. J., Ostrin, E. J., Mardon, G., & Hegde, R. S. (2003). Eyes absent represents a class of protein tyrosine phosphatases. *Nature, 426*(6964), 295-298.

Reddig, P. J., & Juliano, R. L. (2005). Clinging to life: cell to matrix adhesion and cell survival. *Cancer and Metastasis Reviews, 24*(3), 425-439.

Ren, T., Jiang, B., Xing, X., Dong, B., Peng, L., Meng, L., . . . Shou, C. (2009). Prognostic significance of phosphatase of regenerating liver-3 expression in ovarian cancer. *Pathology & Oncology Research, 15*(4), 555-560.

Ren, X. D., Kiosses, W. B., & Schwartz, M. A. (1999). Regulation of the small GTP-binding protein Rho by cell adhesion and the cytoskeleton. *EMBO Journal, 18*(3), 578-585.

Renshaw, M. W., Ren, X. D., & Schwartz, M. A. (1997). Growth factor activation of MAP kinase requires cell adhesion. *EMBO Journal, 16*(18), 5592-5599.

Ridley, A. J. (2004). Rho proteins and cancer. *Breast Cancer Research and Treatment, 84*(1), 13-19.

Rouleau, C., Roy, A., St Martin, T., Dufault, M. R., Boutin, P., Liu, D., . . . Teicher, B. A. (2006). Protein tyrosine phosphatase PRL-3 in malignant cells and endothelial cells: expression and function. *Molecular Cancer Therapeutics, 5*(2), 219-229.

RStudio (Version 0.94.92). Available from http://www.rstudio.org

Ruan, F., Lin, J., Wu, R. J., Xu, K. H., Zhang, X. M., Zhou, C. Y., & Huang, X. F. (2010). Phosphatase of regenerating liver-3: a novel and promising marker in human endometriosis. *Fertility and Sterility, 94*(6), 1980-1984.

Rundle, C. H., & Kappen, C. (1999). Developmental expression of the murine Prl-1 protein tyrosine phosphatase gene. *Journal of Experimental Zoology, 283*(6), 612-617.

Saha, S., Bardelli, A., Buckhaults, P., Velculescu, V. E., Rago, C., St Croix, B., . . . Vogelstein, B. (2001). A phosphatase associated with metastasis of colorectal cancer. *Science, 294*(5545), 1343-1346.

Scarlato, M., Beesley, J., & Pleasure, D. (2000). Analysis of oligodendroglial differentiation using cDNA arrays. *Journal of Neuroscience Research, 59*(3), 430-435.

Schmidt, J., de Avila, J., & McLean, D. (2006). Regulation of protein tyrosine phosphatase 4a1, B-cell translocation gene 2, nuclear receptor subfamily 4a1 and diacylglycerol O-acyltransferase 1 by follicle stimulating hormone in the rat ovary. *Reproduction Fertility and Development, 18*(7), 757-765.

Schneider, C. A., Rasband, W. S., & Eliceiri, K. W. (2012). NIH Image to ImageJ: 25 Years of Image Analysis. *Nature Methods, 9*, 671-675.

Schwartz, M. A., & Assoian, R. K. (2001). Integrins and cell proliferation: regulation of cyclin-dependent kinases via cytoplasmic signaling pathways. *Journal of Cell Science, 114*(Pt 14), 2553-2560.

Schwering, I., Brauninger, A., Distler, V., Jesdinsky, J., Diehl, V., Hansmann, M. L., . . . Kuppers, R. (2003). Profiling of Hodgkin's lymphoma cell line L1236 and germinal center B cells: identification of Hodgkin's lymphoma-specific genes. *Molecular Medicine, 9*(3-4), 85-95.

Semba, S., Mizuuchi, E., & Yokozaki, H. (2010). Requirement of phosphatase of regenerating liver-3 for the nucleolar localization of nucleolin during the progression of colorectal carcinoma. *Cancer Science, 101*(10), 2254-2261.

Shiohama, A., Sasaki, T., Noda, S., Minoshima, S., & Shimizu, N. (2007). Nucleolar localization of DGCR8 and identification of eleven DGCR8-associated proteins. *Experimental Cell Research, 313*(20), 4196-4207.

Si, X., Zeng, Q., Ng, C. H., Hong, W., & Pallen, C. J. (2001). Interaction of farnesylated PRL-2, a protein-tyrosine phosphatase, with the beta-subunit of geranylgeranyltransferase II. *Journal of Biological Chemistry, 276*(35), 32875-32882.

Silvius, J. R. (2002). Mechanisms of Ras protein targeting in mammalian cells. *Journal of Membrane Biology, 190*(2), 83-92.

Simoncic, P. D., McGlade, C. J., & Tremblay, M. L. (2006). PTP1B and TC-PTP: novel roles in immune-cell signaling. *Canadian Journal of Physiology and Pharmacology, 84*(7), 667-675.

Simpson, J. C., & Jones, A. T. (2005). Early endocytic Rabs: functional prediction to functional characterization. *Biochemical Society Symposia*(72), 99-108.

Sipos, F., & Galamb, O. (2012). Epithelial-to-mesenchymal and mesenchymal-to-epithelial transitions in the colon. *World Journal of Gastroenterology, 18*(7), 601-608.

Soulsby, M., & Bennett, A. M. (2009). Physiological signaling specificity by protein tyrosine phosphatases. *Physiology (Bethesda), 24*, 281-289.

St Croix, B., Rago, C., Velculescu, V., Traverso, G., Romans, K. E., Montgomery, E., . . . Kinzler, K. W. (2000). Genes expressed in human tumor endothelium. *Science, 289*(5482), 1197-1202.

Stahlhut Espinosa, C. E., & Slack, F. J. (2006). The role of microRNAs in cancer. *Yale Journal of Biology and Medicine, 79*(3-4), 131-140.

Stam, M., Mol, J. N. M., & Kooter, J. M. (1997). The Silence of Genes in Transgenic Plants. *Annals of Botany (London), 79*, 3-12.

Stenmark, H., & Olkkonen, V. M. (2001). The Rab GTPase family. *Genome Biology, 2*(5), REVIEWS3007.

Stephens, B., Han, H., Hostetter, G., Demeure, M. J., & Von Hoff, D. D. (2008). Small interfering RNA-mediated knockdown of PRL phosphatases results in altered Akt phosphorylation and reduced clonogenicity of pancreatic cancer cells. *Molecular Cancer Therapeutics, 7*(1), 202-210.

Stephens, B. J., Han, H., Gokhale, V., & Von Hoff, D. D. (2005). PRL phosphatases as potential molecular targets in cancer. *Molecular Cancer Therapeutics, 4*(11), 1653-1661.

Sun, J. P., Luo, Y., Yu, X., Wang, W. Q., Zhou, B., Liang, F., & Zhang, Z. Y. (2007). Phosphatase activity, trimerization, and the C-terminal polybasic region are all required for PRL1-mediated cell growth and migration. *Journal of Biological Chemistry, 282*(39), 29043-29051.

Sun, J. P., Wang, W. Q., Yang, H., Liu, S., Liang, F., Fedorov, A. A., . . . Zhang, Z. Y. (2005). Structure and biochemical properties of PRL-1, a phosphatase implicated in cell growth, differentiation, and tumor invasion. *Biochemistry, 44*(36), 12009-12021.

Suzuki, T., Higgins, P. J., & Crawford, D. R. (2000). Control selection for RNA quantitation. *BioTechniques, 29*(2), 332-337.

Takano, S., Fukuyama, H., Fukumoto, M., Kimura, J., Xue, J. H., Ohashi, H., & Fujita, J. (1996). PRL-1, a protein tyrosine phosphatase, is expressed in neurons and oligodendrocytes in the brain and induced in the cerebral cortex following transient forebrain ischemia. *Brain Research. Molecular Brain Research, 40*(1), 105-115.

Tarn, W. Y., & Steitz, J. A. (1996). A novel spliceosome containing U11, U12, and U5 snRNPs excises a minor class (AT-AC) intron in vitro. *Cell, 84*(5), 801-811.

Tautz, L., Pellecchia, M., & Mustelin, T. (2006). Targeting the PTPome in human disease. *Expert Opinion on Therapeutic Targets, 10*(1), 157-177.

Taylor, G. S., Maehama, T., & Dixon, J. E. (2000). Myotubularin, a protein tyrosine phosphatase mutated in myotubular myopathy, dephosphorylates the lipid second messenger, phosphatidylinositol 3-phosphate. *Proceedings of the National Academy of Sciences of the United States of America, 97*(16), 8910-8915.

Taylor, W. P., & Widlanski, T. S. (1995). Charged with meaning: the structure and mechanism of phosphoprotein phosphatases. *Chemistry and Biology, 2*(11), 713-718.

Tonks, N. K. (2006). Protein tyrosine phosphatases: from genes, to function, to disease. *Nature Reviews Molecular Cell Biology, 7*(11), 833-846.

Tonks, N. K., & Neel, B. G. (2001). Combinatorial control of the specificity of protein tyrosine phosphatases. *Current Opinion in Cell Biology, 13*(2), 182-195.

Vadlamudi, R. K., Li, F., Adam, L., Nguyen, D., Ohta, Y., Stossel, T. P., & Kumar, R. (2002). Filamin is essential in actin cytoskeletal assembly mediated by p21-activated kinase 1. *Nature Cell Biology, 4*(9), 681-690.

Vandesompele, J., De Preter, K., Pattyn, F., Poppe, B., Van Roy, N., De Paepe, A., & Speleman, F. (2002). Accurate normalization of real-time quantitative RT-PCR data by geometric averaging of multiple internal control genes. *Genome Biology, 3*(7), RESEARCH0034.

Varedi, K. S., Ventura, A. C., Merajver, S. D., & Lin, X. N. (2010). Multisite phosphorylation provides an effective and flexible mechanism for switch-like protein degradation. *PLoS ONE, 5*(12), e14029.

Vasudevan, S. (2012). Posttranscriptional upregulation by microRNAs. *Wiley Interdiscip Rev RNA, 3*(3), 311-330.

Virshup, D. M., & Shenolikar, S. (2009). From promiscuity to precision: protein phosphatases get a makeover. *Molecular Cell, 33*(5), 537-545.

von Roretz, C., & Gallouzi, I. E. (2010). Protein kinase RNA/FADD/caspase-8 pathway mediates the proapoptotic activity of the RNA-binding protein human antigen R (HuR). *Journal of Biological Chemistry, 285*(22), 16806-16813.

Wang, E. (2008). MicroRNA Systems Biology. In V. A. Erdmann, W. Poller & J. Barciszewski (Eds.), *RNA Technologies in Cardiovascular Medicine and Research* (pp. 69-86). Berlin-Heidelberg, Germany: Springer.

Wang, H., Quah, S. Y., Dong, J. M., Manser, E., Tang, J. P., & Zeng, Q. (2007). PRL-3 down-regulates PTEN expression and signals through PI3K to promote epithelial-mesenchymal transition. *Cancer Research, 67*(7), 2922-2926.

Wang, H., Vardy, L. A., Tan, C. P., Loo, J. M., Guo, K., Li, J., . . . Zeng, Q. (2011). PCBP1 suppresses the translation of metastasis-associated PRL-3 phosphatase. *Cancer Cell, 18*(1), 52-62.

Wang, J., Kirby, C. E., & Herbst, R. (2002). The tyrosine phosphatase PRL-1 localizes to the endoplasmic reticulum and the mitotic spindle and is required for normal mitosis. *Journal of Biological Chemistry, 277*(48), 46659-46668.

Wang, L., Peng, L., Dong, B., Kong, L., Meng, L., Yan, L., . . . Shou, C. (2006). Overexpression of phosphatase of regenerating liver-3 in breast cancer: association with a poor clinical outcome. *Annals of Oncology, 17*(10), 1517-1522.

Wang, L., Shen, Y., Song, R., Sun, Y., Xu, J., & Xu, Q. (2009). An anticancer effect of curcumin mediated by down-regulating phosphatase of regenerating liver-3 expression on highly metastatic melanoma cells. *Molecular Pharmacology, 76*(6), 1238-1245.

Wang, Q., Holmes, D. I., Powell, S. M., Lu, Q. L., & Waxman, J. (2002). Analysis of stromal-epithelial interactions in prostate cancer identifies PTPCAAX2 as a potential oncogene. *Cancer Letters, 175*(1), 63-69.

Wang, Y., & Lazo, J. S. (2012). Metastasis-associated phosphatase PRL-2 regulates tumor cell migration and invasion. *Oncogene, 31*(7), 818-827.

Wang, Y., Li, Z. F., He, J., Li, Y. L., Zhu, G. B., Zhang, L. H., & Li, Y. L. (2007). Expression of the human phosphatases of regenerating liver (PRLs) in colonic adenocarcinoma and its correlation with lymph node metastasis. *International Journal of Colorectal Disease, 22*(10), 1179-1184.

Wang, Y., Shibasaki, F., & Mizuno, K. (2005). Calcium signal-induced cofilin dephosphorylation is mediated by Slingshot via calcineurin. *Journal of Biological Chemistry, 280*(13), 12683-12689.

Wang, Z., Cai, S. R., He, Y. L., Zhan, W. H., Zhang, C. H., Wu, H., . . . Song, W. (2009). Elevated PRL-3 expression was more frequently detected in the large primary gastric cancer and exhibits a poor prognostic impact on the patients. *Journal of Cancer Research and Clinical Oncology, 135*(8), 1041-1046.

Wang, Z., He, Y. L., Cai, S. R., Zhan, W. H., Li, Z. R., Zhu, B. H., . . . Zhang, L. J. (2008). Expression and prognostic impact of PRL-3 in lymph node metastasis of gastric cancer: its molecular mechanism was investigated using artificial microRNA interference. *International Journal of Cancer, 123*(6), 1439-1447.

Welsh, C. F., Roovers, K., Villanueva, J., Liu, Y., Schwartz, M. A., & Assoian, R. K. (2001). Timing of cyclin D1 expression within G1 phase is controlled by Rho. *Nature Cell Biology, 3*(11), 950-957.

Werner, S. R., Lee, P. A., DeCamp, M. W., Crowell, D. N., Randall, S. K., & Crowell, P. L. (2003). Enhanced cell cycle progression and down regulation of p21(Cip1/Waf1) by PRL tyrosine phosphatases. *Cancer Letters, 202*(2), 201-211.

Wiederkehr, A., & Caroni, P. (1995). Widely used enhancer of eukaryotic expression vectors is strongly and differentially regulated in fibroblast, myoblast, and teratocarcinoma cell lines. *Experimental Cell Research, 219*(2), 664-670.

Wu, X., Zeng, H., Zhang, X., Zhao, Y., Sha, H., Ge, X., . . . Xu, Q. (2004). Phosphatase of regenerating liver-3 promotes motility and metastasis of mouse melanoma cells. *American Journal of Pathology, 164*(6), 2039-2054.

Wu, Z. S., Wu, Q., Wang, C. Q., Wang, X. N., Wang, Y., Zhao, J. J., . . . Xu, X. C. (2010). MiR-339-5p inhibits breast cancer cell migration and invasion in vitro and may be a potential biomarker for breast cancer prognosis. *BMC Cancer, 10*, 542.

Xiao, W., Bao, Z. X., Zhang, C. Y., Zhang, X. Y., Shi, L. J., Zhou, Z. T., & Jiang, W. W. (2012). Upregulation of miR-31* is negatively associated with recurrent/newly formed oral leukoplakia. *PLoS ONE, 7*(6), e38648.

Xing, X., Peng, L., Qu, L., Ren, T., Dong, B., Su, X., & Shou, C. (2009). Prognostic value of PRL-3 overexpression in early stages of colonic cancer. *Histopathology, 54*(3), 309-318.

Xu, J., Cao, S., Wang, L., Xu, R., Chen, G., & Xu, Q. (2011). VEGF promotes the transcription of the human PRL-3 gene in HUVEC through transcription factor MEF2C. *PLoS ONE, 6*(11), e27165.

Xu, Y., Zhu, M., Zhang, S., Liu, H., Li, T., & Qin, C. (2010). Expression and prognostic value of PRL-3 in human intrahepatic cholangiocarcinoma. *Pathology & Oncology Research, 16*(2), 169-175.

Yarovinsky, T. O., Rickman, D. W., Diamond, R. H., Taub, R., Hageman, G. S., & Bowes Rickman, C. (2000). Expression of the protein tyrosine phosphatase, phosphatase of regenerating liver 1, in the outer segments of primate cone photoreceptors. *Brain Research. Molecular Brain Research, 77*(1), 95-103.

Yonemura, S., Matsui, T., & Tsukita, S. (2002). Rho-dependent and -independent activation mechanisms of ezrin/radixin/moesin proteins: an essential role for polyphosphoinositides in vivo. *Journal of Cell Science, 115*(Pt 12), 2569-2580.

Yoon, C. H., Miah, M. A., Kim, K. P., & Bae, Y. S. (2010). New Cdc2 Tyr 4 phosphorylation by dsRNA-activated protein kinase triggers Cdc2 polyubiquitination and G2 arrest under genotoxic stresses. *EMBO Reports, 11*(5), 393-399.

Yu, L., Kelly, U., Ebright, J. N., Malek, G., Saloupis, P., Rickman, D. W., . . . Bowes Rickman, C. (2007). Oxidative stress-induced expression and modulation of Phosphatase of Regenerating Liver-1 (PRL-1) in mammalian retina. *Biochimica et Biophysica Acta, 1773*(9), 1473-1482.

Yuan, L., Chen, J., Lin, B., Zhang, J., & Zhang, S. (2007). Differential expression and functional constraint of PRL-2 in hibernating bat. *Comparative Biochemistry and Physiology. Part B, Biochemistry and Molecular Biology, 148*(4), 375-381.

Yuvaniyama, J., Denu, J. M., Dixon, J. E., & Saper, M. A. (1996). Crystal structure of the dual specificity protein phosphatase VHR. *Science, 272*(5266), 1328-1331.

Zeng, Q., Dong, J. M., Guo, K., Li, J., Tan, H. X., Koh, V., . . . Hong, W. (2003). PRL-3 and PRL-1 promote cell migration, invasion, and metastasis. *Cancer Research, 63*(11), 2716-2722.

Zeng, Q., Hong, W., & Tan, Y. H. (1998). Mouse PRL-2 and PRL-3, two potentially prenylated protein tyrosine phosphatases homologous to PRL-1. *Biochemical and Biophysical Research Communications, 244*(2), 421-427.

Zeng, Q., Si, X., Horstmann, H., Xu, Y., Hong, W., & Pallen, C. J. (2000). Prenylation-dependent association of protein-tyrosine phosphatases PRL-1, -2, and -3 with the plasma membrane and the early endosome. *Journal of Biological Chemistry, 275*(28), 21444-21452.

Zhang, L., Ding, L., Cheung, T. H., Dong, M. Q., Chen, J., Sewell, A. K., . . . Han, M. (2007). Systematic identification of C. elegans miRISC proteins, miRNAs, and mRNA targets by their interactions with GW182 proteins AIN-1 and AIN-2. *Molecular Cell, 28*(4), 598-613.

Zhang, Y., & Zhang, M. (2011). Crystal structure of Ssu72, an essential eukaryotic phosphatase specific for the C-terminal domain of RNA polymerase II, in complex with a transition state analogue. *Biochemical Journal, 434*(3), 435-444.

Zhang, Z. Y., & Dixon, J. E. (1993). Active site labeling of the Yersinia protein tyrosine phosphatase: the determination of the pKa of the active site cysteine and the function of the conserved histidine 402. *Biochemistry, 32*(36), 9340-9345.

Zhao, W. B., Li, Y., Liu, X., Zhang, L. Y., & Wang, X. (2008). Evaluation of PRL-3 expression, and its correlation with angiogenesis and invasion in hepatocellular carcinoma. *International Journal of Molecular Medicine, 22*(2), 187-192.

Zhao, Z., Lee, C. C., Monckton, D. G., Yazdani, A., Coolbaugh, M. I., Li, X., . . . Caskey, C. T. (1996). Characterization and genomic mapping of genes and pseudogenes of a new human protein tyrosine phosphatase. *Genomics, 35*(1), 172-181.

Zheng, P., Liu, Y. X., Chen, L., Liu, X. H., Xiao, Z. Q., Zhao, L., . . . Li, J. M. (2010). Stathmin, a new target of PRL-3 identified by proteomic methods, plays a key role in progression and metastasis of colorectal cancer. *Journal of Proteome Research, 9*(10), 4897-4905.

Zheng, P., Meng, H. M., Gao, W. Z., Chen, L., Liu, X. H., Xiao, Z. Q., . . . Li, J. M. (2011). Snail as a key regulator of PRL-3 gene in colorectal cancer. *Cancer Biology and Therapy, 12*(8), 742-749.

Zhou, J., Bi, C., Chng, W. J., Cheong, L. L., Liu, S. C., Mahara, S., . . . Chen, C. S. (2011). PRL-3, a metastasis associated tyrosine phosphatase, is involved in FLT3-ITD signaling and implicated in anti-AML therapy. *PLoS ONE, 6*(5), e19798.

Zhou, J., Wang, S., Lu, J., Li, J., & Ding, Y. (2009). Over-expression of phosphatase of regenerating liver-3 correlates with tumor progression and poor prognosis in nasopharyngeal carcinoma. *International Journal of Cancer, 124*(8), 1879-1886.

APPENDICES

Appendix A Literature Reports of PRL Expression in Normal Tissues

Table A.1 Instances where positive PRL expression has been reported in the literature for normal tissues

Tissue	Molecule	Species*	Detection Methods	Reference*
Adipose Tissue (Fat)	PRL-1	Human	ISH	Dumaual 2006
	PRL-2	Human; Bat	ISH; PCR	Dumaual 2006; Yuan 2007
Adrenal Gland (Adult)	PRL-1	Human	ISH; Northern Blot	Dumaual 2006; Guo 2006
	PRL-2	Human; Rat	ISH; Northern Blot	Dumaual 2006; Carter 1998
Adrenal Gland (Developing)	PRL-1	Mouse	ISH	Rundle 1999
Appendix (Adult)	PRL-1	Human	ISH	Dumaual 2006
	PRL-2	Human	ISH	Dumaual 2006
Bladder (Adult)	PRL-1	Human	ISH	Dumaual 2006
	PRL-2	Human	ISH	Dumaual 2006
Bone/Cartilage (Developing)	PRL-1	Mouse	ISH	Rundle 1999
Bone Marrow (Adult)	PRL-1	Human	PCR	Gjorloff-Wingren 2000
	PRL-2	Human	PCR	Gjorloff-Wingren 2000
Brain (Adult)	PRL-1	Human; Rat	ISH; Northern Blot	Dumaual 2006; Diamond 1994, Takano 1996, Guo 2006
	PRL-2	Human; Mouse, Rat; Bat	ISH; Northern Blot; PCR	Dumaual 2006; Carter 1998, Zhao 1996, Zeng 1998, Guo 2006; Yuan 2007
Brain (Developing)	PRL-1	Rat, Mouse; Human	ISH; Northern Blot	Takano 1996, Rundle 1999; Guo 2006
	PRL-2	Human	Northern Blot	Zhao 1996
	PRL-3	Human	Northern Blot	Guo 2006
Breast (Adult)	PRL-1	Human	ISH; PCR	Dumaual 2006; Guo 2003
	PRL-2	Human	ISH	Dumaual 2006
Cervix (Adult)	PRL-1	Human	ISH	Dumaual 2006
	PRL-2	Human	ISH	Dumaual 2006
Colon (Adult)	PRL-1	Human	ISH; Northern Blot	Dumaual 2006; Guo 2006
	PRL-2	Human	ISH; Northern Blot	Dumaual 2006; Guo 2006, Montagna 1995, Zhao 1996
	PRL-3	Human	IHC**	L. Peng 2004**
Colon (Developing)	PRL-1	Rat	IHC	Kong 2000
Esophagus (Developing)	PRL-1	Rat	IHC	Kong 2000
Eye (Adult Retina)	PRL-1	Human; Monkey	ISH; IHC, Southern, Western	Dumaual 2006; Yarovinsky 2000
	PRL-2	Human	ISH	Dumaual 2006
Heart (Adult)	PRL-1	Human	Northern Blot	Guo 2006
	PRL-2	Human; Mouse, Rat; Bat	ISH; Northern Blot; PCR	Dumaual 2006; Carter 1998, Zhao 1996, Zeng 1998, Guo 2006; Yuan 2007
	PRL-3	Human; Mouse	ISH; Northern Blot	Guo 2006; Zeng 1998, Matter 2001, Wu 2004
Heart (Developing)	PRL-3	Human; Rat	IHC; Northern Blot	Guo 2006
Hyaline Cartilage (Adult)	PRL-2	Human	ISH	Dumaual 2006
Kidney (Adult)	PRL-1	Human; Rat	ISH; Northern Blot; IHC	Dumaual 2006; Diamond 1994, Guo 2006; Kong 2000
	PRL-2	Human; Mouse; Rat	ISH; Northern Blot	Dumaual 2006; Zhao 1996, Carter 1998, Zeng 1998
Kidney (Developing)	PRL-1	Human; Mouse; Rat	Northern Blot; ISH; IHC	Guo 2006; Rundle 1999; Kong 2000
	PRL-2	Human	Northern Blot	Zhao 1996
	PRL-3	Human	Northern Blot	Guo 2006
Liver (Adult)	PRL-1	Human; Rat	ISH; Northern Blot; IHC	Dumaual 2006; Diamond 1994, Haber 1995, Guo 2006; Diamond 1996, Kong 2000
	PRL-2	Human; Mouse	ISH; Northern Blot	Dumaual 2006; Zeng 1998
	PRL-3	Human	Northern Blot	Wu 2004
Liver (Developing)	PRL-1	Rat; Mouse; Human	ISH; IHC; Northern Blot; PCR	Haber 1995, Rundle 1999; Guo 2006; Gjorloff-Wingren 2000
	PRL-2	Human	Northern Blot; PCR	Zhao 1996, Guo 2006; Gjorloff-Wingren 2000
	PRL-3	Human	Northern Blot	Guo 2006
Lung (Adult)	PRL-1	Human; Rat	ISH; IHC	Dumaual 2006; Kong 2000
	PRL-2	Human; Mouse	ISH; Northern Blot	Dumaual 2006; Zeng 1998
	PRL-3	Human; Mouse	Northern Blot	Guo 2006, Zeng 1998
Lung (Developing)	PRL-1	Human; Mouse; Rat	Northern Blot; ISH; IHC	Guo 2006; Rundle 1999; Kong 2000
	PRL-2	Human	Northern Blot	Guo 2006, Zhao 1996
	PRL-3	Human	Northern Blot	Guo 2006

Table A.1 Cont.

Tissue	Molecule	Species*	Detection Methods	Reference*
Lymph Node (Adult)	PRL-1	Human	ISH; PCR	Dumaual 2006; Gjorloff-Wingren 2000
	PRL-2	Human	ISH; PCR	Dumaual 2006; Gjorloff-Wingren 2000
Ovary (Adult)	PRL-1	Human	ISH	Dumaual 2006
	PRL-2	Human	ISH; Northern Blot	Dumaual 2006; Montagna 1995, Zhao 1996
Pancreas (Adult)	PRL-1	Human	ISH; Northern Blot	Dumaual 2006; Guo 2006
	PRL-2	Human	ISH; Northern Blot	Dumaual 2006; Zhao 1996
	PRL-3	Human	Northern Blot	Guo 2006, Matter 2001
Parathyroid (Adult)	PRL-1	Human	ISH	Dumaual 2006
	PRL-2	Human	ISH	Dumaual 2006
Placenta	PRL-1	Human	ISH; Northern Blot	Dumaual 2006; Guo 2006
	PRL-2	Human	ISH	Dumaual 2006
Prostate (Adult)	PRL-1	Human	ISH; Northern Blot	Dumaual 2006; Guo 2006
	PRL-2	Human	ISH; Northern Blot	Dumaual 2006; Montagna 1995, Zhao 1996
	PRL-3	Human	Northern Blot	Guo 2006
Skeletal Muscle (Adult)	PRL-1	Rat; Human	Northern Blot; ISH	Diamond 1994, Guo 2006; Dumaual 2006
	PRL-2	Mouse; Human; Bat	Northern Blot; ISH; PCR	Zhao 1996, Zeng 1998, Guo 2006; Dumaual 2006; Yuan 2007
	PRL-3	Human; Mouse	Northern Blot	Guo 2006, Matter 2001, Wu 2004, Zeng 1998
Skin (Adult)	PRL-1	Human	ISH	Dumaual 2006
	PRL-2	Human	ISH	Dumaual 2006
Small Intestine (Adult)	PRL-1	Human; Rat	ISH; Northern Blot; IHC	Dumaual 2006; Guo 2006; Diamond 1996, Kong 2000
	PRL-2	Human	ISH; Northern Blot	Dumaual 2006; Montagna 199, Zhao 1996
	PRL-3	Human; Mouse	IHC; Northern Blot	Guo 2006; Zeng 2000
Small Intestine (Developing)	PRL-1	Mouse; Rat	ISH; Northern Blot; IHC	Rundle 1999; Diamond 1996; Kong 2000
Spinal Cord (Adult)	PRL-1	Human	Northern Blot	Guo 2006
	PRL-2	Human	Northern Blot	Guo 2006
Spinal Cord (Developing)	PRL-1	Mouse	ISH	Rundle 1999
Spleen (Adult)	PRL-1	Rat; Human	Northern Blot; ISH; PCR	Diamond 1994; Dumaual 2006; Gjorloff-Wingren 2000
	PRL-2	Human	Northern Blot; ISH; PCR	Montagna 1995, Zhao 1996; Dumaual 2006; Gjorloff-Wingren 2000
	PRL-3	Mouse	Northern Blot	Zeng 1998
Spleen (Developing)	PRL-1	Human	Northern Blot	Guo 1996
	PRL-2	Human	Northern Blot	Guo 1996
	PRL-3	Human	Northern Blot	Guo 1996
Stomach (Adult)	PRL-1	Human; Rat	ISH; Northern Blot; IHC	Dumaual 2006; Guo 2006; Kong 2000
	PRL-2	Human	ISH	Dumaual 2006
	PRL-3	Human	IHC; Northern Blot	Dai 2009; Guo 2006
Stomach (Developing)	PRL-1	Rat	IHC	Kong 2000
Testis (Adult)	PRL-1	Human	ISH; Northern Blot	Dumaual 2006; Guo 1996
	PRL-2	Human; Mouse; Rat	ISH; Northern Blot	Dumaual 2006; Montagna 1995, Zhao 1996, Carter 1998, Zeng 1998
	PRL-3	Mouse	Northern Blot	Zeng 1998
Tongue (Adult)	PRL-1	Human	ISH	Dumaual 2006
	PRL-2	Human	ISH	Dumaual 2006
Tonsil (Adult)	PRL-1	Human	PCR	Gjorloff-Wingren 2000
	PRL-2	Human	PCR	Gjorloff-Wingren 2000
Thymus (Adult)	PRL-1	Rat; Huma	Northern Blot; PCR	Diamond 1994; Gjorloff-Wingren 2000
	PRL-2	Human	Northern Blot; PCR	Guo 2006, Montagna 1995, Zhao 1996; Gjorloff-Wingren 2000
Thymus (Developing)	PRL-1	Mouse	ISH	Rundle 1999
	PRL-2	Human	Northern Blot	Guo 2006
	PRL-3	Human	Northern Blot	Guo 2006
Thyroid (Adult)	PRL-1	Human	ISH	Dumaual 2006
	PRL-2	Human	ISH; Northern Blot	Dumaual 2006; Guo 2006
Uterus (Adult)	PRL-1	Human	ISH	Dumaual 2006
	PRL-2	Human	ISH	Dumaual 2006
	PRL-3	Human	Northern Blot	Guo 2006

*Ordered first by the specific detection method that was used and second by the date published.
**Only 7.1% of samples gave positive results
Abbreviations: IHC, immunohistochemistry; ISH, *in situ* hybridization; PCR, polymerase chain reaction.

Table A.2 Reports in the literature where PRL expression was undetectable in normal tissues

Tissue	Molecule	Species*	Detection Methods	Reference*
Adrenal Gland (Adult)	PRL-2	Human	Northern Blot	Guo 2006
	PRL-3	Human	Northern Blot	Guo 2006
Bone Marrow (Adult)	PRL-1	Human	Northern Blot	Guo 2006
	PRL-2	Human	Northern Blot	Guo 2006
	PRL-3	Human	Northern Blot	Guo 2006
Bladder (Adult)	PRL-1	Human	Northern Blot	Guo 2006
	PRL-2	Human	Northern Blot	Guo 2006
	PRL-3	Human	Northern Blot	Guo 2006
Brain (Adult)	PRL-3	Mouse; Human	Northern Blot; ISH; IHC	Zeng 1998, Guo 2006; Matter 2001; Kong 2007
Brain (Developing)	PRL-2	Human	Northern Blot	Guo 2006
Colon (Adult)	PRL-1	Human	IHC	Y. Wang 2007
	PRL-2	Human	IHC	Y. Wang 2007
	PRL-3	Human	IHC; ISH; Northern Blot	Bardelli 2003; Y. Wang 2007; Guo 2006
Esophagus (Adult)	PRL-1	Rat; Human	IHC; Northern Blot	Kong 2000; Guo 2006
	PRL-2	Human	Northern Blot	Guo 2006
	PRL-3	Human	Northern Blot	Guo 2006
Fibrocartilage (Adult)	PRL-1	Human	ISH	Dumaual 2006
	PRL-2	Human	ISH	Dumaual 2006
Heart (Adult)	PRL-1	Human; Rat	ISH; Northen Blot	Dumaual 2006; Diamond 1994
	PRL-3	Human; Rat	IHC	Guo 2006
Heart (Developing)	PRL-1	Mouse; Human	ISH; Northern Blot	Rundle 1999; Guo 2006
	PRL-2	Human	Northern Blot	Guo 2006
Hyaline Cartilage (Adult)	PRL-1	Human	ISH	Dumaual 2006
Kidney (Adult)	PRL-2	Human	Northern Blot	Guo 2006
	PRL-3	Mouse; Human	Northern Blot	Zeng 1998, Matter 2001, Guo 2006
Kidney (Developing)	PRL-2	Human	Northern Blot	Guo 2006
Liver (Adult)	PRL-1	Rat	IHC	Kong 2000
	PRL-2	Human; Rat	Northern Blot	Zhao 1996, Carter 1998, Guo 2006
	PRL-3	Mouse; Human	Northern Blot	Zeng 1998, Matter 2001, Guo 2006
Lung (Adult)	PRL-1	Rat; Human	Northern Blot	Diamond 1994; Guo 2006
	PRL-2	Human	Northern Blot	Zhao 1996, Guo 2006
	PRL-3	Human	Northern Blot	Matter 2001
Lymph Node (Adult)	PRL-1	Human	Northern Blot	Guo 2006
	PRL-2	Human	Northern Blot	Guo 2006
	PRL-3	Human	Northern Blot	Guo 2006
Ovary (Adult)	PRL-1	Human	Northern Blot	Guo 2006
	PRL-2	Human	Northern Blot	Guo 2006
	PRL-3	Human	Northern Blot	Guo 2006
Pancreas (Adult)	PRL-2	Human	Northern Blot	Guo 2006
Placenta	PRL-2	Human	Northern Blot	Zhao 1996, Guo 2006
	PRL-3	Human	Northern Blot	Matter 2001, Guo 2006
Prostate (Adult)	PRL-2	Human	Northern Blot	Guo 2006
Skeletal Muscle (Developing)	PRL-1	Mouse	ISH	Rundle 1999
Small Intestine (Adult)	PRL-1	Rat	Northern Blot	Diamond 1994
	PRL-2	Human	Northern Blot	Guo 2006
Spinal Cord (Adult)	PRL-3	Human	Northern Blot	Guo 2006
Spleen (Adult)	PRL-1	Human	Northern Blot	Guo 2006
	PRL-2	Mouse; Human	Northern Blot	Zeng 1998, Guo 2006
	PRL-3	Human	Northern Blot	Guo 2006
Stomach (Adult)	PRL-1	Rat	Northern Blot	Diamond 1994
	PRL-2	Human	Northern Blot	Guo 2006
Testis (Adult)	PRL-2	Human	Northern Blot	Guo 2006
	PRL-3	Human	Northern Blot	Guo 2006
Thymus (Adult)	PRL-1	Human	Northern Blot	Guo 2006
	PRL-3	Human	Northern Blot	Guo 2006

Table A.2 Cont.

Tissue	Molecule	Species*	Detection Methods	Reference*
Thymus (Developing)	PRL-1	Human	Northern Blot	Guo 2006
Thyroid (Adult)	PRL-1	Human	Northern Blot	Guo 2006
	PRL-3	Human	Northern Blot	Guo 2006
Uterus	PRL-1	Human	Northern Blot	Guo 2006
	PRL-2	Human	Northern Blot	Guo 2006

*Ordered first by the specific detection method that was used and second by the date published.
Abbreviations: IHC, immunohistochemistry; ISH, *in situ* hybridization.

Appendix B Correlation of miRNA and mRNA Expression in HEK293 Cells Stably Transfected with PRL-3

Table B Significant miRNAs and the significant mRNAs which they are predicted to target

The Ingenuity Pathway Analysis tool was used to identify mRNAs that were significantly (Fold Change > 100; FDR < 10%) differentially expressed in HEK293 cells stably transfected with PRL-3 versus those transfected with empty vector and that were also known or predicted targets of miRNAs which were significantly (Fold Change > 2; FDR < 30%) differentially expressed in the same sample set. The resulting list of predicted or known miRNA-mRNA interactions and the fold change differences in expression for each that were observed in the current study are shown.

miR ID	miR Fold Change	Target Prediction Database	Prediction Confidence	mRNA Probe ID	mRNA Gene Symbol	mRNA Fold Change
hsa-miR-98	-14.02	TargetScan Human	High (predicted)	208754_s_at	NAP1L1	-115.477
hsa-miR-98	-14.02	TargetScan Human	Moderate (predicted)	225421_at	PM20D2	-117.803
hsa-miR-98	-14.02	TargetScan Human	High (predicted)	204286_s_at	PMAIP1	-199.922
hsa-miR-98	-14.02	TarBase,TargetScan Human,miRecords	Experimentally Observed, High (predicted)	201589_at	SMC1A	-214.353
hsa-miR-526b*	-4.86	TargetScan Human	Moderate (predicted)	201891_s_at	B2M	-142.07
hsa-miR-526b*	-4.86	TargetScan Human	Moderate (predicted)	208808_s_at	HMGB2	-203.616
hsa-miR-526b*	-4.86	TargetScan Human	High (predicted)	221891_x_at	HSPA8	-307.422
hsa-miR-526b*	-4.86	TargetScan Human	Moderate (predicted)	200603_at	PRKAR1A	-233.943
hsa-miR-526b*	-4.86	TargetScan Human	High (predicted)	222077_s_at	RACGAP1	-107.434
hsa-miR-526b*	-4.86	TargetScan Human	High (predicted)	201417_at	SOX4	-137.064
hsa-miR-526b*	-4.86	TargetScan Human	Moderate (predicted)	201351_s_at	YME1L1	-180.101
hsa-miR-190b	-4.25	TargetScan Human	Moderate (predicted)	224585_x_at	ACTG1	-162.754
hsa-miR-190b	-4.25	TargetScan Human	Moderate (predicted)	205361_s_at	PFDN4	-111.338
hsa-miR-190b	-4.25	TargetScan Human	Moderate (predicted)	225421_at	PM20D2	-117.803

256

Table B Cont.

miR ID	miR Fold Change	Target Prediction Database	Prediction Confidence	mRNA Probe ID	mRNA Gene Symbol	mRNA Fold Change
hsa-miR-141	-4.22	TargetScan Human	High (predicted)	208796_s_at	CCNG1	-102.758
hsa-miR-141	-4.22	TargetScan Human	High (predicted)	208905_at	CYCS	-128.101
hsa-miR-141	-4.22	TargetScan Human	High (predicted)	200934_at	DEK	-150.128
hsa-miR-141	-4.22	TargetScan Human	High (predicted)	224935_at	EIF2S3	-166.898
hsa-miR-141	-4.22	TargetScan Human	High (predicted)	212449_s_at	LYPLA1	-196.579
hsa-miR-141	-4.22	TargetScan Human	Moderate (predicted)	200626_s_at	MATR3	-124.303
hsa-miR-141	-4.22	TargetScan Human	Moderate (predicted)	218499_at	MST4	-106.237
hsa-miR-141	-4.22	TargetScan Human	High (predicted)	208754_s_at	NAP1L1	-115.477
hsa-miR-141	-4.22	TargetScan Human	Moderate (predicted)	200738_s_at	PGK1	-124.247
hsa-miR-141	-4.22	TargetScan Human	Moderate (predicted)	204286_s_at	PMAIP1	-199.922
hsa-miR-141	-4.22	TargetScan Human	High (predicted)	200603_at	PRKAR1A	-233.943
hsa-miR-141	-4.22	TargetScan Human	Moderate (predicted)	208319_s_at	RBM3	-230.462
hsa-miR-141	-4.22	TargetScan Human	Moderate (predicted)	201427_s_at	SEPP1	-174.877
hsa-miR-141	-4.22	TargetScan Human	Moderate (predicted)	217851_s_at	SLMO2	-105.53
hsa-miR-141	-4.22	TargetScan Human	High (predicted)	212160_at	XPOT	-131.845
hsa-miR-210	-2.59	TargetScan Human	Moderate (predicted)	201312_s_at	SH3BGRL	-104.897
hsa-miR-150	2.94	TargetScan Human	High (predicted)	224372_at	DCAF6	-158.764
hsa-miR-150	2.94	TargetScan Human	Moderate (predicted)	1555653_at	HNRNPA3	-175.135
hsa-miR-150	2.94	TargetScan Human	Moderate (predicted)	221553_at	MAGT1	-146.678
hsa-miR-150	2.94	TargetScan Human	High (predicted)	200603_at	PRKAR1A	-233.943
hsa-miR-150	2.94	TargetScan Human	High (predicted)	208694_at	PRKDC	-110.014
hsa-miR-150	2.94	TargetScan Human	Moderate (predicted)	222077_s_at	RACGAP1	-107.434
hsa-miR-570	3.01	TargetScan Human	Moderate (predicted)	208905_at	CYCS	-128.101
hsa-miR-570	3.01	TargetScan Human	High (predicted)	1555653_at	HNRNPA3	-175.135

Table B Cont.

miR ID	miR Fold Change	Target Prediction Database	Prediction Confidence	mRNA Probe ID	mRNA Gene Symbol	mRNA Fold Change
hsa-miR-570	3.01	TargetScan Human	High (predicted)	200914_x_at	KTN1	-106.924
hsa-miR-570	3.01	TargetScan Human	Moderate (predicted)	221553_at	MAGT1	-146.678
hsa-miR-570	3.01	TargetScan Human	High (predicted)	201669_s_at	MARCKS	-203.708
hsa-miR-570	3.01	TargetScan Human	Moderate (predicted)	226091_s_at	MRFAP1	-115.33
hsa-miR-570	3.01	TargetScan Human	High (predicted)	208754_s_at	NAP1L1	-115.477
hsa-miR-570	3.01	TargetScan Human	Moderate (predicted)	204286_s_at	PMAIP1	-199.922
hsa-miR-570	3.01	TargetScan Human	Moderate (predicted)	201589_at	SMC1A	-214.353
hsa-miR-570	3.01	TargetScan Human	High (predicted)	201273_s_at	SRP9	-432.297
hsa-miR-570	3.01	TargetScan Human	Moderate (predicted)	224587_at	SUB1	-119.306
hsa-miR-570	3.01	TargetScan Human	Moderate (predicted)	221493_at	TSPYL1	-101.53
hsa-miR-512-3p	3.03	TargetScan Human	Moderate (predicted)	224585_x_at	ACTG1	-162.754
hsa-miR-512-3p	3.03	TargetScan Human	Moderate (predicted)	208754_s_at	NAP1L1	-115.477
hsa-miR-512-3p	3.03	TargetScan Human	Moderate (predicted)	222077_s_at	RACGAP1	-107.434
hsa-miR-215	3.83	TargetScan Human	Moderate (predicted)	209291_at	ID4	-100.949
hsa-miR-215	3.83	TargetScan Human	Moderate (predicted)	221805_at	NEFL	-182.674
hsa-miR-215	3.83	TargetScan Human	High (predicted)	200603_at	PRKAR1A	-233.943
hsa-miR-517c	4.25	TargetScan Human	Moderate (predicted)	200626_s_at	MATR3	-124.303
hsa-miR-518d-3p	4.37	TargetScan Human	Moderate (predicted)	214039_s_at	LAPTM4B	-158.612
hsa-miR-515-3p	5.12	TargetScan Human	High (predicted)	210211_s_at	HSP90AA1	-556.599
hsa-miR-515-3p	5.12	TargetScan Human	Moderate (predicted)	200603_at	PRKAR1A	-233.943
hsa-miR-515-3p	5.12	TargetScan Human	Moderate (predicted)	201589_at	SMC1A	-214.353
hsa-miR-515-3p	5.12	TargetScan Human	Moderate (predicted)	201417_at	SOX4	-137.064
hsa-miR-515-3p	5.12	TargetScan Human	High (predicted)	201273_s_at	SRP9	-432.297

Table B Cont.

miR ID	miR Fold Change	Target Prediction Database	Prediction Confidence	mRNA Probe ID	mRNA Gene Symbol	mRNA Fold Change
hsa-miR-219-1-3p	5.2	TargetScan Human	Moderate (predicted)	217719_at	EIF3L	-170.601
hsa-miR-219-1-3p	5.2	TargetScan Human	High (predicted)	200914_x_at	KTN1	-106.924
hsa-miR-219-1-3p	5.2	TargetScan Human	Moderate (predicted)	200650_s_at	LDHA	-145.996
hsa-miR-219-1-3p	5.2	TargetScan Human	Moderate (predicted)	200738_s_at	PGK1	-124.247
hsa-miR-219-1-3p	5.2	TargetScan Human	High (predicted)	224587_at	SUB1	-119.306
hsa-miR-487a	5.31	TargetScan Human	Moderate (predicted)	201443_s_at	ATP6AP2	-150.744
hsa-miR-487a	5.31	TargetScan Human	Moderate (predicted)	218499_at	MST4	-106.237
hsa-miR-487a	5.31	TargetScan Human	Moderate (predicted)	225421_at	PM20D2	-117.803
hsa-miR-133a	6.17	TargetScan Human	High (predicted)	201443_s_at	ATP6AP2	-150.744
hsa-miR-133a	6.17	TargetScan Human	High (predicted)	200084_at	C11orf58	-100.286
hsa-miR-133a	6.17	TargetScan Human	Moderate (predicted)	1555653_at	HNRNPA3	-175.135
hsa-miR-133a	6.17	TargetScan Human	High (predicted)	209291_at	ID4	-100.949
hsa-miR-133a	6.17	TargetScan Human	High (predicted)	217851_s_at	SLMO2	-105.53
hsa-miR-133a	6.17	TargetScan Human	High (predicted)	201417_at	SOX4	-137.064
hsa-miR-372	9	TargetScan Human	High (predicted)	224372_at	DCAF6	-158.764
hsa-miR-372	9	TargetScan Human	Moderate (predicted)	222077_s_at	RACGAP1	-107.434
hsa-miR-372	9	TargetScan Human	Moderate (predicted)	211942_x_at	RPL13A	-245.93
hsa-miR-372	9	TargetScan Human	Moderate (predicted)	201351_s_at	YME1L1	-180.101
hsa-miR-372	9	TargetScan Human	Moderate (predicted)	212426_s_at	YWHAQ	-116.345
hsa-miR-129-3p	9.01	TargetScan Human	High (predicted)	1555653_at	HNRNPA3	-175.135
hsa-miR-129-3p	9.01	TargetScan Human	Moderate (predicted)	201417_at	SOX4	-137.064
hsa-miR-129-3p	9.01	TargetScan Human	Moderate (predicted)	201273_s_at	SRP9	-432.297

Table B Cont.

miR ID	miR Fold Change	Target Prediction Database	Prediction Confidence	mRNA Probe ID	mRNA Gene Symbol	mRNA Fold Change
hsa-miR-346	10.8	TargetScan Human	Moderate (predicted)	212449_s_at	LYPLA1	-196.579
hsa-miR-346	10.8	TargetScan Human	High (predicted)	200738_s_at	PGK1	-124.247
hsa-miR-519a	15.14	TargetScan Human	Moderate (predicted)	200934_at	DEK	-150.128
hsa-miR-519a	15.14	TargetScan Human	Moderate (predicted)	221891_x_at	HSPA8	-307.422
hsa-miR-519a	15.14	TargetScan Human	Moderate (predicted)	222077_s_at	RACGAP1	-107.434
hsa-miR-519a	15.14	TargetScan Human	Moderate (predicted)	201417_at	SOX4	-137.064
hsa-miR-128	16.52	TargetScan Human	Moderate (predicted)	201443_s_at	ATP6AP2	-150.744
hsa-miR-128	16.52	TargetScan Human	High (predicted)	208796_s_at	CCNG1	-102.758
hsa-miR-128	16.52	TargetScan Human	High (predicted)	214039_s_at	LAPTM4B	-158.612
hsa-miR-128	16.52	TargetScan Human	High (predicted)	201669_s_at	MARCKS	-203.708
hsa-miR-128	16.52	TargetScan Human	Moderate (predicted)	200006_at	PARK7	-131.528
hsa-miR-128	16.52	TargetScan Human	Moderate (predicted)	201273_s_at	SRP9	-432.297
hsa-miR-509-5p	20.48	TargetScan Human	Moderate (predicted)	201016_at	EIF1AX	-329.726
hsa-miR-509-5p	20.48	TargetScan Human	Moderate (predicted)	201669_s_at	MARCKS	-203.708
hsa-miR-509-5p	20.48	TargetScan Human	Moderate (predicted)	212160_at	XPOT	-131.845
hsa-miR-509-5p	20.48	TargetScan Human	Moderate (predicted)	201351_s_at	YME1L1	-180.101
hsa-miR-576-3p	21.15	TargetScan Human	Moderate (predicted)	208905_at	CYCS	-128.101
hsa-miR-576-3p	21.15	TargetScan Human	Moderate (predicted)	200934_at	DEK	-150.128
hsa-miR-576-3p	21.15	TargetScan Human	Moderate (predicted)	201016_at	EIF1AX	-329.726
hsa-miR-576-3p	21.15	TargetScan Human	Moderate (predicted)	209291_at	ID4	-100.949
hsa-miR-576-3p	21.15	TargetScan Human	Moderate (predicted)	201669_s_at	MARCKS	-203.708
hsa-miR-576-3p	21.15	TargetScan Human	Moderate (predicted)	204286_s_at	PMAIP1	-199.922

Table B Cont.

miR ID	miR Fold Change	Target Prediction Database	Prediction Confidence	mRNA Probe ID	mRNA Gene Symbol	mRNA Fold Change
hsa-miR-576-3p	21.15	TargetScan Human	High (predicted)	200603_at	PRKAR1A	-233.943
hsa-miR-576-3p	21.15	TargetScan Human	High (predicted)	222077_s_at	RACGAP1	-107.434
hsa-miR-576-3p	21.15	TargetScan Human	Moderate (predicted)	217851_s_at	SLMO2	-105.53
hsa-miR-576-3p	21.15	TargetScan Human	Moderate (predicted)	201589_at	SMC1A	-214.353
hsa-miR-576-3p	21.15	TargetScan Human	Moderate (predicted)	201417_at	SOX4	-137.064
hsa-miR-576-3p	21.15	TargetScan Human	Moderate (predicted)	221493_at	TSPYL1	-101.53
hsa-miR-576-3p	21.15	TargetScan Human	Moderate (predicted)	212426_s_at	YWHAQ	-116.345
hsa-miR-605	24.04	TargetScan Human	Moderate (predicted)	208905_at	CYCS	-128.101
hsa-miR-605	24.04	TargetScan Human	Moderate (predicted)	224935_at	EIF2S3	-166.898
hsa-miR-605	24.04	TargetScan Human	Moderate (predicted)	214039_s_at	LAPTM4B	-158.612
hsa-miR-605	24.04	TargetScan Human	Moderate (predicted)	212449_s_at	LYPLA1	-196.579
hsa-miR-605	24.04	TargetScan Human	High (predicted)	221553_at	MAGT1	-146.678
hsa-miR-605	24.04	TargetScan Human	Moderate (predicted)	208754_s_at	NAP1L1	-115.477
hsa-miR-605	24.04	TargetScan Human	Moderate (predicted)	225421_at	PM20D2	-117.803
hsa-miR-605	24.04	TargetScan Human	High (predicted)	201589_at	SMC1A	-214.353
hsa-miR-605	24.04	TargetScan Human	Moderate (predicted)	201273_s_at	SRP9	-432.297
hsa-miR-605	24.04	TargetScan Human	Moderate (predicted)	212320_at	TUBB	-171.879
hsa-miR-605	24.04	TargetScan Human	Moderate (predicted)	212160_at	XPOT	-131.845
hsa-miR-642	24.04	TargetScan Human	Moderate (predicted)	204102_s_at	EEF2	-284.914
hsa-miR-642	24.04	TargetScan Human	Moderate (predicted)	212320_at	TUBB	-171.879
hsa-miR-375	25.84	TargetScan Human	Moderate (predicted)	200934_at	DEK	-150.128
hsa-miR-375	25.84	TargetScan Human	High (predicted)	213564_x_at	LDHB	-128.475

Table B Cont.

miR ID	miR Fold Change	Target Prediction Database	Prediction Confidence	mRNA Probe ID	mRNA Gene Symbol	mRNA Fold Change
hsa-miR-375	25.84	TargetScan Human	Moderate (predicted)	225421_at	PM20D2	-117.803
hsa-miR-622	29.65	TargetScan Human	Moderate (predicted)	208796_s_at	CCNG1	-102.758
hsa-miR-622	29.65	TargetScan Human	High (predicted)	201016_at	EIF1AX	-329.726
hsa-miR-622	29.65	TargetScan Human	High (predicted)	201503_at	G3BP1	-113.556
hsa-miR-622	29.65	TargetScan Human	Moderate (predicted)	208754_s_at	NAP1L1	-115.477
hsa-miR-622	29.65	TargetScan Human	Moderate (predicted)	208319_s_at	RBM3	-230.462
hsa-miR-622	29.65	TargetScan Human	High (predicted)	221452_s_at	TMEM14B	-120.017
hsa-miR-622	29.65	TargetScan Human	High (predicted)	223105_s_at	TMEM14C	-221.955

VITA

VITA

Carmen Michelle Dumaual

EDUCATION

Ph.D.	Purdue University Biology	Dec. 2012
B.S.	Ball State University Cellular & Molecular Biology *summa cum laude*	1998

PROFESSIONAL EXPERIENCE

Associate Consultant Scientist, Pharmacogenomics — 2010-2012
Eli Lilly and Company, Indianapolis, IN
Pharmacogenomics liaison for Autoimmune platform

Assistant Senior Scientist, Diagnostic and Experimental Medicine — 2007-2010
Eli Lilly and Company, Indianapolis, IN
Development and validation of pharmacogenomic assays

Senior Associate, Diagnostic and Experimental Medicine — 2002-2007
Eli Lilly and Company, Indianapolis, IN
Assay development and validation for clinical trial support

Associate Biologist, Molecular Pathology — 2000-2002
Eli Lilly and Company, Indianapolis, IN
Immunohistochemistry for early stage molecule development.

Research Assistant, Department of Biology — 1998-2000
IUPUI, Indianapolis, IN
Characterization of the PRL family of phosphatases

Undergraduate Research Fellow, Department of Biology 1997-1998
Ball State University, Muncie, Indiana
Optimization of field methods for DNA collection

Laboratory Technician, Pathologists Associated 1995-1998
Ball Memorial Hospital, Muncie, Indiana

SUPERVISORY EXPERIENCE

Three years experience with supervision of laboratory research associates from a broad range of technical backgrounds and professional experience.

TEACHING/ORGANIZATIONAL EXPERIENCE

Instructor, DMET Genotyping Training Course 2005-2009
Eli Lilly and Company, Indianapolis, IN

Organizer/Coordinator, Intensive Immunology Course 2002-2004
Eli Lilly and Company, Indianapolis, IN

Teaching Assistant, Anatomy Course, Department of Biology 1998-1999
IUPUI, Indianapolis, IN

AWARDS, ACHIEVEMENTS, AND HONORS

President's Award, Eli Lilly and Company 2007
Regional Solution Achievement Award, Eli Lilly and Company 2007
Undergraduate Fellowship, Ball State University 1997
Dean's list, Ball State University 1995-1998
Westfield Teachers Association Scholarship 1993

PRESENTATIONS AND ABSTRACTS

Dumaual CM. MicroRNAs: Small molecules with big functions. An introduction to microRNA biogenesis, function, and role in disease pathology. Student seminar presentation, IUPUI. October, 2012.

Dumaual CM, Banerjee P, Krueger J, Fretzin S, Dow E, Nantz E, Komocsar W, Phipps K, Cameron G, McColm J, Penny MA, Banerjee S, Hoffman RW. IL-17 blockade demonstrates central role of Th17 in the pathogenesis of psoriasis. *Poster presentation, Tailored Therapeutics Learning Forum, Eli Lilly and Company.* March 2012.

Dow E, **Dumaual CM**, Banerjee P, Komocsar W, Nantz E, Yang Y, Santa P, Bishop J, Hoffman RW. Tailored therapeutics in rheumatoid arthritis. *Poster presentation, Tailored Therapeutics Learning Forum, Eli Lilly and Company.* March 2012.

Dumaual CM, Njau R, Man M, Farmen M, Teng C, Moser B, Irie S, Noh GJ, close S, Wise S, Hockett R. Comparison of genetic variation in drug metabolizing enzyme and transporter genes in three major ethnic groups. *Poster presentation, Lilly Expo, Eli Lilly and Company.* April 2009.

Grondin J, Ivanova Y, Bauer N, **Dumaual C**, Farmen M, Njau R. Evaluation of a multiplex assay for genotyping of drug metabolic enzyme and transporter gene polymorphisms*. Poster presentation, Lilly Expo, Eli Lilly and Company.* April 2009.

Dumaual, CM. Validation of a multiplex assay for comprehensive genotyping of drug metabolic enzyme and transporter gene polymorphisms. 39th Annual Oak Ridge Conference: Harnessing New Technology for Clinical Diagnostics, St. Louis, MO. April 2007.

Dumaual, CM, Hockett, R., and Duffin, K. Technology validation and its relevance to tailored therapeutics. **Invited Speaker:** Tailored Therapeutics Learning Forum. Eli Lilly and Company. February 2007.

Dumaual, CM. Genotyping genetic polymorphisms in drug metabolic enzyme and transporter genes, using the MegAllele genotyping platform. **Invited Speaker and panelist:** Incorporating Pharmacogenomics in Clinical Studies conference. Hyatt, Baltimore, Maryland. September, 2006.

Dumaual CM, Dotson CA, Bauer NL, Farmen MW, Mukhopadhyay N, Kadam SK, Hockett RD, Daly TM. Precision profiling and components of variability analysis for Affymetrix microarray assays. *Poster presentation, Lilly Expo, Eli Lilly and Company.* April 2005.

Dumaual CM, Dotson CA, Farmen MW, Mukhopadhyay N, Kadam SK, Daly TM, Hockett RD. Clinical validation of the Affymetrix microarray system. *Poster presentation, 7th Annual Affymetrix User Group Meeting, San Francisco, CA.* May, 2004.

Zambrano, CM. Immunohistochemical analysis of the APO-1/Fas and Bcl-2 proteins in formalin-fixed tissues of various species. Sigma Zeta Honorary Science Society National Conference. Coastal Carolina University, South Carolina. March, 1998.

Zambrano, CM. Immunohistochemical analysis of the APO-1/Fas and Bcl-2 proteins in formalin-fixed tissues of various species. Indiana Academy of Sciences, 114th annual meeting. St. Joseph's College, Rensselaer, Indiana. October, 1997.

Zambrano, CM. Immunohistochemical analysis of the APO-1/Fas and Bcl-2 proteins in formalin-fixed tissues of various species. Lilly Intern Poster Session, Eli Lilly and Company, Indianapolis, Indiana. August, 1997.

PUBLICATIONS RELATED TO THIS DISSERTATION

Dumaual CM, Steere BA, Walls CD, Zhang ZY, Randall SK. Novel insights to PRL-1 signaling gained through integrated analysis of mRNA and protein expression data. *Manuscript in Preparation.*

Dumaual CM, Steere BA, Randall SK. PRL-1 expression alters cellular microRNA levels. *Manuscript in Preparation*.

Dumaual CM, Sandusky GE, Soo HW, Werner SR, Crowell PC, Randall SK. Tissue-specific alterations of PRL-1 and PRL-2 expression in cancer. *Am J Transl Res*. 2012. 4(1):83-101.

Dumaual CM, Sandusky GE, Crowell PL, Randall SK. Cellular localization of PRL-1 and PRL-2 gene expression in normal adult human tissues. *J Histochem Cytochem*. 2006, 54(12):1401-1412.

OTHER ORIGINAL REPORTS

Man M, Farmen M, **Dumaual C**, Teng C, Moser B, Irie S, Noh GJ, Njau R, Close S, Wise S, Hockett R. Genetic variation in metabolizing enzyme and transporter genes: Comprehensive assessment in three major East Asian subpopulations with comparison to Caucasians and Africans. Submitted to *J. Clin Pharm*. 2010. 50:929-940.

Sandusky G, **Dumaual C**, Cheng L. Human tissues for discovery biomarker pharmaceutical research: The Experience of the Indiana University Simon Cancer Center-Lilly Research Labs Tissue/Fluid BioBank. *Vet Pathol*. 2009. 46(1):2-9.

Dumaual C, Miao X, Daly TM, Bruckner C, Njau R, Fu DJ, Close-Kirkwood S, Bauer N, Watanabe N, Hardenbol P, Hockett RD. Comprehensive assessment of metabolic enzyme and transporter genes using the Affymetrix Targeted Genotyping platform. *Pharmacogenomics* 2007, 8(3): 293-305.

Daly TM, **Dumaual CM**, Miao X, Farmen MW, Njau RK, Fu DJ, Bauer NL, Close S, Watanabe N, Bruckner C, Hardenbol P, Hockett RD. Multiplex assay for comprehensive genotyping of genes involved in drug metabolism, excretion, and transport. *Clin Chem.* 2007, 527: 1222-1230.

Ray C, **Dumaual C**, O'Brien PJ, Gourley I, Devanarayan V, Konrad RJ. Optimization of ex vivo stimulation of TNF-α release in whole blood. *J Pharm Biomed Anal.* 2006, 41:189-195.

Daly TM, **Dumaual CM**, Dotson CA, Farmen MW, Kadam SK, Hockett RD. Precision profiling and components of variability analysis for Affymetrix microarray assays run in a clinical context. *J Mol Diagn.* 2005, 7(3):404-412.

Alvarez E, Westmore M, Sells Galvin RJ, Clapp CL, Considine EL, Smith SJ, Keyes K, Iversen PW, Delafuente DM, Sulaimon S, **Zambrano C**, Ma L, Sato M, Martin TJ, Teicher BA, Galbreath EJ. Properties of bisphosphonates in the 13762 rat mammary carcinoma model of tumor-induced bone resorption. *Clin Ca Res.* 2003, 9:5705-5713.

Sandusky GE, Galbreath EJ, Fouts R, Mintze K, **Zambrano C**. Use of tissue microarrays to determine gene expression in tumor specimens. *Vet Pathol* 1999, 36:495.